Characterization of $CD4^+$ T-cell expansion after cord blood transplantation and its role in anti-leukaemic effects

PRASHANT RAMDAS HIWARKAR

UNIVERSITY COLLEGE LONDON

GREAT ORMOND STREET HOSPITAL INSTITUE OF CHILD HEALTH

A thesis submitted for the degree of Doctor of Philosophy

Declaration

I, Prashant Hiwarkar, confirm that the work presented in this thesis is my own. Where information has been derived from other sources, I confirm that this has been indicated in the thesis.

Abstract

In the absence of serotherapy, cord blood transplantation (CBT) is followed by a rapid and unique $CD4^+$ biased immune reconstitution derived from T cells within the graft. The mechanism for this enhanced $CD4^+$ biased reconstitution which differs from that of other stem cell sources and correlates with rapid anti-viral and enhanced graft-versus-leukaemia responses is not known. Lymphopoiesis following stem cell transplantation may be derived from foetal or adult haematopoietic stem cells. We therefore sought to determine whether recapitulation of foetal lymphopoiesis mediates rapid expansion of cord blood $CD4^+$ T cells into the lymphopenic environment created by transplant conditioning. We compared the foetal $CD4^+$ T-cell transcriptome with the transcription profile of naïve $CD4^+$ T cells from normal donor cord blood (*n=9*), normal donor peripheral blood (*n=9*), and reconstituting naïve $CD4^+$ T cells following CBT (*n=3*) and bone marrow transplant (BMT) (*n=3*). Our findings confirm that cord blood $CD4^+$ T cells and $CD4^+$ T cells reconstituting after CBT retain the properties of foetal ontogenesis and can rapidly restore the $CD4^+$ T-cell biased adaptive immunity through enhanced T-cell receptor (TCR) signalling. TCR sensitivity dictates the ability of T cells to respond to self-peptide and foreign antigens, and the emerging data suggests that unrelated CBT, particularly in the context of HLA-mismatching and a T-cell replete graft, may reduce leukaemic relapse. Therefore, I aimed to study the role of foetal-derived adaptive immune system following T-cell replete CBT in mediating graft-versus-tumour responses and dissect the underlying cellular mechanisms. To do this, the ability of HLA-mismatched cord blood and adult peripheral blood T cells to eliminate Epstein-Barr virus (EBV)-driven human B-cell lymphoma was compared, in a xenogeneic NOD/SCID/$IL2rg^{null}$ mouse model. In our model, cord blood T cells mediated enhanced anti-tumour effects by rapid infiltration of the tumour with $CCR7^+$ $CD8^+$ T cells, and prompt induction of cytotoxic $CD8^+$ and Th1 $CD4^+$ T cells in the tumour microenvironment. Conversely, in the peripheral blood group, this anti-lymphoma effect was impaired because of delayed tumoural infiltration of peripheral blood T cells, and a relative bias toward suppressive Th2 and T regulatory cells. Our data suggest that, despite being naturally programmed toward tolerance, reconstituting T cells after unrelated T-cell replete CBT may provide superior Tc1-Th1 anti-tumour effects against high-risk haematological malignancies.

Acknowledgements

To Waseem, thank you for giving me the opportunity to work on the project of viral-specific immune system in haematopoietic cell transplantation. During those 4 months, I learnt some of the basic techniques in the laboratory. I am also grateful to you for helping me to design the murine experiments.

To Persis, thank you helping me in writing the grant and supervising me throughout my time at the Institute of Child health, UCL. This would not have happened without your supervision.

To Paul, thank you for encouraging me to take up this project, helping me in writing the grant and always having an open door for discussing the project.

To Waseem, Persis and Paul, thank you for teaching me and inspiring me every step of the way. I feel privileged for having the opportunity to work with you.

To Kimberly and Aurore, special thanks to you for the fruitful discussions and valuable advice on the laboratory techniques.

To Mike, Debbie and Nick, I will be indebted to you for assisting with the *in vivo* work.

To Sarah and Ida, thank you for teaching me techniques in the lab. It was pleasure working with you.

To Ayad, thank you for helping with the flow cytometry and cell sorting.

Thanks to members of Laboratory Immunology Unit from Great Ormond Street hospital and members of Molecular and Cellular Immunology Unit, Institute of Child health, UCL, for helping me with the reagents and laboratory techniques.

To my parents, for always encouraging me to do my best.

To my wife Swati, thank you for endless patience and support throughout my time in research. I could not have done any of this without you.

Table of contents

Index of Figures

Index of Tables

Abbreviations

ALL	Acute lymphoblastic leukaemia
AML	acute myeloid leukaemia
ATG	anti-thymocyte globulin
BMT	Bone marrow transplant
CBMC	Cord blood mononuclear cells
CBT	Cord blood transplant
CD	Cluster of differentiation marker
CFSE	carboxy-fluorescein diacetate succinimidyl ester
CLs	Circulating lymphocytes
CML	Chronic myeloid leukaemia
CsA	Ciclosporin
CTLs	cytotoxic T cells
DLI	Donor lymphocyte infusion
DLI	Donor lymphocyte infusion
DNA	Deoxyribonucleic Acid
EBV	Epstein-Barr virus
FACS	Flourescence activated cell sorting
Fluc	Firefly luciferase
Foxp3	Forkhead box p3
GFP	Green fluorescent protein
GSEA	Gene set enrichment analysis
GvHD	Graft versus host disease
GvL	Graft versus leukaemia
HCT	Haematopoietic cell transplantation
HLA	Human leukocyte antigen
i.v.	intravenous

IFN-γ	Interferon-gamma
IL	Interleukin
IVIS	In vivo imaging system
JAK	Janus kinase
KIR	killer cell immunoglobulin
LCLs	Lymphoblastoid cells
MAIT	Mucosal-associated invariant T cells
MFI	Mean flourescence intensity
mHAgs	Minor histocompatibility antigens
MHC	Major histocompability complex
MSD	meso-scale discovery
NK	natural killer cells
NOD	Nonobese diabetic
PBMC	Peripheral blood mononuclear cells
PBS	Phosphate buffered saline
PCA	Principal component analysis
PFA	paraformaldehyde
PI	Proliferative index
PMA	phorbol 12-myristate 13-acetate
RAG	Recombination-activating gene
REC	Research ethics committee
RMA	Robust Multi-array Average
RNA	Ribonucleic acid
ROI	Region of interest
RTE's	Recent thymic emigrants
SCID	severe combined immune deficiency
STAT	Signal Transducer and Activator of Transcription

TCR	T-cell receptor
TILs	Tumour infiltrating lymphocytes
TNF-α	Tumour necrosis factor-alpha
TRECs	T-cell receptor excision circles
WT1	Wilm's tumour protein

Chapter one

Introduction

1.1 History of haematopoietic cell transplantation

Haematopoietic cell transplantation (HCT) has become a life-saving procedure for malignant haematological diseases and a wide variety of non-malignant diseases. Ironically the era of HCT began just four years after the 1945 atomic bomb explosions when Jacobson *et al.,* observed that the bone marrow of mice was protected by shielding their spleens with lead (Jacobson *et al.,* 1949). This was followed by a report in 1951, stating that the intravenous infusion of bone marrow also provided similar protection against radiation in murine models (Lorenz *et al.,* 1951). This observation led to the humoural hypothesis of bone marrow regeneration, with growth factors being secreted by the spleen or bone marrow. However, it was not until the mid-1950s, when it was shown that this radiation protection was due to regeneration of protected or transplanted stem cells (Barnes *et al.,* 1954; Ford *et al.,* 1956; Nowell *et al.,* 1956). Finally, the bone marrow cells of recipients were shown to have cytogenetic features of the donor (Ford *et al.,* 1956). These observations confirmed the cellular hypothesis of protection against radiation.

These exciting and novel discoveries were thought to have therapeutic applications, especially in the field of haematological malignancies. However, the first attempts to understand this process in a laboratory were not very successful, and it was thought that overcoming the transplantation barrier between individuals might not be possible (Uphoff *et al.,* 1958). Further experiments with large non-bred animals gave encouraging results (Storb *et al.,* 1967), and this set the stage for treating patients with haematological diseases. The initial therapeutic test was performed using increasing doses of radiation to kill the recipient bone marrow, along with the malignant cells. The radiotherapy-conditioned recipient bone marrow was then rescued with an intravenous infusion of donor bone marrow.

Barnes *et al.,* demonstrated that murine leukaemia could be cured by supralethal radiation, followed by bone marrow infusion (Barnes *et al.,* 1956). This was followed by attempts to treat human patients with intravenous infusion of allogeneic marrow after chemotherapy and radiotherapy in 1957 (Thomas *et al.,* 1957). This also led to autologous harvesting of marrow prior to high dose chemotherapy and then infusing it after high dose chemotherapy to facilitate the marrow recovery (Kurnick *et al.,* 1958). In 1959, Thomas *et al.,* reported the treatment of advanced leukaemia with supralethal radiation, followed by marrow infusion from identical

twins leading to prompt haematological recovery (Thomas *et al.,* 1959). Although a relapse of leukaemia was observed a few months later, this provided the proof-of-principle for using allogeneic bone marrow to cure haematological diseases.

In 1956, the immune-reaction of donor marrow against the host was reported as a wasting syndrome known as graft-versus-host disease (GvHD) (Barnes *et al.,* 1956), which was shown to be ameliorated with the use of methotrexate (Uphoff *et al.,* 1958; Lochte *et al.,* 1962). In parallel to the discovery of immunosuppressive drugs to tame the immune system, approximately 200 human allogeneic stem cell transplantations were carried out between 1950 and 1960. However, the only successful transplants were those carried out using the marrow of an identical twin (Thomas *et al.,* 1959), which demonstrated the role of histocompatibility in marrow grafting. Therefore, experiments were conducted in dogs to understand the process of marrow grafting, such as engraftment failure, graft rejection, and GvHD.

Dausset *et al.* and van Rood *et al.,* identified the human leukocyte antigen (HLA) groups, and these were thought to be important in transplantation (Dausset, *et al.,* 1958; van Rood, *et al.,* 1958). The proof-of-principle that determined the importance of the HLAs was obtained from studies in dogs and showed that dog leukocyte antigen-matched marrow grafts significantly improved survival (Epstein, *et al.,* 1969). The canine experiments also confirmed the role of methotrexate in suppressing GvHD (Storb *et al.,* 1970a), and also encouraged trials using sibling bone marrow grafts.

During these trials in the second half of the 1960s, high dose conditioning regimens with or without radiotherapy were developed (Buckner *et al.,* 1970; Thomas *et al.,* 1975). Alongside these advances in conditioning regimens, an improved understanding of HLA allowed grafting from an histocompatible donors. Despite using histocompatible donors and methotrexate, GvHD was still a problem in 50% of marrow recipients (Thomas *et al.,* 1975; Storb *et al.,* 1977), which led to studies optimizing the use of methotrexate and calcineurin inhibitors, such as ciclosporin and tacrolimus for inhibiting T-cell activation. Thus, these advances in conditioning regimens, GvHD prophylaxis, alongside improvements in supportive care and blood component technology set the stage for the modern era of HCT.

During this modern era of HCT, which started towards the end of the 1960s, three successful transplantation procedures were carried out in children with severe combined

immunodeficiencies (SCID), using HLA-matched sibling grafts (Gatti *et al.,* 1968; Bach *et al.,* 1968; deKoning *et al.,* 1969). These were followed by more than 100 allogeneic bone marrow transplant (BMT) procedures for aplastic anaemia and leukaemia across the USA (Thomas, *et al.,* 1972; Storb *et al.,* 1974), which included some patients with advanced leukaemia becoming long-term survivors. In particular, this led to the use of HLA-matched grafts for treating chronic myeloid leukaemia (CML) with very encouraging results (Fefer *et al.,* 1973; Clift *et al.,* 1982).

The success of BMTs in the 1970s led to the application of bone marrow grafting for a variety of other non-malignant disorders. After 1975, non-malignant haematological conditions, such as thalassaemia and sickle cell disease were grafted using HLA-matched sibling donors (Thomas *et al.,* 1982; Lucarelli *et al.,* 1984; Johnson *et al.,* 1984). In 1980, this was followed by the first HLA-matched sibling bone marrow transplant in a child with Hurler's syndrome (Hobbs *et al.,* 1980). Thus, providing proof-of-concept that bone marrow transplant corrects not only haematological defects, but also enzyme deficiencies, and halts the clinical deterioration of inherited metabolic disorders like Hurler's syndrome. By the year 2008, more than 1000 transplants had been performed world-wide for inherited metabolic disorders (Prasad *et al.,* 2008).

The success of bone marrow grafting has led to an increased number of bone marrow donors registered world-wide (van Rood *et al.,* 2008). New techniques for isolating haematopoietic stem cells (HSCs) from peripheral blood using G-CSF stimulation were developed in 1980 (To & Juttner, 1987; Kessinger *et al.,* 1988; Gianni *et al.,* 1989; Juttner *et al.,* 1990). This led to the easy collection of stem cells through apheresis of the donor's peripheral blood, providing adult donors with the choice of donating stem cells without general anaesthesia.

In the late 1980s it was discovered that cord blood was a source of HSCs, and provided another vital discovery in the field of stem cell transplantation (Broxmeyer *et al.,* 1989). In 1988, the first successful cord blood transplantation (CBT) for Fanconi anaemia was performed (Gluckman *et al.,* 1989), and in 1992, another patient with leukaemia was successfully transplanted with cord blood (Rubinstein *et al.,* 1998). In the past three decades, more than 30,000 cord blood transplants have been performed for haematological and inherited metabolic disorders (Ballen *et al.,* 2013). In instances, where a single unit of cord blood has an insufficient cell dose, two units of cord blood (double cord blood transplantation) are used (Majhail *et al.,*

2006). The growing adult donor registry has made it relatively easy to find an unrelated 10/10 HLA-matched donor in the Caucasian population, but less frequently in ethnic minorities populations. The cord blood registry has benefited ethnic minority populations by targeting cord collections in areas of ethnic diversity and because of less stringent requirements of HLA-matching for cord blood compared to an adult donor. These advances in stem cell grafting and molecular HLA matching, along with the exponential growth of donor registries over the past two decades have set the stage for the current transplantation program worldwide. Finally, if both adult and cord donors are not available, advances in haploidentical transplantation, such as post-transplant cyclophosphamide (Berger *et al.,* 2016) and T-cell receptor alpha/beta, and B-cell depletion (Bertaina *et al.,* 2014) have made it possible to transplant with acceptable morbidity and mortality.

These advances have made stem cell grafting safer and provided a number of different ways of performing transplant procedures. There is a choice of stem cell source, *in vivo* T-cell depletion using anti-thymocyte globulin or alemtuzumab, T-cell replete haploidentical transplant using post-transplant cyclophosphamide *vs* TCR alpha-beta and B-cell deplete haploidentical transplant; each may have a role in specific diseases. For instance, cord blood graft may mediate better enzyme delivery in metabolic disorders (Aldenhoven *et al.,* 2015). Similarly, in myeloid leukaemia, graft-versus-leukaemia (GvL) effects may be more pronounced with cord blood (Boelens *et al.,* 2016; Milano *et al* 2016), and conditioning, particularly the use of *in vivo* T-cell depletion, could also play a crucial role. In the context of our work, T-cell replete CBT may facilitate rapid T-cell reconstitution with undifferentiated foetal-derived cord blood T cells, and this may have distinct immunogenic effects compared with T-cell replete BMT.

1.2. T-cell reconstitution after haematopoietic cell transplantation

T-cell reconstitution after HCT occurs via thymus-independent and thymus-dependent pathways (Mackall *et al.,* 1993; Williams *et al.,* 2007).

1.2.1 Thymic dependent T-cell expansion

T cells carried with the stem cell graft have the ability to undergo lympopenia-induced proliferation or proliferation in response to antigens immediately after transplantation (Mackall *et al.,* 1996; Mackall *et al.,* 1997; Ge *et al.,* 2002). T-cell proliferation in the lymphopenic environment is thought to occur in the peripheral lymphoid organs, such as the lymph nodes and gut. The benefit of such a T-cell reconstitution is mostly observed in sibling grafts that are performed using preparative regimens without any T-cell depletion. Generally early T-cell reconstitution is mediated by CD8+ memory T cells, and CD4+ T cells do not appear till thymopoiesis is restored (Mackall *et al.,* 1996).

1.2.2 Thymic independent T-cell expansion

Thymopoiesis provides a *de novo* pool of naïve T cells and is essential for the diverse T-cell repertoire. The dynamics of thymus dependent T-cell reconstitution depends on the state of the thymus after transplantation; therefore, thymopoiesis is determined by the age of the recipient and the occurrence of acute or chronic GvHD.

Children have relatively preserved thymic function compared to adults, so generally thymic output in children begins before six months, and in adults it can sometimes take 9 to 12 months. Early T-cell reconstitution generally exhibits a skewed T-cell repertoire, and with the onset of thymopoiesis the repertoire begins to diversify (Mackall *et al.,* 1996).

1.2.3 Effects of T cell depletion on T-cell reconstitution

The thymus-independent T-cell reconstitution is abrogated using *in vivo* or *ex vivo* T-cell depletion as a part of the conditioning regimen. (Keever *et al.,* 1989). These are used to reduce the risk of severe GvHD in the setting of unrelated or mismatched donors. However, T-cell depletion leads to delays in immune-reconstitution, and hence increases the risk of viral reactivation/infection (Bacigalupo *et al.,* 2001; Socie *et al.,* 2011; Veys *et al.,* 2012). T-cell depletion may also increase the risk of leukaemic relapse, because GvHD and GvL

are mediated by similar effector T-cell functions. Thus, T-cell depletion has both advantages and disadvantages and hence both, T-cell deplete and T-cell replete grafts are being performed world-wide, depending on the local practices.

Ex vivo depletion of donor T cells has been used for over three decades, and *in vivo* T-cell depletion has been used in the last 2 decades (Champlin *et al.,* 2000). *Ex vivo* T-cell depletion is frequently performed via positive selection of $CD34^+$ cells, using immuno-magnetic beads. Recently, an advance in the T-cell depletion technique, using depletion of T-cell receptor alpha/beta and $CD19^+$ lymphocytes has made it to the clinic, whereby negative selectin of CD34+ cells also retains NK cells and gamma delta T cells within the graft allowing haploidentical grafts with a very low incidence of GvHD, and an infection-related mortality of less than 10%. This is an attractive option for non-malignant diseases without an HLA-matched donor, giving improved immune-reconstitution, despite T-cell depletion (Bertaina *et al.,* 2014).

Immune-reconstitution is delayed when T-cell depletion strategies are used. In the setting of cord blood graft, *ex vivo* T-cell depletion cannot be used because of the low number of $CD34^+$ cells. Hence, preparative regimens, consisting of anti-thymocyte globulin (ATG) have been used for *in-vivo* T cell depletion. However, *in vivo* T-cell depletion significantly delays immune-reconstitution after cord blood graft, because cord blood T cells appear to be particularly sensitive to ATG, either because of their low number or naivety (Admiraal *et al*., 2015). Because cord blood grafts were associated with a lower incidence of GvHD (Rubinstein *et al.,* 1998; Rocha *et al.,* 2000; Rocha *et al.,* 2001) and require less stringent HLA-matching, non-serotherapy conditioning regimens were used to improve immune-reconstitution.

We observed an unprecedented, thymus independent T-cell expansion with a $CD4^+$ bias, in contrast to the normal expansion of CD8+ memory cells after transplantation following the omission of serotherapy from the cord blood transplant conditioning regimens at Great Ormond Street hospital (Chiesa *et al.,* 2012). Further investigation of this unique phenomenon formed the basis of this thesis. But, what are the primary drivers of thymic-independent T-cell reconstitution. This type of T-cell expansion is called “lymphopenia-induced proliferation” and is distinct to the steady state homeostatic proliferation.

1.3 Mechanisms of T-cell expansion

1.3.1 Lymphopenia-induced (spontaneous) *vs* homeostatic proliferation

Many studies have used the terms "homeostatic" and "lymphopenia-induced" proliferation interchangeably. However, there are at least two mechanistically distinct modes of proliferation referred to as spontaneous proliferation and homeostatic proliferation.

Spontaneous proliferation or lymphopenia-induced proliferation occurs in extreme lymphopenic settings such as after myelo-ablative HCT without T-cell depletion. Spontaneously proliferating cells divide more than a cell division per day in the absence of cytokines. These spontaneously proliferating cells rapidly differentiate in to memory phenotype cells and thus acquire the ability to produce inflammatory cytokines after stimulation (Min *et al*., 2005; Keiper *et al*., 2005).

In contrast, homeostatic proliferation occurs in lymphoreplete or mildly lymphopenic conditions. This is a slow process. Homeostatically proliferating CD4+ T cells undergo cell division every 3 to 4 days, although CD8+ T cells proliferate rapidly compared to CD4+ T cells.

Tonic TCR signalling and cytokines such as IL-7 play role in both homeostatic and lymphopenia-induced proliferation (Do *et al*., 2009; Tan *et al*., 2002). It is intriguing that one is rapid and other is a slow process. Min proposed quantitative and qualitative signalling models for explaining spontaneous proliferation in the lymphopenic environment and steady-state homeostatic proliferation (Min *et al*., 2018). The quantitative signalling model for homeostatic proliferation postulates that the relative amount of resources such as IL-7 and self-MHC determines T-cell proliferation [Figure 1 (a)]. In contrast, the qualitative signalling model for spontaneous proliferation postulates the nature of signals that T cells receive is fundamentally different from those that T cells receive in the lymphocyte replete environment [Figure 1 (a)]. The model further proposes relative TCR signal strength determines which T cells undergo spontaneous proliferation in extreme lymphopenic environment [Figure 1 (b)].

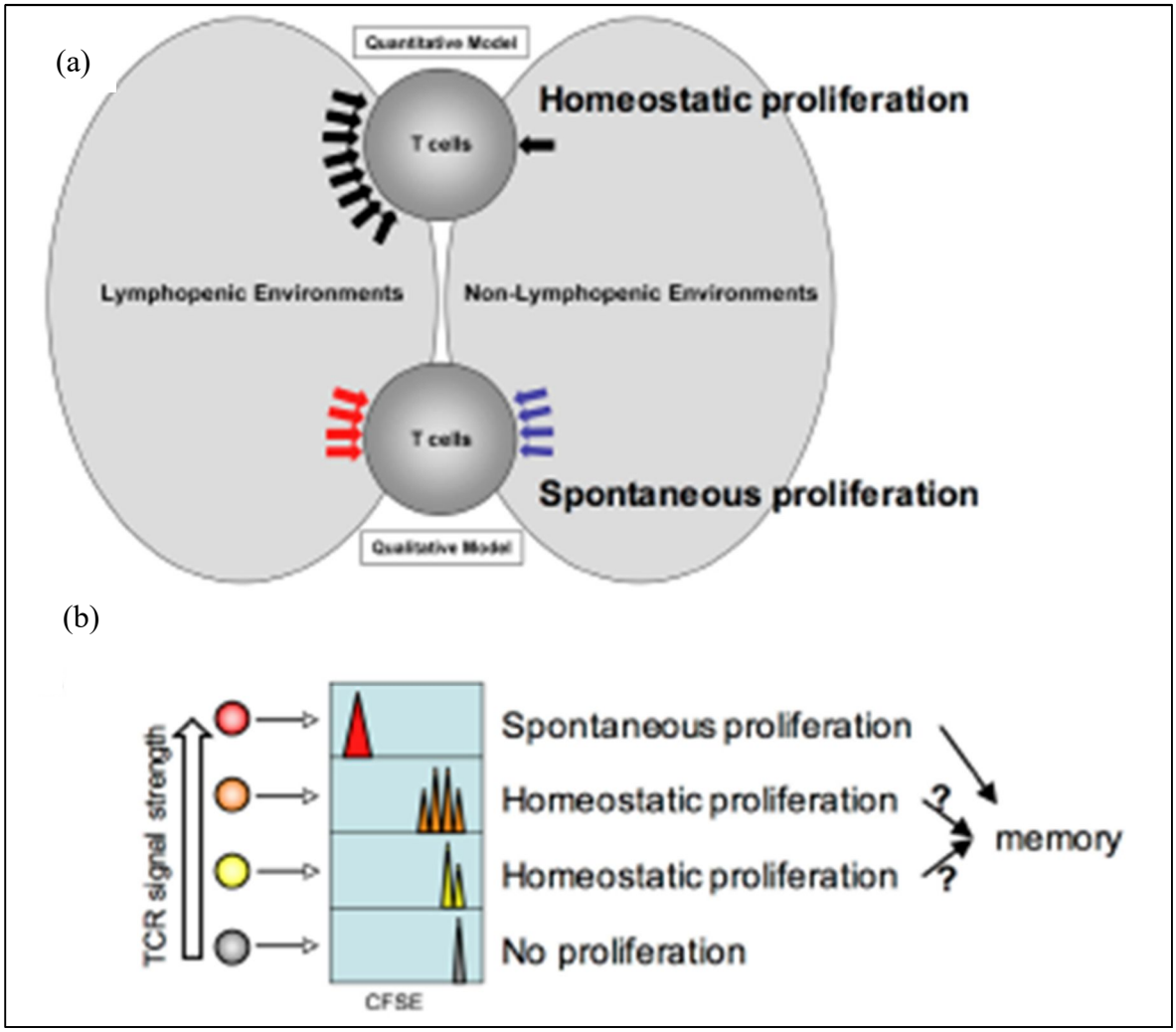

Figure 1: Model for homeostatic and spontaneous proliferation. Quantitative and qualitative signalling model. (a) The model depicts potential signalling mechanisms during homeostatic and spontaneous proliferation. Homeostatic proliferation is triggered by excessive soluble resources available under lymphopenic environments. In contrast, spontaneous proliferation is triggered by different types of signalling mechanism only available under lymphopenic conditions. (b) Relative T-cell receptor signal strength against self-MHC:peptide determines which T cells undergo lymphopenia-induced (spontaneous) proliferation *vs* homeostatic proliferation. Higher the TCR signal strength is, the more likely T cells undergo spontaneous proliferation. Adapted from Min *et al*., 2018.

1.3.2 TCR signalling

Adaptive immunity represents a system of intercellular communication mediated by soluble molecules, where two cells can transmit signals through membrane-associated receptors and

ligands. Typically, during an adaptive immune response, the major histocompatibility complex (MHC) protein on the surface of antigen-presenting cells interacts with the TCR on T lymphocytes initiating TCR signalling.

The antigen specificity of T-cell is defined by its TCR, which acts as an antigen detector. The interaction between TCR and peptide-bound MHC of the right complementarity results in tyrosine phosphorylation of the TCR (referred to as TCR "triggering") and the initiation of signals that activate the T-cell. Adhesion molecules stabilise this immunological synapse, and costimulatory pathways must also be triggered to deliver co-ordinated signals to the nucleus of the T cell, resulting in effective activation. The most important of these being binding of CD28 on the T-cell by CD80/86 on the target antigen presenting cell, although several other possible costimulatory pathways that can substitute for CD28. Although TCR is sufficient for pMHC recognition, the associated invariant CD3 and zeta chains are required for signalling to occur. The cytoplasmic domains of CD3 and zeta chains contain sequence motifs called immunoreceptor tyrosine-based activation motif (ITAMs).

The TCR has no intrinsic kinase activity, unlike many other receptors, and instead relies upon on a T-cell specific kinase called Lck. Also distinct from other systems, the phosphorylatable tyrosine residues of the TCR (the ITAMs) do not reside on the polypeptides that contact the pMHC (α, β) but instead are contained on tightly associated CD3 subunits (γ, δ, ε_2, ζ_2).

On pMHC binding to the TCR, the kinase Lck is recruited to the TCR complex by the colocalization of CD4 or CD8 coreceptors to pMHC molecules where Lck can phosphorylate ITAM signalling motifs. ITAM motifs each contain two tyrosines that, when phosphorylated, create binding sites for the tandem SH2 domains of the Zap70 kinase. The phosphorylated ITAMs then bind a second kinase, ZAP70, which is subsequently activated and drives downstream signalling.

Before TCR engagement, Zap70 predominately resides in the cytoplasm where it is autoinhibited. By binding to phosphorylated ITAMs, Zap70 is recruited to the plasma

membrane and its autoinhibited conformation is disrupted. The active conformation of Zap70 is further stabilized through phosphorylation of its interdomain linker and activation loop by Lck.

Following ligation of the TCR, several phosphatases are activated and initiate signalling through four main pathways. With help from the CD45 molecule, the Src family kinases Lck and Fyn dephosphorylate ZAP-70 and Syk. Once recruited and activated, Zap70 is then able to propagate signalling events from the TCR. Specifically, Zap70 phosphorylates the linker for activation of T cells (LAT), which serves as a signalling hub (Balgopalan *et al*., 2010; Wange *et al*., 2000) leading to activation of phospholipase Cγ1 (PLCγ1). This results in hydrolysis of Phosphatidylinositol-5,4-bisphosphate (PIP2) to diacyl glycerol (DAG) and inositol phosphate3 (IP3), simultaneously activating three pathways: the Ras pathway, resulting in Erk translocation to the nucleus, protein kinase C θ (PKCθ) activation initiates the NFκB pathway (nuclear factor kappa light chain enhancer of activated B cells), and the Calmodulin/Calcineurin pathway activating the nuclear factor of activated T cells (NFAT).

In contrast to IP3, DAG remains in the plasma membrane where it activates protein kinase C (PKC) and RasGRP, which can activate Ras. In addition, recruitment of SOS to LAT via Grb2 results in the activation of the RAS pathway. The combined actions of RasGRP and SOS lead to rapid, bistable amplification of Ras activation. Ras-mediated activation of Raf leads to activation of MEK, and ultimately the MAP kinase ERK (Das *et al*., 2009). The MAP kinases respond to diverse signalling inputs and activate p38 and Jnk, allowing entry to the nucleus and the presence of activated Fos and Jun. Binding of CD28 leads to activation of PIP3, which in conjunction with PKCθ (activated by DAG), leads to activation and translocation of NFκB (Aringer *et al*., 2002). Thus, complex signalling pathways and network regulate T-cell activation (Smith-Garvin *et al*., 2009). T cell activation remains under continued investigation, however a simplified illustration of the understanding of these pathways to date in shown in Figure 2.

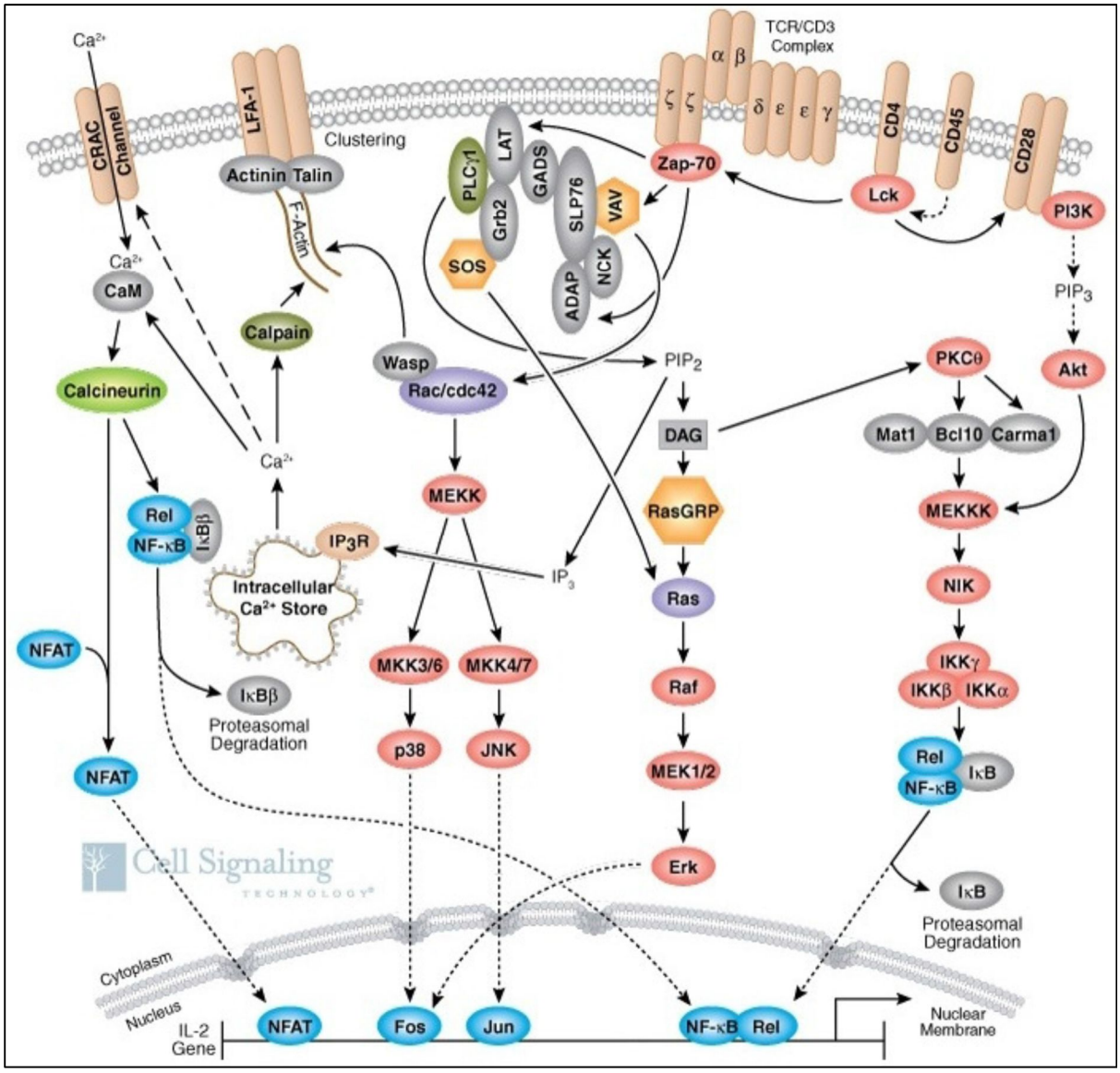

Figure 2: Illustration of T cell receptor signal pathways. From Cell Signalling Technologies (http://www.cellsignal.com/reference/pathway/T_Cell_Receptor.html)

1.4 T-cell differentiation

1.4.1 Models of T-cell differentiation

T-cell differentiation is still being understood (Ganusov *et al*., 2007). Currently, there are 3 models of T-cell differentiation – 1) stem cell associated differentiation 2) linear differentiation and 3) progressive differentiation.

Stem cell differentiation model – In this model, during expansion phase, memory "stem" cells divide and differentiate into nondividing activated effectors. During the contraction phase, effectors die.

Linear differentiation model - In this model, during the expansion phase, activated cells proliferate and become effectors. During the contraction phase, some activated cells (having phenotype of effector cells) die and others differentiate into memory cells.

Progressive differentiation model – In this model, activated cells proliferate during the expansion phase and progressively differentiate from naïve to memory to effectors. During the contraction phase, activated effectors die and are survived by memory cells.

1.4.2 Phenotypic classification of T cells

Although, the mechanisms of T-cell differentiation is less understood, T-cell phenotypic classification is better understood. Using four markers i.e. CD45RA, CCR7, CD27 and CD28, CD4+ T cells can be classified in to naïve, central memory, Th0 effector memory, Th2 effector memory and Th1 or Th2 effector T cells (Okada *et al*., 2008) [Figure 3].

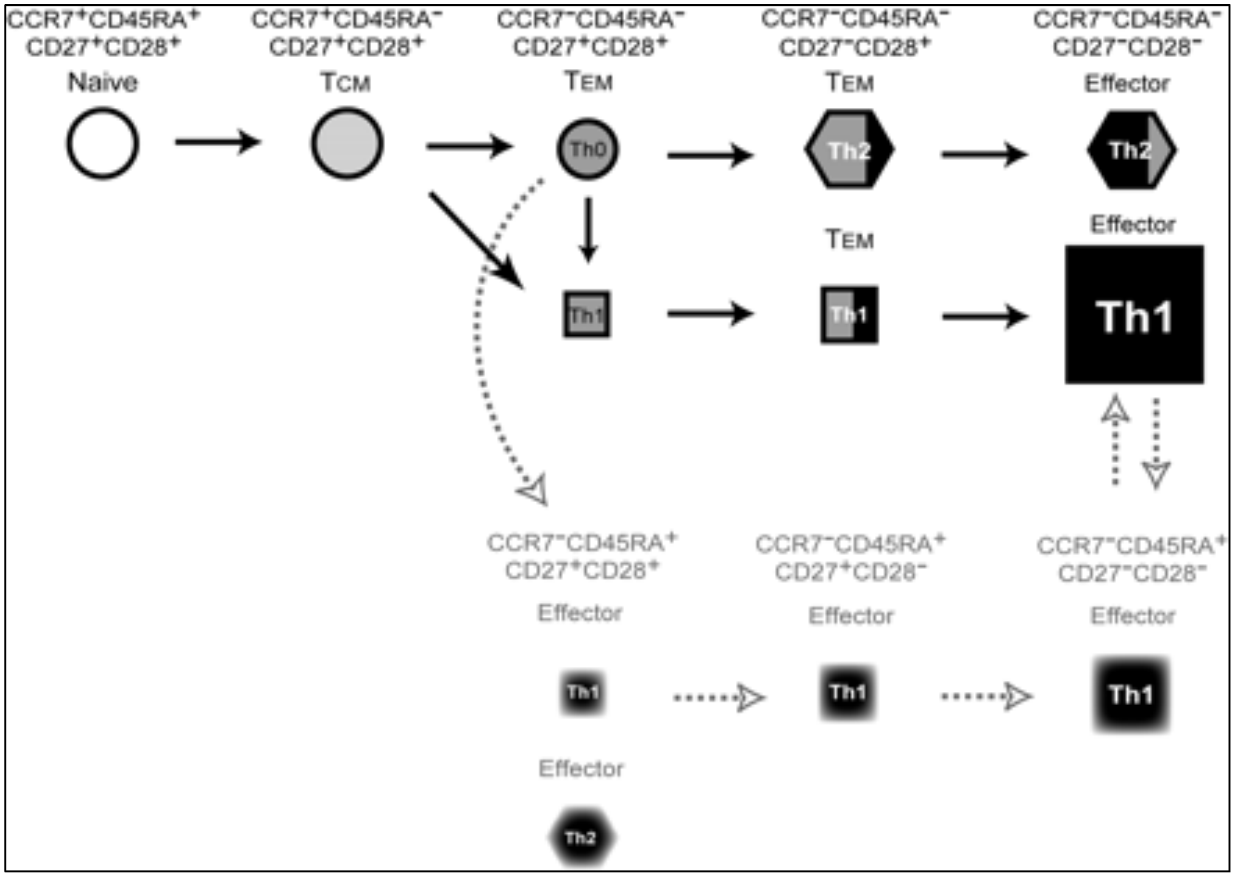

Figure 3: Differentiation pathway of human $CD4^+$ T cells. (TCM=central memory, TEM=effector memory) Adapted from Okada *et al*., 2008.

1.5 Cord blood transplantation

The first successful HLA-identical, sibling cord blood transplant for Fanconi anaemia was performed in 1988 (Gluckman *et al.,* 1989), and provided proof-of-concept for the feasibility of cord blood transplantation (CBT). Following this success, the development of cord blood banks for related and unrelated transplants started in Paris, Dusseldorf, New York, and Milan, The first unrelated cord blood transplant was performed in 1993 (Kurtzberg *et al.,* 1993). The success of these cord blood transplants prompted the development of the Eurocord Netcord network. It was soon realized that cord blood was less HLA-restricted, and hence led to less GvHD compared to adult stem cell sources, but with comparable long-term leukaemia free survival in both children and adults (Rubinstein *et al.,* 1998; Rocha *et al.,* 2000; Rocha, *et al.,* 2001; Barker *et al.,* 2015; Ponce, *et al.,* 2015). The low cell dose in cord blood grafts led to a high incidence of graft failures in adults, but this was significantly reduced by using double cords to increase the cell dose (Barker *et al.,* 2005). The cord blood grafts were also observed to mediate a distinct immunological reaction in the form of an increased incidence of engraftment syndrome (Kanda *et al.,* 2013; Park *et al.,* 2013; Patel *et al.,* 2010). Thus, the propensity to mediate an engraftment syndrome yet with low incidence of GvHD, and with comparable rates of long-term leukaemia-free survival, suggested that there might be significant differences in the properties of T cells contained within cord blood grafts and bone marrow grafts.

1.5.1 Differences in graft composition - cord blood *vs* adult sources

Compared with stem cells from adult sources (bone marrow or peripheral blood), cord blood is a distinct source because of the following seven reasons: (1) cord blood contains one log lower $CD34^+$ cells compared to an adult source (Table 1); (2) cord blood has one log lower T cells compared to an adult source (Table 1); (3) the majority of T cells in cord blood are undifferentiated naïve T cells, compared with a mixture of naïve, memory, and effector T cells in bone marrow and peripheral blood stem cell grafts (De Waele *et al.,* 1988; Zhao *et al.,* 2002); (4) cord blood lymphocytes have been shown to have reduced expression of transcription factors associated with T-cell activation (Kaminski *et al.,* 2003); (5) cord blood lymphocytes have a diminished ability to secrete cytokines (Nitsche, *et al.,* 2007); (6) cord blood T cells are skewed towards a Th2/Tc2 phenotype (Marchant *et al.,* 2005; White *et al.,*

2002); and (7) cord blood dendritic cells have a Th2 bias, associated with lower antigen presenting activity, reduced expression of co-stimulatory molecules, reduced cytokine production, and induction of a Th2 bias (Langrish, *et al.,* 2002).

Cell source	**Target cell dose**	**Median number of $CD34^+$ cells ($x\ 10^6$/kg)**	**Median number of T cells ($x\ 10^6$/kg)**
CB	> 3 x 10^7 TNC/kg	0.2	2.5
BM	> 2 x 10^8 TNC/kg	2-3	25
PBSC	5-10 x 10^6 $CD34^+$/kg	8	250

Table1. Main differences between haematopoietic cell sources (Gluckman *et al.,* 2012)

1.5.2 T-cell deplete cord blood transplantation

As mentioned earlier, *in vivo* T-cell depletion was routinely employed in the context of unrelated bone marrow grafts in Europe, and this practice also extended to unrelated cord blood grafts. In studies of CBT employing *in vivo* T-cell depletion in the conditioning regimen, T-cell reconstitution was delayed (Renard *et al.,* 2011; Niehues *et al.,* 2001). A study by Renard *et al.,* showed that after unrelated CBT, the median time to achieve a $CD4^+$ T-cell count of $0{\cdot}2 \times 10^9$/L and $0{\cdot}5 \times 10^9$/L was five and nine months, respectively. Similarly, $CD8^+$ T-cell count was delayed after *in vivo* T-cell depletion and took approximately eight months to reach a count of 0.25 x 10^9/L. In adult recipients, cord blood grafting with *in vivo* T-cell depletion results in a significant delay in T-cell reconstitution, with a recovery of absolute $CD4^+$ and $CD8^+$ T-cell number after 9 to 12 months. The delayed immune-recovery is often characterized by impaired thymopoiesis and late memory T-cell skewing (Komanduri *et al.,* 2007).

1.5.3 T-cell replete cord blood transplantation

In contrast, following T-cell replete CBT in children, we observed unprecedented $CD4^+$ T-cell

recovery. Two months post-CBT, the median $CD4^+$ T-cell count was $0{\cdot}56 \times 10^9$/L and $CD8^+$ T-cell count was 0.25×10^9/L (Chiesa *et al.,* 2012). Following T-cell replete double cord blood transplantation in adults, the median time to reach a $CD4^+$ T-cell count > $0{\cdot}2 \times 10^9$/L was four months, and six months to reach a $CD8^+$ T-cell count > 0.09×10^9/L (Sauter *et al.,* 2011). In a report comparing practices in two different centres, circulating $CD4^+$ T-cell count was 1 log higher at two months in the no ATG group compared with the group that received ATG (Lindemans *et al.,* 2014).

Within our own centre, we compared the immune-reconstitution following CBT with ATG (n = 7) and without ATG (n = 30). Following CBT without ATG, we found unprecedented recovery of $CD4^+$ T cells, with median $CD3^+/CD4^+/CD8^+$ T cell counts of $840/560/150 \times 10^6$/L at two months, compared to $70/20/20 \times 10^6$/L following conventional CBT incorporating ATG serotherapy [Figure 4].

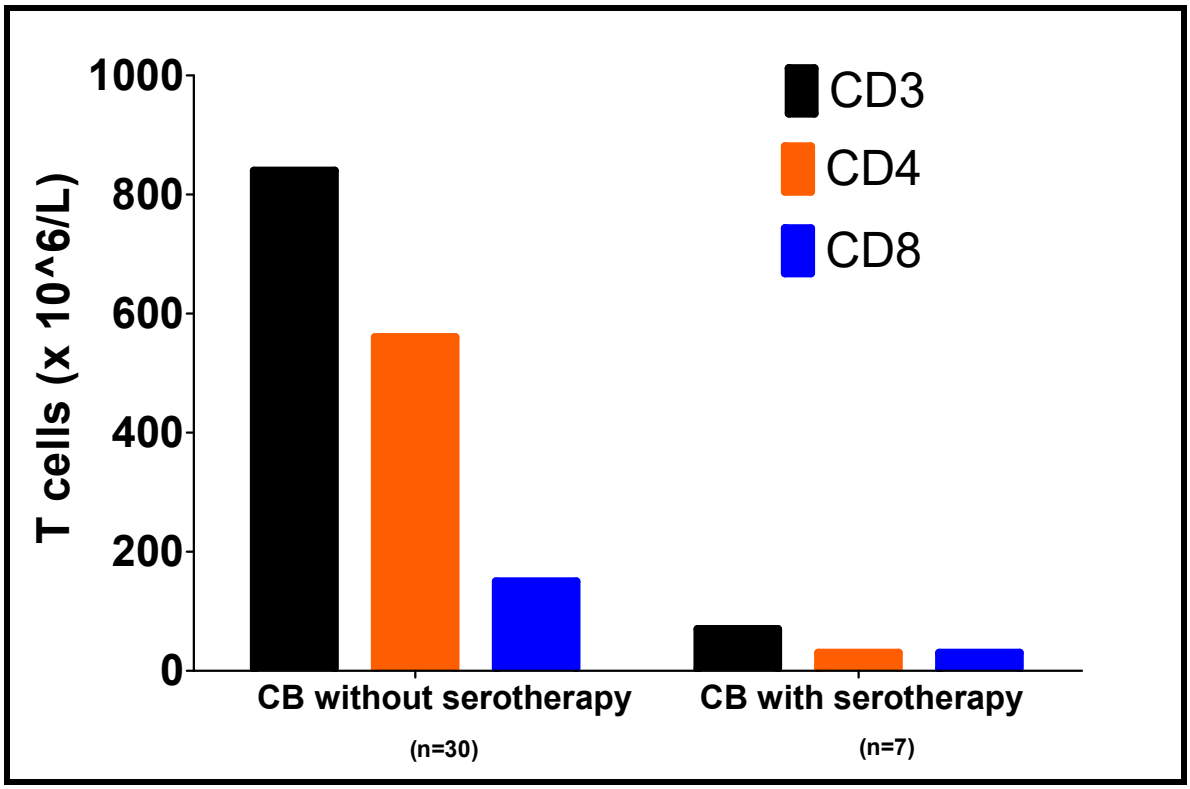

Figure 4: Comparison of immune-reconstitution two months after CBT with and without ATG. Median $CD3^+$, $CD4^+$ and $CD8^+$ T cells are shown. Unprecedented early immune-reconstitution was observed after CBT, when ATG was omitted.

Thus, CBT without *in vivo* T-cell depletion mediates a rapid T-cell reconstitution with a striking asymmetric $CD4^+$ T-cell bias, especially at early time-points. Hence, the characteristic CD4:CD8 inversion observed after adult sources, such as bone marrow and peripheral blood stem cells, is not observed after CBT. Further analysis suggested that this $CD4^+$ T cell expansion after CBT is thymic independent (i.e. in the absence of an increase in T-cell receptor excision circle (TREC) numbers) [Figure 5] and involved a rapid shift from naïve to central memory phenotype (Chiesa *et al.,* 2012). Thus, omission of *in vivo* T-cell depletion promotes a unique thymic-independent $CD4^+$ T cell reconstitution after unrelated CBT in children.

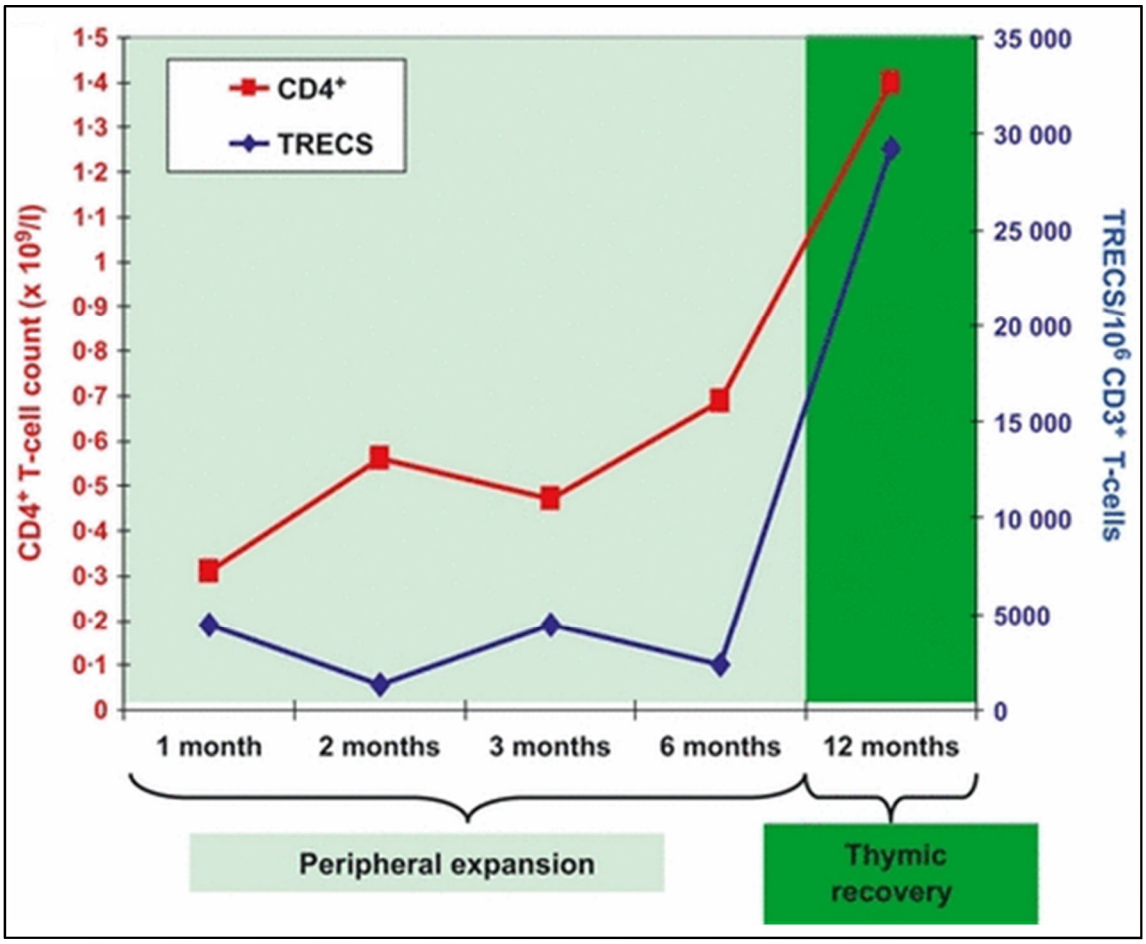

Figure 5: Early CD4+ T-cell expansion is thymic-independent. Median $CD4^+$ T-cell count (red line) and the median number of TRECs (blue line) after CBT are shown. $CD4^+$ T-cell recovery over the first six months after CBT is due to peripheral expansion of the lymphocytes infused with the graft, since TRECs are low during this period. Six months after unrelated CBT, there is a concomitant increase in both $CD4^+$ T cells and TRECs, suggesting a return of thymopoiesis. Figure adapted from Chiesa *et al.,* 2012.

Interestingly, we also noted that the early and rapid T-cell reconstitution also occurred with a

diverse T-cell repertoire. Cord blood $CD4^+$ T cells are enriched in recent thymic emigrants (RTEs) compared to peripheral blood $CD4^+$ T cells (Swainson *et al.,* 2007). This may be the reason for the robust proliferation of cord blood $CD4^+$ T cells. However, using a RAG2p-GFP mouse model, Opiela *et al.,* have shown that RTEs from murine neonates and adults are phenotypically and functionally distinct, and that neonatal, but not adult, RTEs showed early proliferation in response to stimulation with interleukin-7 (IL-7) alone (Opiela *et al.,* 2009). This observation suggests that preferential $CD4^+$ T-cell proliferation may be a property, peculiar to foetal T-cell homeostasis.

It is also important to note that the average CD4/CD8 ratio is 3.9 ± 1.3 in the cord blood, compared to 1.9 ± 0.7 in the adult blood, and this ratio declines gradually with age (Gasparoni *et al.,* 2003; Neubert *et al.,* 1998). Thus, the observation of a $CD4^+$ T-cell biased immune system following CBT, and $CD8^+$ T-cell biased immune system following BMT, coupled with a higher CD4/CD8 ratio in neonates compared to adults, suggests that (1) $CD4^+$ T-cell proliferative and survival mechanisms are significantly up-regulated in cord blood compared to peripheral blood, and (2) the equilibrium of proliferative and survival advantage shifts from $CD4^+$ to $CD8^+$ T cells as the transition from foetal to adult immune system occurs.

1.6 Are cord blood and adult blood T cells distinct?

T-cell reconstitution patterns observed after CBT and BMT indicate that T cells carried with the cord blood and bone marrow graft may be distinct. Here, I have therefore attempted to layout the development of T cells in foetus and phenotypic, functional, and homeostatic differences between cord blood and peripheral blood T cells.

1.6.1 Snapshot of haematopoiesis in the foetus

The first stage of human foetal haematopoiesis occurs in the mesoderm of the yolk sac and the extraembryonic mesenchymal tissue. Pluripotent erythroid and granulo-macrophage progenitors can be detected in the yolk sac at 3 to 4 weeks of gestation. These primitive cells then migrate to the liver and are hence detected in circulation from 4 weeks of gestation. Liver becomes a major site of haematopoiesis from 5 to 6 weeks onwards. From 5 weeks onwards, liver – the key foetal haematopoietic organ, and thymus – the key organ for T-cell development undergo dramatic increase in size. From 12 weeks onward bone marrow starts to develop and gradually becomes the key organ for haematopoiesis [Figure 6].

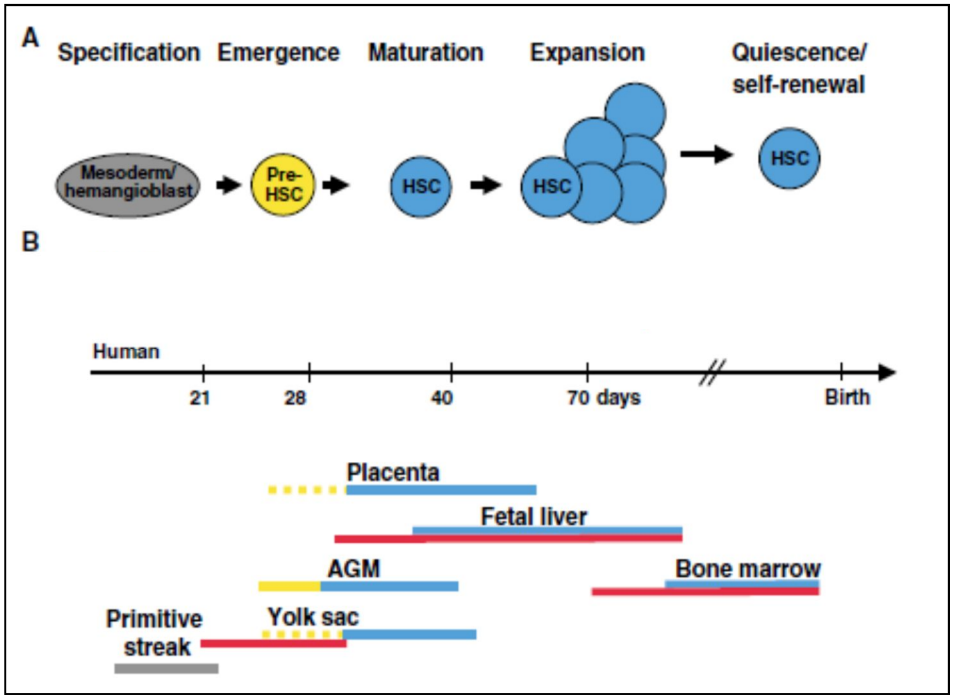

Figure 6: Illustration of establishment of definitive HSC pools in human foetus.

(a) Hematopoietic development starts as primitive streak mesoderm (gray) into hematopoietic and vascular fates. Nascent HSCs undergo a maturation process (blue) that allows them to engraft, survive and self-renew in future hematopoietic niches. Subsequently, foetal HSCs expand rapidly, after which a steady state is established in which HSCs reside in a relatively quiescent state in the bone marrow.

(b) The ages at which human haematopoietic sites are active. Gray bars, mesoderm; red bars, active hematopoietic differentiation; yellow bars, HSC genesis; blue bars, presence of HSCs. Broken yellow bars for yolk sac and placenta indicate that de novo HSC genesis has not been experimentally proven.

AGM – aorto-gonad mesonephros; Adapted from Mikkola *et al*., 2006

The transition of foetal to adult haematopoiesis could be dependent on generation of foetal *vs* adult haematopoietic stem cell from a single precursor or could be related to the environment of haematopoiesis such as liver *vs* bone marrow [Figure 7].

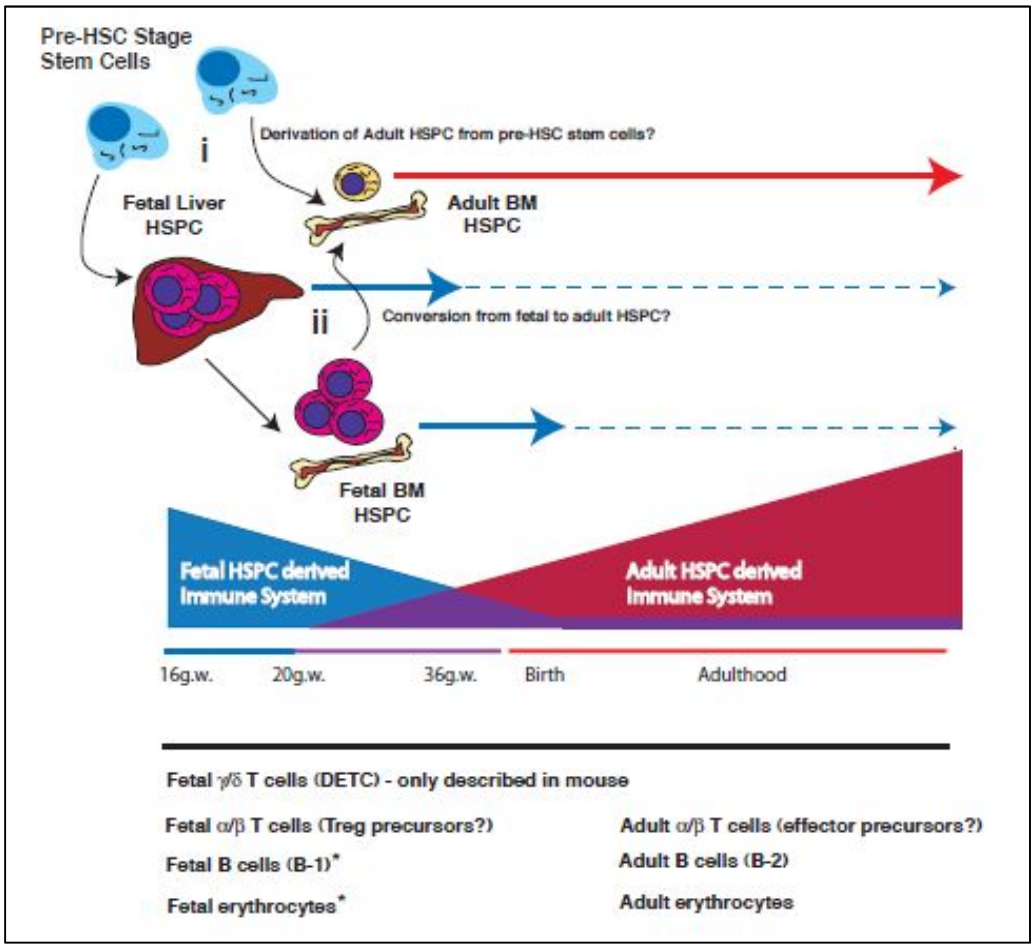

Figure 7: Mold *et al.,* 2010 proposed the model of transition of foetal to adult haematopoiesis. The two proposed theories of switch from foetal to adult haematopoiesis and therefore switch from foetal to adult immune system are 1) generation of separate i.e. foetal *vs* adult haematopoietic stem cells from a single precursor population 2) a transition from foetal to adult haematopoiesis may be related to environment in which they reside for eg. liver *vs* bone marrow. Adapted from Mold *et al*., 2010.

1.6.2 T-cell development in the foetus

7 to 10 weeks

T-cell progenitors can be identified in the foetal liver from 7 weeks of gestation (Haynes *et al*., 1989). These are highly proliferative cells positive for CD7, CD45, and cytoplasmic CD3, without surface CD3, TCR β chain, or terminal deoxynucleotidyl transferase (TdT is involved in diversification of the DJ region of Ig heavy chain and the TCR).

Initially the T-cell precursors are not TCR δ or β positive. Rearranged TCR δ genes are seen in

the liver and primitive gut between 6 and 9 weeks of gestation prior to being detectable in the thymus (McVay *et al*., 1998). T-cell precursors start seeding the thymus at 8 to 9 weeks of gestation. TCR β cells are detected from 9 to 10 weeks of gestation and percentage of these cells increase to form over 90% of the CD7+ population at birth (Campana *et al*., 1989).

10 to 18 weeks

T-cell progenitors with surface CD3 are detected after week 10 of gestation (Haynes *et al*., 1988; Haynes *et al*., 1989). Foetal gastrointestinal tract is most likely to be the site of extrathymic differentiation of T cells, as has been demonstrated in the mouse (Fichtelius *et al*., 1967). Human foetal intestinal mucosa has T cells detectable in the lamina propria and epithelium from 12 to 14 weeks of gestation (Spencer *et al*., 1986). T cells in foetal ileum epithelium are mostly CD8+, and many of these express CD8αα. Almost half of the CD8+ T cells in the lamina propria are also CD8αα. Peyer's patches start to develop between 16 to 19 weeks, and unlike dominance of CD8αα T cells in the lamina propria and epithelium, CD8αβ T cells predominate in the Peyer's patches (Latthe *et al*., 1994).

18 to 24 weeks

T cells from 18 weeks of gestation are most studied because of access to the circulating T cells in the foetus, pre-term and term neonates. The peripheral compartment is populated with single positive CD4+ and CD8+ mature T cells from second trimester on onwards. More than 90% of circulating T cells are CD45RA+ naïve T cells from 18-week onwards. The mesenteric lymph nodes are also populated with high percentage of CD45RA+ naïve T cells but very few B cells or monocytes and the foetal spleen has equal numbers of T cells, B cells and monocytes/macrophages (von Hoegen *et al*., 1995). Interestingly, spleen has relatively higher numbers of CD45RO+ T cells compared to circulating cells, lymph nodes.

Lymph node and thymus T cells at these gestational ages do not proliferate in response to the mitogen phytohaemagglutinin or anti-CD3 stimulation. In contrast, splenic T cells do proliferate to phytohaemagglutinin and anti-CD3. T cells from foetal spleen have adult levels of CD3, CD4, and CD8, and expressed CD2 and CD11a. Thus, the spleen is considered already fully immunocompetent by 18 weeks of gestation, having sufficient accessory cells to ensure T-cell activation, whereas the mesenteric lymph nodes are deficient in accessory cells

numerically or functionally (von Hoegen *et al*., 1995).

24 weeks to term

Neonatal T cells differ significantly from adult T cells. CD4+ T cells outnumber CD8+ T cells during foetal life. CD4:CD8 ratio is significantly CD4+ T-cell biased during the foetal life with higher frequency of T-regulatory cells. At 25 weeks of gestational age, 12% of CD4+ T cells are T-regulatory cells and at term the frequency of T-regulatory cells is 3% i.e. similar to adults (Michaelsson *et al*., 2006). The foetal exposure to foreign antigens is largely restricted to non-inherited maternal allo-antigens. Hence, the function of early-life T cells is different from adult T cells. For example, foetal naive $CD4^+$ T cells respond strongly to allo-antigens, but they tend to develop towards $Foxp3^+$ $CD25^+$ regulatory T cells (T_{reg}) through the influence of TGF-β (Mold *et al*., 2010), and thus rapidly promote tolerance.

Activation of foetal and neonatal T cells with allo-antigens results in a response that is skewed towards Th2 immunity (Hebek *et al*., 2014). Th2 biased response is also supported by the neonatal dendritic cells and T-cell epigenetics. Very early-life adaptive T-cell immunity is thus characterized by enhanced allogeneic responses with a tolerogenic bias.

In contrast to the conventional αβ T cells that recognize peptide antigens in the context of classical MHC molecules, there are populations of MHC independent innate-like T cells. These include functionally competent γδ TCR-positive T cells and iNKT cells that rapidly produce IFN-γ, mucosal-associated invariant T (MAIT) cells (Leeansyah *et al*., 2014) and the recently described interleukin-8 (CXCL8)-secreting naive T cells (Gibbons *et al*., 2014). MAIT cells develop in the thymus, but their maturation can take place in foetal mucosal tissues before microbial colonization. The CXCL8-producing T cells produce important effector functions in human newborns as they have the potential to activate antimicrobial neutrophils and γδ T cells. They appear to be particularly active at the mucosal barriers of premature and term infants, though their frequency decreases with age. In contrast to adult blood, where the repertoire of γδ TCR is restricted, neonatal blood γδ T cells display a variety of receptor chain combinations that change with gestation (Silva-Santos *et al*., 2012). γδ T cells can produce significant amounts of IFN-γ, after brief polyclonal stimulation, compensating for the immaturity of the more classical Th1-type T-cell response to neonatal infections (Gibbons *et al*., 2009). Thus, the

immune system carried with the cord blood graft is distinct to the immune system carried with related or unrelated peripheral blood or bone marrow graft.

1.6.3 Phenotypic differences in cord blood and adult blood T cells

Peripheral blood T cells comprise approximately 45% $CD4^+$ T cells and 70% $CD8^+$ T cells with a naïve phenotype, whereas more than 90% of cord blood $CD4^+$ and $CD8^+$ T cells have a naïve phenotype (De Waele *et al.,* 1988; Zhao *et al.,* 2002). In cord blood, approx. 80% of these naïve T cells are thymic naïve ($CD31^+$), and the remaining 16 to 18% are central naïve ($CD31^-$). The percentage of thymic naïve $CD31^+$ $CD4^+$ T cells and central naïve $CD31^-$ T cells decreases to 65% and 10%, respectively, towards the end of the first year. This decrease in percentage parallels with the increase in $CD45RA^-CD31^-$ memory T cells (Collier *et al.,* 2015).

Analysis of lymphocyte subsets shows that 0.35 - 9.07% and 1.7 - 7% of T-regulatory cells have been reported in cord blood and peripheral blood, respectively (Kim *et al.,* 2012). Although, T-regulatory content is not dissimilar between cord blood and peripheral blood, the percentage of resting T-regulatory cells, activated T-regulatory cells, and activation-induced FoxP3 T cells gradually increase in the first year of life (Collier *et al.,* 2015). Whereas the increase in resting regulatory T cells is modest, from 4 to 5%, and the increase in activated T-regulatory cells and activation-induced FoxP3 T cells is reported to be significant. Activated T-regulatory cells and activation-induced FoxP3 T cells have been reported to increase from 0.72% to 1.91%, and 0.53% to 2.65% respectively. Thus, these phenotypic differences may have an influence on immune-reconstitution after T-cell replete CBT.

1.6.4 Functional differences between cord blood and adult blood T cells

Components of the naïve immune system carried with the cord blood graft have to undergo memory-effector differentiation and gain functionality. IL-12 secretion and expression of co-stimulatory molecules by antigen-presenting cells (APCs) supports the process of memory-effector differentiation. Neonatal APCs have diminished IL-12 secretion and defective expression of co-stimulatory molecules. These features in neonatal dendritic cells have been reported to play a role in the defective secretion of Th1 cytokines by naïve cord blood $CD4^+$ T cells (Langrish *et al.,* 2002). Although the APCs present in cord blood mediate

a Th2 biased response, the residual host antigen presentation may mediate a Th1 response. In addition, it is well established that cord blood T cells, in particular cord blood $CD4^+$ T cells, have decreased ability to secrete Th1 cytokines compared with peripheral blood $CD4^+$ T cells (Marchant *et al.,* 2005). This is because cord blood $CD4^+$ T cells are hypermethylated at CpG and non-CpG sites within the IFN-γ promoter compared to adult naive T cells, and hence produce lower levels of IFN-γ (White *et al.,* 2002).

This lack of ability to mediate Th1 responses *in vitro* explains why neonates and infants cannot efficiently develop responses to certain vaccines or cannot fight viral infections. In particular, infants develop lower Th1 responses to vaccines, such as hepatitis B, measles, and oral polio vaccine (Ota *et al.,* 2004; Vekemans *et al.,* 2002; Gans *et al.,* 2001). They also develop attenuated responses to CMV, HSV, and HIV infections (Tu *et al.,* 2004; Feeney *et al.,* 2003; Burchett, *et al.,* 1992). Furthermore, the foetal immune system is immunotolerant (Silverstein *et al.,* 1964a; Silverstein *et al.,* 1964b). It is well-established that although cord blood and peripheral blood have similar percentages of T-regulatory cells, a significant proportion of cord blood T cells have a propensity to acquire T-regulatory phenotype in a mixed lymphocyte reaction (Mold *et al.,* 2010).

However, despite the immunotolerant immune system and the lack of ability to mediate Th1 responses *in vitro,* and to vaccines, and viral infections as described above*,* neonates can mount efficient Th1 responses to *Bordetella pertussis* and BCG vaccine, and also develop an adult-like $CD8^+$ response to *Trypanosoma cruzi* infection (Henderson *et al.,* 1997; Tonon *et al.,* 2002; Hermann *et al.,* 2002).

These observations indicate that cord blood T cells can mount efficient antigenic responses under appropriate conditions. Leukaemia-free survival rates following CBT are comparable to adult sources (Wagner, *et al.,* 2014; Brunstein, *et al.,* 2011; Barker, *et al.,* 2015), and we also have observed early CMV-specific and ADV-specific immune responses after T-cell-replete CBT (Chiesa, *et al.,* 2012). Thus, these observations make it important to understand how the early adaptive immune system could mediate anti-leukaemic responses to haematological malignancies after T-cell replete CBT.

1.6.5 T-cell homeostasis in cord blood and adult blood T cells

Three processes drive T-cell expansion following HCT, lymphopenia-induced expansion, antiviral expansion and allo-reactive expansion (Maury *et al.,* 2001). Non-host reactive donor T cells proliferate in response to lymphopenic space and homeostatic signals, and thus contribute to a beneficial T-cell peripheral reconstitution. In contrast, host reactive donor T cells proliferate in response to allo-antigens, causing GvHD and virus-specific T cells expansion occurs in response to viral reactivation.

Lymphopenia-induced expansion is predominantly dependent on MHC class I and II and/or cytokines (Tan *et al.,* 2001; Seddon *et al.,* 2002; Kieper *et al.,* 2004). Allo-reactive expansion depends on the recognition of MHC/antigen complex by the T-cell receptor, and subsequent engagement of co-stimulatory molecules and clonal expansion of T cells. The most well characterized co-stimulatory molecule is the CD28/B7 family (Acuto *et al.,* 2003), however, the role of several members of the tumour-necrosis factor receptor (TNFR) superfamily - OX40, CD40, 4-1BB, CD27, CD30, and HVEM (herpes-virus entry mediator) - in providing co-stimulation that is distinct to that of CD28/B7 has also been recognized (Croft *et al.,* 2003). The allo-reactive expansion is largely inhibited with immunosuppression following HCT, and homeostatic expansion is thought to be the primary mechanism of replenishing the lymphopenic environment.

In the lymphopenic and lymphoreplete environment, $CD4^+$ and $CD8^+$ T cells compete for proliferation and survival (Butz *et al.,* 1998; Kedl *et al.,* 2000; Kedl *et al.,* 2002) [Figure 8]. It has been suggested that $CD8^+$ T cells are better competitors than $CD4^+$ T cells, hence, $CD8^+$ T cells have a proliferative and survival advantage over $CD4^+$ T cells (Bender *et al.,* 1999; Ernst *et al.,* 1999; Ferriera *et al.,* 2000). This may also be because the homeostatic expansion of $CD8^+$ T cells (but not $CD4^+$ T cells) can occur outside of the normal secondary lymphoid organs (Dai *et al.,* 2001). It has also been suggested that dendritic cell-secreted IL-7, rather than stromal-secreted IL-7 controls $CD4^+$ T-cell proliferation (Saini *et al.,* 2009; Guimond *et al.,* 2009; Martin *et al.,* 2010; Kaye *et al.,* 2009). These findings indicate that $CD4^+$ T cells have a more stringent requirement, such as lymphoid APCs, compared to $CD8^+$ T cells, which may contribute to the control of $CD4^+$ and $CD8^+$ T-cell expansion.

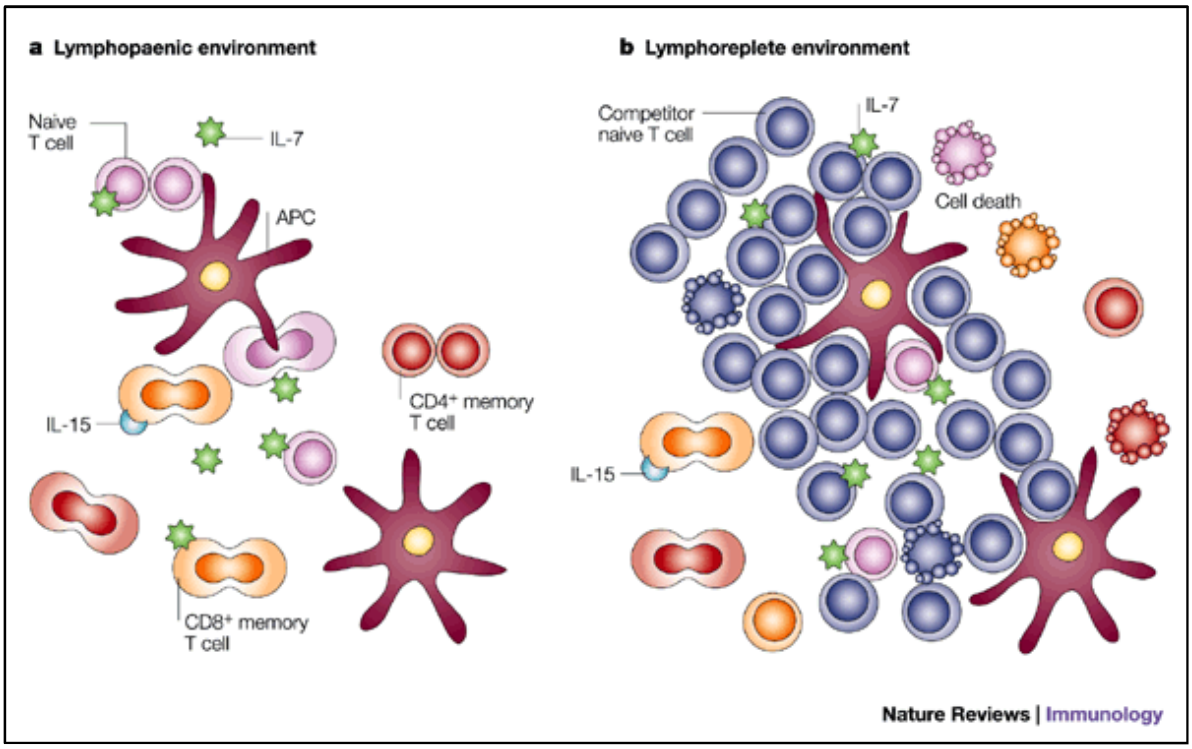

Figure 8: Naive and memory T cells in lymphopenic versus normal (lympho-replete) environments. (a) In the lymphopenic host, naive T cells have increased access to IL-7 and self-MHC molecules on APCs, which allows the cells to homeostatically proliferate. (b) In the lympho-replete host, the presence of competitor naive T cells restrains clonal expansion and limits survival by competing for these resources. Memory $CD8^+$ T cells can proliferate in response to IL-15 or IL-7, but competition with naive T cells limits access to IL-7 in lympho-replete hosts. Figure adapted from Jameson *et al*., 2002.

The rapid $CD4^+$ T-cell biased peripheral expansion after T-cell-replete CBT, but relatively delayed $CD8^+$ T-cell biased expansion after T-cell-replete BMT, indicates that the cord blood and peripheral blood T cells may have distinct interactions with APCs and/or cytokines during lymphopenia-induced proliferation. It has been reported that compared to peripheral blood, cord blood $CD4^+$ and $CD8^+$ T cells are explicitly responsive to IL-7, and cord blood $CD8^+$ T cells are selectively responsive to IL-15 (Schonland *et al.,* 2003). Similarly, cord blood T cells are in a state of high proliferative turn over despite retaining a naïve (resting) phenotype. In addition, there are 10-fold higher Ki67-expressing naïve T cells in the cord blood, than in the peripheral blood (Schonland *et al.,* 2003).

Since naïve T cells require both MHC and IL-7 for homeostatic expansion, how do these two signals co-operate to keep naïve cord blood T cells in a state of high proliferative turn over? It is well-established that there is a co-ordinated network between these two pathways. The

ligation of IL7R increases the expression of TCR co-receptors, and thus, allows TCR to signal when bound to MHC self-ligands. The TCR signal blocks the IL-7 signal, down-regulating the TCR co-receptors, and allowing T cells to respond to IL-7 again (Takada *et al.,* 2009; Surh *et al.,* 2008; Sprent *et al.,* 2011; Seddon *et al.,* 2003; Goldrath *et al.,* 1999; Tscheltzoff *et al.,* 2013). Using T cells from normal mice and 7RTg mice, researchers recently showed that normal T cells grow in TCR sufficient conditions but failed to grow in TCR deficient mice. However, T cells from 7RTg mice did proliferate in both TCR sufficient and deficient conditions, although fewer T cells were isolated from the TCR deficient animals. Thus, it was concluded that IL-7 can promote T-cell proliferation but fails to promote survival in the absence of a TCR signal. They further showed that in 7RTg cells, continuous exposure of IL-7 initially led to proliferation, followed by IFN-γ induced cell death, and intermittent exposure of IL-7 maintained naïve $CD8^+$ T cells in a quiescent state, without proliferation. It was further shown that the stronger the TCR signal, the more IL-7 signal was interrupted, and the more cells survived. Therefore, it appears that the TCR mediated interruption of IL-7 signalling is required for the survival of T cells *in vivo* (Kimura *et al.,* 2013).

Given the complex interplay between the TCR and IL-7 signalling pathways to maintain T-cell homeostasis, and the distinct feature of early T-cell immune-reconstitution after T-cell-replete CBT and BMT, it is likely that the distinct regulation of these homeostatic pathways during the developing immune system may endow cord blood T cells with the enhanced ability to reconstitute in a lymphopenic environment, such as following CBT.

1.6.6 The foetal *versus* adult adaptive immune system

The phenotypic differences between cord blood and peripheral blood T cells are a result of the immune system being at different stages of maturation. Cord blood T cells are predominantly undifferentiated naïve T cells, whereas peripheral blood T cells are a mixture of naïve, memory, and effector T cells. Thus, the undifferentiated naïve cord blood T cells may proliferate with a CD4 bias, whereas the differentiated immune system proliferates with a CD8 bias because of the relatively enhanced proliferative capability of memory $CD8^+$ T cells, compared with memory $CD4^+$ T cells. However, the functional differences, such as the ability to secrete cytokines and distinct T-cell homeostasis - in particular, the rapid kinetics of immune-reconstitution after CBT, despite one log lower T cells carried with a cord blood graft, compared to an adult graft source may indicate the

influence of foetal ontogeny. The evidence of two distinct lymphoid systems derived from foetal and adult haematopoietic stem cells is increasing (Mold *et al.,* 2010; Copley *et al.,* 2013), a so-called a layered immune system, similar to that of avian and murine species (Morrison *et al.,* 1995; Zanjani *et al.,* 1993; Harrison *et al.,* 1997; Ikuta *et al.,* 1990; Montecino-Rodriguez *et al.,* 2006; Havran *et al.,* 1988). It has been shown that the Lin28b-let7 axis determines the self-renewal potential of HSCs, and upregulation of Lin28b in adult HSCs mediates a foetal-like erythroid and lymphoid differentiation (Copley *et al.,* 2013; Yuan *et al.,* 2012; Lee *et al.,* 2013). These findings suggest that the physiological demands of the foetal-stage haematopoietic system are met by Lin28b upregulated HSCs. Foetal lymphopoiesis derived from Lin28b upregulated HSCs is therefore likely to be distinct to adult lymphopoiesis that is influenced by let-7 miRNA biogenesis. Foetal lymphocytes may be endowed with the ability to rapidly repopulate the lymphopenic environment of the foetus. It is possible that a significant population of cord blood T cells may be derived from Lin28b upregulated foetal HSCs and could retain the property of foetal ontogenesis. Hence, it is also possible that the rapidly repopulating lymphoid systems after T-cell replete cord blood transplantation could also mediate distinct immunological effects.

1.7 Graft-versus-Leukaemia effect

An immune response mediated by allogeneic cells to suppress residual leukaemia is termed as graft-versus-leukaemia effect. The rationale for using allogeneic transplantation to cure leukaemia is based upon the following observations.

1. The risk of leukaemic relapse is associated with the absence of alloreactivity. For example, there is increased risk of relapse after syngeneic transplant, and after T-cell depleted BMT (Gale *et al.,* 1994; Apperley *et al.,* 1888; Marmont *et al.,* 1991; Goldman *et al.,* 1988).

2. An association between GvHD and risk of relapse is well-known; patients who get GvHD have an increased chance of leukaemia-free survival (Weiden *et al.,* 1979 and 1981).

3. Donor lymphocyte infusions for leukaemia relapse, following allogeneic stem cell transplant, can mediate an anti-leukaemic effect, especially in chronic myeloid leukaemia and juvenile myelomonocytic leukaemia (Levine *et al.,* 2002; Yan *et al.,* 2012).

4. Withdrawal of immunosuppression can sometimes reinduce remission especially in patients with relapsing chronic myeloid leukaemia (Elmaagacli *et al.,* 1999; Mehta *et al.,* 1996).

Donor lymphocyte infusion is less effective in other haematological malignancies, such as acute myeloid leukaemia (AML), myelodysplasia, myeloma, Hodgkin's lymphoma, chronic lymphocytic leukaemia (CLL), and Philadelphia positive acute lymphoblastic leukaemia. Thus the GvL effect depends upon the type of leukaemia, the burden of leukaemia, and the potential for alloreactivity.

1.7.1 Mechanisms of the GvL effect

The cell populations capable of recognizing and killing malignant targets are: T cells and natural killer cells. T cells mediate the GvL effect in an HLA-restricted manner, and it is thought that T cells mediate the GvL effect in three ways:

1) Direct killing by cytotoxic lymphocytes ($CD4^+$, $CD8^+$, and NK cells) via perforin and granyzymes (Kagi *et al.,* 1994).

2) Apoptotic death, induced by cytotoxic lymphocytes ($CD4^+$ and $CD8^+$ T cells) via the Fas/Fas ligand pathway (Kagi *et al.,* 1994).

3) Cytokine-mediated leukaemia cell death (e.g. IFN-γ, TNF-α), or control of proliferation by $CD4^+$ T cells; (Susskind *et al.,* 1996).

$CD4^+$ T cells are now thought to play a dual role as orchestrators and effectors in the GvL response (Barrett *et al.,* 1997) [Figure 9]. $CD4^+$ T cells are central to immune system function, and $CD4^+$ helper T-cell activity is crucial for promoting $CD8^+$ T-cell and NK cell activity. Both $CD8^+$ T cells and NK cells have been implicated in the GvL effect following CBT.

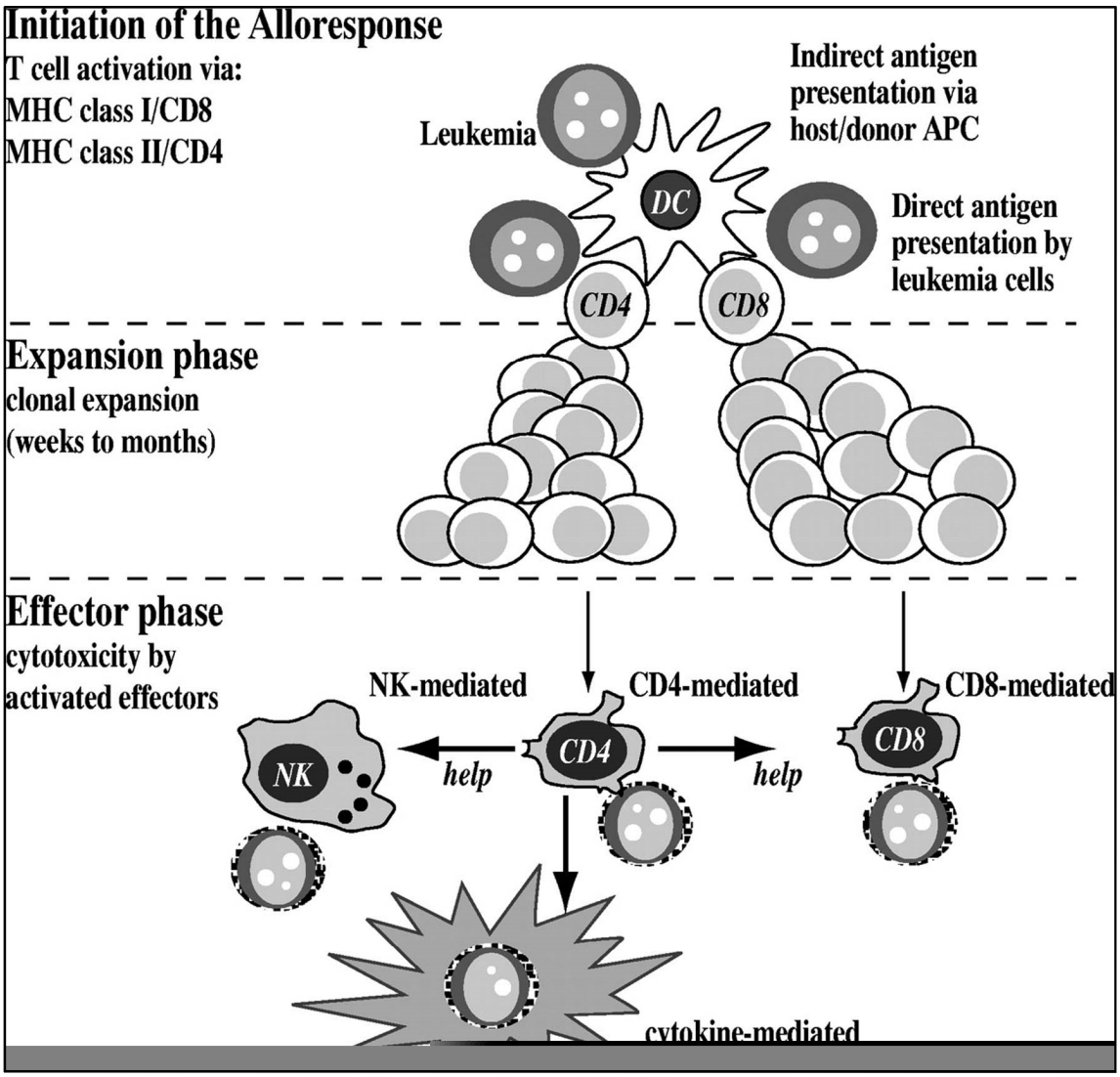

Figure 9: A three phase model of the GvL response. $CD4^+$ T cells have dual roles, as orchestrators and effectors. Figure adapted from Barrett *et al.,* 1997

Cytotoxic $CD8^+$ T cells have been shown to be responsible for single unit predominance following double CBT (Gutman *et al.,* 2010). As early as 28 days following a double CBT,

$CD8^+$ T cells from the winning cord exhibits cytotoxicity against targets from the losing cord. There is also increasing evidence, both in animal (Xie Y *et al.,* 2010; Quezada SA *et al.,* 2010) and clinical studies (Hunder *et al.,* 2008*),* for the direct anti-tumour effects of $CD4^+$ T cells. Furthermore, in clinical studies of chronic myeloid leukaemia, it has been demonstrated that $CD4^+$ donor lymphocyte infusions (DLI), to treat CML relapse after HCT have induced durable remissions (Shimoni *et al.,* 2001). More elaborate studies, however, have shown that $CD4^+$ lymphocyte infusions led to the expansion of $CD8^+$ donor T cells, inducing their cytotoxic activity (Zorn *et al.,* 2002). Another recent study has also demonstrated that the response to $CD4^+$ DLI is predicted by the percentage of pre-DLI bone marrow $CD8^+$ T-cell infiltrates (Bachireddy *et al.,* 2014). These observations indicate that although cytotoxic T cells mediate an effector response, $CD4^+$ T cells play a crucial role in orchestrating an immune response against recipient malignant cells.

1.7.2 Targets for the GvL effect

Cytotoxic T cells (CTLs) recognize recipient haematopoietic and malignant cells as foreign. Donor CTL responses against the recipient leukaemic cells are directed against five broad classes of antigen, (1) major histocompatibility antigens, (2) minor histocompatibility antigens, (3) tumour associated antigens, (4) viral antigens, and (5) killer cell immunoglobulin (KIR)-ligand incompatibility

1) Major histocompatibility antigens

Cord blood grafts pose a lower risk and severity of chronic GvHD compared to adult grafts (Rubinstein *et al.,* 1998; Rocha *et al.,* 2001). HLA-mismatched CBT is now being recommended for leukaemia in the absence of a matched adult donor (Grewal *et al.,* 2003; Apperley *et al.,* 2012). For the same reason, while adult grafts are increasingly matched for 10 HLA loci (A, B, C, DR, and DQ), cord blood grafts are matched only for six HLA loci (A, B, and DR). Thus, in contrast to unrelated donor BMT, unrelated CBTs are frequently mismatched, so, T cells that recognize ubiquitous antigens presented by mismatched-HLA alleles may play a key role in mediating a GvL effect. This has been indicated by the powerful GvL effect observed after HLA-mismatched CBT (Eapen *et al.,* 2007). Additionally, CBT is increasingly performed without *in vivo* T-cell depletion for treating acute leukemia, and such, a T-cell replete CBT may significantly augment this alloreactive effect (Wagner *et al.,* 2014;

Brunstein, *et al.,* 2011; Barker *et al.,* 2015). One major difference between the alloreactivity mediated by CBT and BMT, is that the incidence of chronic GvHD is significantly lower following CBT, compared to an adult source such as bone marrow or peripheral blood stem cells (Rubistein *et al.,* 1998; Rocha *et al.,* 2001). Thus, T-cell replete CBT may mediate enhanced GvL effects with minimal risk of chronic GvHD.

2) Minor histocompatibility antigens

Another crucial mechanism of the GvL effect is through recognition of mismatched minor histocompatibility antigens. Minor histocompatibility antigens (mHAgs) are highly immunogenic peptides, recognized by T cells in an HLA restricted manner. mHAgs are also highly polymorphic, and hence, incompatibility between the donor and the host allows a strong alloreactive effect.

A well-known example of such an alloreactive effect is GvHD observed in male recipients of an HLA identical graft from the female donors. This effect is due to the recognition of minor antigen (HY), encoded by the Y chromosome. Some mHAgs are present ubiquitously (e.g. HY), and thus, CTLs directed against these antigens will result in GvL and GvHD. Others, such as HA-1 and HA-2, are only present on haematopoietic tissues, and should only elicit GvL responses, although in fact, HA-1 mismatching has been associated with GvHD (Goulmy *et al.,* 1996).

HA-1 and HA-2 are encoded by bi-allelic gene systems, with one being immunogenic, and the other non-immunogenic (Di Terlizzi *et al.,* 2006). The immunogenic peptides encoded by HA-1^{H} and HA-2^{V} are presented on HLA-A2 molecules, which are solely recognized by HLA-A2-restricted CTLs. A GvL effect through HA-1 mismatching is estimated to occur in 10-15% of sibling transplants (Schetelig *et al.,* 2005). After infusion of DLI, following HA-1/HA-2 mismatch transplant, only 33% of CTL clones were specific for HA-1 and HA-2. The other 67% of leukaemia-reactive CTLs were thought to be against a variety of antigens of unknown specificity (Scheteli, *et al.,* 2005), showing that the immune system reacts against a variety of antigens to eradicate leukaemic clones.

3) Tumour associated antigens

Tumour associated antigens are those that are expressed in cancer cells, but at low levels, or not at all, in normal tissue. Whilst considerable effort has been made to identify tumour specific neo-epitopes created by leukaemic fusion genes, such as BCR-ABL, there is little evidence that such epitopes are processed and presented *in vivo,* or that they are significant targets for a GvL response. However, an increasing body of evidence suggests that over expressed tumour-associated antigens may be used as targets to augment GvL responses.

Proteinase 3 is a tumour-associated antigen that is over expressed in both CML and AML. PR1 is an HLA-A2 restricted peptide derived from proteinase 3. PR1-specific CTLs have been shown to kill myeloid leukaemic colonies that over express proteinase 3, but not normal marrow cells (Molldrem *et al.,* 1999). High avidity PR1 CTLs are increased in CML patients who develop cytogenetic remission in response to IFN-α (Schetelig *et al.,* 2005). PR1 CTLs are also found in healthy donors, albeit in low frequency (Rezvani *et al.,* 2003).

Wilm's Tumour Protein (WT1) is another tumour-associated antigen that is over expressed in myeloid malignancies. WT1, a zinc-finger transcription factor, was initially described as a tumour-suppressor gene in childhood Wilms' tumours. It is abundantly over-expressed in most human leukaemia cells, including AML, CML, and ALL, with higher levels associated with a worse prognosis. Leukaemia stem cells express from 10- to >100-fold more WT1 protein than normal $CD34^+$ cells. T cells can distinguish this difference in protein expression because $CD8^+$ CTLs generated against WT1 lyse leukaemic $CD34^+$, but not normal $CD34^+$ cells, and inhibit the growth of leukaemic, but not normal myeloid colonies (Appelbaum *et al.,* 2001). Therefore, like PR3, WT1 might serve as a useful target for adoptive T-cell therapy.

4) Viral antigens

Latent EBV infection is associated with non-Hodgkin's lymphoma, Burkitt's lymphoma, NK cell lymphoma, lymphoproliferative disease, Hodgkin's lymphoma, and nasopharyngeal carcinoma, making adoptive T-cell strategies that target EBV a potential option (Rooney *et al.,* 1998).

5) Killer cell immunoglobulin (KIR) ligand incompatibility

The importance of NK activity in this setting has also been demonstrated by the observation that killer cell immunoglobulin (KIR)-ligand incompatibility in the graft-versus-host direction is associated with reduced relapse incidence, and improved leukaemia and overall survival, after CBT for acute leukaemia (Willemze *et al.,* 2009; Sekine *et al.,* 2016).

1.7.3 GvL in acute lymphoblastic leukaemia

There is very little effect of T-cell depletion on leukaemia-free survival following allogeneic HCT for B-cell acute lymphoblastic leukaemia (ALL) (Veys *et al.,* 2012). Similarly, the response of ALL to DLI is significantly inferior to that of AML (Collins *et al.,* 1997). In the NSG mouse model of ALL, the effect of DLI in suppressing tumour growth only lasted for a few weeks (Nijmeijer *et al.,* 2002). The limited effect of DLI in B-cell ALL is thought to be associated with tolerance induction because of the lack of co-stimulatory molecules (Cardoso *et al.,* 1996). In T-cell ALL, and particularly cutaneous T-cell lymphoma, DLI has been shown to mediate durable responses. Despite DLI having little effect in ALL, the role of GvHD in mediating GvL against both T-cell and B-cell ALL has been observed (Passweg *et al.,* 1998).

1.7.4 GvL in Acute myeloid leukaemia

The effect of T-cell depletion on AML relapse is not as pronounced as CML (Horowitz *et al.,* 1990). This is thought to be because of the pace of the disease itself, and because more than 80% of patients with AML do not express CD86 co-stimulatory molecules (Dermime, *et al.,* 1996). The effect of DLI in AML is significantly inferior compared to CML, and the best results of DLI in relapsed AML are obtained in patients who relapse six months post-transplant (Levine *et al.,* 2002). Although generally, the GvL effect in AML is inferior, foetal-derived cord blood T cells may mediate a distinct GvL effect, compared to peripheral blood T cells. Interestingly, the GvL effect mediated by cord blood T cells was observed in AML, but not in ALL (Admiraal *et al.,* 2016), and very recently in AML with minimal residual disease prior to transplantation (Milano *et al.,* 2016).

1.8 Humanized mouse models of GvL

Immuno-deficient *IL2ry*^{null} mice permits engraftment with many primary tumours (Shultz *et al.,* 2007). Human acute leukemia cells injected in NOD/LtSz-scid/IL-2Rgamma null mice, generate a faster and more efficient leukaemia model, compared to other NOD/scid strains, such as NOD-*scid* β*2m*^{null} mice (Agliano *et al.,* 2008). Hence, NOD/LtSz-scid/IL-2Rgamma null mice have been favoured for studying graft-versus-tumour effects. In these models, primary tumours, such as lung tumours, have been tested to recapitulate *in vivo* tumour characteristics, including maintenance of stroma and conversion of naïve to effector T cells in the tumour microenvironment (Simpson-Abelson *et al.,* 2008). Therefore, we decided to use this triple knock out model for studying potential GvL effects of cord blood T cells.

1.9 Measurement of tumours *in vivo*

Palpation of subcutaneous tumours and/or calliper measurement of accessible lesions were the key methods of assessing tumour progression in early studies of tumour development. More recently, bioluminescent imaging technology has allowed the precise tracking and quantification of xenografted tumour cells.

Bioluminescence refers to the production and emission of light by naturally occurring luciferase enzymes. The light is emitted upon oxidation of luciferin substrates to non-reactive oxyluciferins (Berger *et al.,* 2008). The most widely used luciferase-luciferin system is from the common firefly, *Photinus pyralis* (Chandran *et al.,* 2009). Isolation of firefly luciferase, and purification of the D-luciferin substrate has allowed the application of this technology to scientific research.

Luciferase reporter assay, a technology using *in vitro* reporter genes, has been routinely used for many years, and allows the easy detection through luminometers, due to the low background in biological systems and concurrent low signal-to-noise ratio (Nguyen *et al.,* 1988). The development of sensitive charged coupled device (CCD) cameras, and subsequently the Xenogen IVIS imaging system, has also allowed the application of bioluminescence to *in vivo* systems (Contag *et al.,* 1998). The serial measurement of bioluminescent signal allows a sensitive, non-invasive technique for monitoring tumour progression and regression (Foste *et al.,* 2008).

Bioluminescent imaging has become widely used for *in vivo* monitoring, including application to the EBV-PTLD model. These studies have shown serial tumour monitoring using luciferase transduced LCL, demonstrating progression and regression upon treatment (Foster *et al.,* 2008). These studies have established that bioluminescent imaging does not interfere with the utility of the SCID mouse EBV-PTLD model. We, therefore, used a similar technique to monitor xenografted tumours in our triple knockout mouse model.

1.10 Project aims

- To characterize $CD4^+$ T-cell reconstitution and study the differences in immune-reconstitution after T-cell-replete cord blood and bone marrow transplantation.

- To study the role of homeostatic signals in cord blood $CD4^+$ T-cell proliferation.

- To investigate the role of foetal ontogeny in rapid $CD4^+$ T-cell reconstitution after T-cell-replete CBT and explore the underlying mechanisms.

- To establish a tumour model for comparing the GvL effect mediated by rapidly reconstituting cord blood T cells and dissect the underlying immune mechanisms.

Chapter two

Materials and Methods

2.1 Materials

2.1.1 Reagents

General reagents and enzymes:

Cyclosporin A (Sandimmune)	478941 Sandoz Pharmaceuticals
D-Luciferin - K+ Salt	122796 Perkin Elmer
Ficoll-Paque PLUS	17-1440-02 Amersham Biosciences
Matrigel HESC Matrix 5ml	354277 Beckton Dickinson
Recombinant human IL-2	200-02 Peprotech
Recombinant human IL-7	200-07 Peprotech
Recombinant human IL-15	200-15 Peprotech
AP-1 inhibitor (SR 11302)	2476/10 Tocris Bioscience
CellTrace CFSE Cell Proliferation Kit	C34554 Invitrogen
Penicillin-Streptomycin, liquid	15140122 ThermoFisher scientific
Red cell Lysis Buffer	00-4333 EBioscience
Retronectin	T100B TaKara
PMA	V1171 Promega
Ionomycin	0215961101 ThermoFisher scientific
GolgiPlug™ (containing brefeldin A)	555029, BD

Tissue culture media and supplements:

Medium	Supplements
Foetal Bovine Serum (Sigma F7524)	
Complete RPMI (Invitrogen 61870-010)	10% FBS, 100U/ml penicillin, 100µg/ml streptomycin
2x freezing medium	60% FBS, 20% DMSO (Sigma D2650), 20% complete RPMI
AIM V (Invitrogen 12055- 091)	No additions

2.1.2 Buffers and solutions

All buffers and solutions were prepared in double distilled water (ddH20), sterile solutions were prepared in ddH20, autoclaved for 15 minutes at 121^{O}C or sterile filtered through a 0.22.im filter. Composition of buffers and solutions is listed below.

Buffer	**Ingredients**
Flow Cytometry staining buffer (FACS buffer)	PBS, 0.5% FBS
Flow cytometry fixing buffer (FACS fixing buffer)	FACS buffer + 0.5% Paraformaldehyde (Sigma 441244)
Fixation buffer	No additions (BD Cytofix 554655)
PhosFlow Perm Buffer III	No additions (BD 558050)
FoxP3 Staining Buffer set	No additions (eBioscience 00-5523)

2.1.3 Kits

Human IL-7 Ultra-Sensitive Kit	K151AMC-1 Meso Scale discovery
Human Th1/Th2/Th17 Phenotyping Kit	560751 BD Pharmigen

2.1.4 Magnetic selection beads (Milteyni)

CD3 microbeads human, 130-050-101

CD45RA microbeads, 130-045-901

CD235a microbeads, 130-050-501

Pan T Cell Isolation Kit II, human 130-091-156

2.1.5 Flow cytometry antibodies

CD8 BV 421 anti-human, BioLegend, 301036

CD8 PE anti-human, BD, 555635

CD4 BV 605 anti-human, BioLegend, 317438

CD4 FITC anti-human, BD, 555346

CD4 PerCP/Cy5.5 anti-human, BioLegend, 344608

CD25 BV 421 anti-human, BioLegend, 302629

CD45 RO PerCP-Cy5.5 anti-human, BioLegend, 304222

FoxP3 APC anti-human, eBioscience, 17-4777-42

CD3 APC/Cy7 anti-human, BioLegend, 300426

CD197 (CCR7) APC anti-human, BioLegend, 353214

CD197 (CCR7) PE antihuman, eBioscience, 12-1979-42

CD45RA APC anti-human, BioLegend, 304112

CD127 FITC anti-human, BD, 561697

MHC Class I FITC anti-human, BD, 557348

HLA-DRB PE anti-human, BD, 557348

CD80 FITC anti-human, BD, 557226

CD86 PE anti-human, BD, 560957

CD83 PE anti-human, BD, 556855

2.1.6 Reagents for RNA isolation

RNase-Free DNase Set (Qiagen 79245) - RNase-free DNase I, RNase-free Buffer RDD, and RNase-free water for 50 RNA minipreps. For DNase digestion during RNA purification.

RNeasy Plus Micro Kit (Qiagen 74034) - For 50 micropreps: RNeasy MinElute Spin Columns, gDNA Eliminator Spin Columns, Collection Tubes, Carrier RNA, RNase-Free Water and Buffers. For purification of total RNA from small cell and tissue samples using gDNA.

2.1.7 Reagents for gene profiling

NuGEN WT-Ovation, NuGEN - 3302-12

QIAquick PCR purification kit, Qiagen - 28104

Ovation RNA Amplification System V2, NuGEN - 3100-12

Affymerix HuGene ST 1.0 arrays

2.1.8 Cell lines

B958 Marmoset cell line releases high titres of EBV. This cell line is used for transforming B-cell lymphocytes from normal donors to lymphoblastoid cell lines

LCL Human lymphoblastoid cell line (EBV-transformed)

Kasumi 1 Human acute myeloid leukaemia t(8;21) cell line

MV4-11 Human biphenotypic B-myelomonocytic leukaemia cell line

THP-1 Human monocytic leukaemia cell line

K562 Human erythroleukaemia cell line

Human cell lines namely LCL, Kasumi 1, MV4-11, THP-1 and K562 were studied for their antigen presenting properties. Expression of antigen presenting molecules such as MHC Class I, HLA-DR, CD80, CD86 and CD83 in these cell lines is shown below [Figure 10].

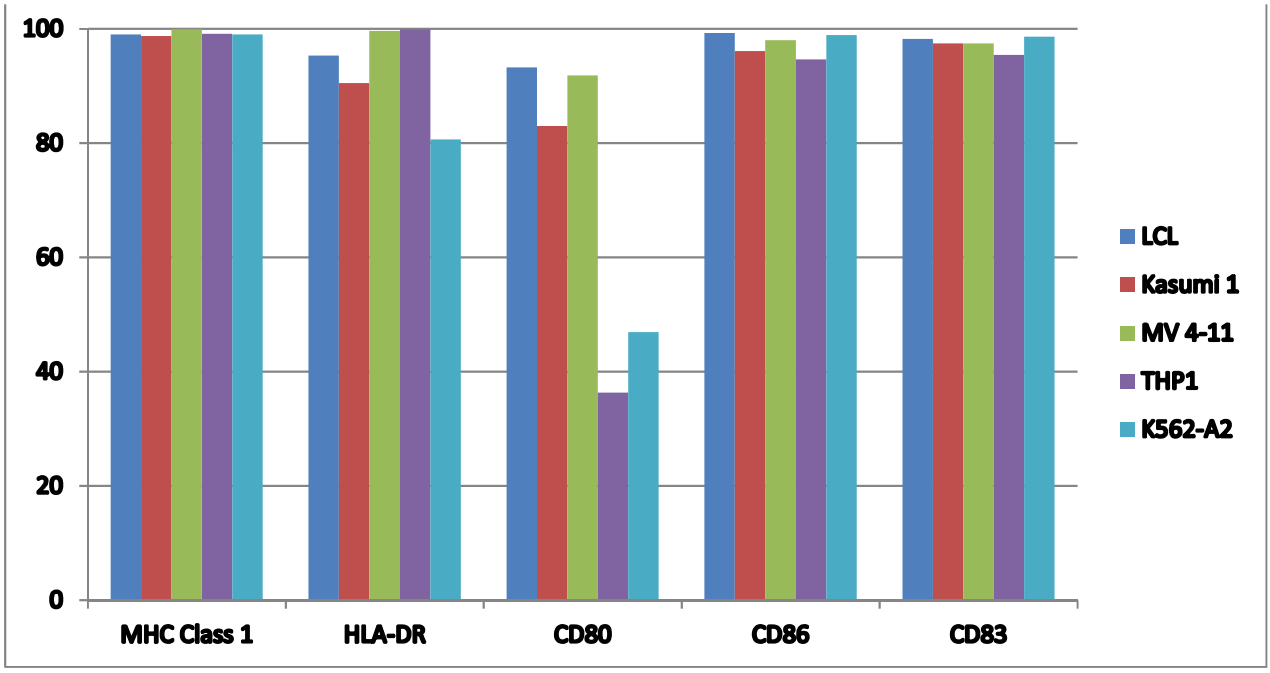

Figure 10: High expression of MHC Class I, HLA-DR, CD86 and CD83 in all cell lines. However, CD80 was highly expressed in LCL, Kasumi 1 and MV 4-11 only. Thus, suggesting these cell lines may have good antigen-presenting ability.

2.2 Methods

2.2.1 Cell isolation

Mononuclear cells were isolated from 1) random healthy adult and cord blood donors and 2) peripheral blood of patients following CBT or BMT using standard cell separation techniques (Ficoll-Paque, GE Healthcare 17-1440-03).

2.2.2 CD4+ T-cell subset analysis

CD4 T-cell subset analysis was performed on day 30, day 60 and day 180 following CBT without serotherapy. This was compared with those receiving BMT without serotherapy. All our recipients were children between 0.1 and 12 years of age, with median age of 2 years.

2.2.2.1 T-regulatory staining

Surface staining of PBMCs was performed using anti-mouse human CD4 PerCP Cy5.5, CD25 PE, CD127 FITC (BD Biosciences) for 20 mins.

Intracellular staining for Foxp3 protein was performed using fixation and permeabilization buffers provided by the Foxp3 kit (eBioscience) and Foxp3APC (eBioscience). RatIgG2a K APC was used for isotype control. Ten thousand lymphocyte gate events were acquired on BD LSR II flow cytometer and analysed by FACSDiva software (BD Biosciences).

2.2.2.2 Th1, Th2, Th17 staining

Th1, Th2, Th17 staining was performed using HumanTh1/Th2/Th17 Phenotyping Kit from BD Pharmingen™. 1 million PBMCs were stimulated with PMA/Ionomycin (at 50 ng/ml and 1 µg/ml respectively) in the presence of BD GolgiStop™ Protein Transport Inhibitor for 5 hours at 37ºC. A negative control was 1 million PBMCs incubated at 37ºC without any stimulation. Significant down regulation of CD4 receptor is observed after PMA/Ionomycin stimulation[52], hence to reliably identify CD4+ T cells additional surface staining of CD3 APC-Cy7 (eBioscience) was performed. Manufacturer's instructions were followed for fixation and permeabilization. Human Th1/Th2/Th17 Phenotyping Cocktail was used for surface staining of CD4 and cytokine staining of IFN-y, IL-4 and IL-17. A minimum of 2000 CD4 T cell events were acquired on_BD LSR II flow cytometer and analysed by FACSDiva software (BD Biosciences).

2.2.2.3 Naïve-memory-effector differentiation

T cells were classified using PerCP-Cy5.5-conjugated CD4, APC-conjugated CD45RA and PE-conjugated CD27PE. CD45RA+CD27+ were classed as naïve, CD45RA-CD27+ cells were classed as central memory, and CD45RA+CD27- were classed as effectors.

2.2.3 CFSE proliferation assay

For measurement of cell proliferation, cells were incubated at 37ºC with 10μM carboxy-fluorescein diacetate succinimidyl ester (CFSE; Invitrogen) in X-VIVO 10 for 7 minutes. CFSE-labelled cells were washed 3 times in X-VIVO 10 containing 10% Human AB serum to remove the excess CFSE. The cells were then suspended in X-VIVO 10 media and incubated at the appropriate concentration in 24-well flat bottom plates. Cells were either unstimulated (control) or stimulated with irradiated (30Gy) allogeneic LCLs (at ratio 10:1) or stimulated with IL-2 (20 U/ml; Pepro Tech), IL-7 (10 ng/ml; Pepro Tech) and IL-15 (12 ng/ml; Pepro Tech). Concentrations of cytokines were chosen based on previous work by other co-workers (Swainson *et al.,* 2007; Schonland *et al.,* 2003; Dardhalon *et al.,* 2001) Unstimulated samples were analysed on day 0 to verify CFSE labelling of cells and were used as negative controls. Stimulated samples were analysed at day 7 following allogeneic stimulation or day 9 following cytokine stimulation. At least 10,000 lymphocyte gate events were acquired on BD LSR II flow cytometer and analysed by FACSDiva software (BD Biosciences).

Proliferative index was calculated as follows -

Sum of the cells in all generations ÷ Calculated number of original parent cells

2.2.4 STAT5 phosphorylation

One million PBMCs and CBMCs were isolated and stimulated with varying concentrations of IL-7 and IL-2 for 10 minutes at 37ºC. IL-7 was used at the concentration of 10 ng/ml, 1 ng/ml, 0.1 ng/ml and 0.01 ng/ml and IL-2 was used at the concentration of 1000 U/ml, 100 U/ml and 20 U/ml. Unstimulated PBMCs and CBMCs were used as controls. The cells were then fixed using Phos flow lyse/fix buffer, washed and permeabilised using Phos Flow Perm Buffer III (BD Biosciences). The cells were then incubated for 30 minutes at 4ºC. At the end of the incubation, cells were washed twice and stained with CD4 PerCP (SK3 clone, BD Biosciences) and Alexa Fluor 488 Anti-Stat5 (pY694) (BD Biosciences). Flow cytometry was performed on FACS Calibur and at least 10,000 lymphocyte gate events were acquired. The acquired flow cytometry files were analysed using CellQuest software (BD Biosciences).

2.2.5 Measurement of plasma cytokines

Plasma samples of children were stored at day+30, day+60 and day+90 following CBT (*n=6*) and BMT (*n=6*). Plasma IL-7 levels were measured in these samples.

All reagents were provided with the Meso-scale discovery kit. Each 96-well plate had a carbon electrodes in the bottom of each well, pre-coated with anti-IL-7 antibody. The standards were reconstituted in the assay diluent provided. Assay diluent (25 µl) was added to all wells and the plate sealed and incubated for 30 sec at room temperature on an orbital shaker (600 rpm). Following addition of 25 µl diluent to each well, samples and standards were added at 25 µl per well. The plate was sealed and incubated for 2 hours at room temperature on an orbital shaker (600 rpm). At the end of the incubation the wells were washed three times using 200 µl PBS + 0.05%Tween 20, soaking for 30 sec and then discarding. Detection antibody was added at 25 µl per well, and the plate sealed and incubated for 1 hour at room temperature on an orbital shaker (600 rpm). At the end of the incubation the plate was washed three times as before. 150 µl of the MSD Read Buffer was added to each well and the MSD plates were measured on the MSD Sector Imager 2400 plate reader. The raw data was measured as electrochemiluminescence signal (light) detected by photodetectors and analysed using the Discovery Workbench 3.0 software (MSD). A 4-parameter logistic fit curve was generated for IL-7 using the standards and the concentration of each sample calculated. The limit of detection was between 0 and 2500 pg/ml.

2.2.6 Fluorescence Activated Cell Sorting (FACS)

Mononuclear cell preparations were incubated in FACS staining buffer (PBS with 2% FBS and 2mM EDTA) with surface antibodies conjugated to fluorochromes. CD4-FITC (BD Biosciences), CCR7-PE (eBioscience), CD45RA-APC (BD Biosciences) were used for surface staining of naïve CD4+ T cells and FACS sorting was performed on BD FACS Aria III cell sorter.

2.2.7 Preparation of RNA for microarray analysis

CD4+CD45RA+CCR7+ naïve T cells from blood samples of 1) normal donor cord blood and peripheral blood and 2) patients 2 months after receiving T-replete CBT and BMT were checked for high purity (>98%) after cell sorting. Naïve CD4+ T cells were then immediately resuspended in RNA lysis buffer (RNAeasy mini-kit) and stored at -80°C. RNA was isolated according the manufacturer's protocol and yield was determined on a Nanodrop spectrophotometer (Thermo Scientific). Samples that had an appropriate yield (typically >10 nanograms total RNA) were subsequently analyzed for RNA integrity using an Agilent Bioanalyzer (Agilent 2100, Agilent Technologies). RNA that was determined to be of high quality was then converted to cDNA and amplified (NuGEN WT-Ovation, NuGEN), purified to remove residual RNA (QIAquick PCR purification kit, Qiagen), fragmented (NuGEN WT-Ovation Kit), and labeled (FL-Ovation cDNA biotin module, NuGEN) for subsequent microarray analysis. Fragmented and labelled cDNA was hybridized to microarray chips (Affymerix HuGene ST 1.0 arrays). Hybridization of samples and data acquisition was performed by the Department of Genomics at University College London.

2.2.8 Experimental design

Three experiments comparing biological replicates of samples from normal donor cord blood (*n=3*) and normal donor peripheral blood (*n=3*) were performed. In the third experiment, samples from cord blood and peripheral blood of same donors were compared, thus allowing a paired analysis of these samples. Along with these paired normal donor samples, biological replicates of reconstituting naïve CD4+ T cells isolated two months after CBT (*n=3*) and BMT (*n=3*) were also performed.

To decipher the relationship of foetal CD4+ T-cell transcriptome with naïve CD4+ T cells from normal donor cord blood, normal donor peripheral blood and during early T-cell reconstitution following T-replete CBT and BMT, Affymetrix Human Genome U133 Plus 2.0 Array dataset of naïve CD4+ T cells isolated from the foetal lymph nodes (18-22 week gestational age) was retrieved (GSE25119; Mold *et al.,* 2010).

An Affymetrix Human Genome U133 Plus 2.0 Array dataset of T-regulatory cells isolated from fetal lymph nodes (18-22 weeks gestational age) and adult PB were also retrieved (GSE25119; Mold *et al.,* 2010). Thus, the relationship between CD4+ T-regulatory cell transcriptome and naive CD4+ T cells from normal donor CB and during early reconstitution after CBT was also elucidated.

2.2.9 Microarray data analysis – Quality control and statistical analysis

All gene expression profiles were determined to be of good quality after a quality control analysis [Figure 11]. Assessment of hybridization quality was performed using Bioconductor package affyPLM (Bolstad *et al.,* 2005).

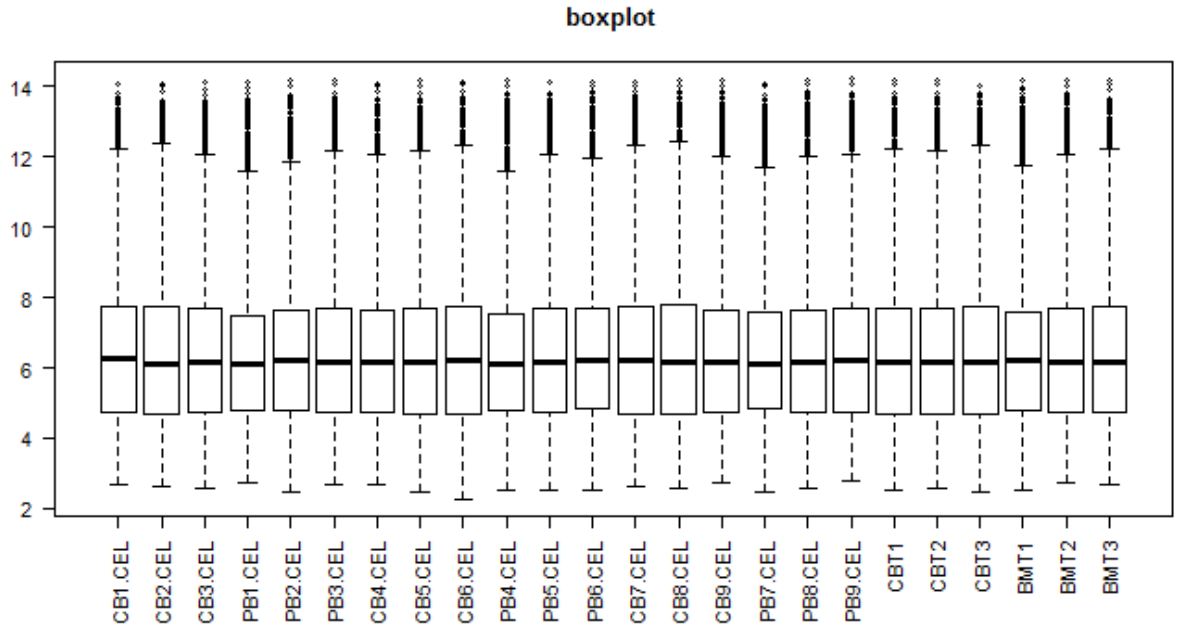

Figure 11: Box plot of log intensities for each microarray. The distribution of data as well as median values are similar for all the arrays. This confirms minimum variability and good quality of gene expression data.

Preprocessing of Affymetrix dataset followed these procedures: background correction, normalization using the quantile method, summarization of probe set values using the RMA (Robust Multi-array Average) method, which fits a specified robust linear model to the probe level data.

Probe sets were mapped to genes using Bioconductor package AnnotationDbi (Pages *et al.,* 2017). Where multiple probe sets representing a gene were available, the probe with maximum average value was chosen. Thus, we identified 17522 genes common to the Affymerix HuGene ST 1.0 and Affymetrix Human Genome U133 Plus 2.0 platform.

The dataset of 17522 genes was combatted to remove the batch effects using Combat function in R as previously described (Johnson *et al.,* 2007). Three-dimensional and two-dimensional principal component analysis was performed on the combatted datasets using DUDI.PCA

function. Hierarchical clustering of gene expression samples on combatted dataset was performed using ward agglomerative hierarchical method.

Differentially expressed genes were identified by comparing the uncombatted data from each individual experiment. Bioconductor package limma - a “moderated t test” application was used, and unpaired or paired analysis was performed to identify differentially expressed genes.[20] The threshold for identifying significant genes was set at a p value of < 0.05 and fold-change (greater than 2) thresholds. All analysis was performed using R (cran.r-project.org) and Bioconductor (www.bioconductor.org).

2.2.10 Pathway analysis

Gene Set enrichment analysis (GSEA) on the data sets was performed to identify differentially regulated pathways (Subramanian *et al.,* 2005). In our analysis, default metric of signal to noise ratio was used to rank the differentially expressed genes. To identify the differentially expressed genes pathways in the naïve CD4+ T cells from normal donor cord blood *vs* peripheral blood, the datasets from the three experiments were pooled and combatted using Combat function in R. When GSEA compared the gene expression profiles from the same experiment, Combat function was not used.

We used Biocarta signalling and KEGG gene set pathways to identify the differentially expressed canonical pathways, and biological gene sets to identify differentially expressed biological processes. Cytoscape software was used to perform enrichment mapping of the pathways upregulated at p value < 0.005 and fdr value < 0.1.

2.2.11 Proliferation assays

CFSE dye dilution experiments were performed to assess the role of upregulated pathways and relevant transcription factor in proliferation of naïve CD4+ T cells.

CD3+ T cells were positively selected from the cord blood and peripheral blood mononuclear cells using human CD3+ microbeads from Milteyni (130-050-101). For measurement of cell proliferation, cells were incubated at 37ºC with 10µM carboxy-fluorescein diacetate succinimidyl ester (CFSE; Invitrogen) in X-VIVO 10 for 7 minutes. CFSE-labelled CD3+ T cells were washed 3 times in X-VIVO 10 containing 10% Human AB serum to remove the excess CFSE. The cells were then suspended in X-VIVO 10 media and incubated at the appropriate concentration in 96-well round bottom plates.

To identify the role of TCR signaling in enhanced proliferation of cord blood CD4+ T cells, CFSE-labelled cord blood and peripheral blood T cells were cocultured with CD3 negative cells (APC fraction) at the APC:T-cell ratio of 1:1, 2:1 and 4:1 for 7 days (Lisciandro, *et al* 2012).

The role of up-regulated transcription factor complex – AP-1 was tested by inhibiting AP-1 with a small molecule inhibitor SR 11302 from R and D systems. CFSE-labelled cord blood CD3+ T cells were cocultured with CD3 negative cells (APC fraction) at APC:T-cell ratio of 4:1 and inhibition of proliferation with 1, 10 and 100 ng/ml of AP-1 inhibitor was assessed after 7 days.

2.2.12 Generation of lymphoblastoid cell lines

$5x10^6$ freshly isolated PBMC from healthy donors were centrifuged and resuspended in 200 µl of EBV supernatant produced from the B95-8 cell line. 1.8 ml complete RPMI containing 1 µg/ml Cyclosporin A (CsA) to inhibit EBV-specific T cell responses and hence facilitate LCL growth was added and 200 µl cells aliquoted into five wells of a flat-bottom 96 well tissue culture plate (96wp) ($5x10^5$/well). 1ml complete RPMI with CsA was added to the remaining 1ml cells and 200 µl aliquotted to 10 further wells ($2.5x10^5$/well). The outer wells were filled with sterile distilled water and the cells were incubated at 37ºC in 5% CO2. The cells were incubated for one week, at which time half media changes were performed as necessary, determined by media colour, until cells were beginning to expand, and clumps appeared. Subsequently, one well seeded with $5x10^5$ cells was combined with two seeded with $2.5x10^5$ cells in a 24 well plate and cells expanded for a further week, whereupon the LCL line was transferred to a vented 25 cm^2 tissue culture flask. Once LCL line was established it was transferred to 75 cm^2 and 150 cm^2 tissue culture flask and finally frozen in aliquots of $5x10^6$ cells/ml.

2.2.13 Firefly Luciferase (F-Luc) transduction of EBV-driven B-cell lymphoma cell lines (B-LCLs)

A total of 5×10^6 freshly isolated mononuclear cells from healthy cord blood or peripheral blood donors were cultured with an EBV supernatant produced from the B95-8 cell line in the presence of 1 µg/mL cyclosporin A to inhibit EBV-specific T-cell responses as described above (Comoli *et al.,* 2002). B-LCL were transduced with an SFG retroviral vector encoding green shifted FLuc and cultured in RPMI medium with 10% fetal calf serum + 1% penicillin/streptomycin (RF10). One week after transduction, LCLs were FACS sorted based on expression of the eBFP reporter gene, to select for transduced cells. The sorted LCLs were then grown and these cells maintained high FLuc expression in cultures. The LCLs were checked for FLuc expression prior to every *in vivo* experiment and cultures with > 90% of LCLs expressing FLuc were used for all the experiments. FLuc allows for non-invasive monitoring of xenografted tumors in mice by luminescent imaging *in vivo*.

2.2.14 T-cell selection

Mononuclear cells were separated from CB and PB using Ficoll-Paque PLUS. Negatively selected CD3+ T cells were isolated using Milteyni Pan T-cell Isolation Kit, human (130-096-535) and counted using a Sysmex XE-5000 automated hematology system. The purity of negatively selected T cells was > 94%.

2.2.15 Xenograft model and tumour imaging

NOD/SCID/IL2rg^{null} mice were obtained from a breeding colony maintained in our institute and housed in individually ventilated cages. Autoclaved food, water and bedding were utilised for these animals and mice were handled under aseptic conditions at all times. Ethical approval for murine work was obtained as per project licence number PPL 70/7294.

All animal studies were approved by the University College London Biological Services Ethical Review Committee and licensed under the Animals (Scientific Procedures) Act 1986 (Home Office, London, United Kingdom). The primary murine modeling experiments were performed to study the differential GvL effect between cord blood and peripheral blood T cells.

2.2.15.1 Subcutaneous injection of LCL

5 million LCLs transduced with the FLuc_eBFP firefly luciferase retroviral vector per animal were washed three times with PBS and resuspended in 50 µl cold plain RPMI. This was mixed with 50 µl cold Matrigel and loaded into a 0.5ml 27-gauge (G) tuberculin syringe. Animals were restrained by scruffing and cells were injected subcutaneously on the nape of the neck on day –2.

2.2.15.2 T-cell injections

To evaluate the anti-tumor activity, 5×10^6 comparably HLA-mismatched CB or PB CD3+ T cells were injected i.v. (by tail vein injection) after 2 days on day +0. HLA typing was performed for A, B, C, DRB1 and DQB1 antigens.

In the first experiment, 10 of 10 and in the second experiment, 7 of 10 HLA antigens were mismatched between CB T cells vs LCLs and PB T cells vs LCLs.

5 million T cells from cord blood and peripheral blood donors were resuspended in 100 µl plain RPMI and transferred to a 0.5ml syringe. Animals were warmed at 37ºC for 10 minutes and T cells were injected into the tail vein using a 27G needle. Pressure was applied to the injection site following administration to reduce bleeding.

2.2.15.3 Monitoring of LCL tumours

The size of LCL tumours was assessed with callipers bi-weekly, in addition to monitoring with bioluminescent imaging using the IVIS imaging system (Xenogen; Caliper Life Sciences, Hopkinton, MA). For imaging, anaesthesia was induced by inhalation of isofluorane with oxygen. 2mg D-Luciferin was injected intraperitoneally in 200 µl volume and animals were

placed in the imaging chamber. Anaesthesia was maintained by delivery of isofluorane and oxygen to individual animals within the imaging chamber. A region of interest (ROI) was delineated around the tumour site and images were captured at two-minute intervals until the signal from each ROI plateaued. Animals recovered individually in warmed chambers. Animals were imaged on day +10, +20, +25, +30, and +35. Photon emission from $FLuc^{+}$ LCLs expressed in photon per second per cm^2 per steradian ($p/s/cm^2/sr$) within each ROI was quantified using Living Image software (Xenogen) as previously described (Savoldo *et al.,* 2007). In addition to monitoring the tumour bioluminescence, two-dimensional caliper measurements of the tumor were performed and tumor volume was derived using the following formula: Tumour volume = $1/2 \times (\text{length} \times \text{width}^2)$. Mice were sacrificed if the tumor growth exceeded the permitted threshold of 10 mm.

Secondary murine modeling experiments were performed to compare the mechanisms of the GvL effect between CB and PB T cells. In these experiments, I examined the differences in xeno-reactive potential of CB and PB T cells and examined the correlation between xeno-reactivity and GvL effect. I also tested if the observed GvL effect was an allo-reactive or an anti-viral effect. Finally, I studied the tumour-infiltrating lymphocytes, their phenotype, stages of differentiation and effector function.

2.2.16 Tumor-infiltrating lymphocytes (TILs)

2.2.16.1 Isolation of TILs

Tumors were minced and incubated in RF10 medium with 0.1 mg/mL collagenase A (Roche) and 60 U/mL DNase I (Sigma-Aldrich) for 30 min at 37°C. Tumors were then homogenized, filtered through a nylon filter (70 µm), and the lymphocytes were isolated in RF-10. TILs were studied for 1) IFN-γ, TNF-α, IL-4 responses, 2) perforin expression, 3) naïve-memory-effector differentiation and FoxP3 staining as detailed below (Law *et al.,* 2009).

2.2.16.2 IFN-γ, TNF-α, IL-4 responses

TILs were separated from lymphoma cells using CD20 microbeads (Milteyni Biotec). Isolated TILs were then re-stimulated at 37°C for 6 h with lymphoma cells from the same donor at the effector:target ratio of (1:10) in the presence of 10 µL of Brefeldin A (1 mg/mL) in 1 mL of RF-10. TILs were then surface stained with mouse anti-human antibodies, including APC-Cy7-conjugated CD3, BV605-conjugated CD4, and BV421-conjugated CD8. Following fixation and intracellular permeabilization with the eBioscience buffer set (00-5523), TILs were stained for PE-conjugated INF-γ, FITC-conjugated TNF-α, and APC-conjugated IL-4.

2.2.16.3 Perforin expression

Unstimulated TILs were surface stained with mouse-antihuman antibodies, including APC-Cy7-conjugated CD3, BV605-conjugated CD4, and BV421-conjugated CD8 for 20 mins. For intracellular perforin staining, TILs were fixed with 1% PFA in PBS for 20 min at room temperature and incubated 10 min with BD perm/wash buffer 1X (BD Biosciences). Cells were washed twice with BD perm/wash buffer 1X and then stained with PE-conjugated mouse anti-human perforin mAb (δG9, IgG2b; BD Biosciences) in BD perm/wash buffer 1X for 30 min at room temperature. Unbound antibodies were removed by washing with perm/wash buffer 1X and fixed again with 1% PFA.

2.2.16.4 Naïve-memory-effector differentiation

Unstimulated TILs were surface-stained with mouse anti-human antibodies, including APC-Cy7-conjugated CD3, BV605-conjugated CD4, BV421-conjugated CD8, PerCP-Cy5.5-conjugated CD45RO, and APC-conjugated CCR7.

2.2.16.5 FoxP3 staining

Unstimulated TILs were surface stained for mouse anti-human antibodies, including FITC-conjugated CD4, PE-conjugated CD8, and BV421-conjugated CD25. Following fixation and intra-cellular permeabilization with the eBioscience FoxP3 buffer set (00-5523), TILs were stained for APC-conjugated FoxP3. T-regulatory cells were identified as CD4+CD25+FoxP3+ cells using a gating strategy based on CD4+ CD25- "non-T-regs" (Law *et al.,* 2009).

2.2.16.6 Th1/Th2 TILs

CD4+ TILs were identified as IFN-γ or TNF-α secreting Th1 cells and IL-4 secreting Th2 cells. Th1/Th2 balance of CD4+ TILs was quantified using IFN-γ/IL-4 and TNF-α/IL-4 ratios.

2.2.16.7 Histology

Immunohistochemical mouse anti-human CD3 staining of tumor sections was performed to study the extent of T-cell infiltration. Using Image J, 10 RGB images of 40× magnification for each tumor slide were converted to black and white mask output using a calibrated threshold for each stack of images and average density of T cells per mm^2 of tumor was calculated as shown in Figure 70 (Loughlin *et al.,* 2007).

2.2.17 Statistics

Statistical analysis was done using GraphPad Prism software. Tumour volumes either photons/sec/cm^2/sr or mm^3 are expressed as mean and standard deviation. Two-tailed t-test was performed for comparisons of experimental groups. A log-rank (Mantel-Cox) test was used to compare survival between different groups of mice.

2.2.18 Ethics

Ethics approval for studying cellular immune-reconstitution following haematopoietic stem cell transplantation was obtained from Central London REC (REC reference 05/Q0508/61).

Ethical approval for comparing the paired gene expression profile of naïve CD4+ T cells from the cord blood and peripheral blood of the same donor was obtained from NRE Committee London – Dulwich (REC reference 11/LO/15089). This ethical approval allowed us to contact families known to Great Ormond Street Hospital who had family-directed cord blood donation in the past but was now no more required for clinical purpose, and hence could be used for research. These families were contacted so that we could collect 20 mls of peripheral blood from the cord blood donor. This allowed paired comparison of naïve CD4+ T cells isolated from the peripheral blood and cord blood of same donors.

Chapter three

Rapid $CD4^+$ T-cell biased immune-reconstitution following CBT may be driven by increased sensitivity of cord blood T cells to homeostatic signals

3.0 Aims

1) To study the kinetics of early immune-reconstitution after T-cell replete cord blood and bone marrow transplantation

2) To perform flow-cytometric phenotyping of $CD4^+$ T cells after T-cell replete cord blood and bone marrow transplantation

- Th1, Th2, Th17 analysis after PMA/Ionomycin stimulation using IFN-γ, IL-4, IL-17 staining

- T-regulatory cell analysis using 4-color ($CD4^+CD25^+CD127^-Foxp3^+$) staining

3) To perform naïve, memory and effector subset analysis of reconstituting $CD4^+$ T cells after T-cell replete cord blood and bone marrow transplantation

4) Measuring IL-7 levels after cord blood and bone marrow transplantation

3.1 Introduction

$CD4^+$ T-cell reconstitution after HCT is predominantly thought to be mediated by the thymic-dependent pathway (Mackall *et al.,* 1997; Williams *et al.,* 2007). Therefore, $CD4^+$ T-cell reconstitution occurs late, typically after 3 to 6 months following transplantation (Mackall *et al.,* 1997; Williams *et al.,* 2007). In contrast, $CD8^+$ T-cell reconstitution occurs early and is thought to be mediated by expansion of cognate memory and effector T cells. The spontaneous expansion of T cells infused with the graft is termed as "homeostatic proliferation (HP)" (Mackall *et al.,* 1996; Mackall *et al.,* 1997; Ge *et al.,* 2002). The relative contribution of thymic-independent and thymic-dependent pathway to replenish the peripheral T-cell pool after HCT depends on the use of serotherapy in the conditioning regimens. In particular, *in vivo* T-cell depleting regimens have a significant effect on thymic-independent homeostatic proliferation (Komanduri *et al.,* 2007; Lindemans *et al.,* 2014; Renard *et al.,* 2011).

Omission of in vivo T-cell depletion from the conditioning regimens allows early T-cell immune-reconstitution which is thymic-independent (Chiesa *et al.,* 2012; Lindemans *et al.,* 2014). This form of conditioning regimen is particularly employed for conditioning of HLA-matched sibling transplants in the context of chemotherapy-resistant leukaemia. Recently, such an approach has also been used for conditioning of unrelated cord blood grafts because of low risk of graft-versus-host disease (Chiesa *et al.,* 2012; Sauter *et al.,* 2011).

We published results of rapid $CD4^+$ T-cell biased immune-reconstitution following cord blood transplantation in 30 patients (Chiesa *et al.,* 2012). Intrigued by this novel $CD4^+$ T-cell biased reconstitution following cord blood transplantation, we decided to explore the mechanisms of early T-cell reconstitution following T-cell replete cord blood graft. Firstly, we compared the differences in $CD4^+$ T-cell reconstitution after transplantation from cord blood and bone marrow. We compared the 1) kinetics of $CD4^+$ T-cell reconstitution, 2) functionality i.e. cytokine-secreting ability of $CD4^+$ T cells, 3) suppressive function i.e. recovery of T-regulatory cells and 4) phenotype of T cells i.e. naïve, memory, effector T cells. We also measured decline in IL-7 levels following cord blood and bone marrow transplantation.

In this chapter, we have studied the differences in kinetics of early T-cell reconstitution (< 6 months) after T-cell replete cord blood and bone marrow transplantation. In addition, we also performed phenotypic analysis of peripherally expanding T cells at early time-points after T-cell replete grafts.

3.2 Patient and graft characteristics of T-cell replete cord blood and bone marrow transplants

To underline the important differences in early thymic-independent T-cell reconstitution after T-cell replete cord blood and bone marrow grafts, we performed analysis on 70 consecutive T-cell replete transplantations. 30 children received cord blood and 40 children received bone marrow grafts. These demographics and relevant transplant characteristics of the two groups are presented in Table 2.

	CBT (*n = 30*; 26 single and 4 double cord)	BMT (*n = 40*)
Age at transplant	1 year (0.1 – 12)	4.3 years (0.6 – 12)
Diagnosis	Acute leukaemia 12 (40%) Myelodysplastic syndrome/Chronic myeloid leukaemia 2 (6%) Immunodeficiency 12 (40%) Haemophagocytic lymphohistiocytosis 4 (14%)	Acute leukaemia 17 (42%) Myelodysplastic syndrome/Chronic myeloid leukaemia 3 (8%) Immunodeficiency 13 (32%) Haemophoagocytic lymphohistiocytosis 5 (13%) Metabolic 2 (5%)
Conditioning	Myeloablative conditioning 29 (97%) (TBI or Bu-based or Treosulfan-based) No conditioning 01 (3%)	Myeloablative conditioning 40 (100%) (TBI or Bu-based or Treosulfan-based)
HLA matching	≤8/10 = 17 9/10 = 14 10/10 = 03	10/10 = 40 (all matched sibling donors)
Acute GVHD	Grade II = 10 (33%) Grade III-IV = 5 (16%)	Grade II = 07 (18%) Grade III-IV = 03 (8%)
Viral reactivations	CMV = 04 (13%) ADV = 04 (13%)	CMV = 07 (17%) ADV = 04 (10%)

Table 2 Demographics and transplant characteristics of patients receiving cord blood and bone marrow graft

3.3 Number of T cells infused with cord blood and bone marrow grafts

To understand if in our paediatric cohort (age range: 0 to 13 years), quantity of T cells infused with the haematopoietic stem cell grafts from different sources influenced the T-cell reconstitution, we compared the number of T cells infused with cord blood and bone marrow grafts.

In our cohort, cord blood transplant recipients received a median T-cell dose of 4.75 x10^6 per kilogram (inter-quartile range: 2.5 to 6.7). This T-cell dose was significantly less (approx. 10 times) than the T cells received by bone marrow transplant recipients (median = 45 x 10^6 per kilogram; inter-quartile range: 27 to 67) [$P < 0.0001$, Figure 12]. These T-cell numbers are similar to that described in the literature and in general, cord blood graft contains one log less $CD34^+$ and $CD3^+$ cells per kilogram recipient body weight than bone marrow grafts (Gluckman, 2012).

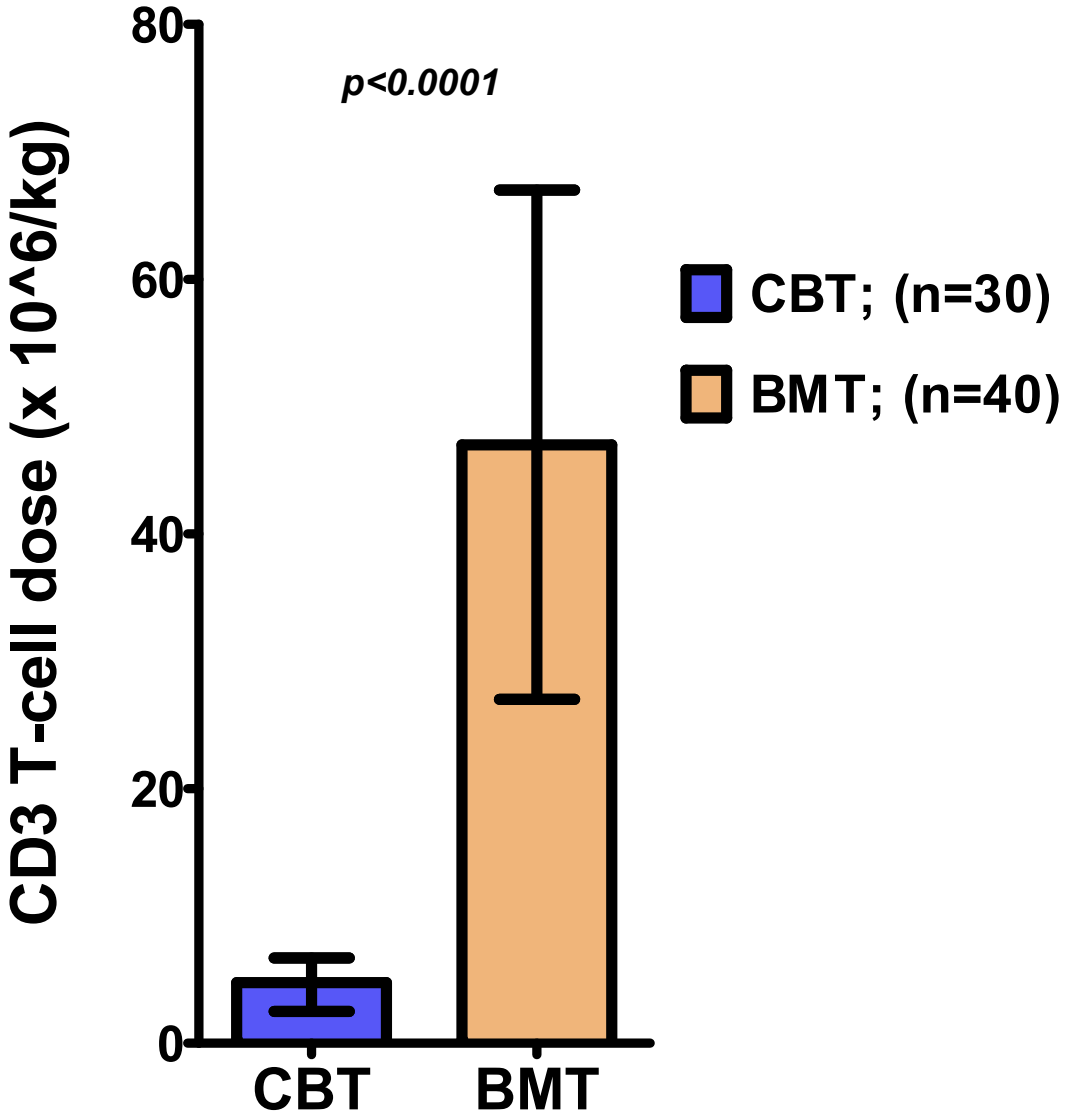

Figure 12: Bar plot of T cells carried with a cord blood and a bone marrow graft. A median of 4 x 10^6/kg T cells are infused with a cord blood graft compared with 10 times more T cells (45 x 10^6/kg) infused with a bone marrow graft (unpaired t-test; *p<0.0001*). The bar graph represents median and error bars represent interquartile range.

3.4 T-cell immune-reconstitution after T-cell replete CBT and BMT

3.4.1 T-cell reconstitution - 2 months after CBT and BMT

Despite a lower number of T cells infused with the cord blood graft, we observed a higher $CD3^+$ T-cell recovery after cord blood transplantation. In particular, two months following cord blood transplantation, we observed unprecedented expansion of the peripheral T-cell pool with a median T-cell count of 840 x 10^6 per kilogram (interquartile range: 575 to 1115). In comparison to the cord blood transplantation, two months following bone marrow transplantation, $CD3^+$ T-cell recovery was significantly lower with a median T-cell count of 500 x 10^6 per kilogram ($P < 0.05$; interquartile range: 280 to 980, Figure 13). The kinetics of recovery of $CD3^+$ T cells at 1, 2 and 6 months is shown in Figure 14.

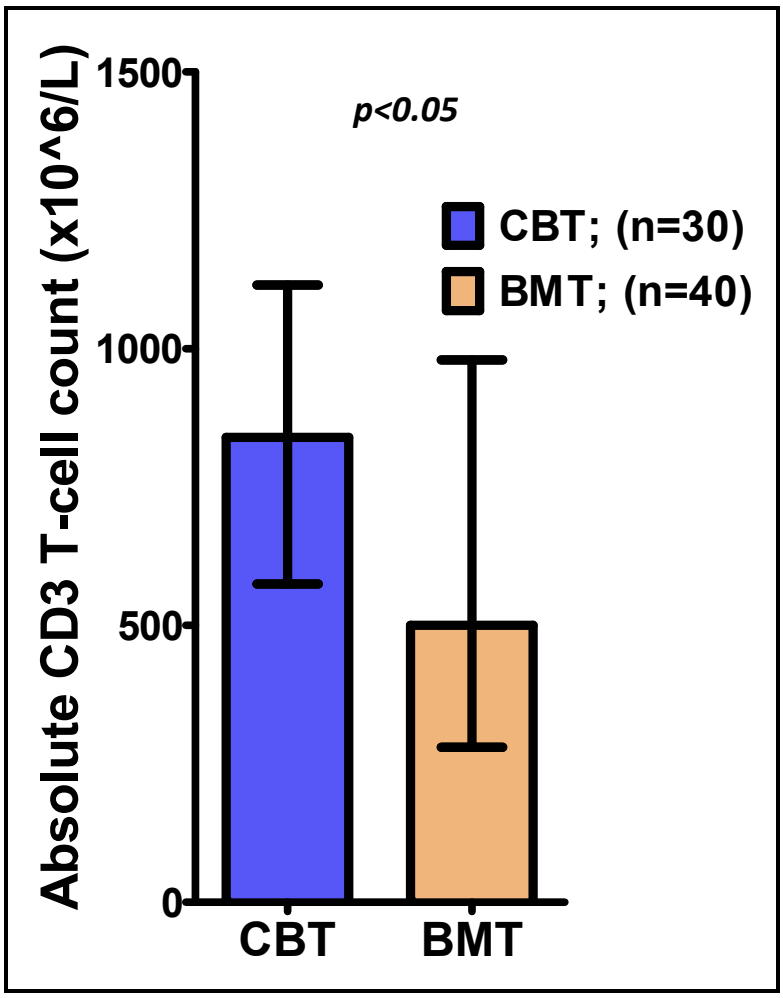

Figure 13: Absolute $CD3^+$ T-cell count two months after cord blood and bone marrow transplant. T-cell reconstitution after CBT was significantly higher than after BMT (unpaired t-test; $p<0.05$). The bar graph represents median and error bars represent interquartile range.

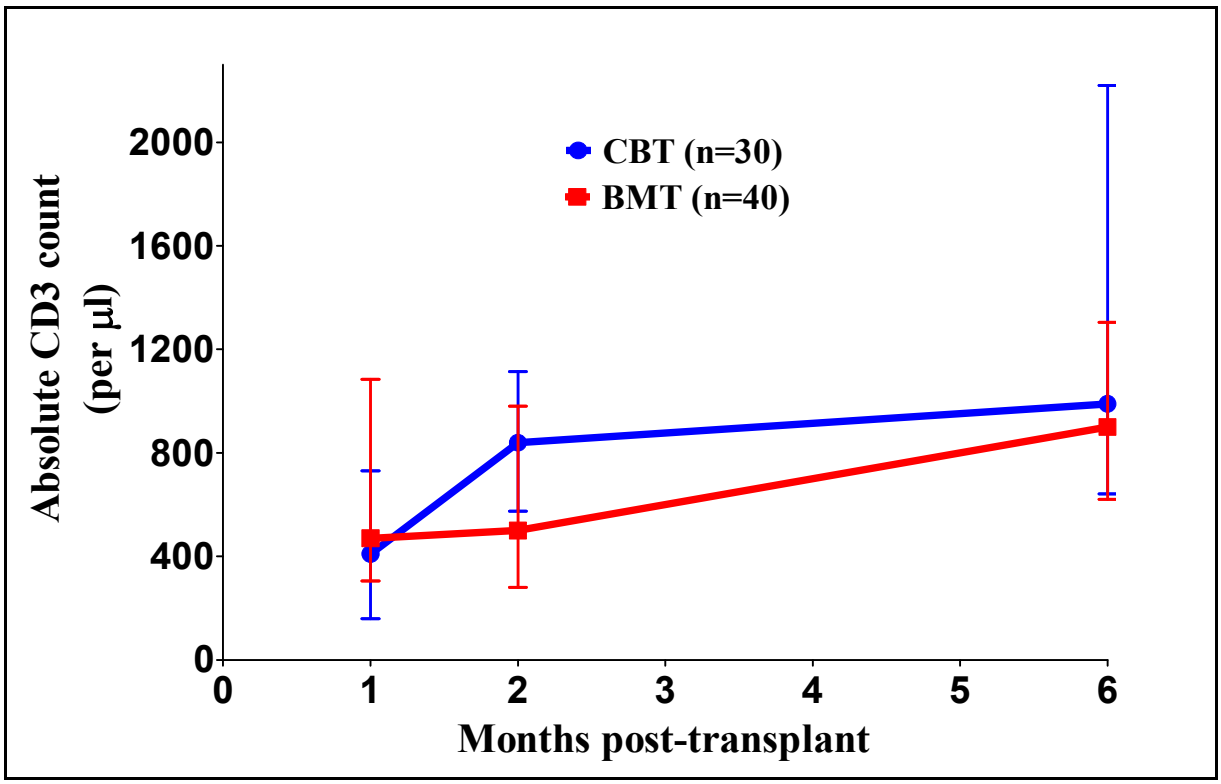

Figure 14: Line graph of T-cell reconstitution after T-replete CBT and BMT. Despite 10 times lower number of T cells infused with the cord blood graft, a significantly higher $CD3^+$ T-cell recovery is observed 2 months post-CBT compared with after BMT. The dots represent the median, and the error bars represent the 25th and 75th centile.

3.4.2 Comparing the kinetics of early $CD4^+$ and $CD8^+$ T-cell reconstitution after cord blood and bone marrow transplantation

We further studied the differences in $CD4^+$ or $CD8^+$ T-cell compartment after cord blood and bone marrow transplantation. Interestingly, this early expansion after bone marrow transplantation was $CD8^+$ T-cell biased which is in sharp contrast to the observed $CD4^+$ T-cell biased immune-reconstitution after cord blood transplantation. In particular, T-cell reconstitution after cord blood transplantation was strikingly $CD4^+$ T-cell biased after one month with an asymmetric CD4:CD8 ratio of 4.5. Further the T-cell reconstitution after cord blood transplantation continued to be numerically superior at 1, 2 and 6 months compared to bone marrow transplantation, albeit with a $CD4^+$ T-cell bias [Table 3 and 4; Figure 15 (a) and (b)].

Post-transplant	**BMT**	**CBT**	
1 month	180 (125 – 365)	310 (100 – 580)	*P = NS*
2 months	180 (105 – 305)	560 (340 – 800)	*P < 0.0001*
6 months	330 (245 – 455)	690 (445 – 1062)	*P < 0.001*

Table 3 shows statistically significant difference in $CD4^+$ T-cell expansion at and after two months CBT *versus* BMT.

Post-transplant	**BMT**	**CBT**	
1 month	200 (105 – 685)	70 (40 – 110)	*P < 0.001*
2 months	330 (150 – 710)	150 (100 – 340)	*P < 0.01*
6 months	380 (255 – 795)	250 (100 – 530)	*P = NS*

Table 4 shows statistically significant difference in $CD8^+$ T-cell expansion at one and two months after CBT *versus* BMT. There is no difference in $CD8^+$ T cells at 6 months.

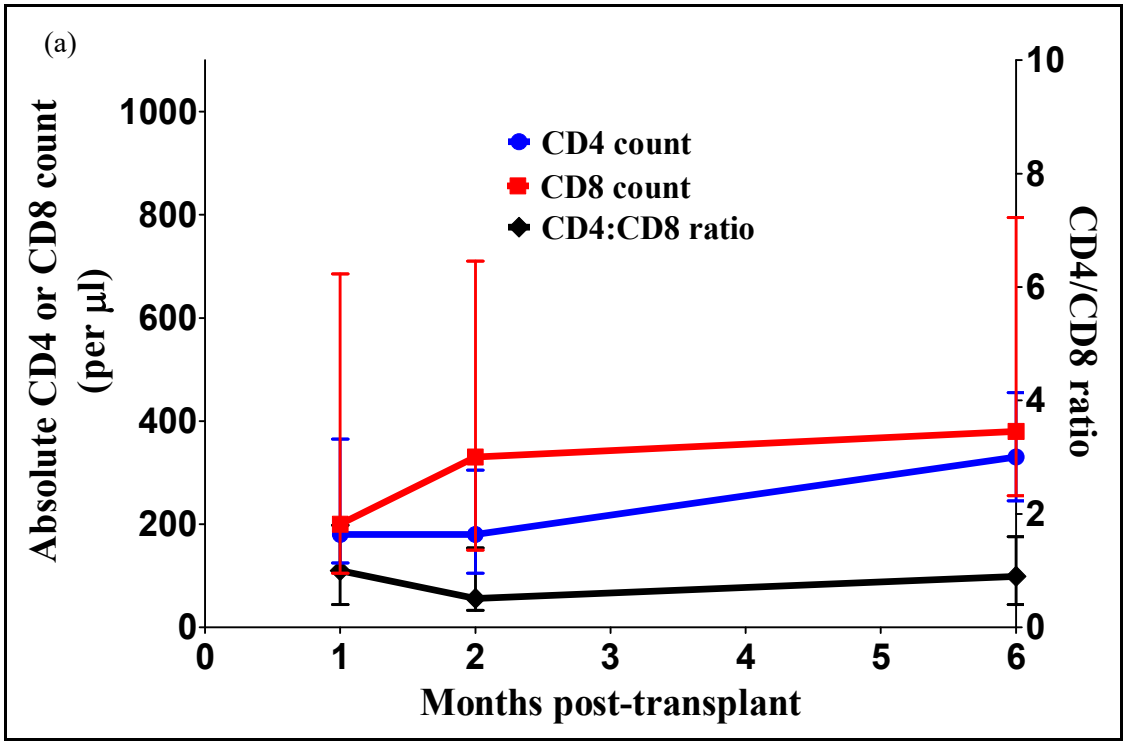

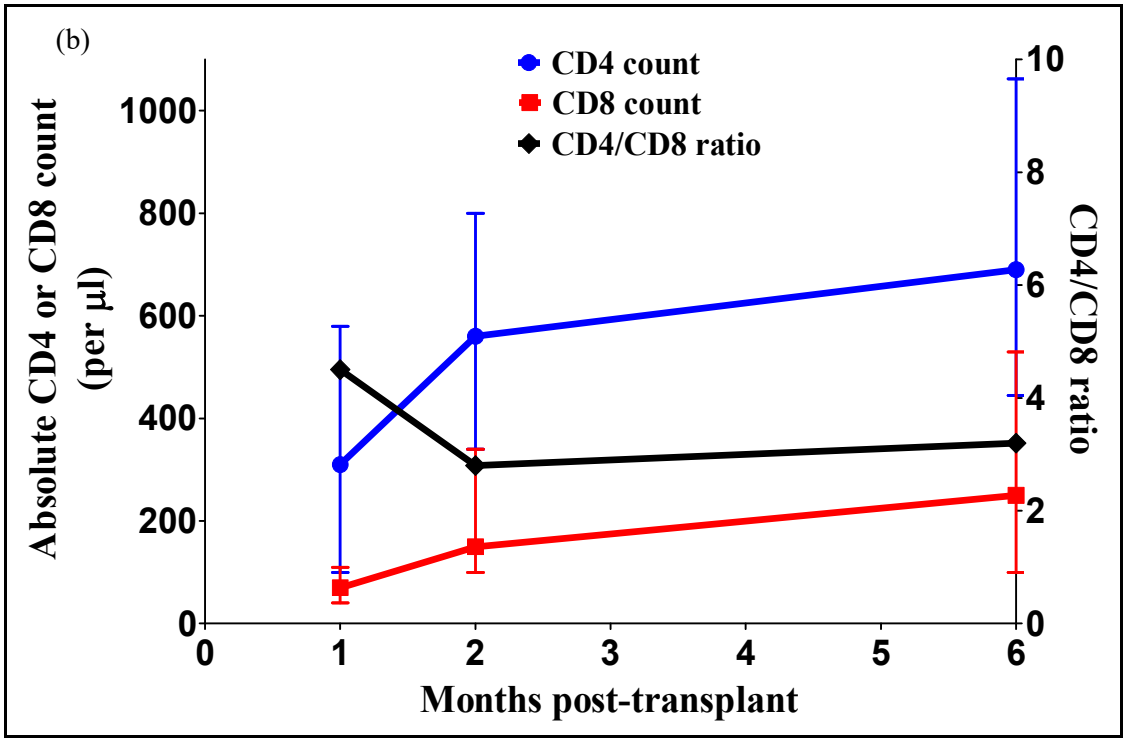

Figure 15 (a) and (b): Line graph showing $CD4^+$ and $CD8^+$ T-cell recovery after BMT and CBT respectively. The T-cell recovery observed after T-replete CBT was asymmetrically $CD4^+$ T-cell biased in contrast to the $CD8^+$ T-cell biased immune-reconstitution after T-replete BMT. The dots represent the median and the error bar represent interquartile range. The black line represents CD4:CD8 ratio plotted on right Y axis. The dots represent the median, and the error bars represent the 25th and 75th centile.

3.5 Comparing the functionality of reconstituting $CD4^+$ T cells after cord blood and bone marrow transplantation i.e. Th1, Th2, Th17 and T-regulatory cells

Since the adaptive immune system in cord blood is predominantly biased towards adopting a T–regulatory fate (Takahata *et al.,* 2004; Michaëlsson *et al.,* 2006; Silverstein *et al.,* 1964a; Silverstein *et al.,* 1964b), we compared Th subsets at day 30, 90 and 180 following cord blood *(n = 10)* and bone marrow *(n = 10)* transplantation to gain more insight into the function of these rapidly expanding $CD4^+$ T cells after cord blood and bone marrow transplantation.

Th1, Th2 and Th17 subsets were identified by intracellular cytokine staining following PMA/Ionomycin stimulation for 5 hours (Baran *et al.,* 2001). T-regulatory cells were identified using 4 colour $CD4^+CD25^+CD127^-FoxP3^+$ staining.

Th1, Th2, Th17 and T-regulatory staining – one month after cord blood and bone marrow transplantation is shown in Figure 16, 17 and 18.

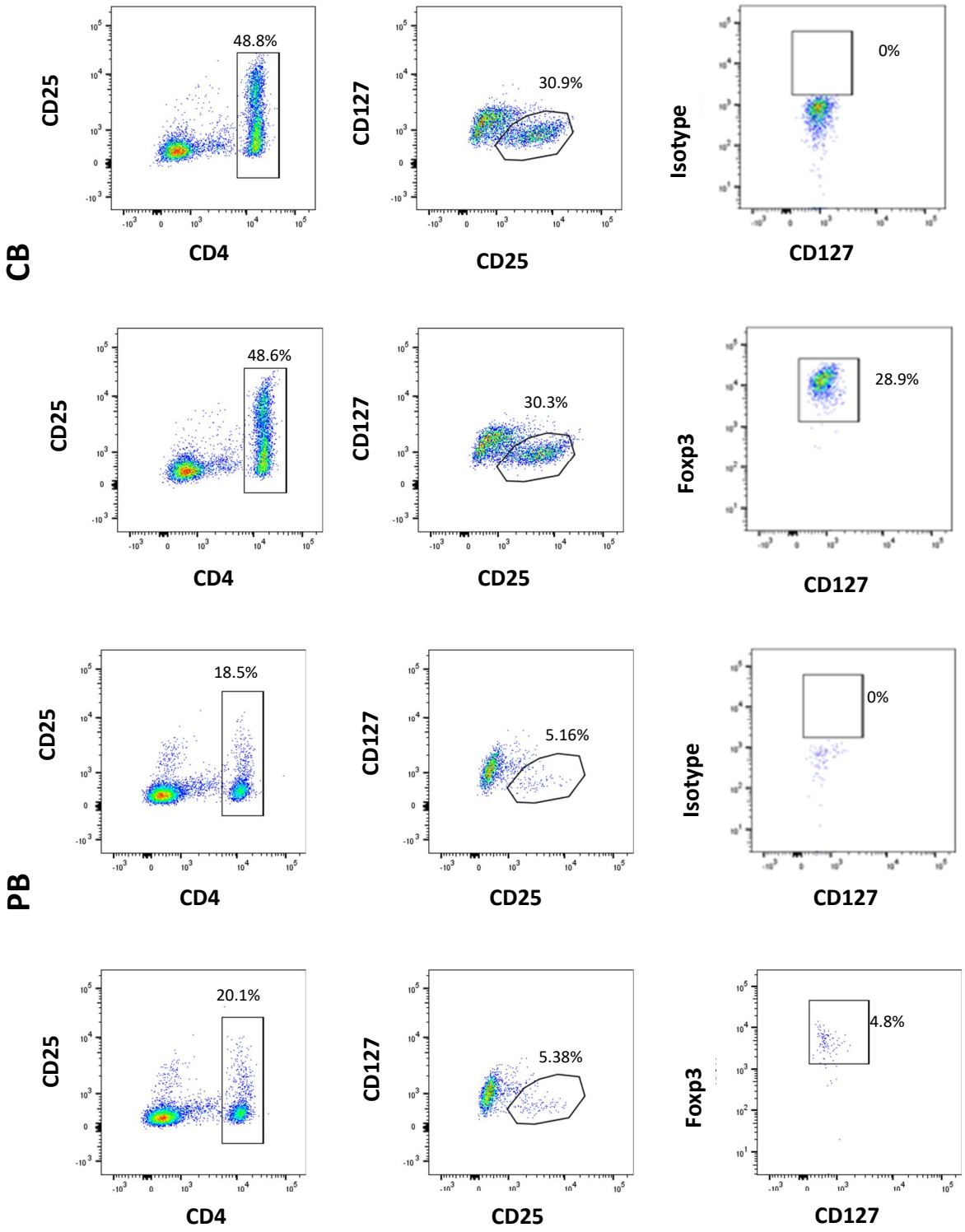

Figure 16: Representative flow cytometry dot plots of $CD4^{+}CD25^{+}CD127^{+}Foxp3^{+}$ T-regulatory cells, 30days after T-replete CBT and BMT. T-regulatory cells were identified as CD4+CD25+CD127-Foxp3+. Top two panels are cord blood (CB) and bottom two panels are peripheral blood (PB). Isotype control and Foxp3 antibody was added at the final step. CD4+ T cells are shown as percentage of lymphocytes. CD25+CD127- cells and CD127-Foxp3+ cells are shown as percentage of CD4+ T cells.

Cord Blood

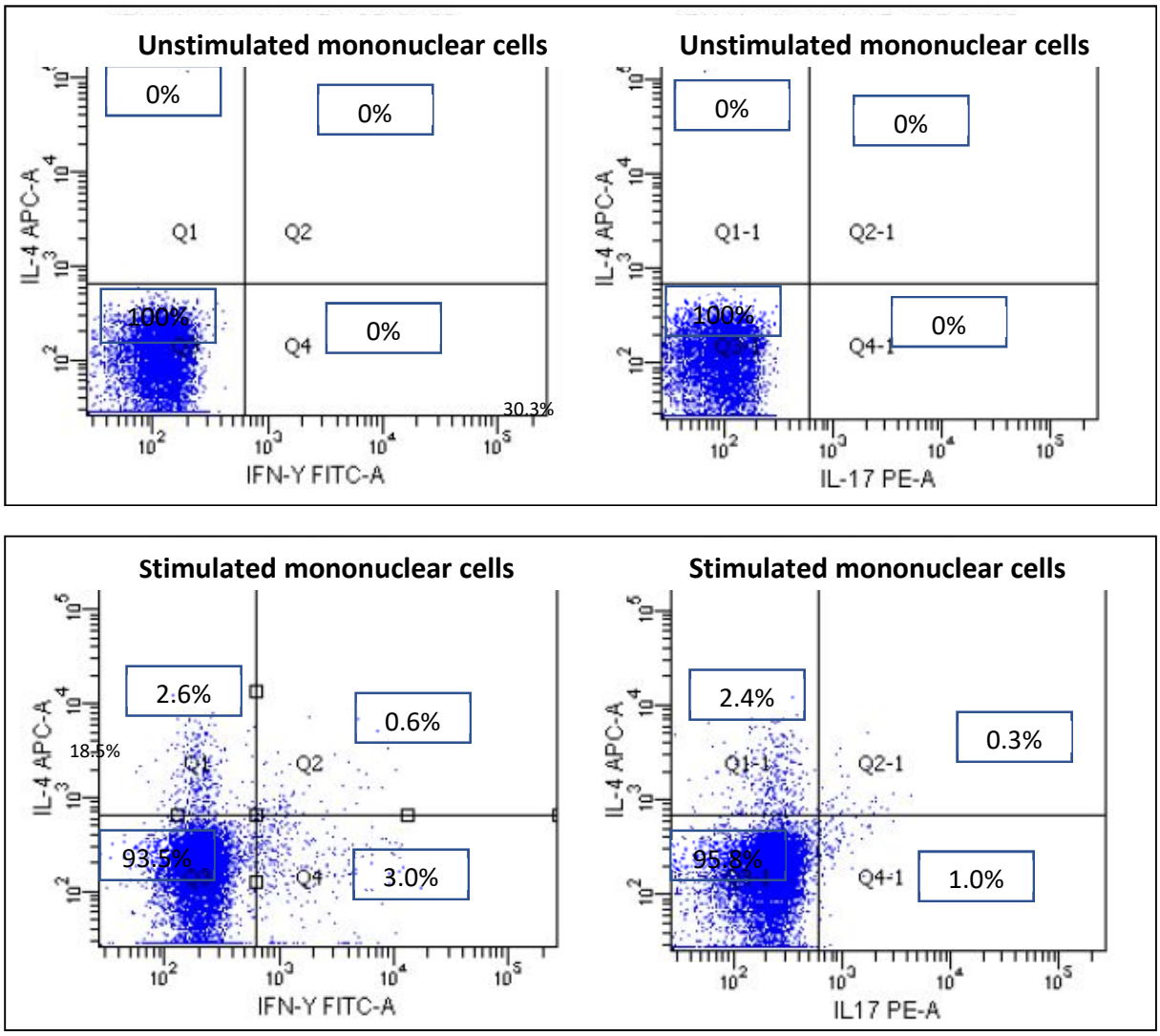

Figure 17: Representative flow cytometry dot plots of IFN-γ secreting Th1 cells, IL-4 secreting Th2 cells and IL-17 secreting Th17 cells are shown on T cells isolated from T-replete CBT recipients after 30 days of transplant. Unstimulated control and PMA-Ionomycin stimulated T cells are shown in the top and bottom panel respectively.

Peripheral Blood

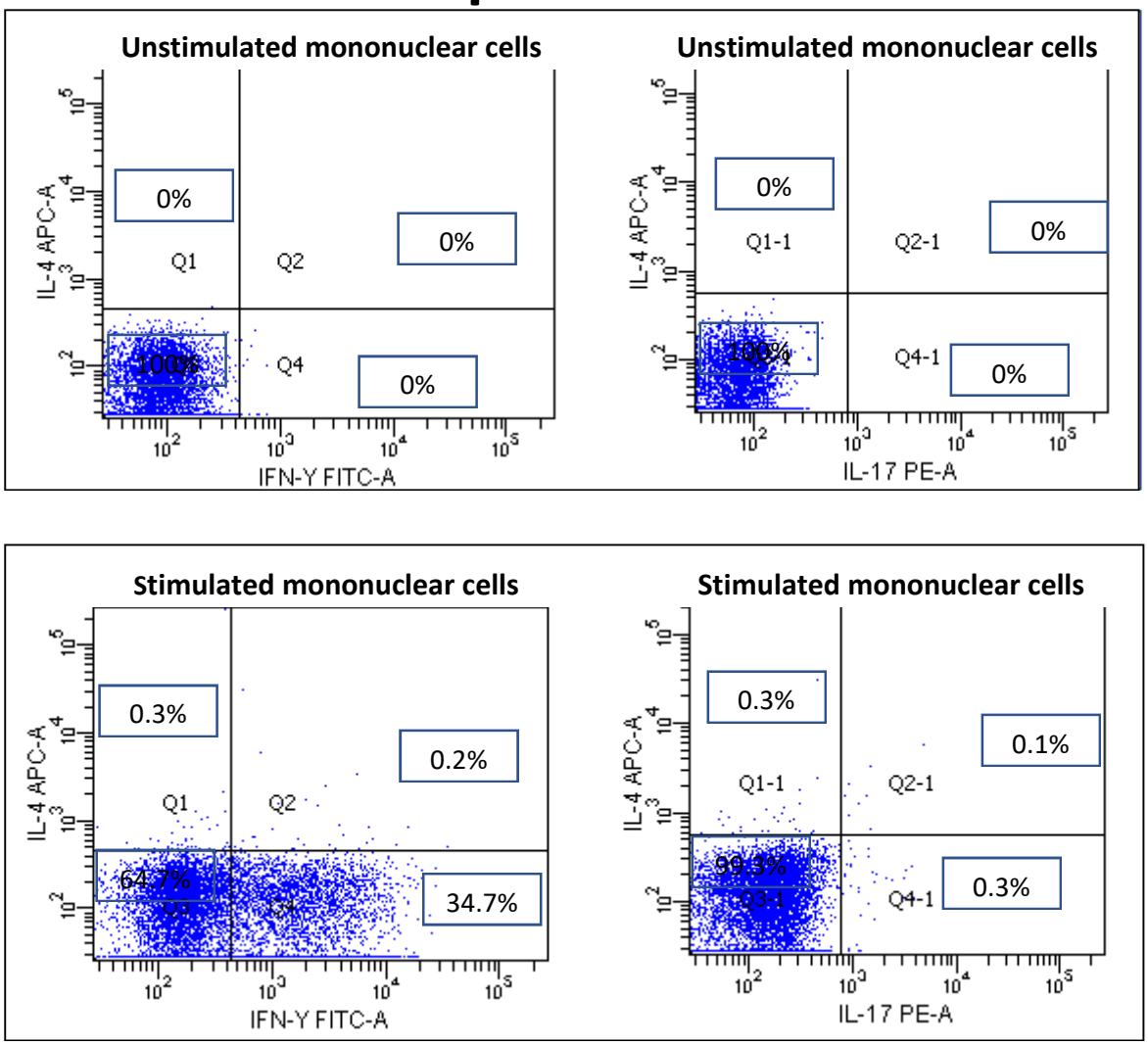

Figure 18: Representative flow cytometry dot plots of IFN-γ secreting Th1 cells, IL-4 secreting Th2 cells and IL-17 secreting Th17 cells are shown on T cells isolated from T-replete BMT recipients after 30 days of transplant. Unstimulated control and PMA-Ionomycin stimulated T cells are shown in the top and bottom panel respectively.

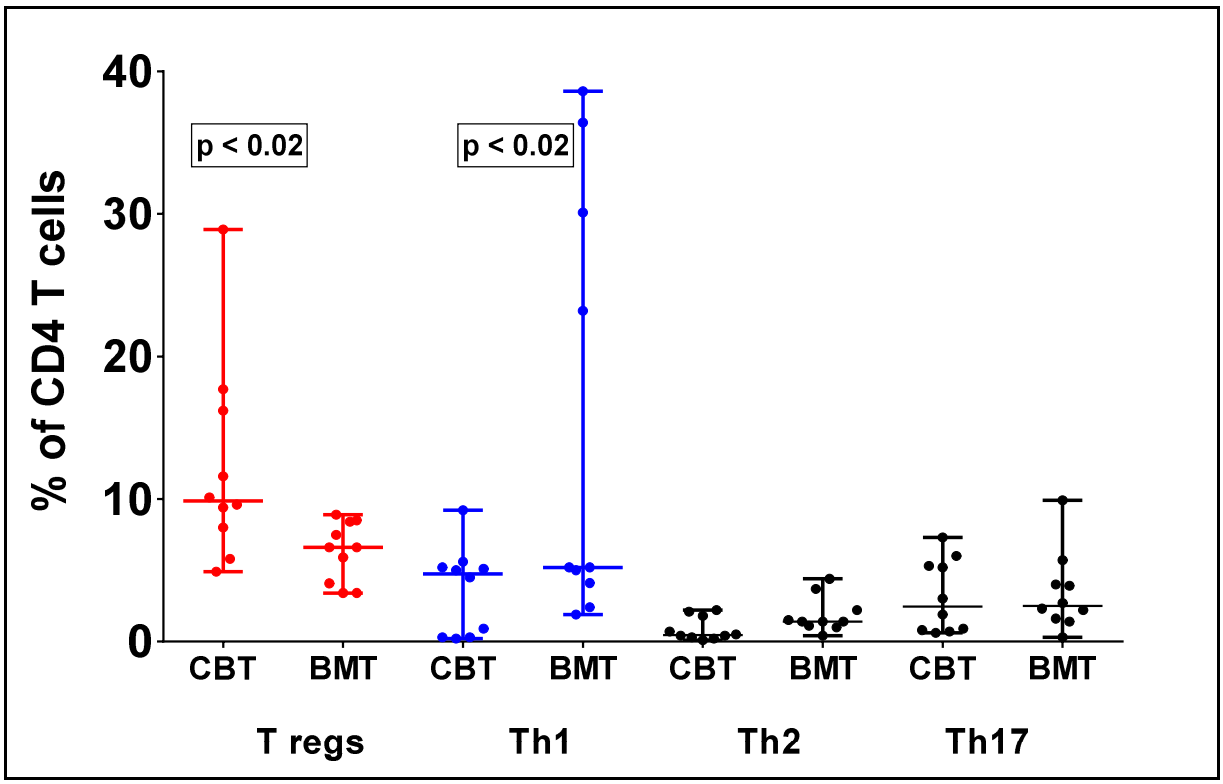

Figure 19: Median and range of T-regulatory, Th1, Th2 and Th17 cells, one month after CBT (*n=10*) and BMT (*n=10*). T-regulatory cells were significantly higher after CBT, in contrast to Th1 cells after BMT.

At 1-month post-transplant, we observed a higher percentage of circulating $CD4^+$ T cells with a T-regulatory phenotype after cord blood transplantation (median = 9.8%, inter-quartile range = 7.4 – 16.5) compared to bone marrow transplantation (median = 6.6%, range = 3.9 – 8.4). In contrast, a lower percentage of Th1 (IFN-γ secreting $CD4^+$ T cells) were observed after cord blood transplantation (median = 4.7%, inter-quartile range = 0.3 – 5.3) compared to bone marrow transplantation (median = 5.2%, inter-quartile range = 3.6 – 31.6) [Figure 16, 17, 18 and 19]. These two observations were statistically significant ($P < 0.02$). No significant differences were observed in circulating Th2 and Th17 cells in the 2 groups [Figure 17, 18 and 19].

Increased percentage of circulating T-regulatory cells observed at 1 month after cord blood grafts reduced significantly at day 180 to a median of 5.4 (interquartile range = 8.9 to 2.1) without increase in Th1 cells. In contrast to this finding, Th1 cells continued to increase following bone marrow transplantation [Figure 20 and 21]. These results confirm the findings of other co-workers suggesting the inability of cord blood $CD4^+$ T cells to secrete pro-inflammatory cytokines like IFN-γ (Krampera *et al.,* 2000; Wiegering *et al.,* 2009).

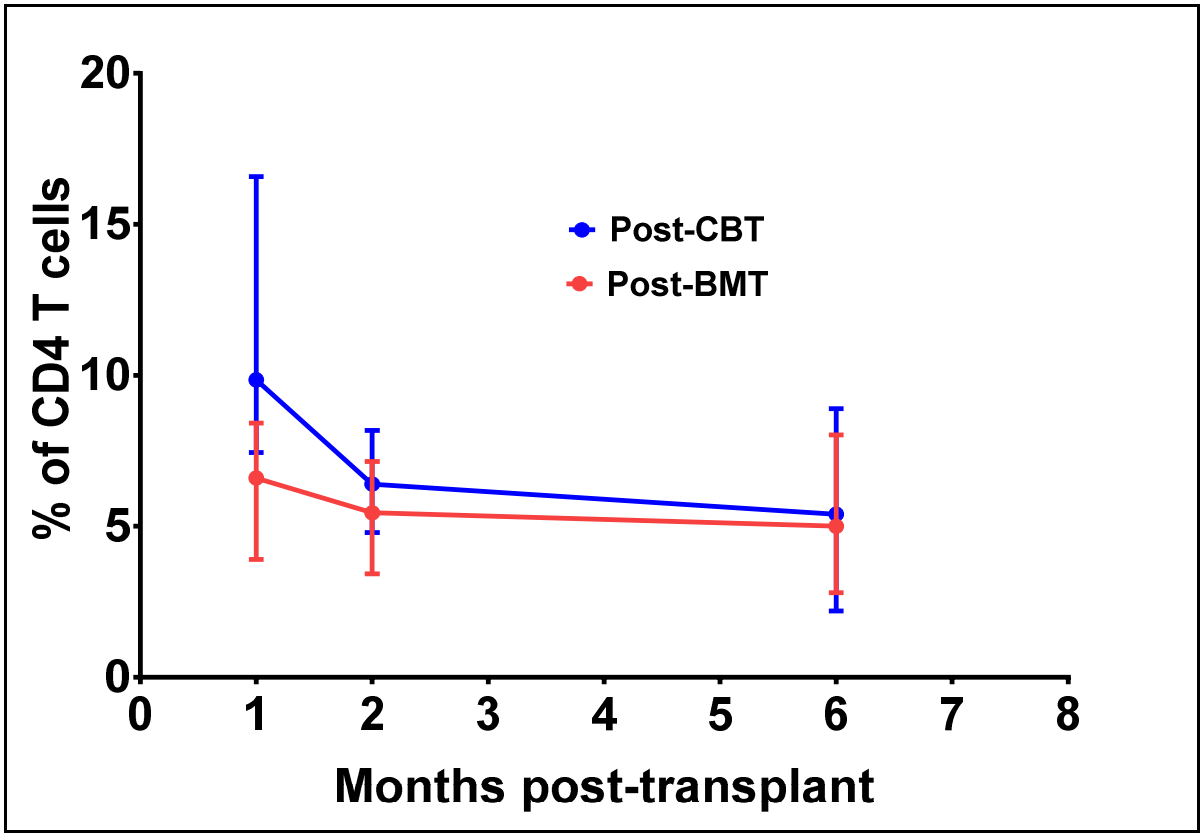

Figure 20: Line graph showing percentage of T-regulatory cells after transplant (median and inter-quartile range shown). A higher percentage of T-regulatory cells after CBT ($n=10$) compared to BMT ($n=10$) was observed ($p < 0.02$). The higher percentage of T-regulatory cells after CBT decreases and reaches levels similar to BMT after 6 months.

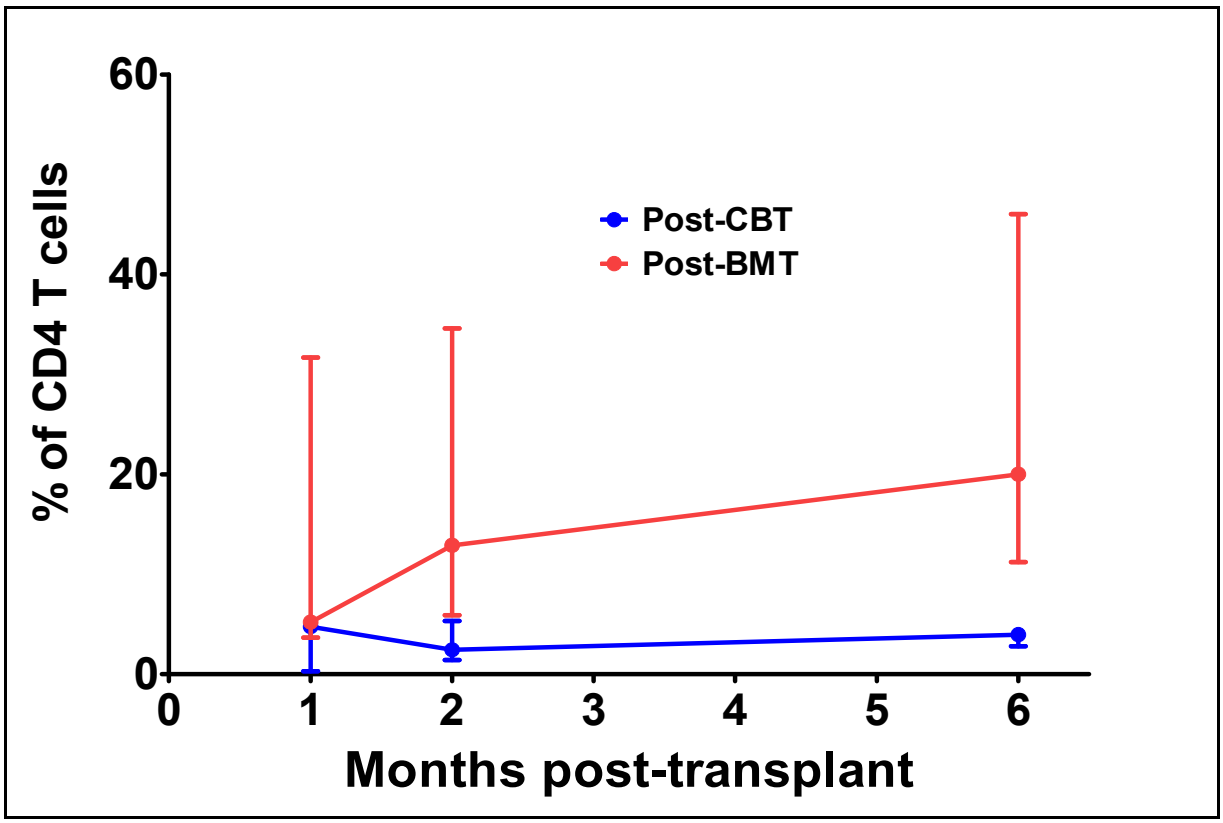

Figure 21: Line graph showing percentage of Th1 cells after transplant (median and inter-quartile range shown). A lower percentage of Th1 cells after CBT (*n=10*) compared to BMT (*n=10*) was observed ($P < 0.02$). The percentage of Th1 cells after CBT remained lower at 6 months post-transplant.

This finding indicates that although increased percentage of $CD4^+$ T cells adopt a T-regulatory fate early after cord blood transplantation, the majority of circulating $CD4^+$ T cells remain non-regulatory. These non-regulatory T cells however do not seem to adopt a functional phenotype such as Th1, Th2 or Th17 on PMA/Ionomycin stimulation.

3.6 Differentiation of reconstituting CD4$^+$ T cells after CBT and BMT

We therefore investigated how rapidly reconstituting naïve cord blood T cells switched their phenotype to memory or effector T cells.

To investigate this CD4$^+$, CD45RA$^+$ and CD27$^+$ markers were used and naïve, memory and effector CD4$^+$ T cells at 1, 2 and 3 after cord blood transplantation *(n=10)* were identified. Figure 22 shows percentage of naïve CD4$^+$ T cells decreased rapidly from first month with a rapid shift towards memory phenotype. In contrast, the percentage of memory CD4$^+$ T cells decreased rapidly after first month with a shift towards effector phenotype in patients undergoing bone marrow transplantation (*n=10*).

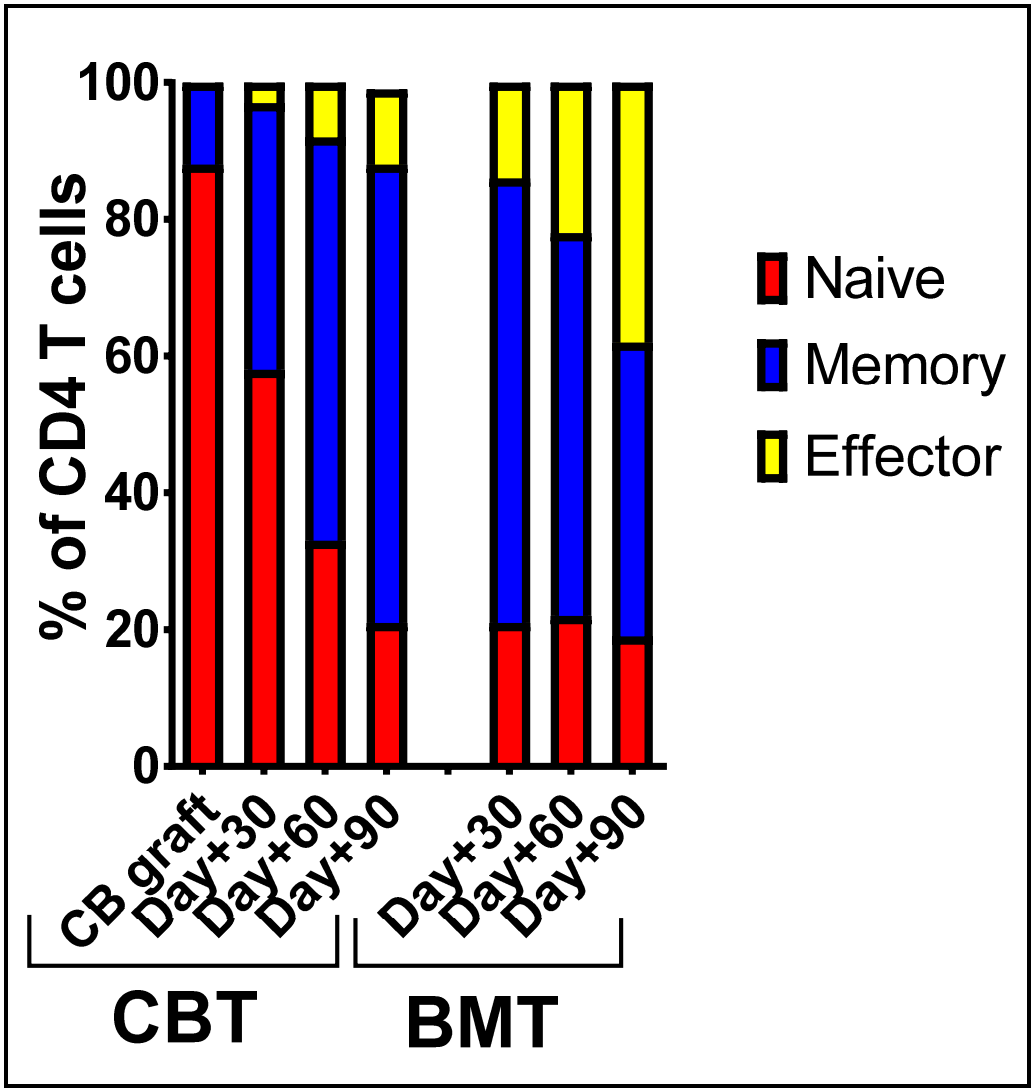

Figure 22: Rapid switch of phenotype from naïve to memory/effector was observed after CBT (*n=10*). In contrast, switch of phenotype from memory to effector was observed after BMT (*n=10*). Median percentage of naïve, memory and effector T cells are shown.

3.7 IL-7 levels after cord blood and bone marrow transplantation

Rapid switching of naïve $CD4^+$ T cells to memory phenotype indicated that this switching in phenotype may be driven by homeostatic mechanisms (Cho *et al.,* 2000). IL-7 is the key homeostatic cytokine and, inverse correlation between $CD4^+$ T cell reconstitution and IL-7 is well-established (Politikos *et al.,* 2015). We therefore investigated whether IL-7 levels declined rapidly after CBT.

We measured plasma IL-7 level at day+30, day+60 and day+90 following CBT (CBT = *6,* BMT = 6). Median plasma level on day+30 after CBT was 14.45 pg/ml (interquartile range = 12 – 16). Plasma IL-7 level decreased significantly to median of 5.1 (interquartile range = 3.3 – 6.9) on day+90 (*P < 0.0001*). In contrast, there was no statistically significant difference between day+30, day+60 and day+90 plasma IL-7 levels after BMT. Median IL-7 levels were 5.5 *vs* 4.1 *vs* 6.5 respectively [Figure 23].

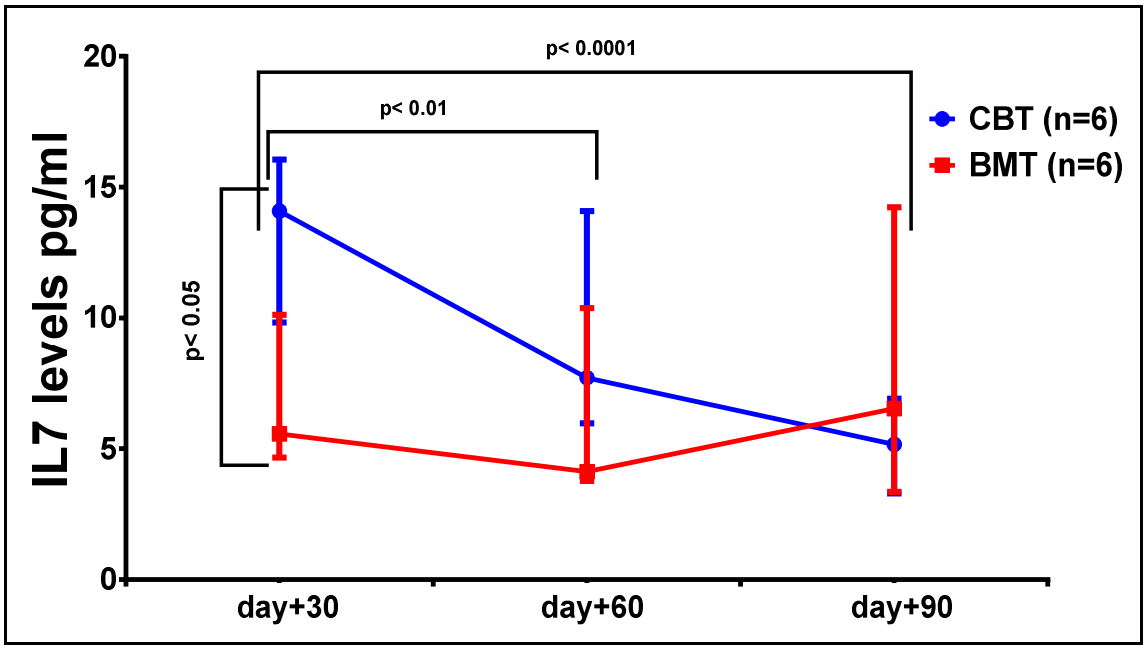

Figure 23: High IL-7 levels at day+30 after CBT (*n=6*) declined rapidly at day+90 (*P < 0.0001*). There was no difference in IL-7 levels at day+30, day+60 and day+90 after BMT (*n=6*).

The high day+30 IL-7 levels possibly reflect the profound lymphopenic environment due to low number of T cells carried with the cord blood graft as previously described (Politikos *et al.,* 2015), and suggests that the cord blood T cells are likely to be exposed to high levels of IL-7 *in vivo* for a longer period of time.

The rapid decline in IL-7 in first 3 months after CBT indicates the role of IL-7 in mediating $CD4^+$ T-cell biased proliferation after CBT.

3.8 CONCLUSION

Early T-cell reconstitution after cord blood transplantation is rapid compared to that of bone marrow transplantation.

T-cell reconstitution after cord blood transplantation is almost always $CD4^+$ T-cell biased compared to $CD8^+$ T-cell biased reconstitution after bone marrow transplantation.

Although early $CD4^+$ T-cell reconstitution after cord blood transplantation is biased towards T-regulatory cells, the majority of circulating T cells were non-regulatory.

In contrast, early $CD4^+$ T-cell reconstitution after bone marrow transplantation is biased towards Th1 cells.

Naïve cord blood T cells rapidly differentiate to memory T cells after cord blood transplantation and this rapid switching to memory phenotype with decline in IL-7 points towards a process of lymphopenia-induced proliferation.

Chapter four

Cord blood T cells are highly sensitive to homeostatic signals (such as TCR and IL-7) in comparison to adult blood T cells

4.0 Aims

1) To study the proliferation of cord blood and adult blood T cells after IL-7, IL-2 and IL15 stimulation using CFSE dye dilution assay

2) To study the differences in IL-7 receptor expression in cord blood and adult blood T cells

3) To study the differences in STAT5 phosphorylation after IL-7 and IL-2 stimulation

4) To study the proliferation of cord blood and adult blood T cells after TCR stimulation using CFSE dye dilution assay

5) To study the proliferation of naïve cord blood and adult blood T cells after TCR stimulation using CFSE dye dilution assay

4.1 Introduction

T-cell homeostasis i.e. survival, proliferation and expansion is mediated by co-operation between homeostatic TCR and IL-7 signals (Surh *et al.,* 2000; Jameson *et al.,* 2005; Deshpande *et al.,* 2013; Hennion-Tscheltzoff *et al.,* 2013; Kimura *et al.,* 2013). It is well known that T cells do not survive in the absence of either self MHC:TCR interactions or IL-7. $CD4^+$ and $CD8^+$ T cells do not survive in the absence of MHC Class II and MHC Class I deficiency respectively. This observation has been well-established in several MHC-deficient models as well as in patients with MHC Class II or Class I deficiency (Brocker *et al.,* 1997; Markiewicz *et al.,* 2003). Similarly, a defect in the IL-7 receptor leads to a $T\text{-}B^+NK^+$ severe combined immunodeficiency (Puel *et al.,* 1998).

Naïve T cells, in particular require both MHC interactions and IL-7 for survival. How these two signals co-operate and maintain T-cell homeostasis during lympho-replete and lympho-depleted conditions is still being understood. Lymphocyte homeostasis in lympho-replete and lympho-deplete conditions are distinct (Surh *et al.,* 2000). In lympho-replete conditions low-affinity TCR:MHC interactions in the periphery provide tonic "survival signals" to naïve T cells without inducing cell division (Surh *et al.,* 2000). However, in lymphopenic environment same homeostatic signals induce T-cell proliferation which is commonly known as lymphopenia-induced homeostatic proliferation (Tchao *et al.,* 2012). In particular, the strength of TCR affinity determines the relative fitness of naïve T cells to compete for factors that support cell survival and homeostatic proliferation (Kieper *et al* 2004; Min *et al.,* 2005).

Recently it has been shown that T-cell receptor triggering modulates the response to IL-7 (Hennion-Tscheltzoff *et al.,* 2013). Increasing T-cell receptor stimulation augments the response to IL-7 and reducing T-cell receptor stimulation decreases the response to IL-7. Another interesting study showed that intermittent IL-7 signalling is essential for survival of T cells (Kimura *et al.,* 2013). In the absence of homeostatic T-cell receptor signalling, naïve T cells receive persistent IL-7 signalling, which instead of promoting survival induce cytokine-induced (IFN-γ) cell death. These reports clearly indicate that T-cell receptor signalling and IL-7 signalling pathways co-operate in maintaining T-cell homeostasis.

T-cell homeostasis in cord blood and adult blood may be regulated distinctly. This is because Cord blood T cells are in a highly proliferative state driven by the relatively lymphopenic environment of the foetus in combination with maximal thymopoiesis (Schonland *et al.,* 2003; Min *et al.,* 2003). In contrast, adult blood T cells are in a state of equilibrium in the lympho-

replete environment and reduced thymopoiesis. We therefore speculated that cord blood T cells may be highly responsive to homeostatic signals compared to adult blood T cells.

In this chapter, we explored if there are differences in these homeostatic mechanisms between cord blood and adult blood T cells. We compared whether cord blood and adult blood T cells responded differently to γ-chain cytokines. In particular, we compared the proliferative potential of T cells to homeostatic cytokines such as IL-7 and IL15, and a conventional cytokine such as IL-2. We also studied differences in IL-7 receptor expression in the cord blood and adult blood T cells and the effect of IL-2 and IL-7 on down-stream signalling such as STAT-5 phosphorylation. Finally, we studied if cord blood T cells and adult blood T cells responded distinctly to T-cell receptor stimulation.

4.2 Comparing the proliferation of cord blood and adult blood T cells to γ-chain cytokines i.e. IL-7, IL-15 and IL-2 using CFSE dye dilution assay

Cord blood mononuclear cells (*n = 5*) and adult blood mononuclear cells (*n = 5*) were labeled with CFSE and stimulated with IL-7 (10 ng/ml), IL-15 (12 ng/ml) and IL-2 (20 U/ml) for 9 days in serum-free media.

Following stimulation with IL-7 (10 ng/ml), we observed that cord blood T cells proliferated rapidly. In comparison to the proliferative index of 1.1 in the adult blood T cells, cord blood T cells had a significantly higher proliferative index of 3. This indicates that in the presence of IL-7, cord blood T cells undergo robust proliferation whereas adult blood T cells undergo minimal proliferation [Figure 24, 25, 26 and 27].

On stimulation with IL-15 (12 ng/ml), cord blood $CD8^+$ T cells proliferated more rapidly with a proliferative index of 1.9, compared to cord blood $CD4^+$ T cells which proliferated at an index of 1.4. Adult blood T cells were not responsive to IL-15 [Figure 24, 25, 26 and 27].

Cord blood and adult blood T cells were not responsive to IL-2 at the concentration of 20 U/ml [Figure 24, 25, 26 and 27].

Thus, our observations confirmed that cord blood T cells are hyper-responsive to IL-7, in comparison to adult blood T cells.

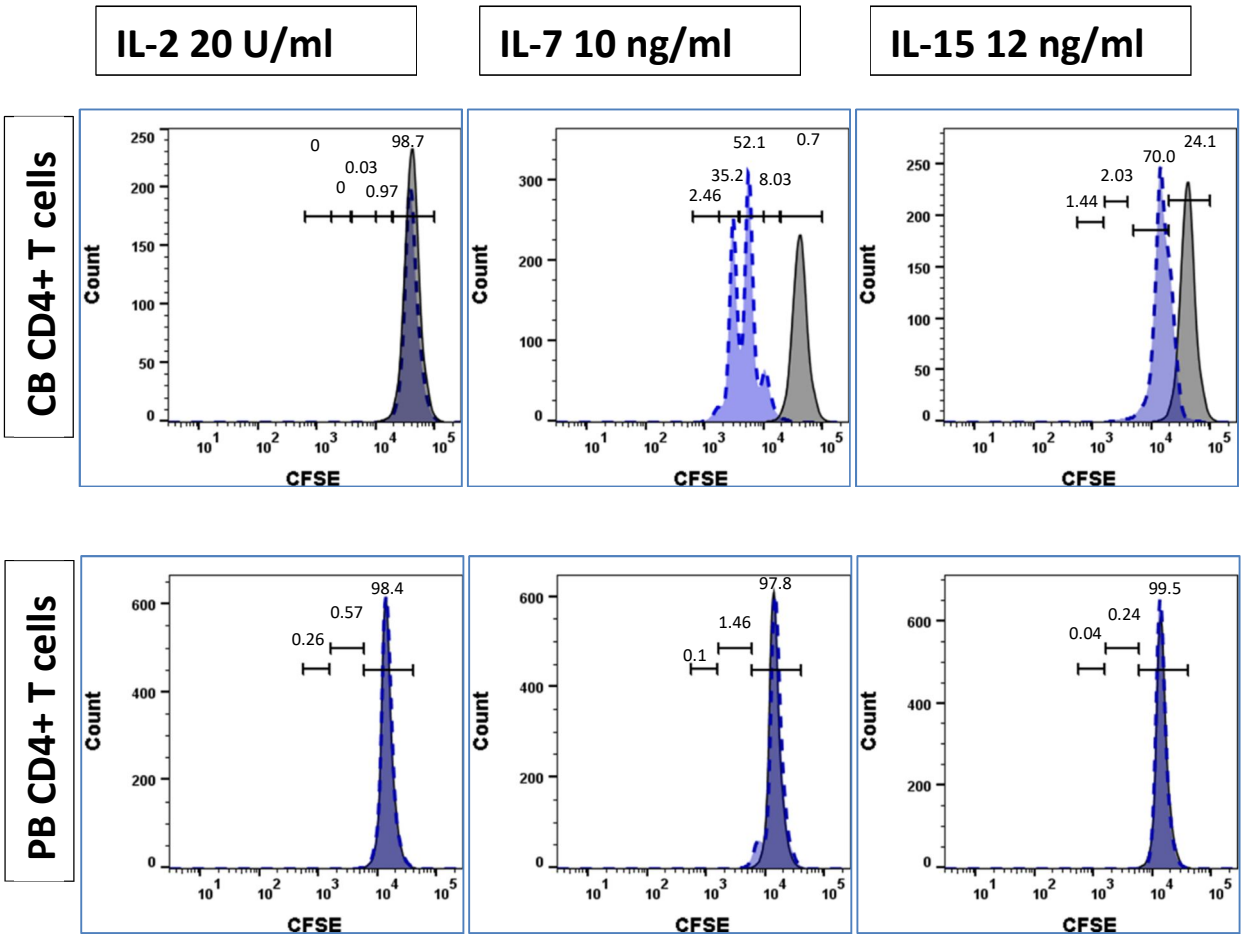

Figure 24: Representative histogram plots of cord blood $CD4^+$ T cells proliferating rapidly in the presence of 10 ng/ml of IL-7. There was some proliferation in the presence of 12 ng/ml of IL-15 and no proliferation in the presence of 20 U/ml of IL-2. Solid line histogram represent cells cultured without cytokine and dashed line histogram represent cells cultured in cytokine. An example of cord blood CD4+ T-cell proliferation in response to IL7 is used below to demonstrate calculation of proliferative index.

Generation	Total number of cells	Total number of parent cells
1	45	45/1=45
2	147	147/2=73.5
3	2104	2104/3=701.3
4	3116	3116/4=779
5	480	480/5=96
Total	**5892**	**1694.8**
Proliferative index = 5892/1694.8 =3.47		

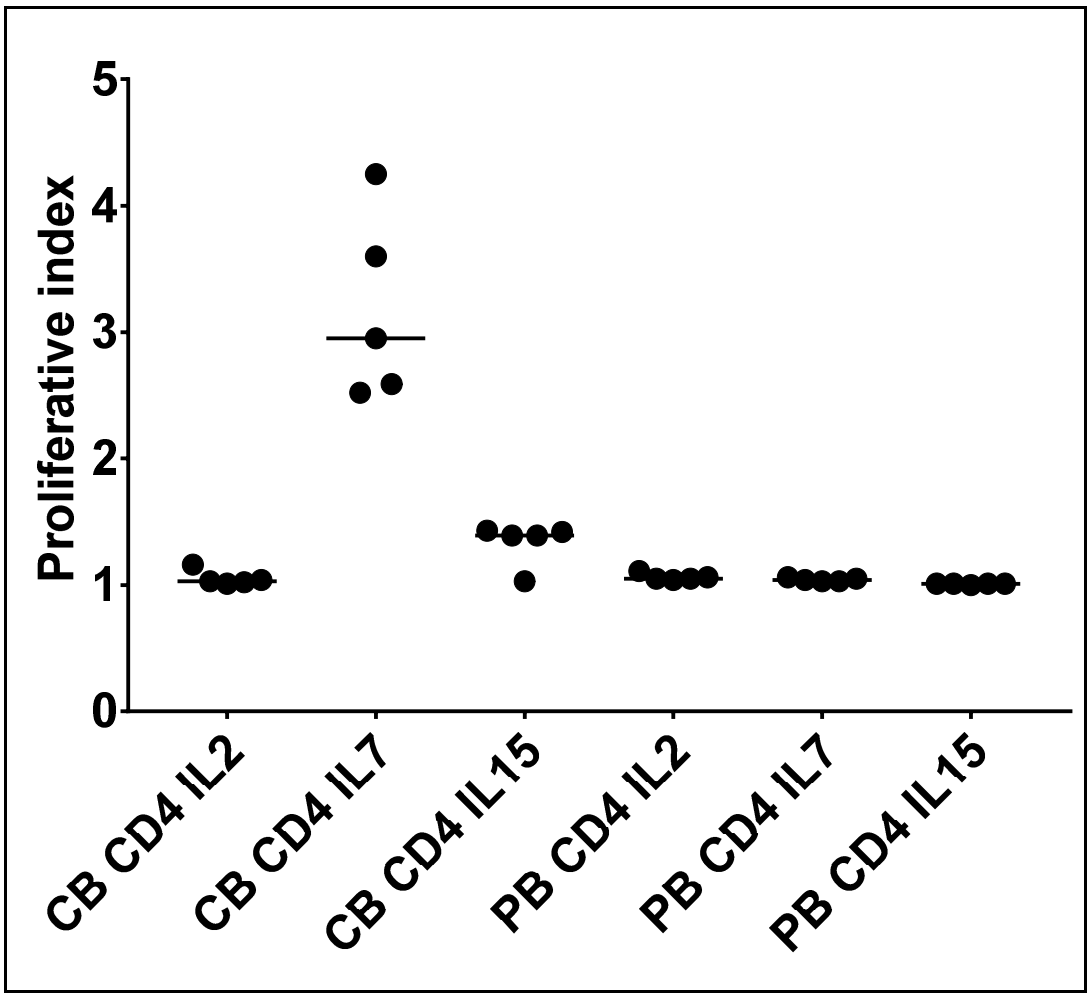

Figure 25: Cord blood $CD4^+$ T cells proliferate rapidly with proliferative index of 3 and 1.4 following stimulation with IL-7 (10 ng/ml) and IL-15 (12 ng/ml) respectively. Cord blood $CD4^+$ T cells do not proliferate in the presence of IL-2 (20 U/ml). In contrast, peripheral blood $CD4^+$ T cells do not proliferate in the presence of IL-7, IL-15 or IL-2 (n = 5 vs 5).

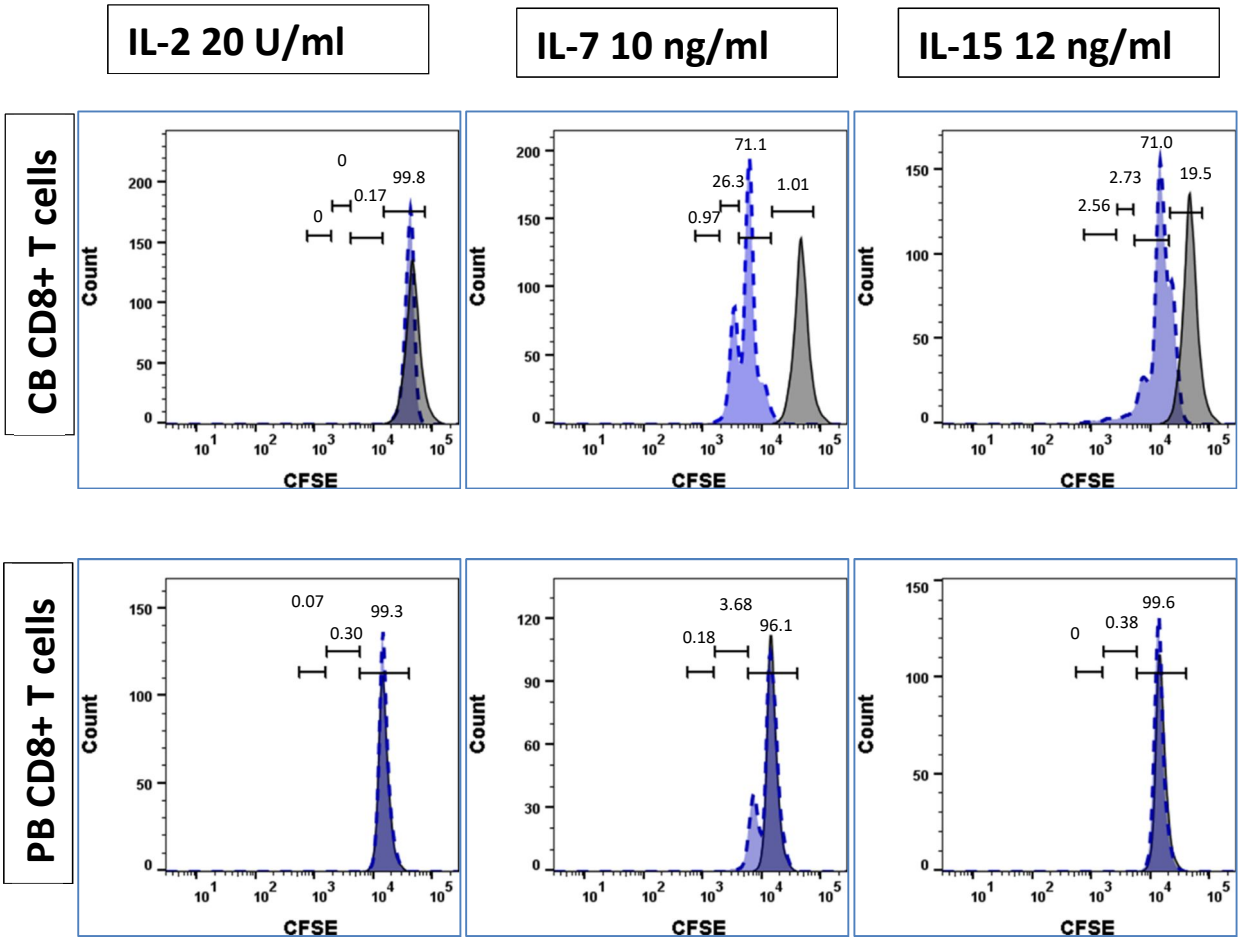

Figure 26: Representative histogram plots of cord blood $CD8^+$ T cells proliferating rapidly in the presence of 10 ng/ml of IL-7. There was some proliferation in the presence of 12 ng/ml of IL-15 and no proliferation in the presence of 20 U/ml of IL-2. Solid line histogram represent cells cultured without cytokine and dashed line histogram represent cells cultured in cytokine.

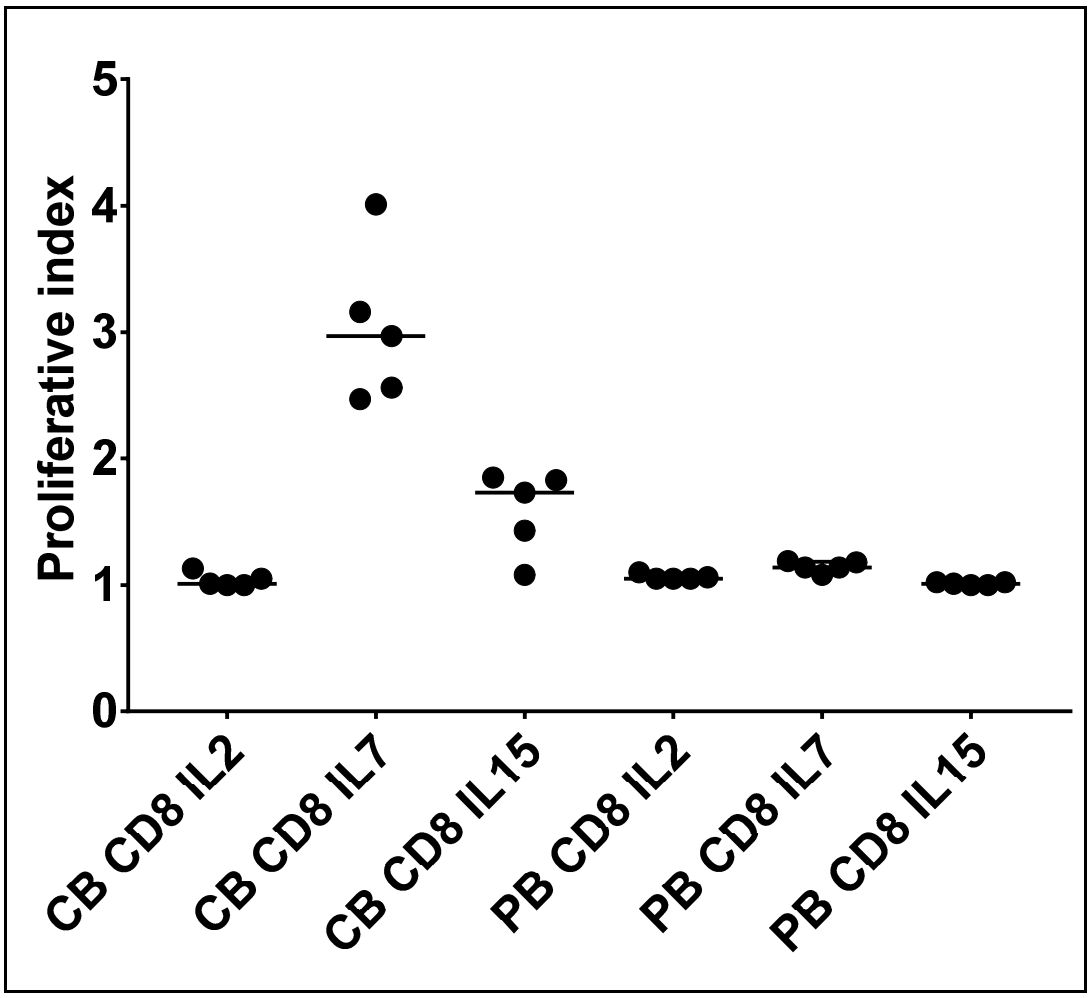

Figure 27: Cord blood $CD8^+$ T cells proliferate rapidly with a median proliferative index of 3 and 1.9 following stimulation with IL-7 (10 ng/ml) and IL-15 (12 ng/ml) respectively. Cord blood $CD8^+$ T cells do not proliferate in the presence of IL-2 (20 U/ml). In contrast, peripheral blood $CD8^+$ T cells do not proliferate in the presence of IL-7, IL-15 or IL-2 (n = 5 vs 5).

4.3 Comparing the IL7R expression in the cord blood and adult blood T cells

Since cord blood T cells are hyper-responsive to IL-7, we compared the IL7R expression of cord blood and adult blood T cells. More than 90% (range = 90 to 97%) of cord blood T cells were positive for IL7R (CD127) whereas, a median of 80% (range = 78 to 84%) and 68% (range = 58 to 78%) of adult $CD4^+$ and $CD8^+$ T cells expressed IL7R (CD127) respectively [Figure 28 and 29]. Similarly, level of IL7R expression, as assessed by median fluorescence intensity was higher in cord blood T cells compared to adult blood T cells [Figure 30]. This finding suggested that upregulated IL7R expression in the cord blood T cells may mediate hyper-responsiveness of cord blood T cells to IL-7.

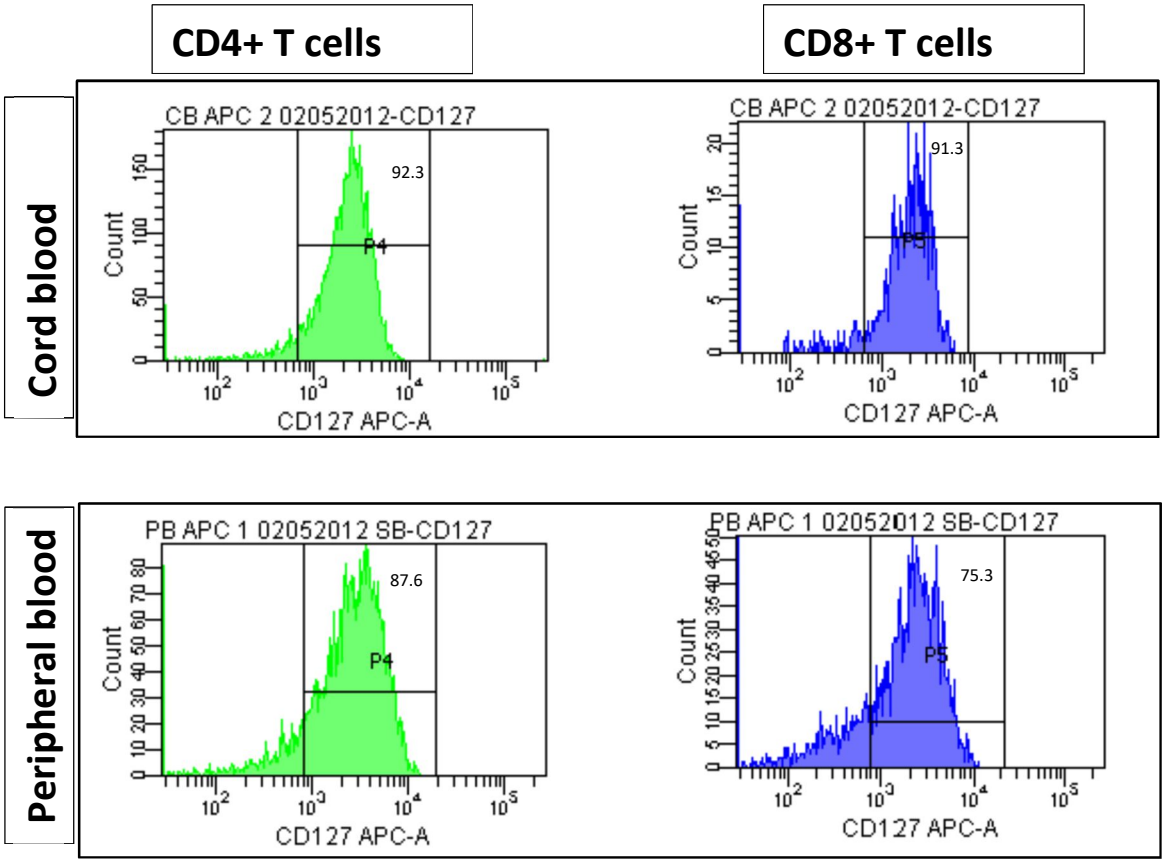

Figure 28: Representative histogram of IL-7R (CD127) expression in cord blood and peripheral blood $CD4^+$ and $CD8^+$ T cells. CD127+ gates were defined using isotype control for each patient.

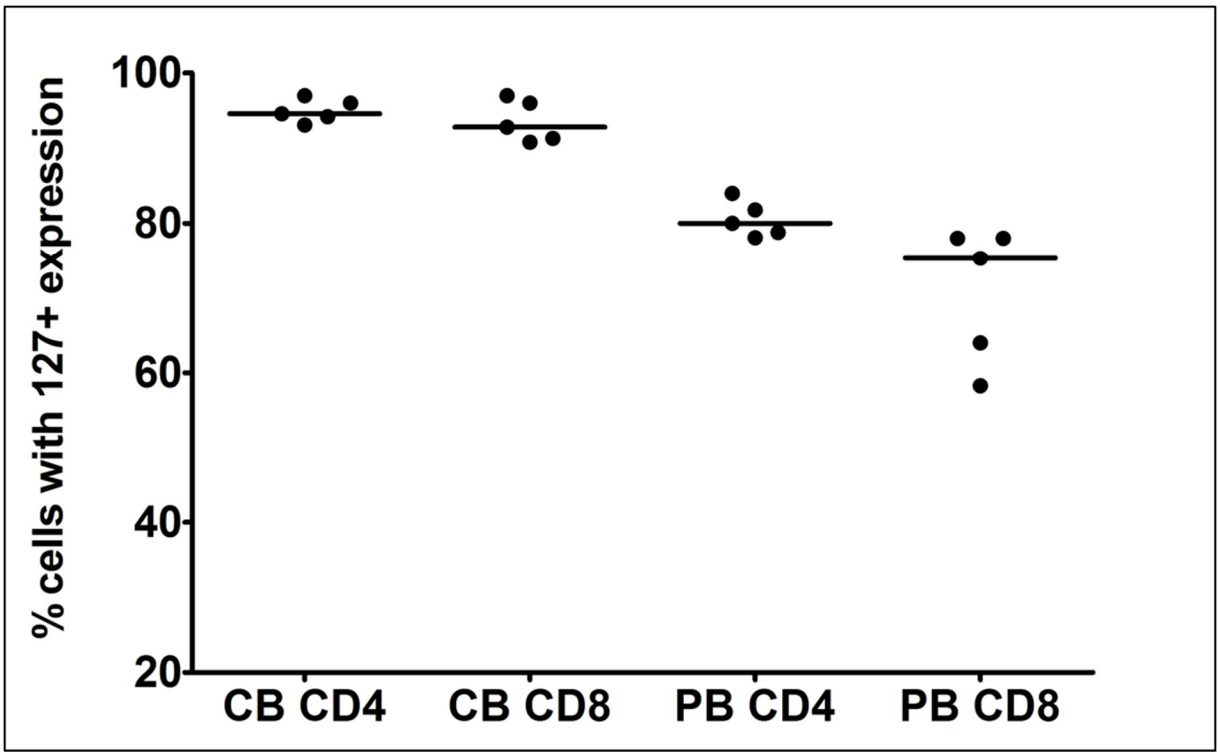

Figure 29: Percentage of IL7R (CD127) positive were higher in cord blood T cells than adult blood T cells (n = 5 *vs* 5; unpaired t-test; *p<0.001*).

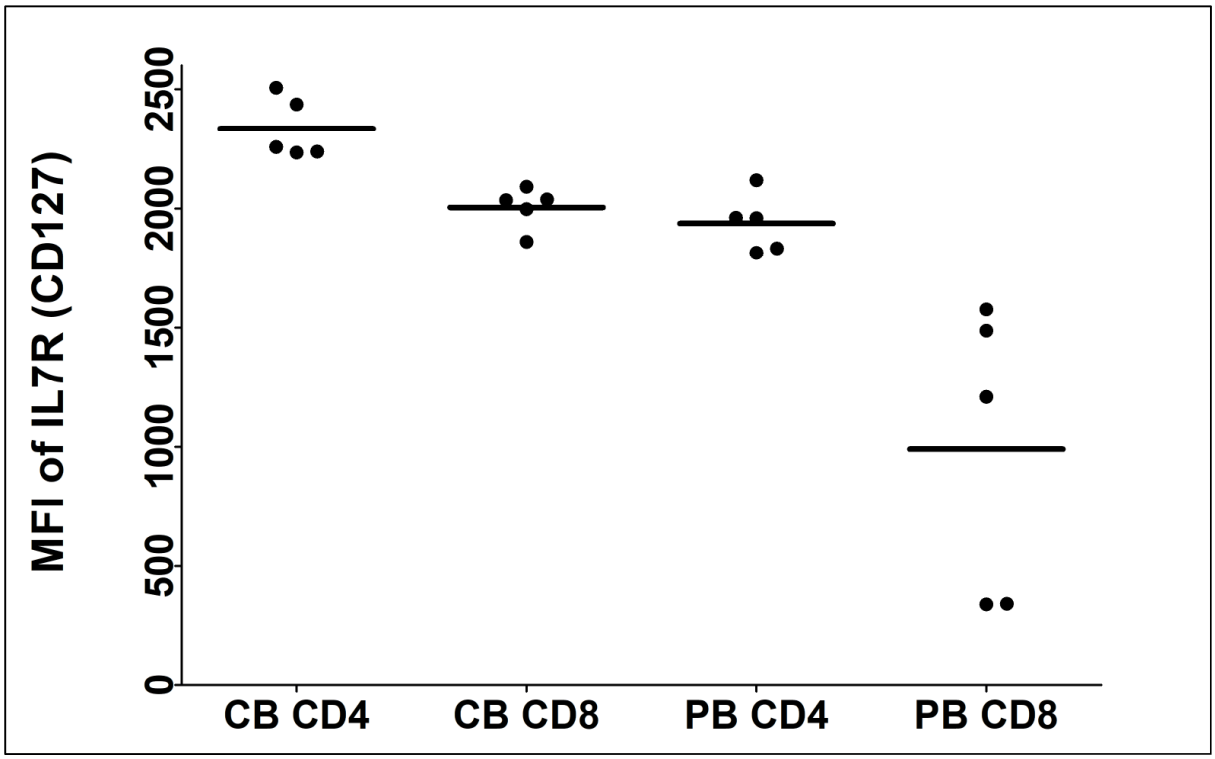

Figure 30: Median fluorescence intensity of IL7R (CD127) was higher in cord blood T cells than in adult blood T cells (n = 5 *vs* 5; unpaired t-test; *p<0.001*).

4.4 Comparing the STAT5 phosphorylation in the cord blood and adult blood T cells

IL-7 is known to activate JAK1 and JAK3 as well as STAT5, which translocates to the nucleus, where it functions as a transcription factor. Since cord blood T cells are hyper-responsive to IL-7 and have increased IL7R expression, we speculated that downstream signalling molecules i.e. STAT5 may undergo increased phosphorylation on stimulation with IL-7. We therefore measured STAT5 phosphorylation in cord blood $CD4^+$ and peripheral blood $CD4^+$ T cells after stimulating CBMCs and PBMCs with varying concentrations of IL-7 (10 ng/ml,1 ng/ml, 0.1 ng/ml, 0.01 ng/ml) and IL-2 (1000 units/ml, 100 units/ml, 20 units/ml). Low level (<10%) STAT5 phosphorylation in cord blood and peripheral blood $CD4^+$ T cells was observed after stimulation with IL-2, regardless of the concentration used. In contrast, following IL-7 stimulation with 10/1/0.1/0.01 ng/ml, STAT5 phosphorylation was observed in 90%, 70%, 10% and < 10% in both cord blood and peripheral blood $CD4^+$ T cells [Figure 31 and 32].

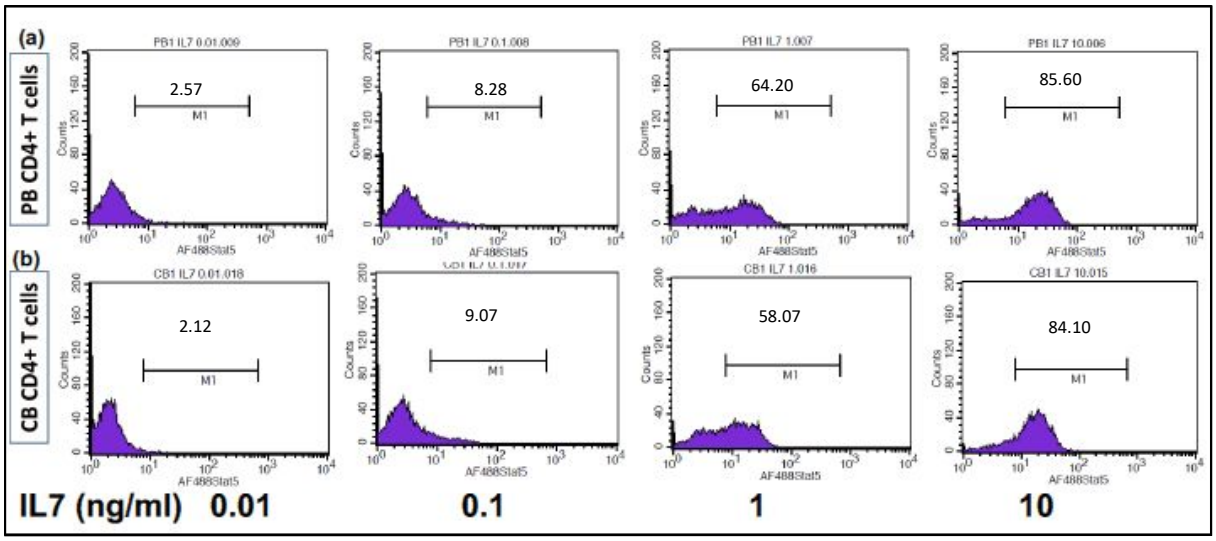

Figure 31: Representative histogram of STAT5 phosphorylation in cord blood and peripheral blood $CD4^+$ T cells to varying degrees of IL-7. Percentage of STAT5 phosphorylated cord blood and peripheral blood CD4+ T cells are shown. Gates were defined using cord blood and peripheral blood CD4+ T cells not stimulated with cytokines.

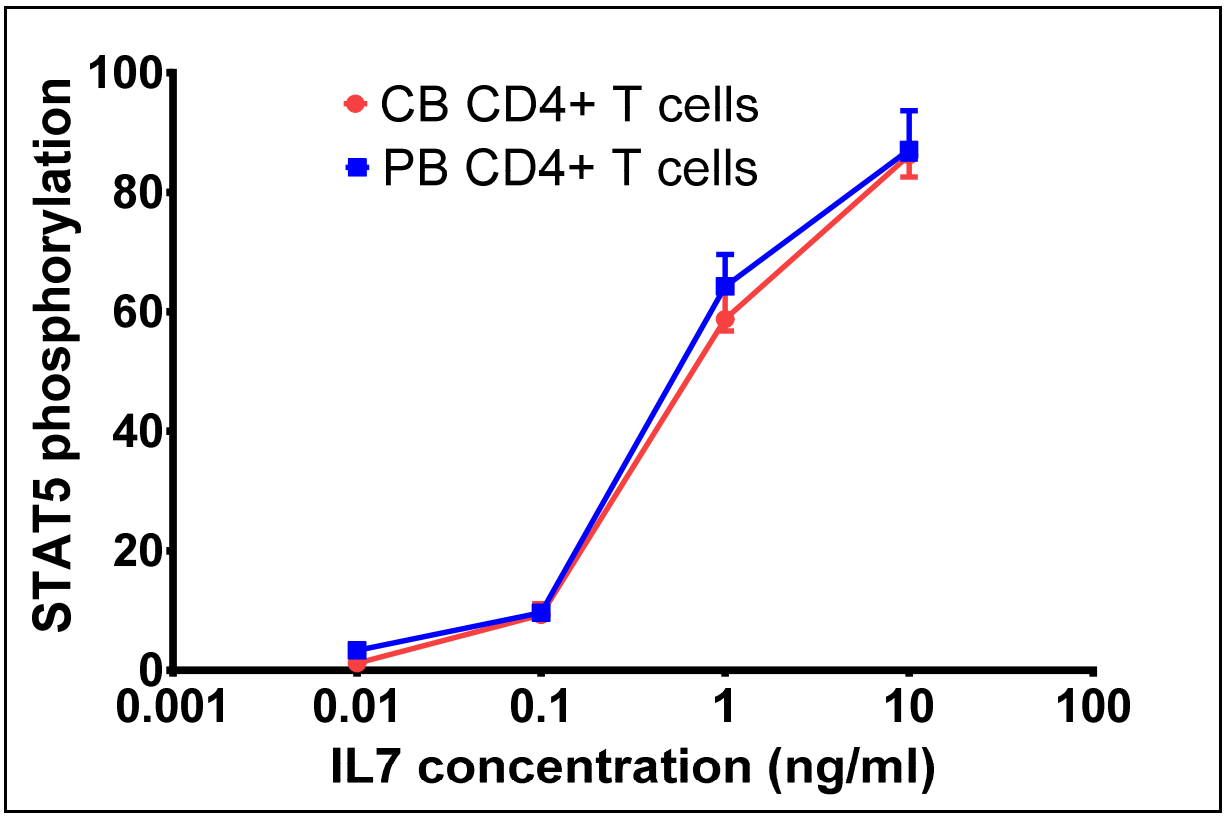

Figure 32: Line graph of STAT5 phosphorylation in cord blood and peripheral blood $CD4^+$ T cells to varying degrees of IL-7. Percentage of STAT5 phosphorylated cord blood and peripheral blood CD4+ T cells are shown. Similar STAT5 phosphorylation was observed in 5 *vs* 5 samples.

Thus, STAT5 phosphorylation in both cord blood and peripheral blood $CD4^+$ T cells occurs in response to IL-7 in a dose dependent manner. This suggests similar down-stream signalling in cord blood and peripheral blood T cells in response to IL-7. It is well-described that although STAT5 phosphorylation occurs in the presence of 1 ng/ml of IL-7, CD4+ T cells do not proliferate in response at the concentration of 1 ng/ml of IL-7 (Swainson *et al*., 2007). Thus, ligation of IL7Ralpha receptor does not explain the differences in proliferation between cord blood and peripheral blood T cells.

4.5 Comparing the T-cell receptor signalling in the cord blood and adult blood T cells

Since an important downstream signalling molecule of IL-7 signalling pathway - STAT5 did not differentially phosphorylate on stimulation with varying concentrations of IL-7, I questioned if upregulated T-cell receptor signalling mediated enhanced proliferation of cord blood T cells.

Cord blood mononuclear cells ($n = 5$) and peripheral blood mononuclear cells ($n = 5$) were labelled with CFSE dye and stimulated with immobilized-CD3 antibody for 7 days in serum free medium to examine TCR-triggered proliferation. We found that by day 7, a high proportion of cord blood $CD4^+$ (mean = 83%, range = 75 to 87%) and cord blood $CD8^+$ (mean = 92%, range = 81% to 99%) T cells go in to cell cycle compared to peripheral blood $CD4^+$ (mean = 19%, range = 9 to 30%) and peripheral blood $CD8^+$ (mean = 42%, range = 34 to 56%) T cells respectively [Figure 33, 34 and 35].

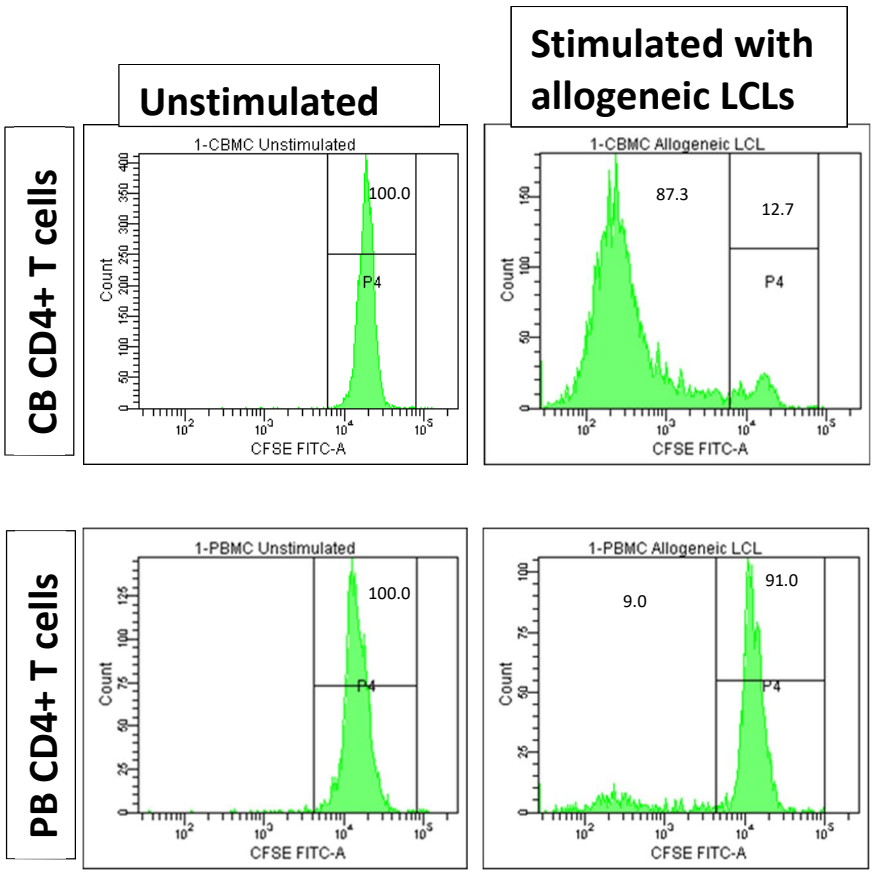

Figure 33: Representative histogram plots of cord blood $CD4^+$ T-cell vs peripheral blood $CD4^+$ T-cell proliferation in response to allogeneic LCLs (at ratio 10 responders:1 allogeneic stimulator). Cord blood $CD4^+$ T cells proliferate rapidly compared to peripheral $CD4^+$ T cells.

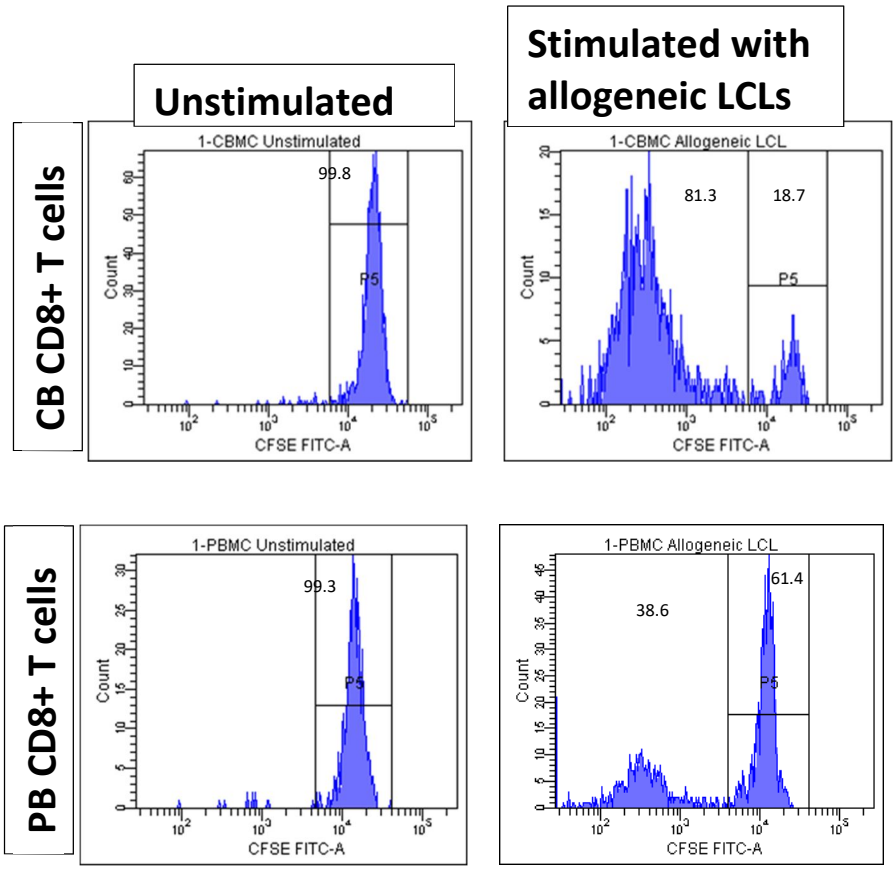

Figure 34: Representative histogram plots of cord blood $CD8^+$ T-cell vs peripheral blood $CD8^+$ T-cell proliferation in response to allogeneic LCLs (at ratio 10 responders:1 allogeneic stimulator). Cord blood $CD8^+$ T cells proliferate rapidly compared to peripheral $CD8^+$ T cells.

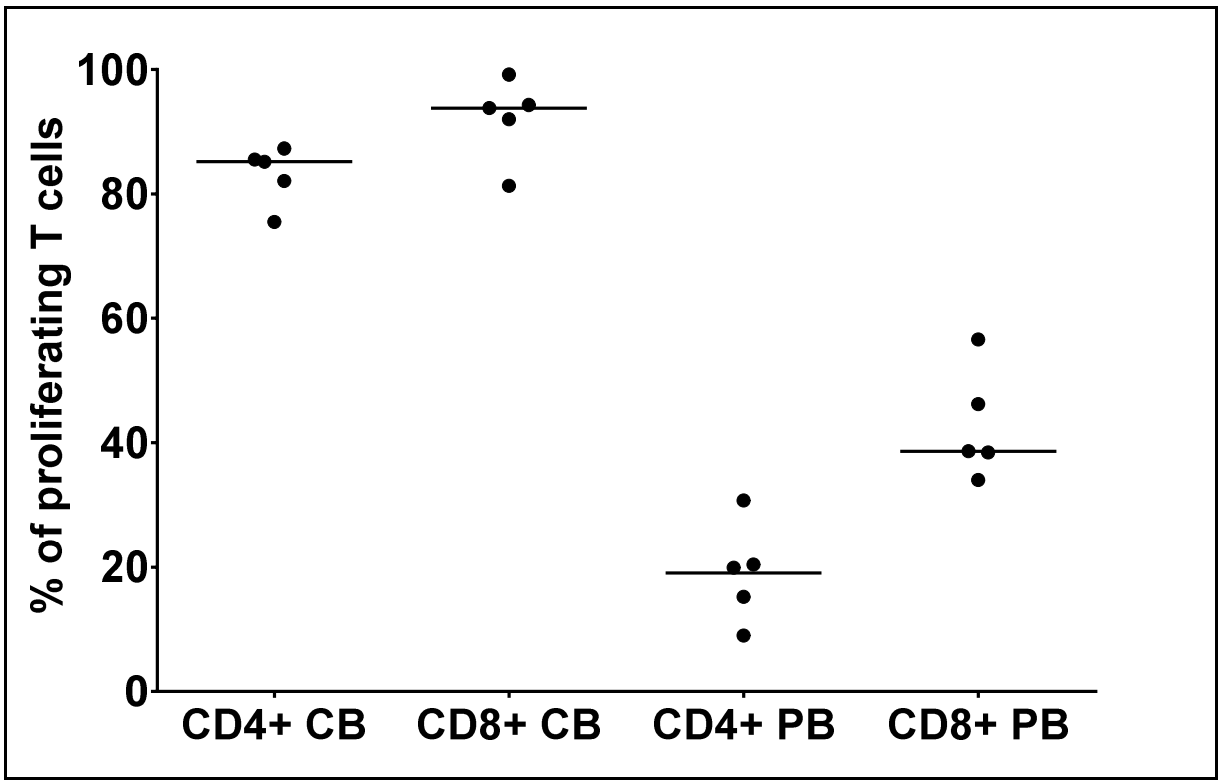

Figure 35: Scatter plot of percentage of proliferating cord blood and peripheral blood T cells after LCL stimulation (5 *vs* 5 samples). 80-90% of cord blood T cells ($CD4^+$ and $CD8^+$) proliferate after allogeneic stimulation compared to 20-40% peripheral blood T cells ($CD4^+$ and $CD8^+$; unpaired t-test; $p<0.0001$).

Additionally, we also observed that asymmetric CD4/CD8 ratio was maintained in cord blood T cells after T-cell receptor stimulation whereas a reduction in CD4/CD8 ratio was observed in peripheral blood T cells ($p<0.02$) [Figure 36].

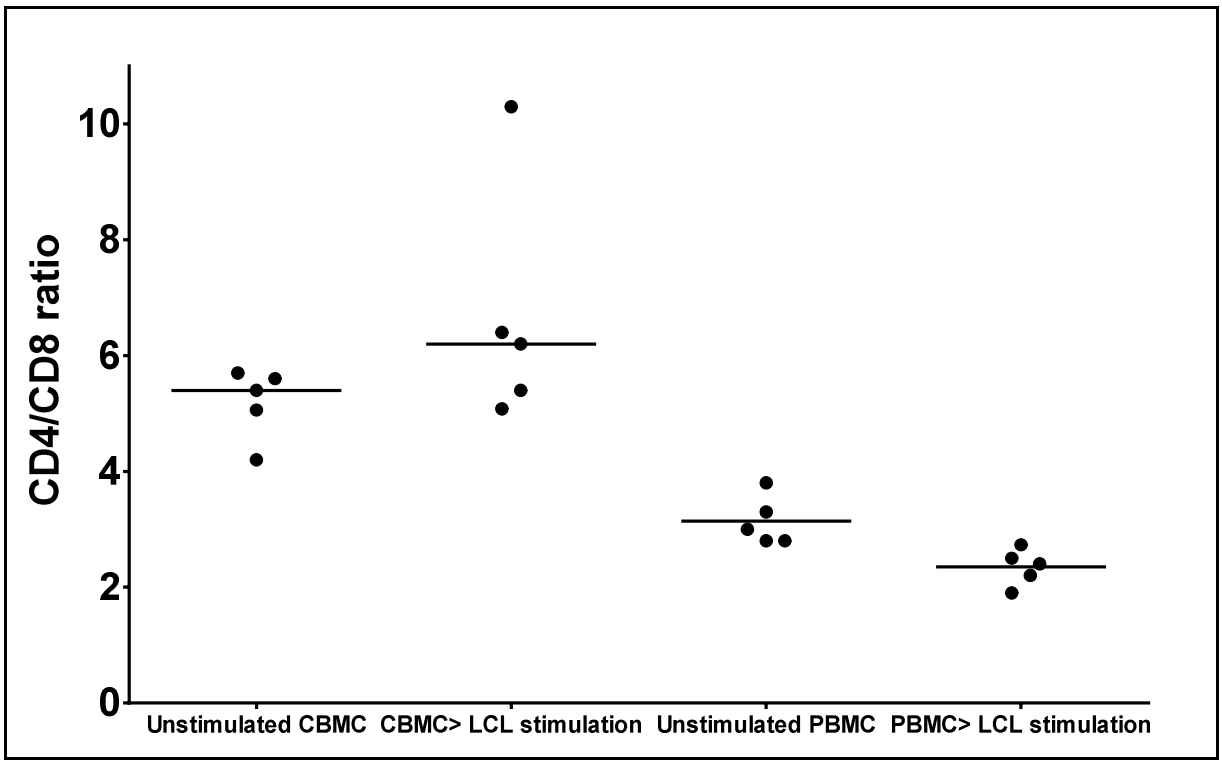

Figure 36: Scatter plot of CD4:CD8 ratio in cord blood and peripheral blood samples (5 *vs* 5) stimulated with allogeneic LCLs. A higher CD4:CD8 ratio was maintained after stimulation of cord blood T cells with allogeneic LCLs. In contrast, a lower CD4:CD8 ratio was observed in PBMC after stimulation with allogeneic LCLs compared to unstimulated PBMC.

This observation suggested that although cord blood T cells are hyper-responsive to T-cell receptor signalling, it also raised the obvious question - whether the naivety of cord blood T cells was responsible for the majority of cells going in to cell cycle following T-cell receptor stimulation.

4.6 Comparing the T-cell receptor signalling in the CD45RA$^+$ enriched (naïve) cord blood and adult blood T cells

We therefore bead sorted CD45RA$^+$ cells to enrich naïve T-cell population from cord blood (*n = 5*) and adult peripheral blood (*n = 5*) [Figure 37]. We found that naïve cord blood T cells proliferated rapidly compared to peripheral blood naïve T-cell enriched population. These results were similar to the previous experiment with unsorted cord blood mononuclear and peripheral blood mononuclear cells.

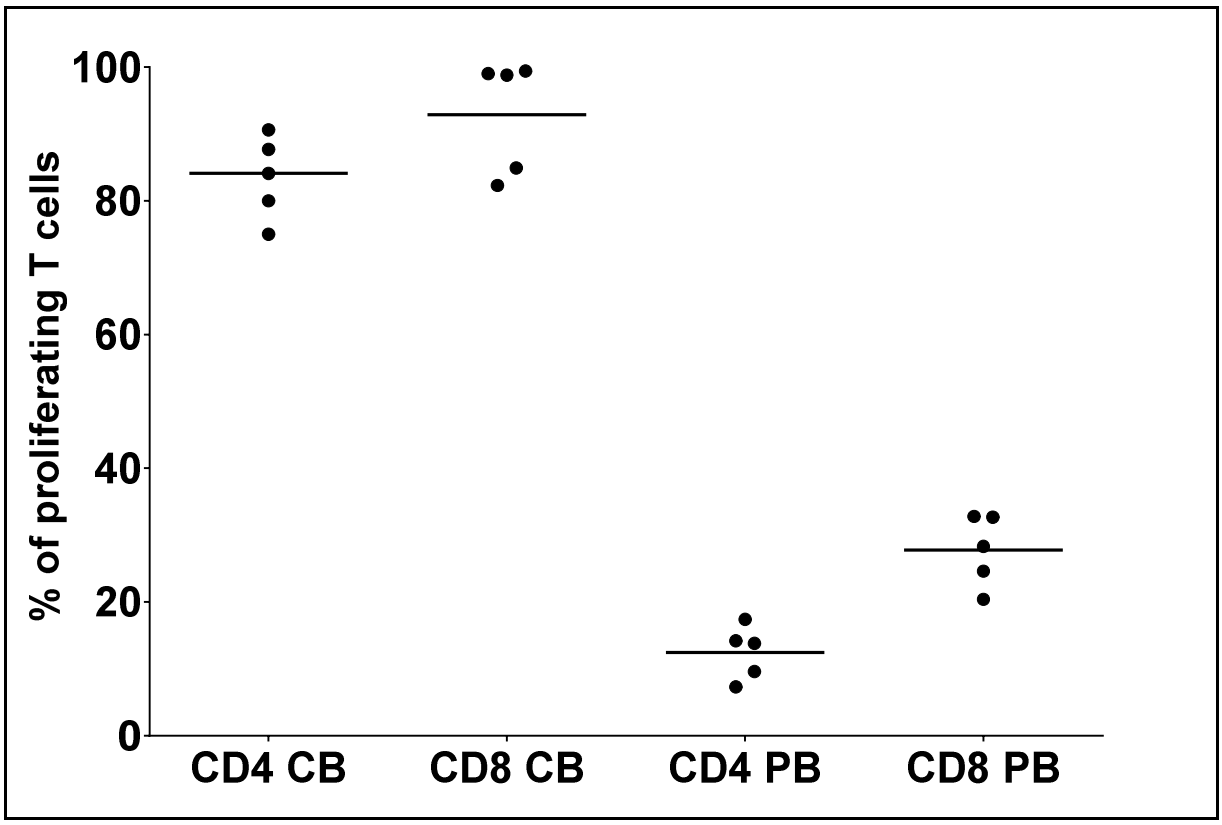

Figure 37: Scatter plot of percentage of proliferating CD4$^+$ and CD8$^+$ T cells in CD45RA$^+$ enriched cord blood and peripheral blood T cells after LCL stimulation (5 *vs* 5 samples). 80-90% of naïve cord blood T cells (CD4$^+$ and CD8$^+$) proliferate after allogeneic stimulation compared to 20-40% naïve peripheral blood T cells (CD4$^+$ and CD8$^+$).

Thus, cord blood T cells are hyper-responsive to T-cell receptor trigger and this hyper-responsiveness appears to be independent of the naivety of T cells.

4.7 CONCLUSION

Cord blood T cells undergo enhanced proliferation to IL-7 (10 ng/ml) compared to adult blood T cells and this indicates the hyper-responsiveness of cord blood T cells to IL-7.

Although cord blood T cells express higher IL-7 receptor expression compared to adult blood T cells, no difference in STAT5 phosphorylation was observed after stimulation with varying concentrations of IL-7. This finding raised question about the role of IL7-STAT5 signalling pathway in differential reconstitution of T cells after cord blood and bone marrow transplantation.

We therefore questioned the role of TCR:MHC interactions in rapid proliferation of cord blood T cells. On TCR stimulation, cord blood T cells were observed to undergo enhanced proliferation compared to adult blood T cells.

Our observations of 1) hyper-responsiveness of cord blood T cells to IL-7 and 2) hyper-responsiveness of cord blood T cells to T-cell receptor stimulation indicated that cord blood T-cell homeostasis may be significantly distinct to T-cell homeostasis in adults. This distinction between cord blood and adult blood T-cell homeostasis may be because of progression of foetal to adult ontogeny and hyper-responsiveness of T cells to homeostatic signals may reduce with the switch over from foetal to adult ontogeny.

Finally, the observation of similar STAT5 phosphorylation to varying concentrations of IL-7 also raised questions about how these homeostatic IL-7 and T-cell receptor signals co-operate during expansion of T cells in the lymphopenic environment.

Chapter five

T-cell replete cord blood transplantation recapitulates foetal ontogeny with a distinct molecular signature

5.0 Aims

1) To establish if cord blood naïve $CD4^+$ T cells are transcriptionally distinct to peripheral blood naïve $CD4^+$ T cells but similar to foetal $CD4^+$ T cells.

2) To establish if recapitulation of foetal T-cell ontogeny occurs after T-cell replete CBT.

3) To identify the genes induced during lymphopenia induced proliferation by comparing the transcriptional profile of naïve $CD4^+$ T cells from steady-state lymphoreplete environment in the peripheral blood with reconstituting T cells after BMT.

4) To identify if reconstituting naive $CD4^+$ T cells after T-cell replete CBT are enriched in the genes induced during lymphopenia induced proliferation.

5) To identify upregulated transcription factors, biological processes and canonical pathways in the naïve cord blood $CD4^+$ T cells.

6) To test the functional relevance of upregulated pathways in the cord blood T cells.

5.1 Introduction

There is a growing evidence supporting distinct ontogenic origins of foetal and adult lymphoid immune systems and so indeed cord blood T cells may have distinct origins compared to peripheral blood T cells. The observations and experiments in chapter three and four indicate that cord blood T cells have proliferative advantage over peripheral blood T cells. We observed unprecedented $CD4^+$ T-cell biased reconstitution after T-cell replete CBT compared with BMT. In addition, we observed a normal T-cell spectratype as early as 30 days after T-cell replete CBT. This suggests distinct ability of cord blood T cells to expand rapidly with a diverse T-cell repertoire in the lymphopenic environment such as post-transplantation and hence implicate that cord blood T cells are distinct compared to adult T cells. Thus, it is likely that foetal origins of cord blood T cells may endow cord blood T cells with the processes that may have a role in lymphopenia-induced proliferation. We also observed that *in vitro*, cord blood T cells undergo enhanced proliferation in response to allogeneic TCR signal from lymphoblastoid cells. Similarly cord blood T cells also show robust proliferation in the presence of high levels of IL-7 (10 ng/ml). These observations suggest that T-cell homeostasis at birth may be regulated distinctly driven by the highly proliferative state of cord blood T cells and relatively lymphopenic environment of the foetus.

The process of lymphopenia-induced proliferation is dependent on TCR signals for peptide/MHC complexes and cytokines such as IL-7 and IL-15. It is therefore plausible that naïve cord blood T cells may have upregulated TCR signalling and/or cytokine signalling pathways which may boost the process of lymphopenia-induced proliferation following T-cell replete CBT.

Therefore, to determine if differential gene expression in cord blood *vs* peripheral blood $CD4^+$ T cells underlies the more rapid $CD4^+$ T-cell proliferation observed after CBT, we set out to identify if cord blood T cells have a distinct and foetal T-cell like gene expression profile and if this foetal ontogeny is recapitulated after T-cell replete CBT. Finally, we aimed to identify the relevant homeostatic pathways and transcription factors that mediate enhanced proliferation after T-cell replete CBT.

5.2 Exploratory data analysis of naïve cord blood and peripheral blood $CD4^+$ T cell gene expression profile

Gene expression profile using Affymetrix Human Gene 1.0 ST array on RNA isolated from flow cytometrically sorted naïve $CD4^+$ T cells ($CD4^+CD45RA^+CCR7^+$) from the normal donor cord blood, adult blood and T-cell replete CBT and BMT recipients was performed.

Two experiments were performed with 3 random donor cord blood and peripheral blood samples (biological replicates). This was followed by 3rd experiment which included 3 paired samples of naïve $CD4^+$ T cells from cord blood and peripheral blood of same donors (age 5 - 8 years old) and from CBT and BMT recipients during early T-cell reconstitution. Gene expression quality control and analysis was performed using R (cran.r-project.org) and Bioconductor (www.bioconductor.org).

The naïve $CD4^+$ T cells from cord blood and peripheral blood clustered into two distinct groups on 3D-principal component analysis and hierarchical clustering. These gene expression profiles were then compared with those of reconstituting naïve $CD4^+$ T cells two months after CBT and BMT. The gene expression profiles of naïve $CD4^+$ T cells after CBT and BMT clustered with the gene expression profiles of naïve $CD4^+$ T cells from cord blood and peripheral blood respectively [Figure 38 and 39]. To determine if cord blood T cells have a transcription profile similar to foetal T cells we retrieved gene expression data set of naïve $CD4^+$ T cells from the foetal mesenteric lymph nodes (gestational age 18 to 22 weeks, Mold *et al*., 2010). Our most notable finding was that the gene expression profiles of naïve $CD4^+$ T cells from cord blood and during early reconstitution following CBT clustered with those of naïve foetal $CD4^+$ T cells [Figure 38 and 39].

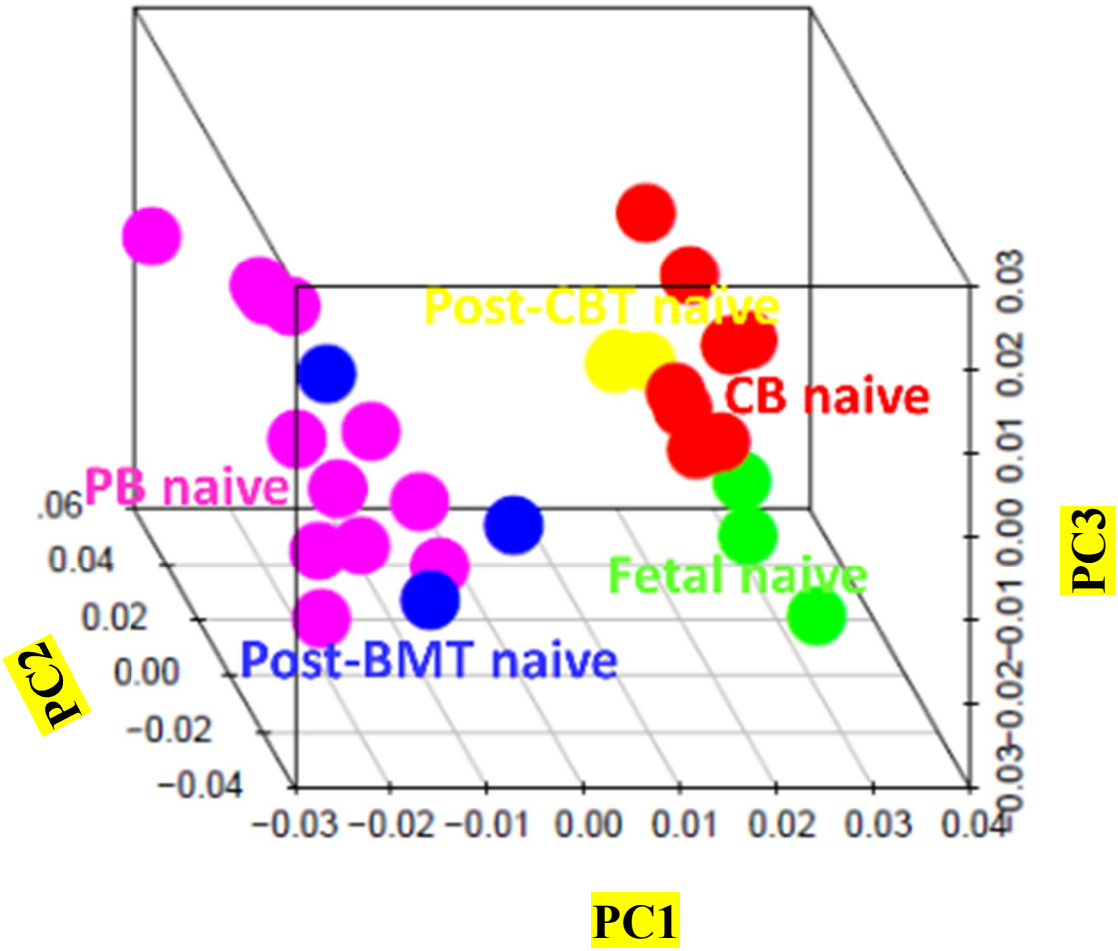

Figure 38: 3D principal component analysis of naive $CD4^+$ T cell transcriptome from cord blood (*n=9*), peripheral blood (*n=12*), fetal mesenteric lymph nodes (*n=3*) and two months after cord blood transplantation (CBT; *n=3*) & bone marrow transplantation (BMT; *n=3*). Naive cord blood $CD4^+$ T cells have a distinct transcription profile to naive peripheral blood $CD4^+$ T cells, but similar to foetal T cells.

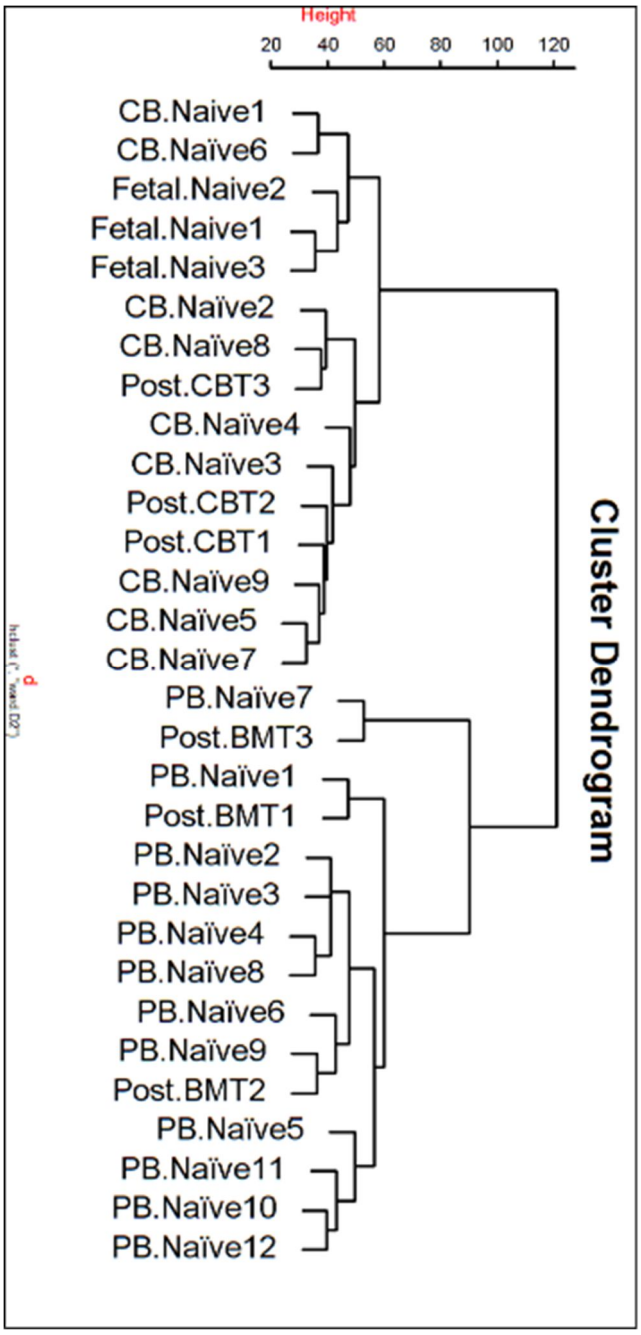

Figure 39: Hierarchical clustering analysis of naive $CD4^+$ T cell transcriptome from cord blood (*n=9*), peripheral blood (*n=12*), fetal mesenteric lymph nodes (*n=3*) and two months after CBT (*n=3*) & BMT (*n=3*). Naive cord blood $CD4^+$ T cells have a distinct transcription profile to naive peripheral blood $CD4^+$ T cells, but similar to foetal T cells.

The foetal immune system is biased towards T-regulatory function. I therefore compared gene expression profile of naïve $CD4^+$ T cells and T-regulatory cells. Naïve $CD4^+$ T cells and T-regulatory cells segregated depending on the developmental stage and T-cell type [Figure 40].

Thus, confirming the distinct gene expression profile of naïve $CD4^+$ T cells after CBT is not due to adoption of T-regulatory function.

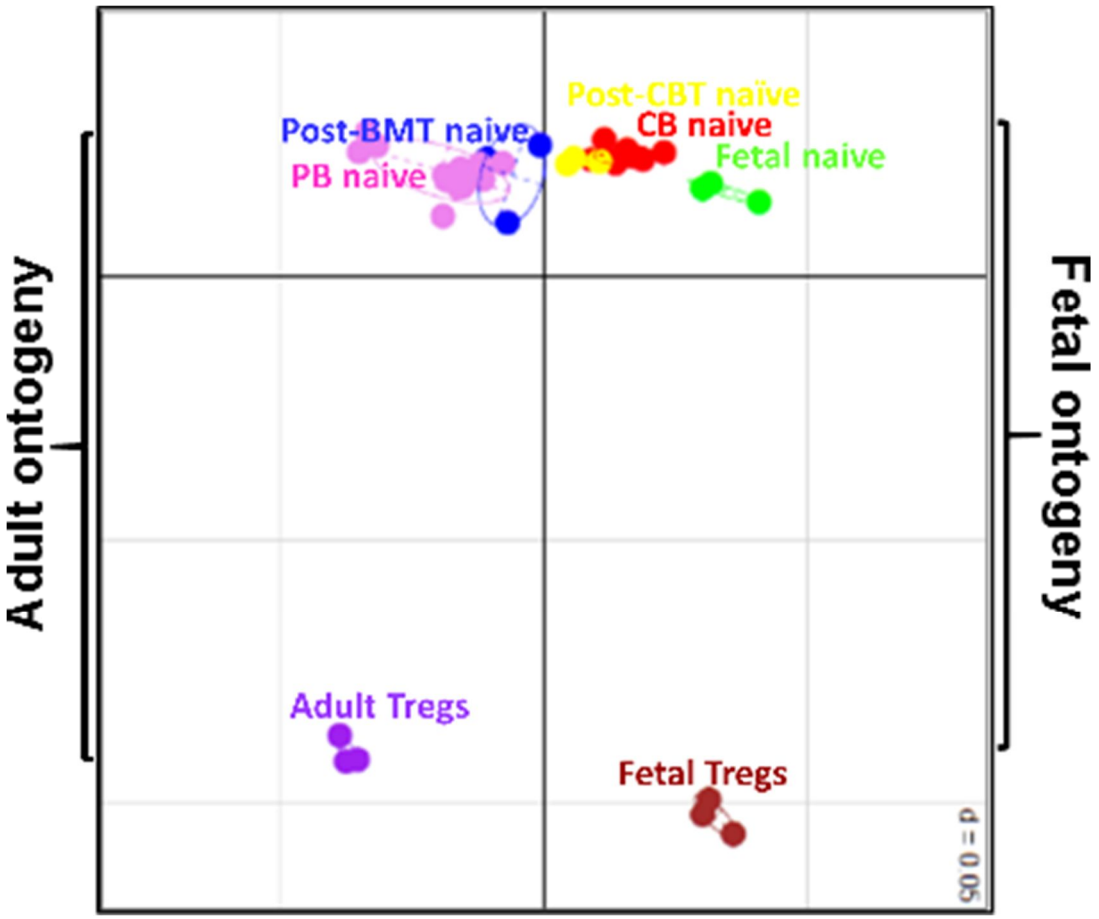

Figure 40: 2D principal component analysis showing relationship between naive $CD4^+$ T cells from cord blood (*n=9*), peripheral blood (*n=9*), foetal mesenteric lymph nodes (*n=3*) and two months after CBT (*n=3*) & BMT (*n=3*) versus T-regulatory cells from foetal mesenteric lymph nodes (*n=3*) and peripheral blood (*n=3*). T cells segregate based on developmental stage and T-cell type. Thus, confirming the distinct transcription profile of naive $CD4^+$ T cells after CBT is not due to adoption of T-regulatory function. (In this graph, each unit is 0.05 and is depicted in the graph as d=0.05)

Thus, these observations indicate that cord blood T cells have a foetal-like transcriptional profile which is distinct to peripheral blood T cells. Most importantly, this foetal ontogeny is recapitulated after T-cell replete CBT thus indicating the role of distinct foetal-like transcription profile in mediating the enhanced T-cell reconstitution after T-cell replete CBT.

5.3 Identifying differentially expressed genes between naïve CD4$^+$ T cells isolated from the cord blood and peripheral blood

We identified the differentially expressed genes in three separate microarray experiments comparing the naïve CD4$^+$ T cells from the CB (*n = 9*) and PB (*n = 9*). In the three experiments, 288, 273 and 213 genes were differentially expressed (Table 5).

Naïve CD4$^+$ T cells (CB vs PB)	**Expt 1 Random donors**	**Expt 2 Random donors**	**Expt 3 Paired donors**
Differentially expressed genes	**288**	**273**	**213**
Up-regulated genes	**206**	**179**	**125**
Down-regulated genes	**82**	**94**	**88**

Table 5 shows differentially expressed genes in the 3 normal donor microarray experiments

Of these differentially expressed genes, sixty genes were common to the three experiments and hence are likely to represent true molecular signature of cord blood CD4$^+$ T cells [Figure 41 (a); Table 6 and 7].

On comparing the gene expression profile of naïve CD4$^+$ T cells from foetal mesenteric lymph nodes and peripheral blood, we found 1133 genes differentially expressed. Of these 1133 genes, 740 were upregulated.

Interestingly, of the sixty genes representing cord blood CD4$^+$ T cell signature, 45 (75%) genes were differentially regulated in the naïve CD4$^+$ T cells from the foetal mesenteric lymph nodes and of these 45 genes, 43 genes had the same direction of regulation [Figure 41 (b)].

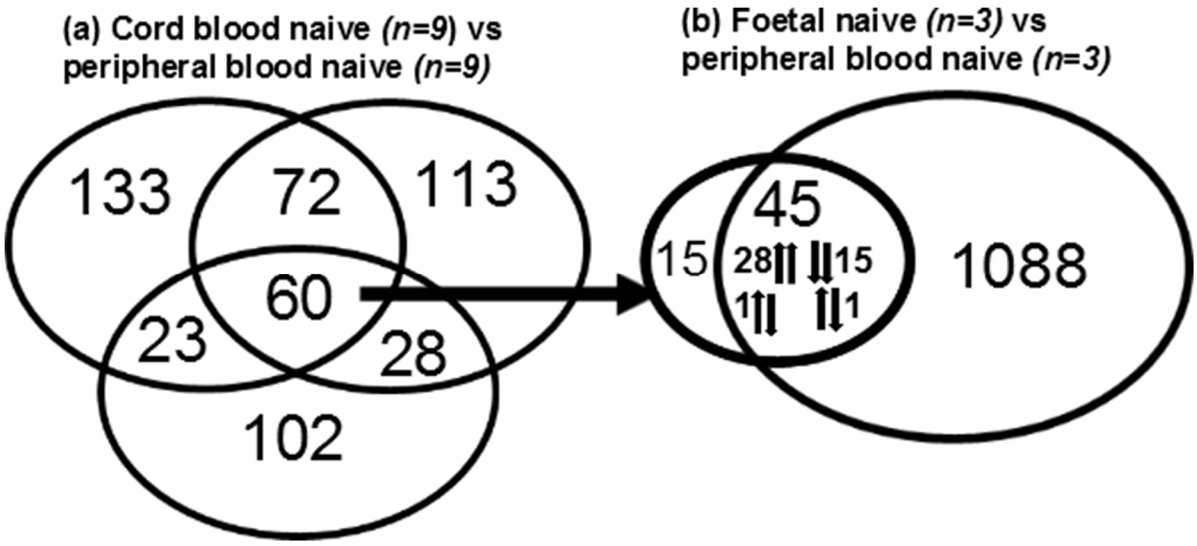

Figure 41: (a) Venn diagram of differentially expressed genes in 3 microarray experiments comparing the naive $CD4^+$ T cells from normal donor cord blood and peripheral blood. Sixty genes overlapped in the 3 experiments. (b) 45 of the 60 overlapping genes were differentially expressed in foetal $CD4^+$ T cells and 43 of these genes had same direction of regulation, confirming that cord blood T cells and foetal T cells have similar transcription profile.

The sixty genes that are differentially expressed are shown in Table 6 and 7 and scatterplot of pairwise global gene expression of naive cord blood $CD4^+$ T cells and naive peripheral blood $CD4^+$ T cells are shown in Figure 42.

	Experiment 1		Experiment 2		Experiment 3	
	logFC	p value	logFC	p value	logFC	p value
GZMA granzyme A	7.535699	1.67E-06	4.31662	0.004528	7.174216	6.45E-05
TNF tumor necrosis factor	6.706227	2.48E-05	6.332923	4.08E-05	4.187791	0.006876
JUN Jun proto-oncogene, AP-1 transcription factor subunit	6.441966	0.012674	6.140109	0.000316	8.667031	0.0001
YBX3 Y-box binding protein 3	5.890719	4.60E-05	3.855246	0.006675	3.579875	0.004035
PMAIP1 phorbol-12-myristate-13-acetate-induced protein 1	5.75521	0.001653	7.430931	9.24E-08	3.450347	0.020954
ERVH48-1 endogenous retrovirus group 48 member 1	5.705971	6.88E-05	5.779196	8.64E-05	4.423607	0.000145
AUTS2 autism susceptibility candidate 2	5.671714	4.95E-06	6.198322	1.36E-07	5.871178	7.46E-05
FOS Fos proto-oncogene, AP-1 transcription factor subunit	5.429297	0.002098	2.920811	0.021043	7.93349	4.09E-05
NREP neuronal regeneration related protein	5.340234	1.62E-05	4.201117	4.23E-05	2.919033	0.000486
BCL11A B-cell CLL/lymphoma 11A	5.044081	6.81E-05	5.652298	1.77E-09	4.843203	3.60E-05
PPP1R15A protein phosphatase 1 regulatory subunit 15A	4.818382	2.31E-06	3.51651	0.000308	7.127937	1.82E-05
RNASE6 ribonuclease A family member k6	4.370133	0.005525	3.076722	0.00724	4.038208	0.001027
SGK1 serum/glucocorticoid regulated kinase 1	4.348108	0.000253	5.288891	2.89E-05	4.057468	0.007536
CKS2 CDC28 protein kinase regulatory subunit 2	4.290451	0.000255	3.210377	0.00014	2.098185	0.020831
HPGD hydroxyprostaglandin dehydrogenase 15-(NAD)	4.182863	0.002524	4.77588	2.96E-05	3.087342	0.019925
RGS1 regulator of G-protein signaling 1	4.129041	0.006686	4.776981	0.000836	6.855456	0.026811
DACH1 dachshund family transcription factor 1	4.003262	3.79E-05	4.102328	5.81E-06	2.290388	0.000493
DUSP1 dual specificity phosphatase 1	3.784847	0.002561	2.173541	0.026407	6.790163	9.84E-06
RAB25 RAB25, member RAS oncogene family	3.509931	4.84E-05	4.399383	6.40E-05	4.726221	0.0007
ZNF462 zinc finger protein 462	3.493374	0.006196	3.802819	8.50E-06	4.444309	0.00019
EPHA4 EPH receptor A4	3.401745	0.003662	2.402585	0.00012	2.231014	0.016643
SOX4 SRY-box 4	3.361926	0.00019	3.878754	8.76E-07	2.052565	0.000975
CD38 CD38 molecule	3.336686	0.00035	3.672497	0.00031	2.212695	0.000832
DAPK1 death associated protein kinase 1	3.307746	0.000202	3.856168	5.42E-06	2.655965	0.000485
SERPINF1 serpin family F member 1	3.30606	0.01073	3.99432	3.43E-05	5.23202	0.000547
TNFAIP3 TNF alpha induced protein 3	3.037118	0.004832	4.137767	0.000261	4.480875	0.012172
MICAL2 microtubule associated monooxygenase, calponin and LI	3.017118	2.69E-05	2.125189	0.002898	2.392789	0.000983
CD69 CD69 molecule	2.973675	0.004498	4.31104	0.000611	4.645605	0.005966
IER2 immediate early response 2	2.949891	0.0003	3.971943	3.28E-08	2.912484	0.000488
ITPRIP inositol 1,4,5-trisphosphate receptor interacting protein	2.941317	0.001875	2.474705	0.000519	2.446789	0.000374
KLF6 Kruppel like factor 6	2.937539	0.000956	2.44734	0.000872	3.459376	0.004316
SLC18A2 solute carrier family 18 member A2	2.91042	0.000807	4.742807	3.17E-05	2.017848	0.008874
KLRG1 killer cell lectin like receptor G1	2.790687	0.007994	2.510963	0.006052	3.407383	0.000289
HILPDA hypoxia inducible lipid droplet associated	2.71938	0.000111	2.059457	1.36E-05	2.294812	0.002073
DDIT4 DNA damage inducible transcript 4	2.55922	0.00181	2.093249	0.002463	2.944853	0.002054
NFKBIA NFKB inhibitor alpha	2.545184	0.019169	3.654324	7.91E-06	4.614546	0.000559
PDE6G phosphodiesterase 6G	2.511184	0.010125	2.262887	0.002368	3.742702	0.00023
LDB2 LIM domain binding 2	2.403874	0.002915	2.334718	0.001334	2.789985	0.000595
CACHD1 cache domain containing 1	2.392288	0.008796	2.670404	6.56E-05	2.153186	0.000715
YARS tyrosyl-tRNA synthetase	2.252624	0.000586	3.234825	6.53E-06	3.321055	0.001332
SEPT11 septin 11	2.24483	0.012034	2.933734	3.90E-06	2.192582	0.004805
DACT1 dishevelled binding antagonist of beta catenin 1	2.09791	0.033199	2.559493	0.006348	2.450052	0.000787
MCTP1 multiple C2 and transmembrane domain containing 1	2.02364	0.00102	2.239509	2.88E-05	2.016444	0.004509

Table 6 Fold-change and p values of upregulated genes in the three experiments are shown separately.

	Experiment 1		Experiment 2		Experiment 3	
	logFC	p value	logFC	p value	logFC	p value
TSHZ2 teashirt zinc finger homeobox 2	-6.65785	7.44E-07	-4.44503	0.000124	-4.15268	5.46E-05
GBP5 guanylate binding protein 5	-5.61794	8.58E-05	-4.78459	0.000959	-8.0585	5.87E-06
NR3C2 nuclear receptor subfamily 3 group C member 2	-5.20196	0.000108	-5.46849	4.40E-07	-5.51365	6.26E-05
ZNF204P zinc finger protein 204, pseudogene	-4.46247	3.86E-06	-2.89953	0.000509	-3.1558	0.006688
ABCD2 ATP binding cassette subfamily D member 2	-3.85728	0.000231	-2.89768	0.00652	-3.75452	5.12E-05
SERPINB6 serpin family B member 6	-3.75117	9.74E-05	-4.05341	3.93E-07	-2.67129	0.001214
TBK1 TANK binding kinase 1	-3.72549	1.90E-06	-2.3558	0.000142	-2.64517	0.004132
MID2 midline 2	-3.60009	6.48E-07	-4.21845	1.85E-06	-3.60814	0.002244
BEX5 brain expressed X-linked 5	-3.55973	4.71E-05	-7.26828	3.95E-06	-5.80275	0.000302
RNF175 ring finger protein 175	-3.5569	7.81E-06	-2.53643	3.34E-05	-2.41742	0.004374
RBM11 RNA binding motif protein 11	-3.43584	0.005858	-2.8751	0.00023	-2.22189	0.001508
HLA-DPA1 major histocompatibility complex, class II, DP alph	-3.06266	0.033783	-3.34038	5.26E-05	-6.31339	3.48E-05
ZBTB38 zinc finger and BTB domain containing 38	-2.63495	0.000584	-3.45025	0.000766	-4.74469	1.92E-05
RNF130 ring finger protein 130	-2.50728	0.00385	-2.50772	9.39E-05	-2.27609	0.00298
TGFBR3 transforming growth factor beta receptor 3	-2.47259	0.016178	-2.27981	0.000273	-2.33925	0.000484
ZNF14 zinc finger protein 14	-2.41439	0.014251	-2.99841	0.002076	-2.3865	0.012378
MT1F metallothionein 1F	-2.05388	0.043655	-3.71048	0.000243	-3.0288	0.00138

Table 7 Fold-change and p values of downregulated genes in the three experiments are shown separately.

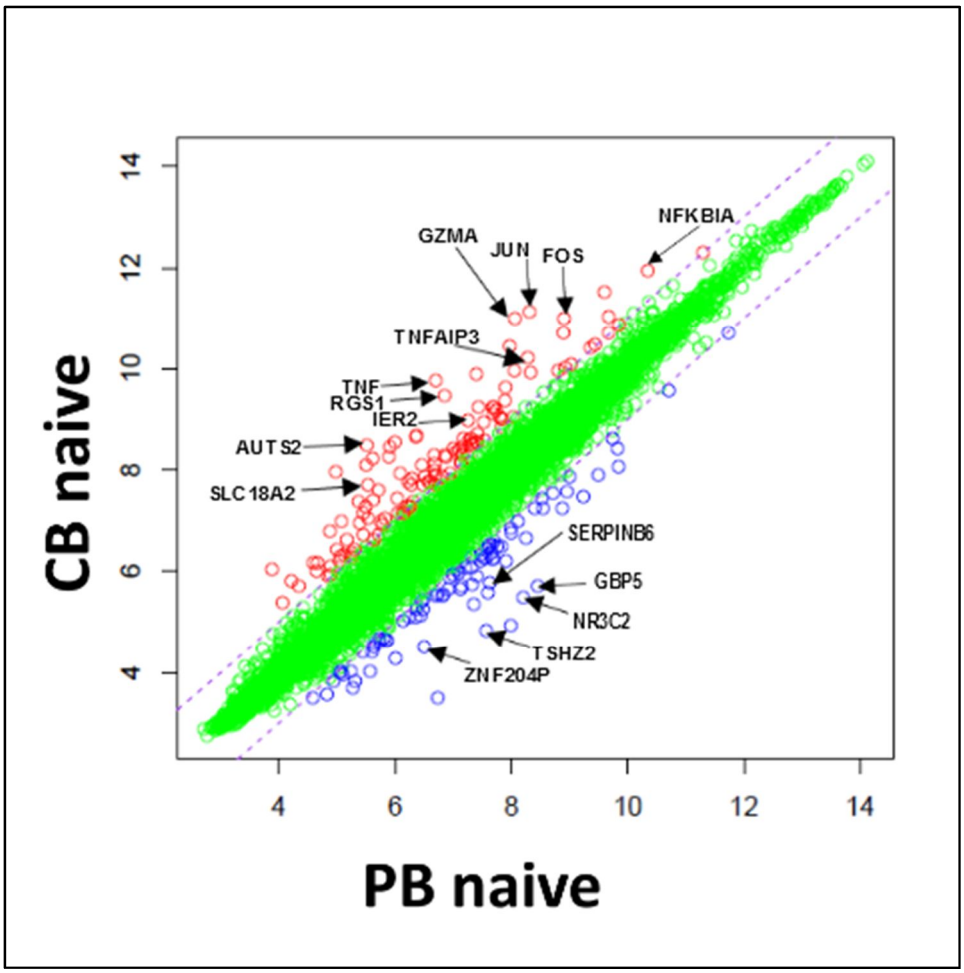

Figure 42: Scatterplot of pairwise global gene expression of naive cord blood $CD4^+$ T cells and naive peripheral blood $CD4^+$ T cells. Gene expression values are plotted on a log scale. Genes that were differentially expressed between groups (determined using p value < 0.05 and fold-change >= 2) are indicated in red and blue. Specific genes that were differentially expressed are highlighted with arrows.

5.4 Identifying molecular signature induced during lymphopenia-induced proliferation

However, since cord blood T cells are in a highly proliferative state, driven by the relatively lymphopenic environment of the foetus, we speculated that a few of these genes may be induced during the process of lymphopenia-induced proliferation.

We identified the genes induced during lymphopenia-induced proliferation taking the advantage of a natural experiment performed during T-cell replete BMT. This allowed us to compare the genes induced in the naïve $CD4^+$ T cells after infusion of a steady lymphoreplete BM graft in a lymphopenic host.

Of the identified sixty genes representing cord blood $CD4^+$ T cell transcriptome, 19 genes were differentially expressed in peripherally expanding naïve $CD4^+$ peripheral blood T cells following T-cell replete BMT. All the 19 genes remained differentially expressed in the reconstituting T cells after CBT, further indicating a role of these genes in lymphopenia-induced proliferation [Figure 43 and 44]. Table 8 is a list of 18 genes that are upregulated in the lymphopenic conditions.

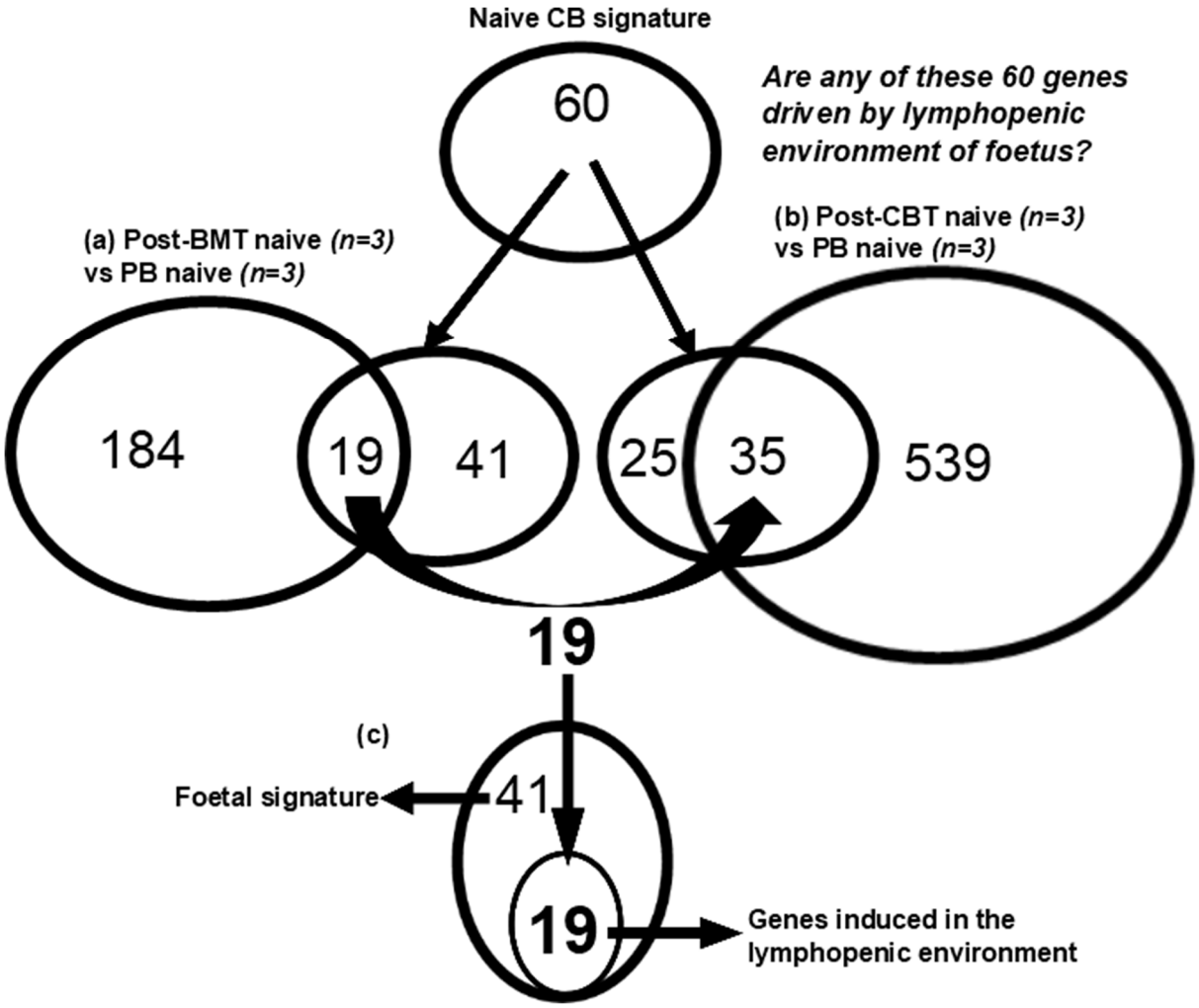

Figure 43: (a) Nineteen of the 60 genes that represent naive cord blood $CD4^+$ T cell signature were induced in the reconstituting naive $CD4^+$ T cells after BMT and (b) all the 19 genes remained differentially expressed in the reconstituting naive $CD4^+$ T cells after CBT. (c) Thus, these 19 genes represent the signature induced in the lymphopenic environment and remaining 41 genes are likely to represent foetal signature.

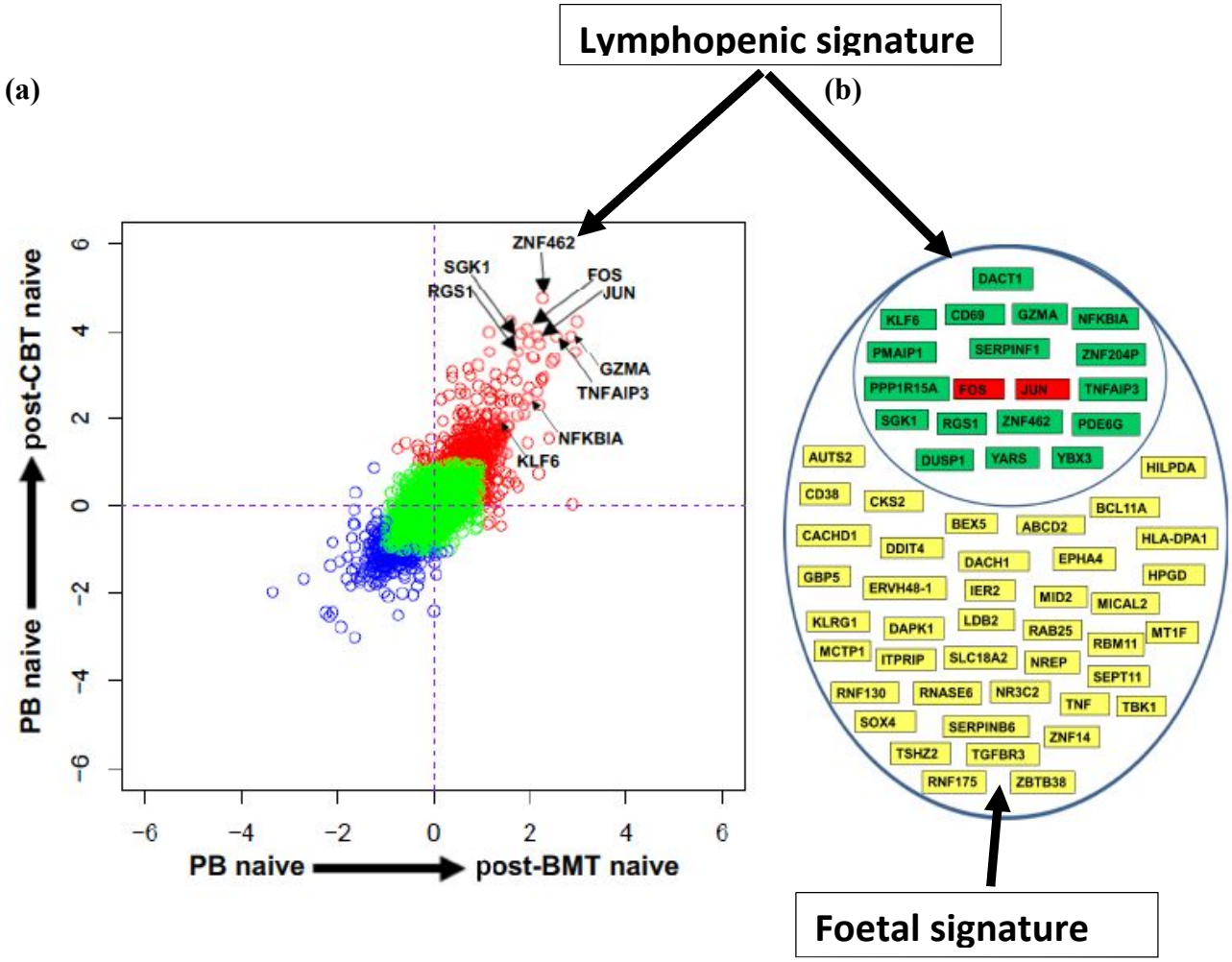

Figure 44: Scatterplot of pairwise global gene expression comparison of naïve $CD4^+$ T cells from two post-transplant environments i.e. cord blood transplantation and bone marrow transplantation. Gene expression values are plotted on a log scale and specific genes upregulated in the lymphopenic environment are highlighted with arrows. (b) Nineteen genes induced in the lymphopenic signature and 41 genes of foetal signature are shown.

	Gene Name	Alternative name/function
High in T cells from lymphopenic environment	FOS	Fos proto-oncogene, AP-1 transcription factor subunit(FOS)
	JUN	Jun proto-oncogene, AP-1 transcription factor subunit(JUN)
	TNFAIP3	TNF alpha induced protein 3
	RGS1	regulator of G-protein signaling 1
	GZMA	granzyme A
	NFKBIA	NFKB inhibitor alpha(NFKBIA)
	PMAIP1	phorbol-12-myristate-13-acetate-induced protein 1
	YARS	tyrosyl-tRNA synthetase
	CD69	CD69 molecule
	PDE6G	phosphodiesterase 6G
	PPP1R15A	protein phosphatase 1 regulatory subunit 15A
	YBX3	Y-box binding protein 3
	KLF6	Kruppel like factor 6
	ZNF462	zinc finger protein 462
	DACT1	dishevelled binding antagonist of beta catenin 1
	DUSP1	dual specificity phosphatase 1
	SGK	serum/glucoorticoid regulated kinase 1
	SERPINF1	serpin family F member 1

Table 8 List of 18 genes upregulated in the lymphopenic environment.

Deducting these 19 genes induced during the process of lymphopenia-induced proliferation, remaining 41 genes are likely to represent the foetal signature of naïve $CD4^+$ T cells [Figure 43]. Figure 45 shows relative transcripts values of genes representing a foetal signature and Table 9 shows selected genes over expressed in cord blood and peripheral blood T cells.

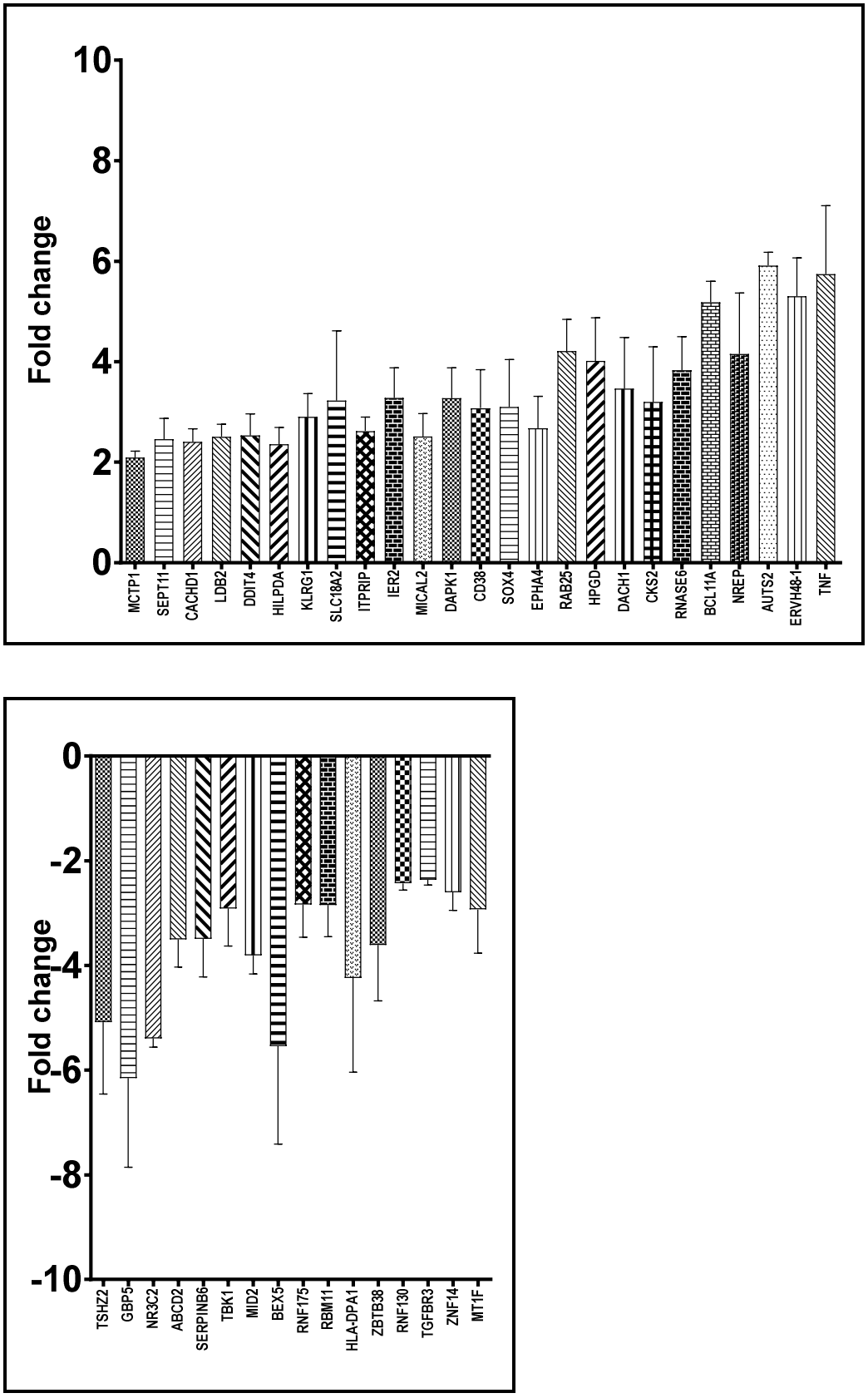

Figure 45: Bar plot showing transcript values (mean and standard deviation) of upregulated and down regulated genes representing foetal signature.

	Gene Name	Alternative name/function
High in cord blood T cells	FOS	Fos proto-oncogene, AP-1 transcription factor subunit(FOS)
	JUN	Jun proto-oncogene, AP-1 transcription factor subunit(JUN)
	SLC18A2	solute carrier family 18 member A2
	TNFAIP3	TNF alpha induced protein 3
	AUTS2	autism susceptibility candidate 2
	RGS1	regulator of G-protein signaling 1
	GZMA	granzyme A
	NFKBIA	NFKB inhibitor alpha(NFKBIA)
	IER2	immediate early response 2(IER2)
	TNF	tumor necrosis factor
High in adult T cells	Gene Name	Alternative name/function
	GBP5	guanylate binding protein 5(GBP5)
	TSHZ2	teashirt zinc finger homeobox 2
	ZNF204P	zinc finger protein 204, pseudogene
	SERPINB6	serpin family B member 6
	NR3C2	nuclear receptor subfamily 3 group C member 2

Table 9 List of selected genes found overexpressed in cord blood and adult blood T cells.

Genes induced during lymphopenia-induced proliferation included 2 important transcription factors of TCR signalling pathway namely c-fos and c-jun which forms an AP-1 complex. Both c-fos and c-jun were highly upregulated during early T-cell reconstitution following CBT and BMT. Interestingly, the upregulation of c-fos and c-jun was significantly higher in reconstituting T cells after CBT than compared with BMT. This upregulation of AP-1 during lymphopenia-induced proliferation suggests a role of TCR signalling during peripheral expansion of T cells infused with stem cell grafts. In particular, higher transcript values of c-fos and c-jun in the reconstituting T cells after CBT suggests that cord blood T cells may have a proliferative advantage over peripheral blood T cells. Figure 46 shows relative transcript values of genes induced during lymphopenia-induced proliferation.

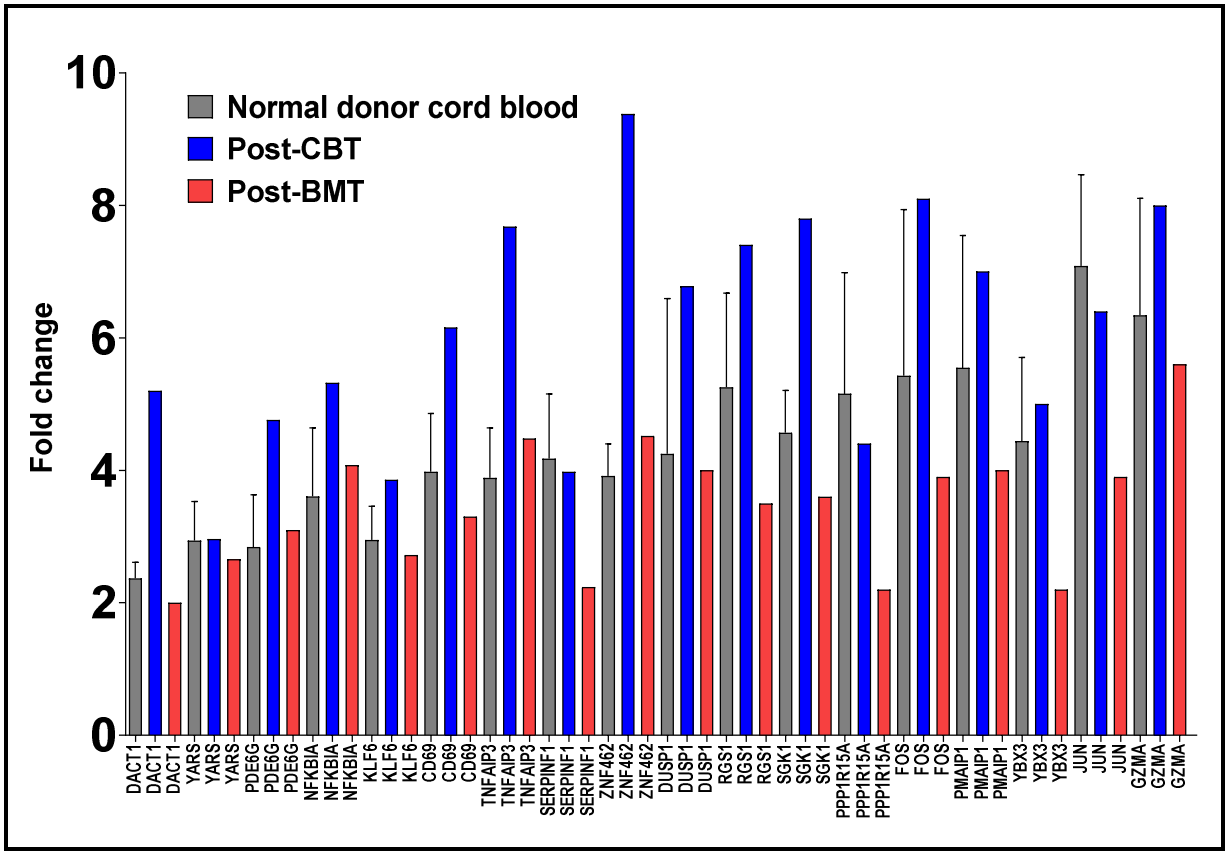

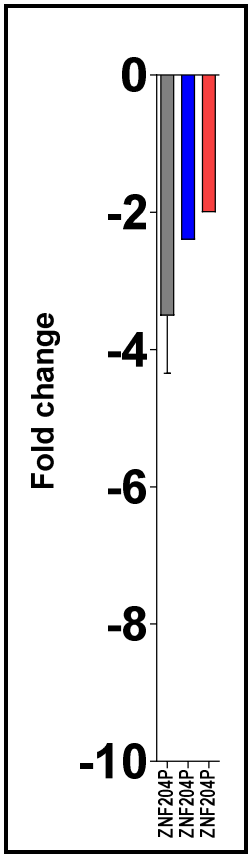

Figure 46: Bar plot showing transcript values (mean and where possible standard deviation) of 19 upregulated/downregulated genes representing genes induced in the lymphopenic environment. Interestingly, the differential regulation of 19 genes was higher in the naive CD4+ T cells from the cord blood and during early reconstitution following cord blood transplantation than compared with bone marrow transplantation.

5.5 Identifying the upregulated biological processes and canonical pathways in the cord blood T cells

Given the distinct transcription profile of cord blood and peripheral blood T cells, we speculated that distinct biological processes and canonical pathways may mediate enhanced T-cell reconstitution after T-cell replete CBT. Firstly, we used 825 gene sets of biological processes from the gene ontology consortium. We found that 27 biological processes were upregulated at p value < 0.001 and fdr q value < 0.1. Table 10 lists the biological processes upregulated in cord blood T cells.

NAME	SIZE	ES	NES	NOM p-val	FDR q-val
DNA_METABOLIC_PROCESS	247	0.5059515	2.1789281	0	0.002307
RESPONSE_TO_DNA_DAMAGE_STIMULUS	155	0.52454346	2.1087008	0	0.005804
CELL_CYCLE_CHECKPOINT_GO_0000075	48	0.6222186	2.054601	0	0.009687
INTERPHASE_OF_MITOTIC_CELL_CYCLE	62	0.5770853	2.0149944	0	0.01112
CELL_CYCLE_GO_0007049	309	0.4655104	2.0182862	0	0.013031
REGULATION_OF_CELL_CYCLE	180	0.47839648	1.9598776	0	0.018691
MITOTIC_CELL_CYCLE	151	0.4827955	1.9438541	0	0.019842
DNA_REPAIR	119	0.51513183	1.9633648	0	0.021051
INTERPHASE	68	0.54464364	1.9261076	0	0.022417
CELL_CYCLE_PHASE	166	0.47129884	1.9061838	0	0.026747
MITOCHONDRION_ORGANIZATION_AND_BIOGENESIS	47	0.5757308	1.8748549	0	0.028571
CELL_CYCLE_PROCESS	189	0.45616704	1.8823042	0	0.03004
NEGATIVE_REGULATION_OF_CELL_CYCLE	79	0.51832753	1.8762827	0	0.030403
RESPONSE_TO_ENDOGENOUS_STIMULUS	191	0.4572464	1.885719	0	0.031494
CELLULAR_COMPONENT_DISASSEMBLY	33	0.5860449	1.8021057	0	0.052743
APOPTOTIC_PROGRAM	59	0.5236585	1.8059676	0.001776199	0.054009
REGULATION_OF_GENE_EXPRESSION_EPIGENETIC	28	0.59163123	1.7378746	0.001956947	0.081819
UBIQUITIN_CYCLE	47	0.5175936	1.7416282	0.001855288	0.08269
APOPTOSIS_GO	415	0.38288313	1.6989125	0	0.086339
PROGRAMMED_CELL_DEATH	416	0.38030535	1.7039883	0	0.088013
DNA_REPLICATION	97	0.45436049	1.7076312	0.001680672	0.088296
REGULATION_OF_PROGRAMMED_CELL_DEATH	328	0.38511395	1.6878171	0	0.089241
REGULATION_OF_APOPTOSIS	327	0.38888615	1.7103146	0	0.089732
PROTEIN_UBIQUITINATION	39	0.5401635	1.7232333	0.003539823	0.090196
M_PHASE	110	0.44338146	1.7104169	0.001739131	0.093471
POSITIVE_REGULATION_OF_DEVELOPMENTAL_PROCESS	210	0.4172443	1.7120072	0	0.09613
NEURITE_DEVELOPMENT	50	0.5046813	1.6658067	0	0.096863
CELL_STRUCTURE_DISASSEMBLY_DURING_APOPTOSIS	18	0.6780949	1.7957022	0.003787879	0.052441

Table 10 Biological processes upregulated in cord blood T cells.

Next I performed enrichment mapping of these pathways and found that naïve cord blood $CD4^+$ T cells were enriched in three clusters relating to cell cycle, DNA metabolism and apoptotis [Figure 47]. The cell cycle and apoptosis pathway were upregulated in all the lymphopenic conditions [Figure 48]. Cell cycle and apoptosis pathway were upregulated in naïve $CD4^+$ T cells after T-replete CBT compared to T-replete BMT.

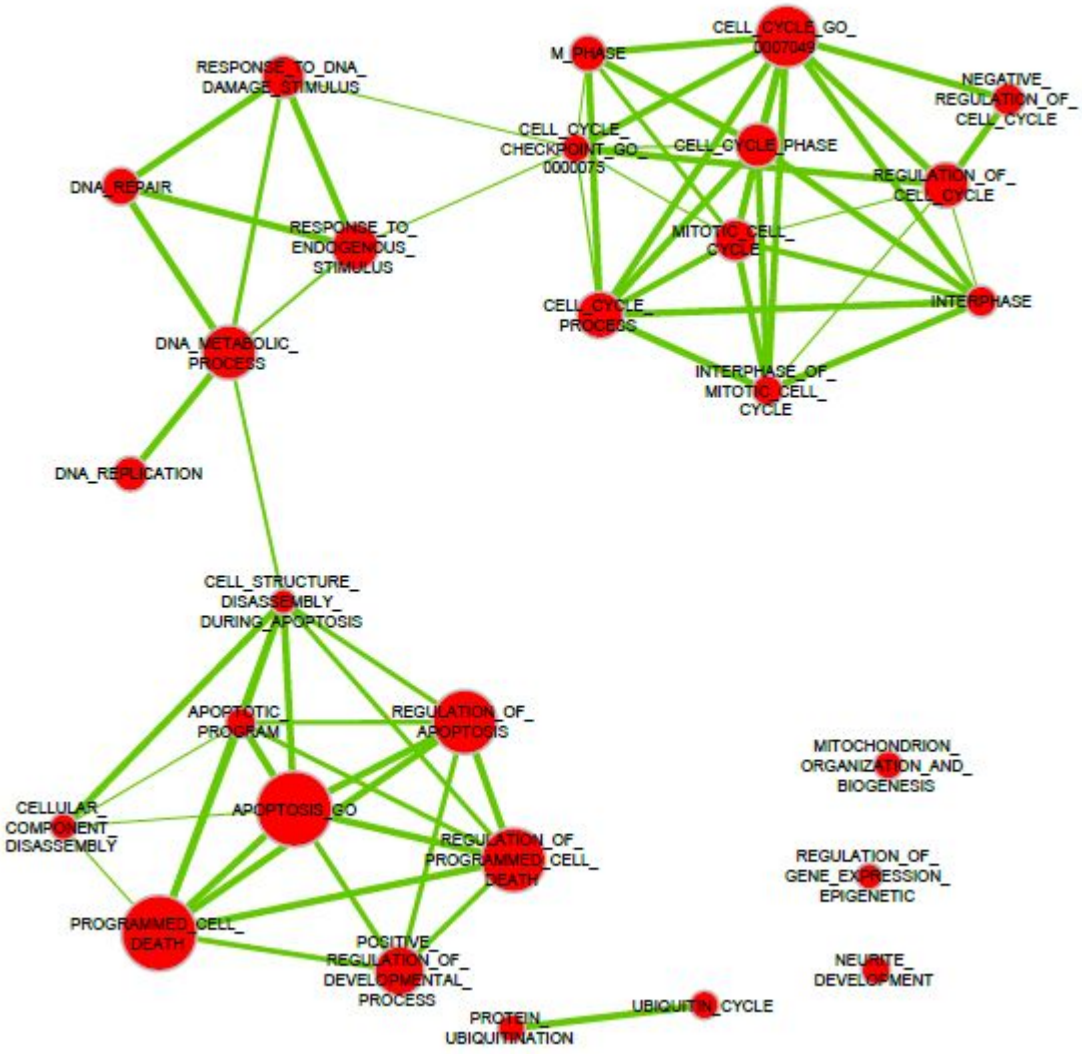

Figure 47: Enrichment map of biological processes upregulated in the naive cord blood $CD4^+$ T cells compared with naive peripheral blood $CD4^+$ T cells. Cell cycle and apoptosis were the two dominant biological processes upregulated in the naive cord blood $CD4^+$ T cells.

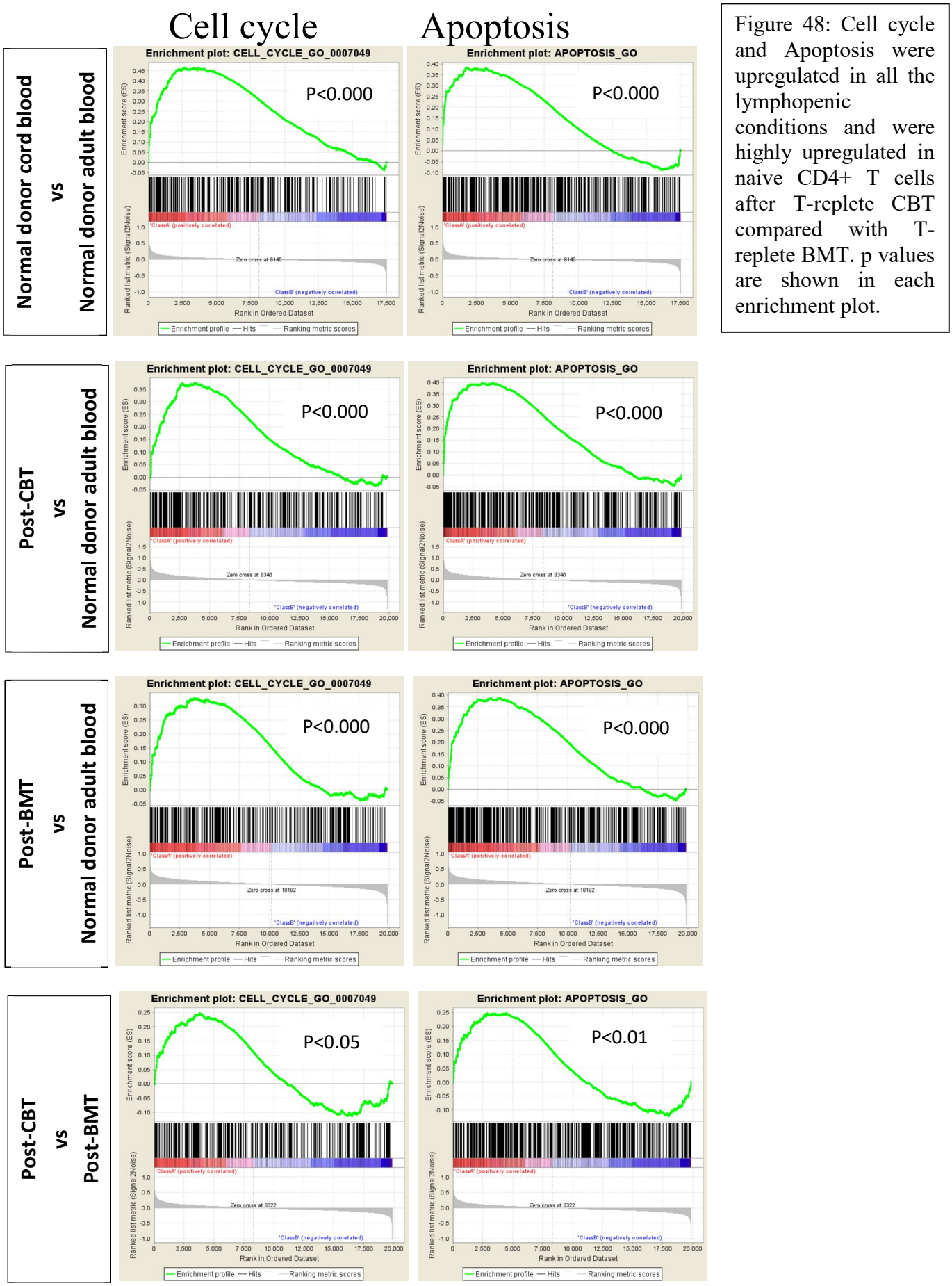

Figure 48: Cell cycle and Apoptosis were upregulated in all the lymphopenic conditions and were highly upregulated in naive CD4+ T cells after T-replete CBT compared with T-replete BMT. p values are shown in each enrichment plot.

To identify the canonical pathways upregulated in naïve CB $CD4^+$ T cells, we used 403 gene sets from BIOCARTA and KEGG database. We found that 26 canonical biological pathways were upregulated at p value < 0.001 and fdr q value < 0.1. Table 11 lists the canonical pathways upregulated in cord blood T cells.

NAME	SIZE	ES	NES	NOM p-val	FDR q-val
BIOCARTA_STRESS_PATHWAY	25	0.747852	2.153037	0	0.002696
BIOCARTA_NTHI_PATHWAY	24	0.705878	2.029868	0	0.004694
KEGG_DNA_REPLICATION	35	0.662369	2.04498	0	0.005209
BIOCARTA_ATM_PATHWAY	20	0.792749	2.161489	0	0.005393
BIOCARTA_TNFR2_PATHWAY	18	0.747083	2.006501	0	0.005757
KEGG_NUCLEOTIDE_EXCISION_REPAIR	44	0.606687	1.968972	0	0.008272
BIOCARTA_GPCR_PATHWAY	32	0.649287	1.973769	0	0.008621
KEGG_T_CELL_RECEPTOR_SIGNALING_PATHW	**107**	**0.511906**	**1.956901**	**0**	**0.009042**
BIOCARTA_MET_PATHWAY	35	0.63085	1.940215	0	0.010134
KEGG_P53_SIGNALING_PATHWAY	67	0.542353	1.911971	0	0.012553
KEGG_CELL_CYCLE	121	0.486363	1.889171	0	0.0141
BIOCARTA_TCR_PATHWAY	**42**	**0.590207**	**1.891878**	**0**	**0.014213**
KEGG_BASE_EXCISION_REPAIR	32	0.617007	1.865055	0	0.017776
BIOCARTA_MAPK_PATHWAY	**86**	**0.490017**	**1.785455**	**0**	**0.023409**
KEGG_MAPK_SIGNALING_PATHWAY	**257**	**0.363248**	**1.548704**	**0.0015873**	**0.096791**
KEGG_OXIDATIVE_PHOSPHORYLATION	110	0.460309	1.750396	0.001675	0.02975
BIOCARTA_PPARA_PATHWAY	54	0.507107	1.717286	0.0017422	0.037614
BIOCARTA_PYK2_PATHWAY	26	0.635627	1.843618	0.0017483	0.019434
BIOCARTA_TNFR1_PATHWAY	29	0.686701	2.047322	0.0018083	0.006946
BIOCARTA_NGF_PATHWAY	18	0.67646	1.788512	0.0018727	0.023704
BIOCARTA_G2_PATHWAY	24	0.623125	1.746379	0.0018797	0.030382
BIOCARTA_TID_PATHWAY	17	0.700731	1.800438	0.0018975	0.023874
BIOCARTA_INTEGRIN_PATHWAY	35	0.568651	1.794564	0.0019048	0.023841
BIOCARTA_ETS_PATHWAY	18	0.675863	1.850606	0.0019342	0.019443
BIOCARTA_HSP27_PATHWAY	15	0.698828	1.79994	0.0019531	0.023302
BIOCARTA_CDMAC_PATHWAY	16	0.768664	1.966973	0.001996	0.008

Table 11 Canonical pathways upregulated in cord blood T cells.

On performing the enrichment mapping, 19 of these pathways clustered in one group and these pathways included TCR and MAPkinase signalling pathways [Figure 49].

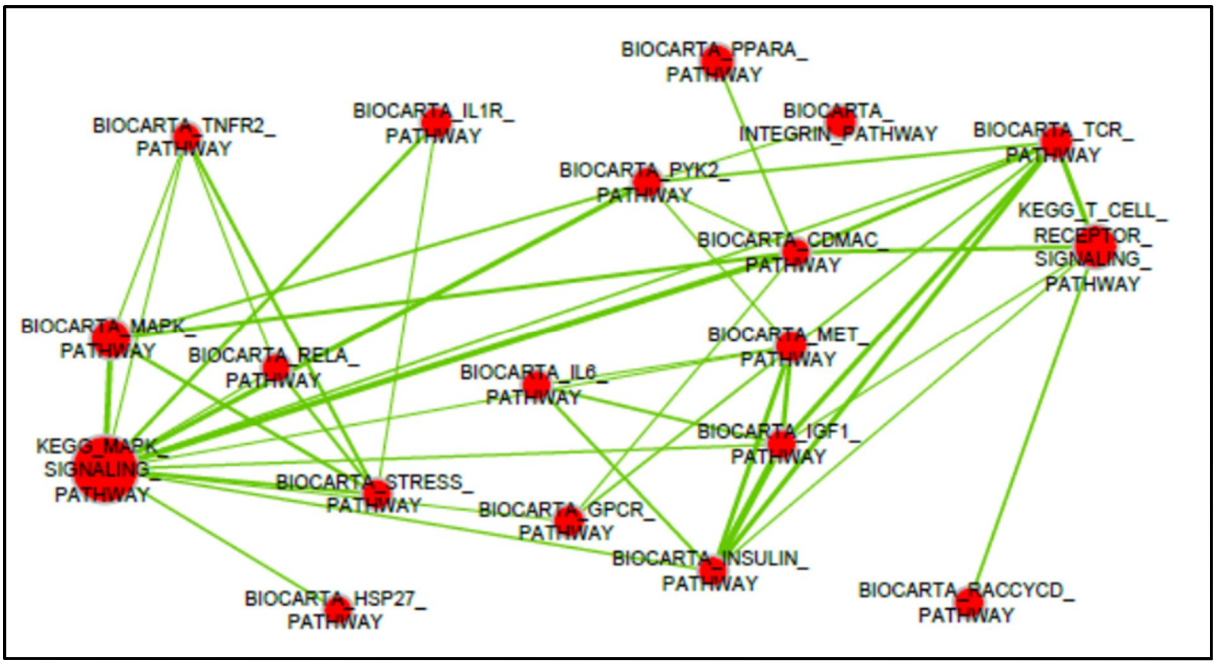

Figure 49: Enrichment map of upregulated canonical pathways in the naive cord blood $CD4^+$ T cells (*n = 9*) compared with naive peripheral blood $CD4^+$ T cells (*n = 9*). The relationship of TCR and MAPK signalling with other upregulated pathways is shown.

Figure 50 shows Blue-Pink O'gram of TCR signalling pathway and Figure 51 shows enrichment plots of TCR and MAPK signalling. The TCR and MAPK signalling pathways were not only upregulated in naïve $CD4^+$ T cells from cord blood but were also upregulated in the reconstituting naïve $CD4^+$ T cells from the lymphopenic environment following CBT and BMT (*P < 0.001, fdr q value 0.1*) [Figure 51]. This indicates induction of TCR-MAPK signals in the lymphopenic environment. Finally, on comparing naïve $CD4^+$ T cells from the two post-transplant lymphopenic conditions i.e. CBT *vs* BMT, TCR and MAPK signalling were found to be upregulated following CBT (*P < 0.02, fdr q value 0.25*) [Figure 51]. Similarly, although c-fos and c-jun were upregulated in the cord blood, during early T-cell reconstitution following CBT and BMT [Figure 51], their upregulation was significantly higher after CBT than after BMT [Figure 51]. Thus, upregulated TCR-MAPK signals and distinctly regulated cell cycle pathways may endow naïve cord blood $CD4^+$ T cells with an enhanced cell cycling ability in the lymphopenic environment.

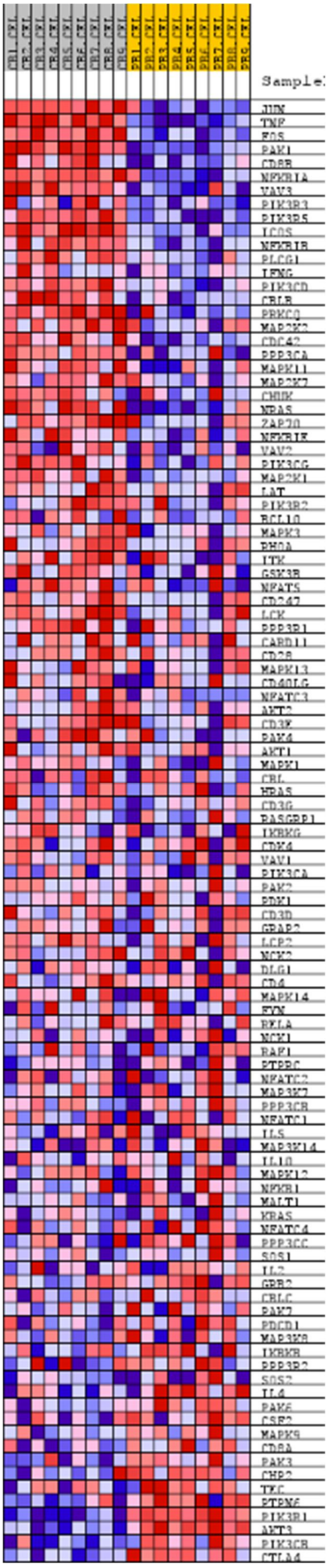

Figure 50: Blue-Pink O'gram of TCR signalling pathway after comparing transcription profiles of naive CD4+ T cells from the cord blood (*n = 9*) and peripheral blood (*n = 9*).

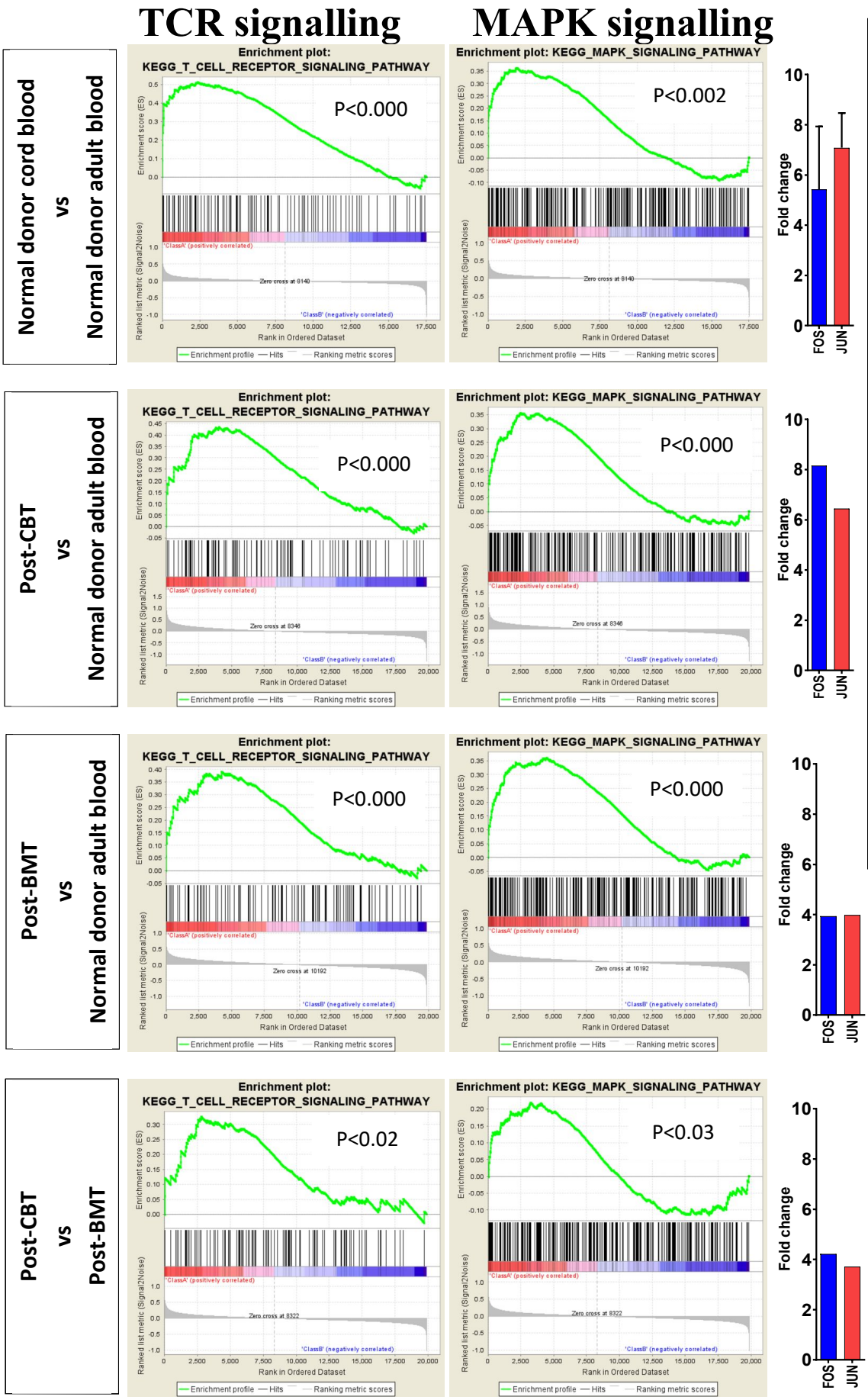

Figure 51: Enrichment plots of TCR and MAPK signalling and the transcript values of two important transcription factors FOS and JUN (AP-1 complex) in the naive CD4+ T cells from lymphopenic conditions such as (a) cord blood (b) and (c) during early T-cell reconstitution following CBT and BMT. FOS and JUN upregulation is expressed as mean (and where possible as standard deviation) (d) When comparing the two lymphopenic conditions i.e. CBT vs BMT, reconstituting naive CD4+ T cells were observed to have an upregulated TCR and MAPK signalling following CBT.

5.6 Testing functional relevance of enhanced TCR signalling in cord blood T cells

In order to study the role of TCR signalling in homeostatic T-cell proliferation and whether TCR:MHC interactions assist in T-cell reconstitution after T-cell replete graft depending on whether the graft source is foetal or adult, we cultured CFSE-labelled CB and PB $CD3^+$ T cells with autologous irradiated non-CD3 fractions. These cultures of non-CD3:$CD3^+$ T-cell were set up in round bottom 96 well plates at the ratio of 1:0 (50000:0), 1:1 (50000:50000), 2:1 (100000:50000) and 4:1 (200000:50000). After 7 days of culture, $CD4^+$ T cells were analysed for proliferation.

Eighty-five to 90% of cord blood $CD4^+$ T cells entered into cell cycle compared with 75% of peripheral blood $CD4^+$ T cells ($P < 0.05$).

The proliferative indices (PIs) of cord blood $CD4^+$ T cells with APC:T cell ratio of 1:1, 2:1 and 4:1 were 2.3 (+/– 0.05), 2.9 (+/– 0.2) and 3.5 (+/– 0.17) respectively [Figure 52 (a) and 53]. In contrast, PIs of peripheral blood $CD4^+$ T cells with APC:T cell ratio of 1:1, 2:1 and 4:1 were 1.8 (+/– 0.1), 1.8 (+/– 0.1) and 1.9 (+/– 0.1) respectively [Figure 52 (b) and 53]. Thus, significantly higher proliferation of cord blood $CD4^+$ T cells occurred compared to peripheral blood $CD4^+$ T cells ($P < 0.05$). A significant effect of increasing APC:T-cell ratio was observed on proliferation of cord blood $CD4^+$ T cells without such an effect on the peripheral blood $CD4^+$ T cells ($P < 0.05$).

Thus, this non-CD3:$CD3^+$ T-cell co-culture system which mimics homeostatic T-cell proliferation show that distinct TCR:MHC interactions occur in cord blood compared with adult blood and this may influence T-cell homeostasis after CBT and BMT.

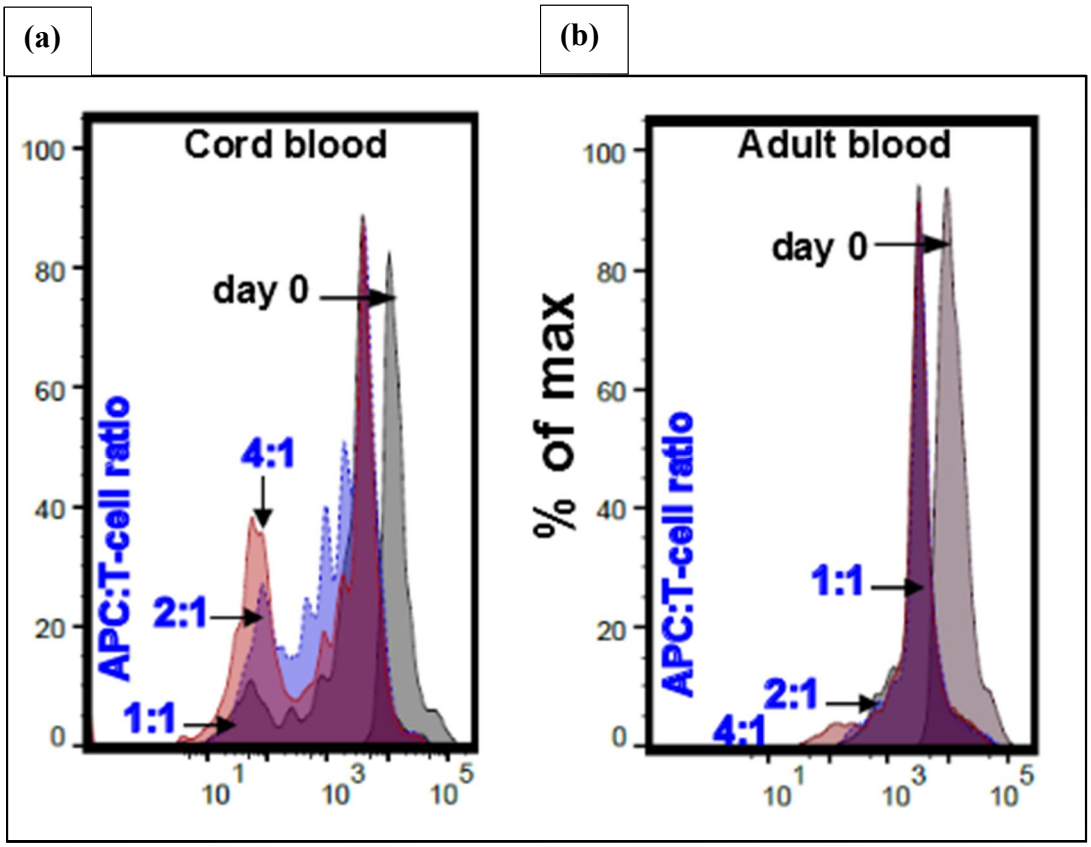

Figure 52: (a) and (b) CFSE proliferation assay of cord blood and peripheral blood $CD4^+$ T cells in response to increasing APC:T-cell ratio of 1:1, 2:1 and 4:1. The proliferation of cord blood $CD4^+$ T cells (*n = 3*) compared with peripheral $CD4^+$ T cells (*n = 3*) was significantly enhanced.

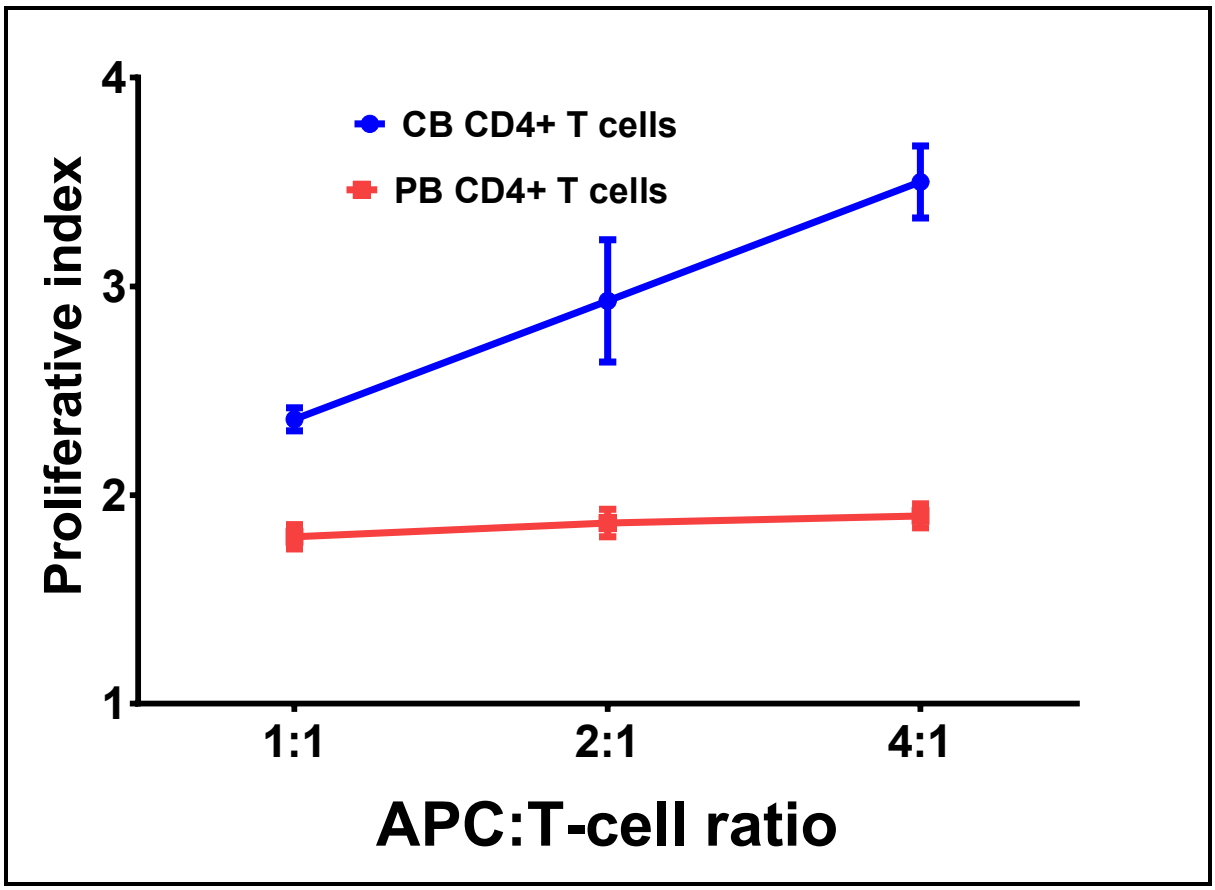

Figure 53: Line graph showing increased proliferation of cord blood $CD4^+$ T cells (*n=3*) with increasing APC:T-cell ratio, however no such effect was observed on peripheral blood $CD4^+$ T cells (*n=3*).

5.7 Testing functional relevance of AP-1 upregulation in cord blood CD4$^+$ T cells

To further determine the role of TCR and MAPkinase signalling in CB T-cell homeostasis, we inhibited the most upregulated transcription factor c-fos, c-jun (AP-1) using AP-1 inhibitor (SR 11302). CFSE-labelled CB CD3$^+$ T cells were cultured with non-CD3 fraction in the non-CD3:CD3 ratio of 4:1 (200000:50000). These cultures were performed without AP-1 inhibitor and with AP-1 inhibitor of 1, 10 and 100 ng/ml.

The PIs of cord blood CD4$^+$ T cells cultured with APC's at APC:T cell ratio of 4:1 and an AP-1 inhibitor concentration of 1 ng/ml, 10 ng/ml and 100 ng/ml were 3.5 (+/– 0.1), 2.7 (+/– 0.1) and 1.9 (+/– 0.1) respectively [Figure 54 and 55]. Thus, increasing concentration of AP-1 inhibitor had an increased inhibitory effect on CB CD4$^+$ T-cell proliferation indicating that AP-1 inhibition abrogated TCR-MAP kinase signals. This suggest that inhibiting TCR signalling abrogates homeostatic T-cell proliferation in non-CD3:CD3$^+$ T-cell coculture system.

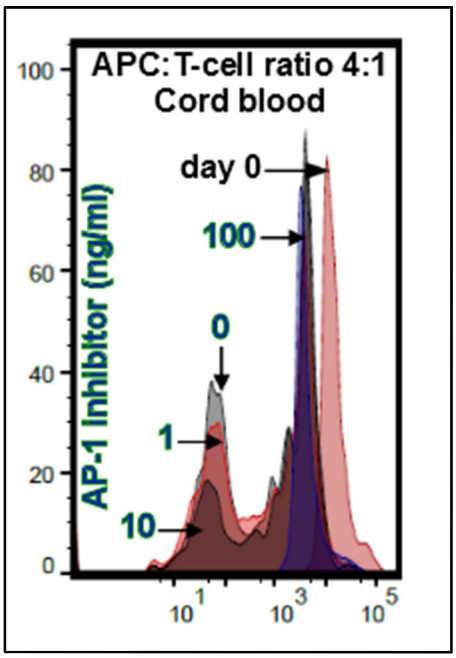

Figure 54: CFSE assay showing proportional inhibition of cord blood CD4+ T-cell proliferation at different concentrations of AP-1 inhibitor.

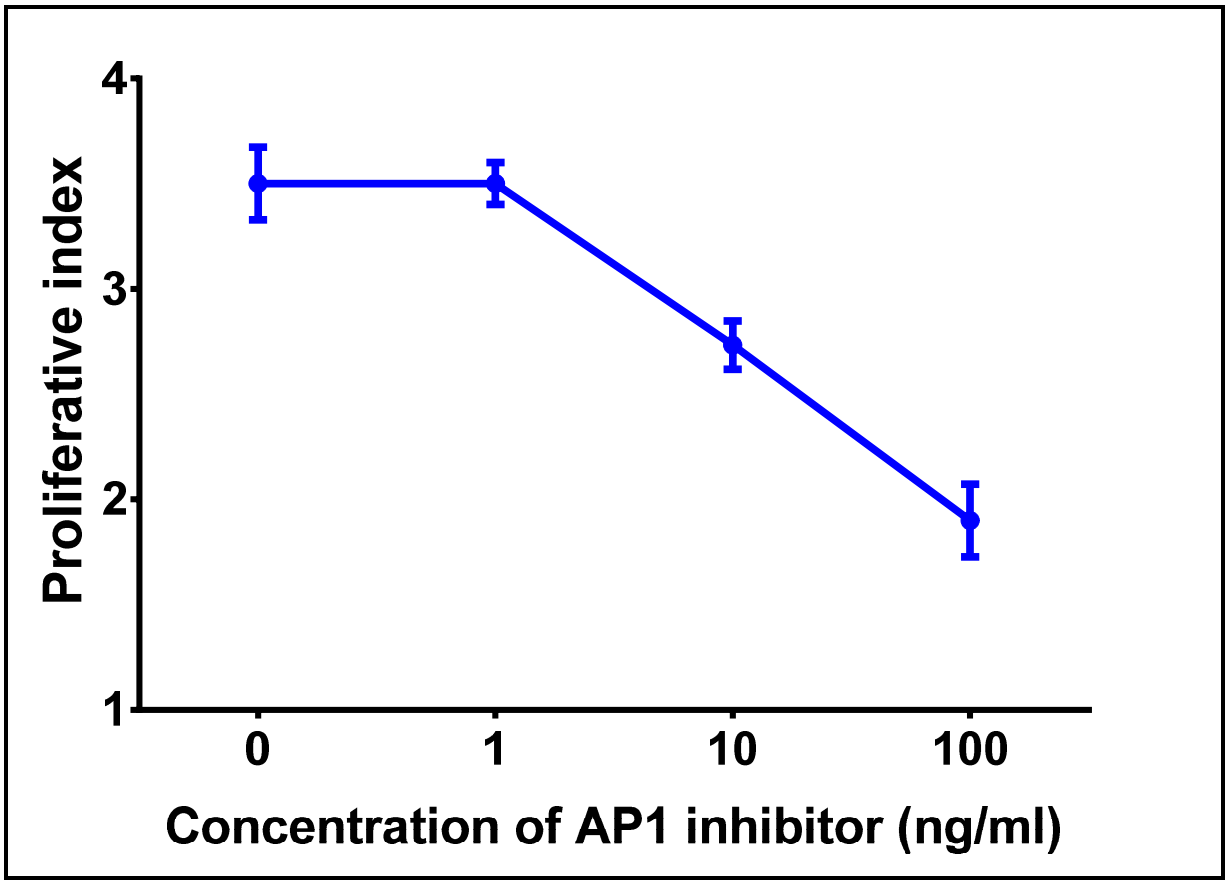

Figure 55: Line graph showing the inhibitory effect on cord blood $CD4^+$ T cells ($n=3$) was proportional to the increasing concentration of AP-1 inhibitor. The dots represent mean and error bars represent standard deviation.

Thus, upregulated TCR signalling may endow naïve cord blood $CD4^+$ T cells with the enhanced ability to proliferate in the lymphopenic environment and hence contribute to unprecedented T-cell reconstitution after CBT.

CONCLUSIONS

We have shown that cord blood T cells and peripheral blood T cells have a distinct transcriptional profile. It has been previously reported that foetal T cells have a distinct gene expression profile compared with adult T cells and our work shows that cord blood T cells also have a distinct gene expression profile compared with adult T cells and that the gene expression profile of cord blood T cells is similar to foetal T cells. This indicates that cord blood T cells have foetal ontogenic origins which is distinct to that of adult ontogeny. Further we have shown that following CBT, there is recapitulation of foetal T-cell ontogeny.

More importantly, gene expression profiles show that AP-1 was significantly upregulated in the cord blood T cells compared with the peripheral blood T cells. AP-1 is an important activator protein which is an important regulator of cell life and death and it plays an important role in TCR-MAPkinase signalling. Further using GSEA and enrichment mapping analysis, we found that biological processes such as cell cycle and apoptosis and canonical pathways such as TCR-MAPkinase signalling were significantly upregulated.

To test the relevance of AP-1 and TCR-MAPkinase signalling pathway we performed functional analysis. Firstly, we cocultured cord blood T cells and peripheral blood T cells with allogeneic lymphoblastoid cells to assess the differences in proliferation in response to non-self MHC peptide. We found that cord blood T cells proliferate rapidly after stimulation with allogeneic lymphoblastoid cells compared with peripheral blood T cells. This proliferation of cord blood T cells was similar to rapid proliferation of foetal T cells after stimulation with allogeneic peripheral blood mononuclear cells as shown previously. This indicates that foetal T cells and cord blood T cells undergo robust proliferation compared with peripheral blood T cells when stimulated with non-self MHC peptide.

To test if these differences in proliferation between cord blood and peripheral blood T cells maintain a similar response during homeostatic proliferation, we compared the proliferation of $CD3^+$ T cells when stimulated with autologous non-CD3 fraction. We found enhanced proliferation of cord blood $CD4^+$ T cells in comparison to peripheral blood $CD4^+$ T cells. This indicates that cord blood T cells are more sensitive to both self and non-self peptide MHC than peripheral blood T cells and this is represented by upregulated TCR-MAPkinase signalling pathway and AP-1 transcription factor. Therefore, AP-1 inhibition assay was performed using a small molecule. These assays showed that AP-1 inhibitor inhibited the proliferation of naïve $CD4^+$ T cells in a dose dependent manner. Thus, these observations indicate a major role of

TCR signalling in homeostatic proliferation following T-replete CBT. Since T cells with enhanced sensitivity to homeostatic cues have been shown to have the ability to mediate enhanced response to foreign antigens too (Fulton *et al.,* 2015), we questioned if cord blood T cells can mediate an enhanced graft-versus-leukaemia effect compared with peripheral blood T cells.

Chapter six

Cord blood T cells mediate enhanced anti-leukaemic effects compared with peripheral blood T cells

6.0 Aims

1) To develop a human T-cell:lymphoma model in an immunodeficient mice.

2) To compare the anti-tumour effect mediated by cord blood T cells and peripheral blood T cells in this model.

6.1 Introduction

We have shown in the previous chapter that foetal ontogeny of cord blood T cells is recapitulated after T-cell replete cord blood transplantation. During recapitulation of foetal ontogeny, we observed enhanced $CD4^+$ T-cell reconstitution with rapid memory-effector differentiation. Thus, cord blood T cells rapidly reconstitute in the lymphopenic environment. We also observed rapid proliferation of cord blood T cells in response to self-MHC and allo-MHC peptides *in vitro*, and that these processes are mediated by upregulated TCR signalling in cord blood T cells.

In addition to being ontogenetically foetal and despite being overtly responsive to self and non-self MHC peptides, cord blood T cells are predominantly antigen-inexperienced $CD45RA^+$ cells. When compared with $CD45RA^+$ "naive" adult T cells, cord blood T cells are Th2-Tc2 biased with reduced inducible expression of Th1-Tc1 cytokines, such as interferon gamma (IFN-γ) (White *et al.,* 2002; Marchant *et al.,* 2005). This is due to relative hypermethylation of cord blood $CD4^+$ T cells at CpG and non-CpG sites within the IFN-γ promoter (White *et al.,* 2002). Th1 responses in cord blood T cells are further attenuated because of reduced ability of neonatal dendritic cells to produce IL-12 (Langrish *et al.,* 2002). In addition, the foetal immune system is generally believed to induce immune tolerance after exposure to foreign antigens (Silverstein *et al.,* 1964a; Silverstein *et al.,* 1964b). These findings suggest that although cord blood T cells undergo enhanced proliferation in response to self and non-self MHC peptides they may not mount efficient allo-reactive response required for eliminating leukemia.

However, CBT is associated with a significantly lower leukemia relapse risk, particularly after HLA-mismatched and T-cell replete CBT (Eapen *et al.,* 2007; Milano *et al.,* 2016). HLA-mismatched CBT is now being recommended in the absence of a matched adult donor because cord blood grafts pose a lower risk of chronic GvHD compared with adult grafts (Gluckman *et al.,* 2012). For the same reason, while adult grafts are increasingly matched for 10 HLA loci (HLA, B, C, DR, and DQ), cord blood grafts are matched only for 6 HLA loci (HLA A, B, and DR) (Gluckman *et al.,* 2012), and additionally, CBT is increasingly being performed without anti-thymocyte globlin (ATG) for treating high risk hematological malignancies (Chiesa *et al.,* 2012; Wagner *et al.,* 2014). We have shown that such a T-cell replete approach leads to enhanced thymus-independent T-cell expansion of donor cord blood T cells (Chiesa *et al.,* 2012; Lindemans *et al.,* 2014). This enhanced thymus-independent T-

cell reconstitution after CBT is always $CD4^+$ T-cell biased, a pattern not observed after transplantation using a bone marrow or peripheral blood stem cell graft, and, intriguingly, occurs despite one log lower T cells in the cord blood graft compared with the bone marrow graft [Figure 12 and 13]. Furthermore, these rapidly expanding naïve cord blood T cells differentiate into viral specific T-lymphocytes within 2 months, leading to rapid clearance of viral infections from the blood (both cytomegalovirus and adenovirus; Chiesa *et al.,* 2012). These observations suggest that despite intrinsic bias towards anti-inflammatory Th2–Tc2 immune responses, naive cord blood T cells can rapidly proliferate and differentiate into antigen-specific T lymphocytes.

Therefore, I questioned whether this rapidly expanding early-life naïve T-cell immunity following unrelated T-cell replete CBT, which is less stringently HLA-matched compared with an adult donor, also accounts for enhanced GvL effects. I set out to establish a model to study the orchestration of these anti-tumour effects mediated by cord blood T cells within the tumour microenvironment. In order to model this, I compared the ability of HLA-mismatched cord blood and peripheral blood T cells to eliminate EBV-driven human B-cell lymphomas in a NOD/SCID/IL2rg^{null} mouse model.

6.2 Cord blood T cells mediate enhanced anti-tumour effects compared with peripheral blood T cells

NOD/SCID/IL2rg^{null} (NSG) mice were chosen because they are deficient in T, B, and NK cells and this allows rapid engraftment of human T cells (Shultz *et al.,* 1995).

EBV-driven human B-cell lymphoma was chosen as human tumour because of our expertise in this tumour model. This tumour can be subcutaneously grafted into the NOD/SCID/IL2rg^{null} mice allowing *in vivo* imaging of tumour using Xenogen-IVIS. In addition, this tumour is known to have professional antigen presenting abilities because of strong expression of MHC Class I and Class II and other co-stimulatory molecules such as CD80, CD86, and CD83.

I initially compared the anti-tumour effects of equivalent doses of T cells derived from cord blood *versus* peripheral blood in this NSG mouse model of EBV-driven B-cell lymphoma.

EBV-driven B-cell lymphoblastoid cells were generated from random donors. These cells were transduced with SFG retroviral vector encoding green shifted Firefly Luciferase (F-Luc). F-Luc positive lymphoblastoid cells were sorted and then grown to perform the experiment. Experimental design involved injecting 5×10^6 human B-cell lymphoma cells on day –2 subcutaneously. Untouched $CD3^+$ T cells were sorted from the fresh cord blood and adult blood mononuclear cells on day 0 and, 5×10^6 peripheral blood or cord blood T cells were injected via tail vein. Mice were then monitored for tumour growth by *in vivo* imaging using Xenogen-IVIS and calliper on day +10, 20, 30, 35, 40, 50, and 60. Mice were also monitored weekly for signs of xeno-reactivity such as ruffled fur, lethargy and weight loss.

Two consecutive experiments with B-cell lymphoma and allogeneic T cells derived from different donors were performed. The degree of HLA-mismatch between the T cells from the cord blood and peripheral blood group and the B-cell lymphoma tumour cell lines was similar in both the experiments. In the first experiment, both the cord blood and peripheral blood T cells were mismatched with the tumour for all 10 HLA antigens and, in the second experiment cord blood and peripheral blood T cells were mismatched with the tumour for 7 of 10 HLA antigens (Table 12).

	HLA A	HLA B	HLA C	HLA DRB1	HLA DQB1
CB donor 1	36 66	15 18	02 07	01 11	05 06
PB donor 1	02 32	07 44	05 07	13 15	06 06
LCL donor 1	24 30	13 51	06 1602	04 07	02 07
CB donor 2	**02** 29	44 51	14 16	**07** 11	**02** 03
PB donor 2	01 68	14 58	**07** 08	**07** 16	**02** 05
LCL donor 2	**02** 24	07 39	**07** 07	**07** 13	**02** 06

Table 12 Cord blood T cells vs LCLs and peripheral blood T cells vs LCLs show a similar degree of HLA-mismatch in the two experiments. All 10 HLA antigens and 7 of 10 HLA antigens were mismatched in experiment 1 and 2 respectively.

	Cord blood	**Peripheral blood**
Expt 1	95.9%	94.6%
Expt 2	95.2%	94.5%

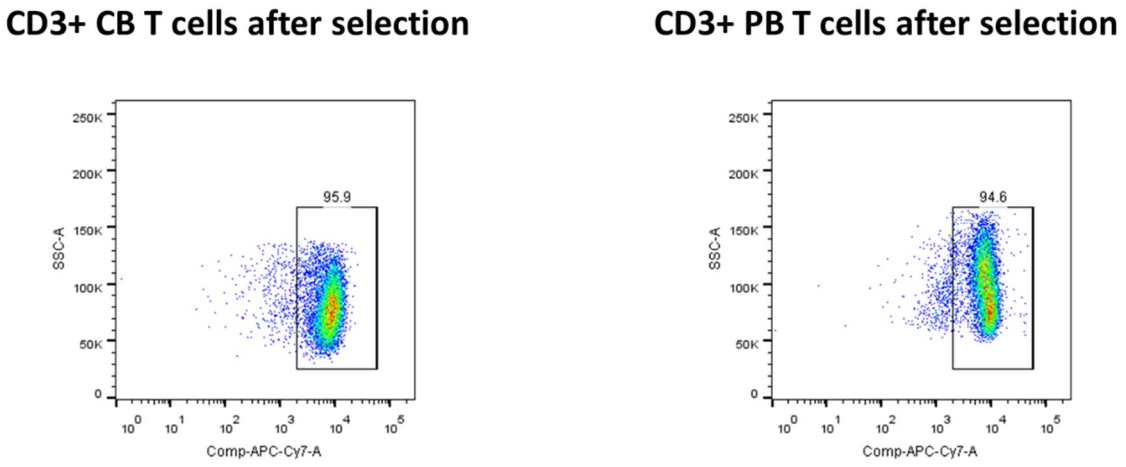

Table 13 Representative $CD3^+$ population obtained after negative selection is shown as APC-Cy7 fluorescence are shown. Cell debris were excluded from the analysis based on scatter signals. The purity of T cells obtained after negative selection was > 94% in the two primary experiments.

Control mice receiving B-cell lymphoma without T cells (*n = 6*) and mice receiving B-cell lymphoma followed by peripheral blood T cells (*n = 10*) exhibited tumour growth exceeding

the threshold limit of 10 mm between 20–22 days following tumour inoculation, and hence these mice were sacrificed. In contrast, 9/10 mice receiving cord blood T cells showed slower tumour growth followed by complete tumour regression [Figure 56]. These findings were confirmed by measuring tumour bioluminescence in photons/sec/cm^2/sr using a Xenogen-IVIS imaging system. The mean tumour bioluminescence of the cord blood group on day +20 was significantly lower than that of the peripheral blood and control group (9.65×10^9 +/− 2.65×10^9 *vs* 3.83×10^{10} +/− 1.075×10^{10} and 3.04×10^{10} +/− 8.42×10^9, respectively; $P < 0.01$) [Figure 57]. These IVIS findings were mirrored by caliper-measured tumour volumes. On day +20, the mean tumour volume in the cord blood group was 204 mm^3 [Figure 58], which was significantly lower than the mean tumour volume of the peripheral blood (814 mm^3) and control (812 mm^3) group ($P < 0.01$).

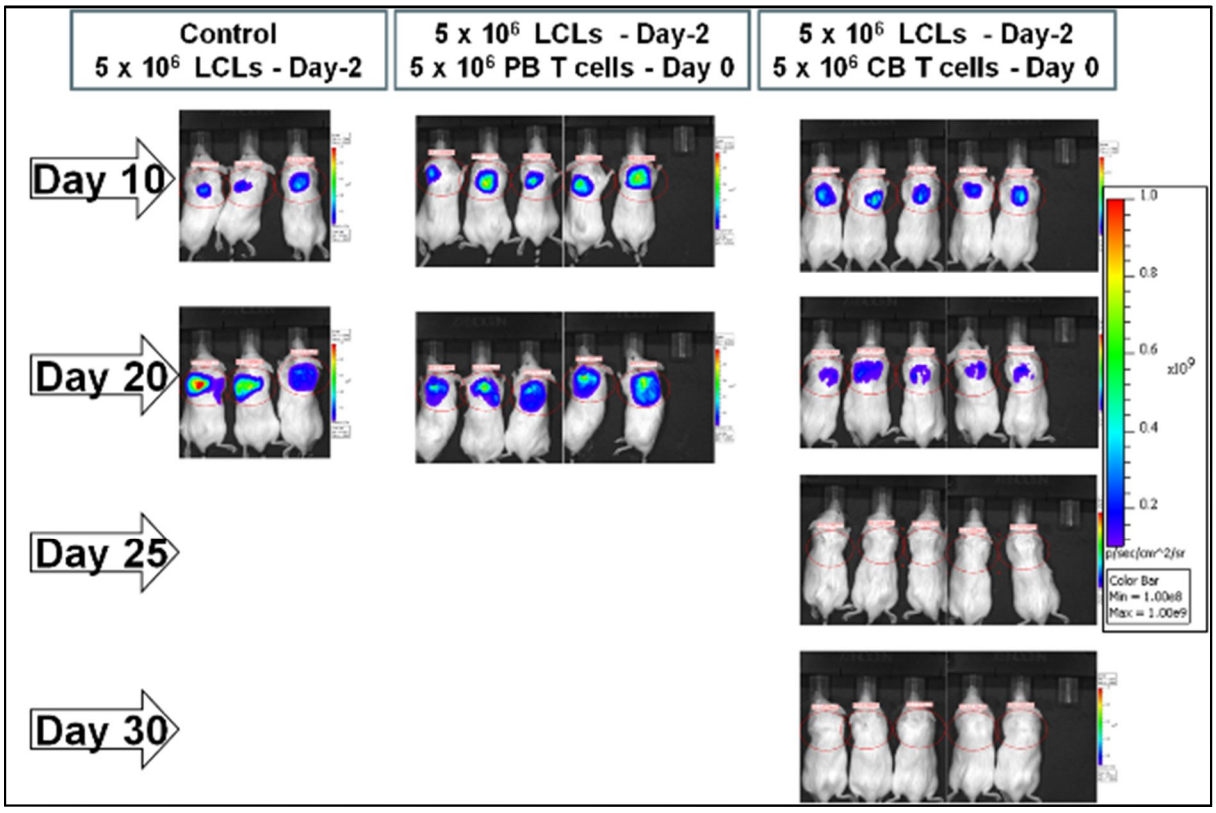

Figure 56: Representative experiment illustrates slower tumour growth followed by rapid rejection of B-cell lymphoma in mice receiving allogeneic cord blood T cells compared with mice receiving allogeneic peripheral blood T cells and control mice. All images are shown on one scale (range: 1.00e8 to 1.00e9 photons/sec/cm^2/sr). Tumour size in control mice and those receiving peripheral blood T cells exceeded threshold of 10 mm and hence these mice were sacrificed.

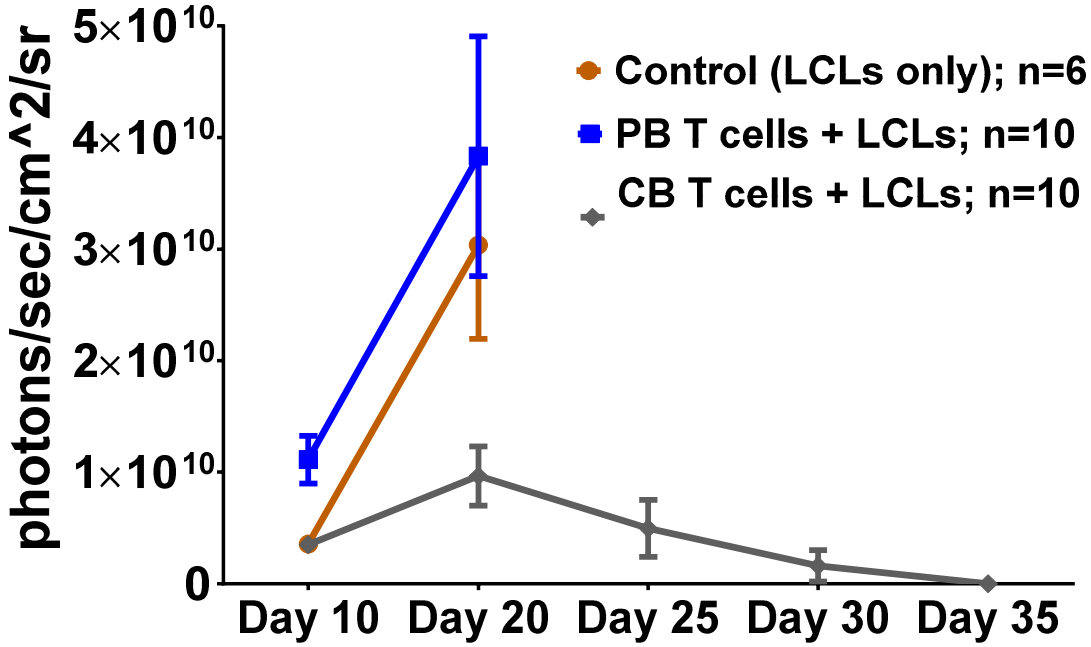

Figure 57: Tumour bioluminescence (photons/sec/cm^2/sr) was measured using Xenogen-IVIS. Cumulative rate of tumour growth (mean and standard error of mean) from two separate experiments are plotted. These plots show significantly slower rate of tumour growth in the mice receiving cord blood T cells compared with the mice receiving peripheral blood T cells and control group. (Two independent experiments)

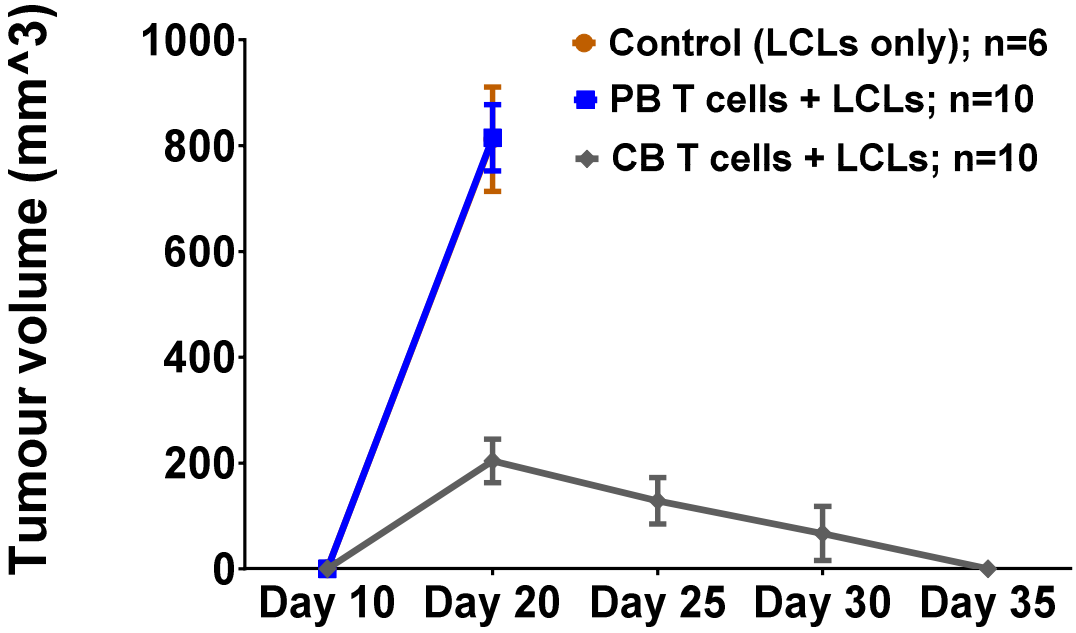

Figure 58: Tumour volume (mm^3) was derived using calliper measurements. Cumulative rate of tumour growth (mean and standard error of mean) from two separate experiments are plotted. These plots show significantly slower rate of tumour growth in the mice receiving cord blood T cells compared with the mice receiving peripheral blood T cells and control group. (Two independent experiments)

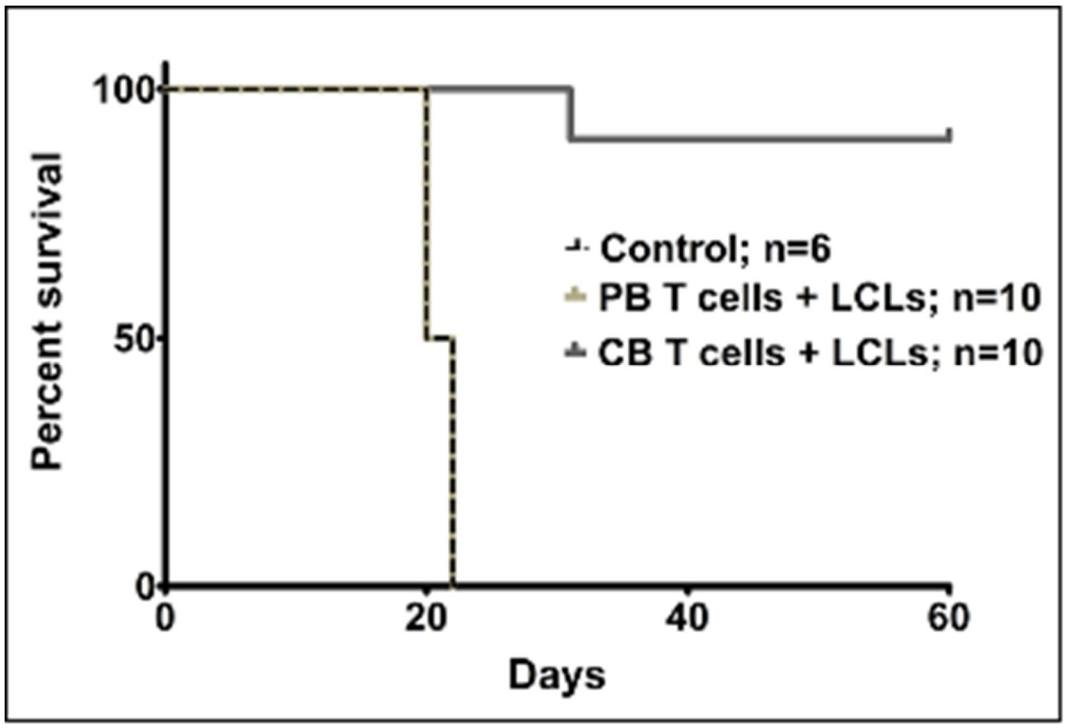

Figure 59: Regression of tumour following infusion of cord blood T cells led to significantly improved survival in this group compared with the peripheral blood group (log rank test; $P < 0.0003$).

Surviving mice in the cord blood group were monitored for 60 days after T-cell injection, and interestingly, there was no relapse of tumour and no evidence weight loss or other signs of xenogeneic GvHD. This led to significantly improved survival in the cord blood group compared with the peripheral blood group ($P < 0.0003$) [Figure 59]. This observation suggests that cord blood T cells can mediate a potent GvL effect without causing xenogeneic GvHD.

6.3 Cord blood T cells are not xeno-reactive, whereas peripheral blood T cells have potent xeno-reactive ability

However, because the xenogeneic GvHD mediated by peripheral blood T cells is well established (King *et al.,* 2009; Ali *et al.,* 2012; Covassin *et al.,* 2011), I next performed xeno-reactive modelling comparing the ability of intravenously injected cord blood *vs* peripheral blood T cells to mediate xenogeneic GvHD.

Untouched $CD3^+$ T cells were sorted from freshly isolated cord blood and peripheral blood mononuclear cells. After injecting 5×10^6 cord blood or peripheral blood T cells via tail vein, mice were monitored for signs of xenogeneic GvHD such as ruffled fur, lethargy and weight loss.

In mice receiving peripheral blood T cells, we observed the onset of xeno-reactivity 3 weeks following T-cell injection. All mice receiving peripheral blood T cells begin to develop weight loss 3 weeks following T cell injections [Figure 60]. In the following week, ruffled fur and lethargy was noticed along with the weight loss of more than 10% and hence the mice receiving peripheral blood T cells had to be sacrificed. In contrast, mice receiving cord blood T cells did not develop any symptoms of xeno-reactivity, during the 60 day period of observation after T-cell injection. This was despite the presence of circulating human T cells at the end of the experiment.

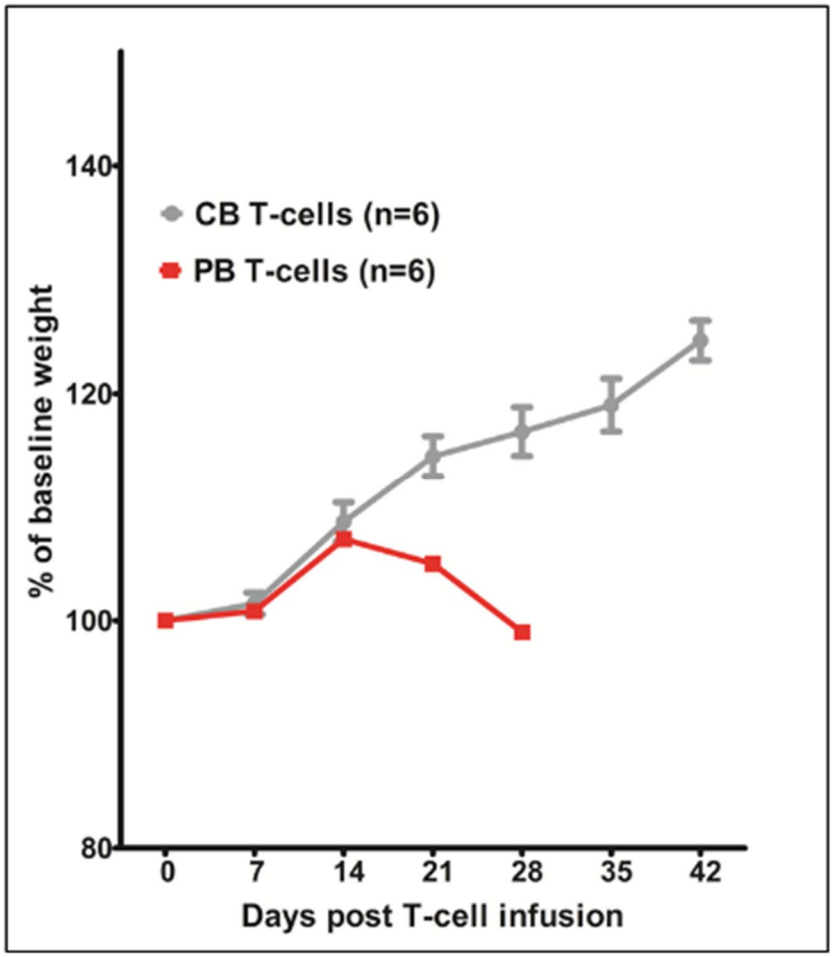

Figure 60: shows onset of weight loss three weeks after peripheral blood T cell injections. 10-15% weight loss occurred by four weeks in the peripheral blood group and hence these mice were sacrificed. No weight loss was observed in mice receiving cord blood T cells up to 6 weeks after the injection of T cells.

The presence of xenogeneic GvHD in the peripheral blood T-cell group was further confirmed by haematoxylin/eosin staining of target GvHD organs such as liver and skin. A significant infiltration of T cells and distortion of normal architecture around the bile ducts and in the intra-dermal region was observed in the peripheral blood group. In contrast, scant T cells and normal histology of liver and skin sections were observed in the cord blood T-cell group [Figure 61].

This was further substantiated by the cleaved-caspase 3 staining to study the apoptosis in the histopathology sections of liver and skin. We observed marked cleaved-caspase 3 staining indicating the apoptotic changes around the bile ducts and in the intra-dermal region of the peripheral blood group. In contrast, no apoptotic changes were seen in the cord blood group [Figure 61].

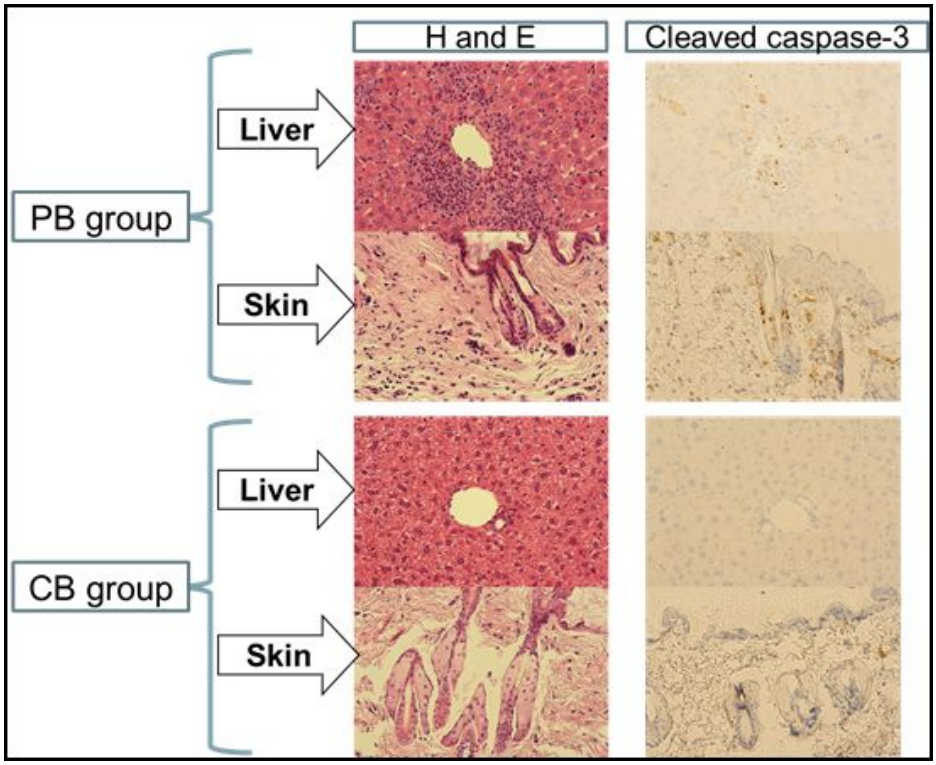

Figure 61: Haematoxylin and eosin sections of liver and skin of mice receiving peripheral blood T cells show infiltrating lymphocytes around the bile duct and in the intra-dermal region. Cleaved caspase-3 staining was apparent at the site of lymphocytic infiltration confirming apoptosis of bile duct epithelium and keratinocytes present in epidermis and hair follicle. Cord blood T cells were not observed to infiltrate either liver or skin.

This indicates that cord blood T cells do not cause xenogeneic GvHD, while peripheral blood T cells mediate potent xenogeneic GvHD.

We then asked the question whether xeno-reactive peripheral blood T cells might also mediate a GvL effect?

6.4 Peripheral blood T cells can mediate GvL effect correlating with the onset of xeno-reactivity

To model any GvL effect mediated by peripheral blood T cells and how this correlates with xenogeneic GvHD following peripheral blood T-cell injection, I performed tumour modeling experiment with a lower burden of B-cell lymphoma. B-cell lymphoma (2.5×10^6 cells) were injected subcutaneously on day –2 in six mice, followed by the tail vein injection of 5×10^6 peripheral blood T cells in the treatment but not the control group.

We observed that the control mice receiving B-cell lymphoma without T cells ($n = 3$) had tumour growth exceeding the threshold limit of 10 mm on day +27 after tumour inoculation, and hence these mice were sacrificed. In mice receiving peripheral blood T cells, tumours continued to grow until 3 weeks. On day +20, there was no statistically significant difference between the tumours in the control and peripheral blood T-cell group (mean tumour bioluminescence = 3.89×10^8 +/− 2.15×10^8 *vs* 5.69×10^8 +/− 1.69×10^8; P = NS). After 3 weeks, the tumours in mice receiving peripheral blood T cells started regressing [Figure 62]. We observed signs such as ruffled fur, lethargy, and, most importantly, the onset of weight loss, an objective measure of xeno-reactivity correlated with the onset of tumour regression [Figure 63]. This confirms that peripheral T cells also mediate a GvL effect in this model, although this effect was apparent only against a lower burden of B-cell lymphoma. Thus, compared with cord blood T cells, peripheral blood T cells appear to mediate an attenuated anti-tumour effect correlating with the onset of xenogeneic GvHD.

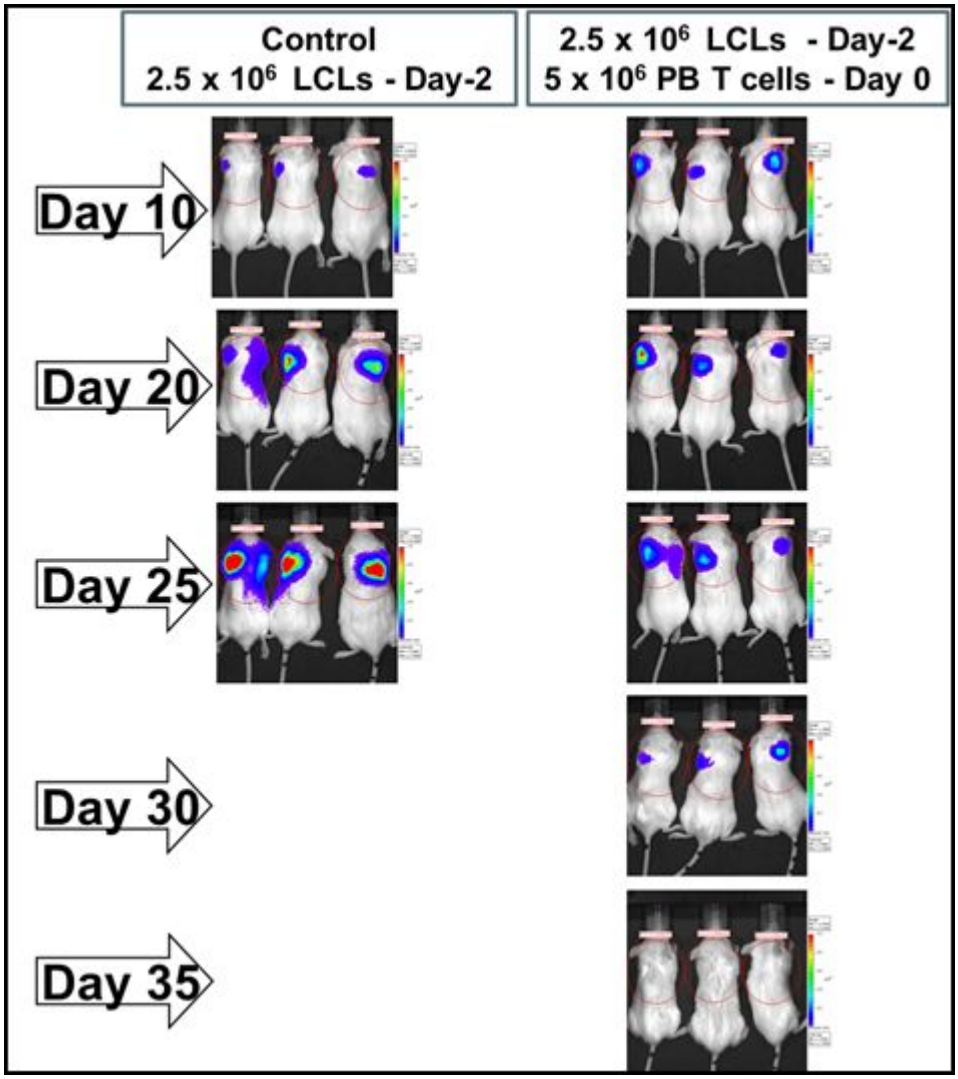

Figure 62: Tumour bioluminescence measured as photons/sec/cm^2/sr using Xenogen-IVIS. All images are shown on one scale (range: 2.00e6 to 1.00e8 photons/sec/cm^2/sec). Tumour regression was observed in the peripheral blood T cells with the onset of signs of GvHD (weight loss, ruffled fur).

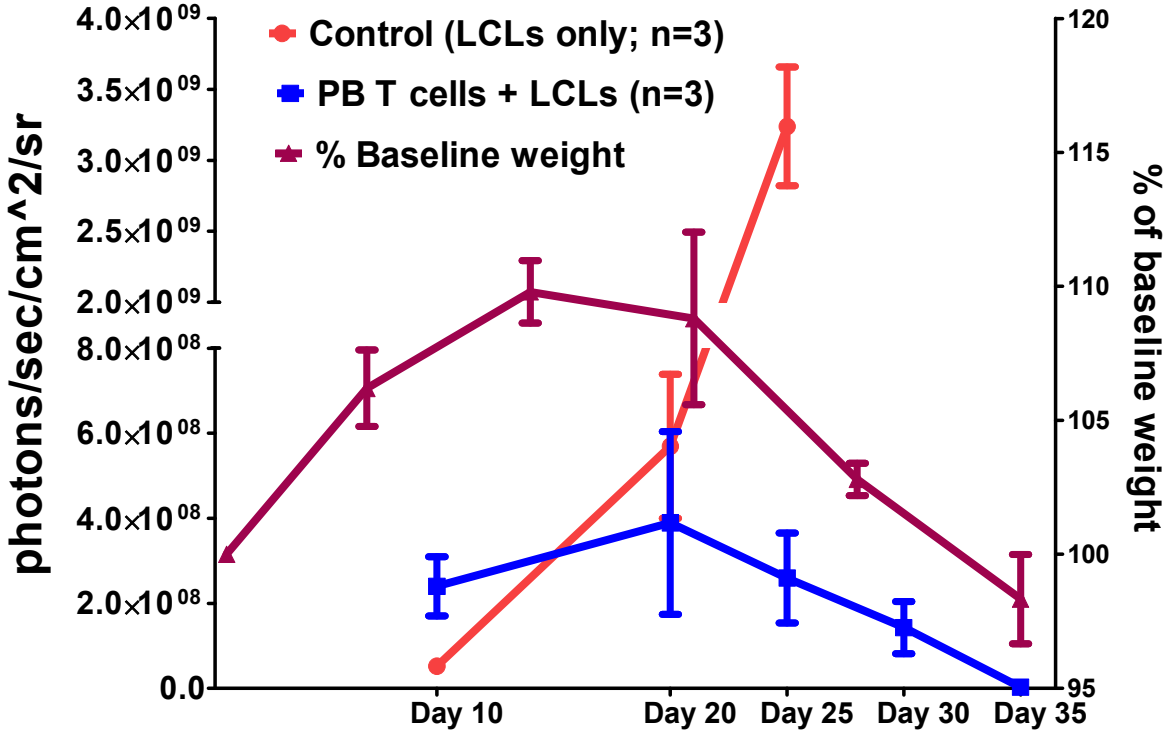

Figure 63: GvL effect mediated by peripheral blood T cells (5 million) against a lower burden of B-cell lymphoma (2.5 million tumour cells) and a correlation between xenoreactivity and tumour regression following peripheral blood T-cell injection. (A) shows serial weekly weight measurements of mice plotted as % of baseline weight (mean and standard error of mean) on right y-axis and bioluminescence of tumour measured as photons/sec/cm^2/sr (mean and standard error of mean) plotted on left y-axis. In this experiment with lower burden of tumour cells, tumour regression correlated with the onset of weight loss, which is an objective measure of xenoreactivity. This experiment suggests that peripheral blood T cells also mediate tumour regression but this effect may be attenuated and typically occurs with the onset of xenoreactivity.

6.5 Anti-tumour effects of cord blood T cells are mediated through allo-reactivity

Lymphoblastoid tumour in our model is an EBV-driven lymphoma. Therefore, it was imperative to determine the anti-tumour effect mediated by cord blood T cells is an anti-leukaemic (allo-reactive) effect and not an anti-EBV effect.

To model this, autologous T cells were first sorted from the cord blood mononuclear cells and stored in liquid nitrogen. The remaining population of cells which included the B cells, were used to generate the lymphoblastoid cells as described in the methods. Subsequently allogeneic T cells were sorted from the cord blood mononuclear cells of another donor and stored in liquid nitrogen.

When the lymphoblastoid cells were generated, they were transduced with SFG retroviral vector encoding green shifted F-Luc. F-Luc positive lymphoblastoid cells were sorted and then grown to perform the experiment.

In this experiment, I compared the ability of autologous and allogeneic cord blood T cells to reject B-cell lymphoma. Mice were injected with B-cell lymphoma (5×10^6 cells) subcutaneously on day –2, followed by the tail vein injection of 5×10^6 stored autologous or allogeneic T cells on day 0.

Control mice receiving B-cell lymphoma without T cells ($n = 3$) and mice receiving B-cell lymphoma followed by autologous cord blood T cells ($n = 5$) had tumour growth exceeding the threshold limit of 10 mm on day +22 after tumour inoculation and were therefore sacrificed. In contrast, mice injected with B-cell lymphoma and allogeneic cord blood T cells ($n = 5$) had slower tumour growth followed by complete tumour regression. On day +22, the autologous cord blood T-cell group had a mean tumour volume (mm^3) and mean tumour bioluminescence (photons/sec/cm^2/sr) of 1223 +/− 72 and 1.323×10^{11} +/− 2.53×10^{10}, respectively. In contrast to these large tumours, the mean tumour volume (mm^3) and mean tumour bioluminescence (photons/sec/cm^2/sr) in the allogeneic cord blood T-cell group were significantly lower, 12 +/− 6 and 1.797×10^9 +/− 1.09×10^9, respectively ($P < 0.01$) [Figure 64, 65 and 66).

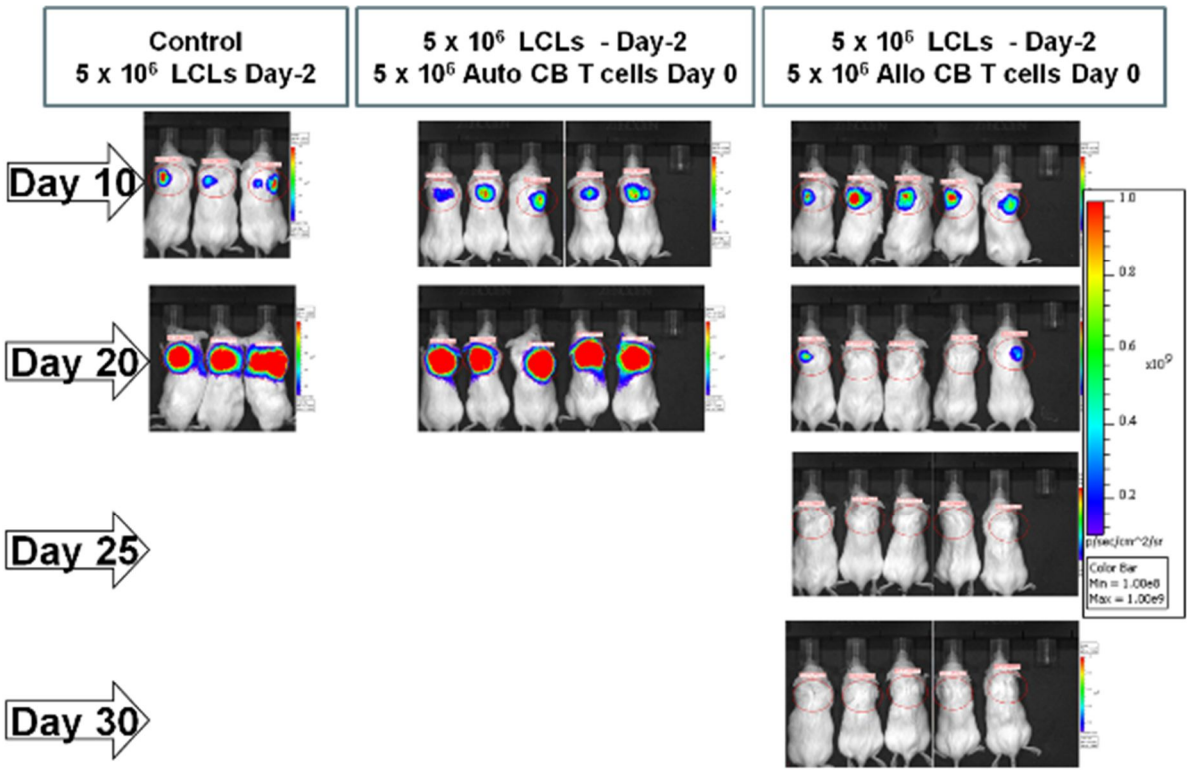

Figure 64: Representative experiment illustrates tumour regression in mice receiving allogeneic cord blood T cells. Tumour size in mice receiving autologous cord blood T cells exceeded 10 mm and hence these mice were sacrificed. This observation suggest that anti-tumour effects against B-cell lymphoma is an allo-reactive effect, and not an EBV-specific response. All images are shown on one scale (range: 1.00e8 to 1.00e9 photons/sec/cm^2/sr).

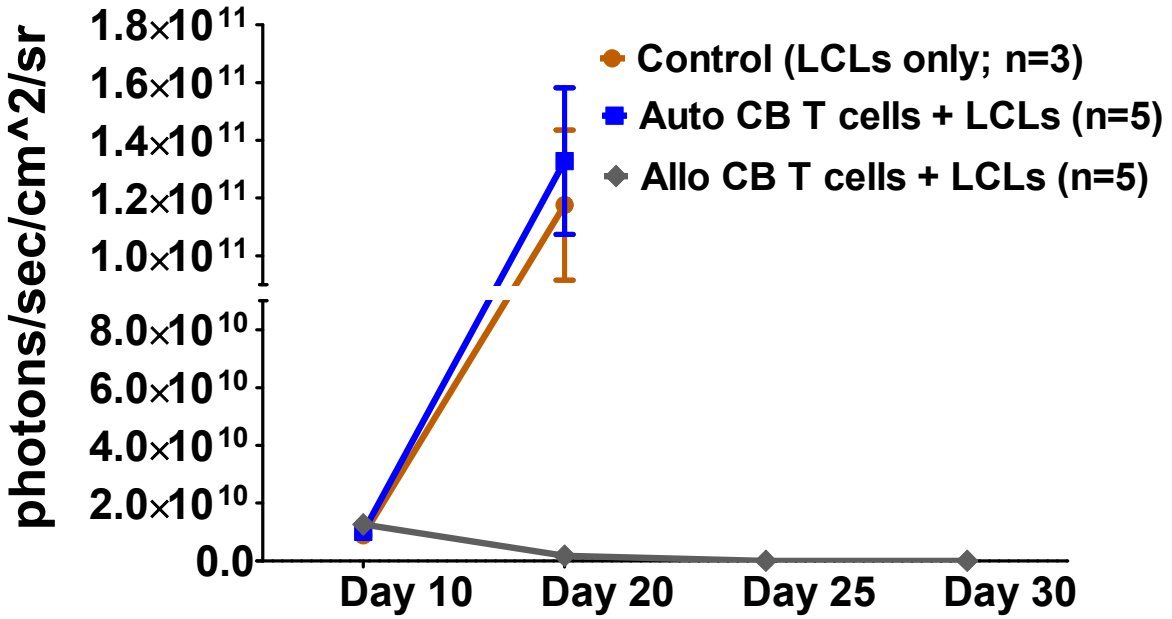

Figure 65: Tumour bioluminescence (photons/sec/cm^2/sr) was measured using Xenogen-IVIS. Rapid tumour regression in mice receiving allogeneic cord blood T cells was observed. Cumulative rate of tumour growth (mean and standard error of mean) are plotted

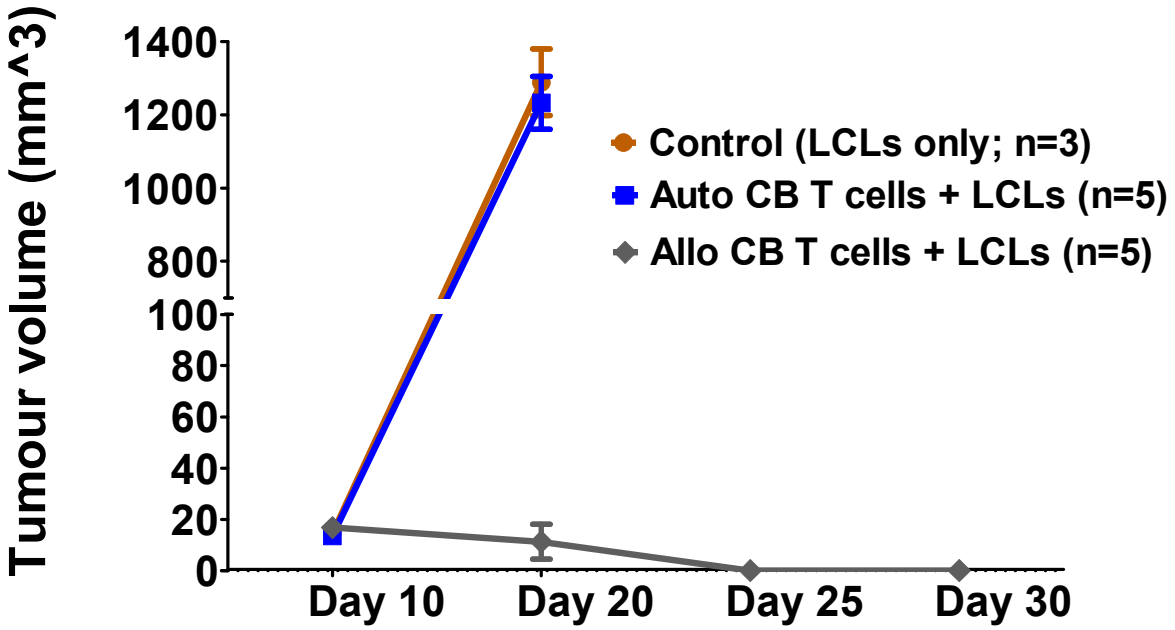

Figure 66: Tumour volume (mm^3) was derived using calliper measurements. Rapid tumour regression in mice receiving allogeneic cord blood T cells was observed. Cumulative rate of tumour growth (mean and standard error of mean) are plotted.

At sacrifice, we performed flow-cytometry on the blood of the mice from the autologous and allogeneic groups to confirm the survival of T cells. In both the groups circulating T cells were present. In the allogeneic group CD4:CD8 ratio was 0.9 (0.7 to 1.2) and in the autologous group CD4:CD8 ratio was 5.4 (4.7 to 5.6) [Figure 67]. This striking reversal of CD4:CD8 ratio in the allogeneic group, in contrast with the $CD4^+$ T-cell biased CD4:CD8 ratio in the autologous group indicates that allogeneic cord blood T cells mediate a $CD8^+$ T-cell response against the B-cell lymphoma. The autologous cord blood T cells failed to mediate any anti-tumour effect confirming that the observed anti-tumour effect is not against EBV antigens. Thus the observed tumour regression appears to be mediated through an allo-reactive T-cell response rather than a HLA-restricted anti-EBV effect.

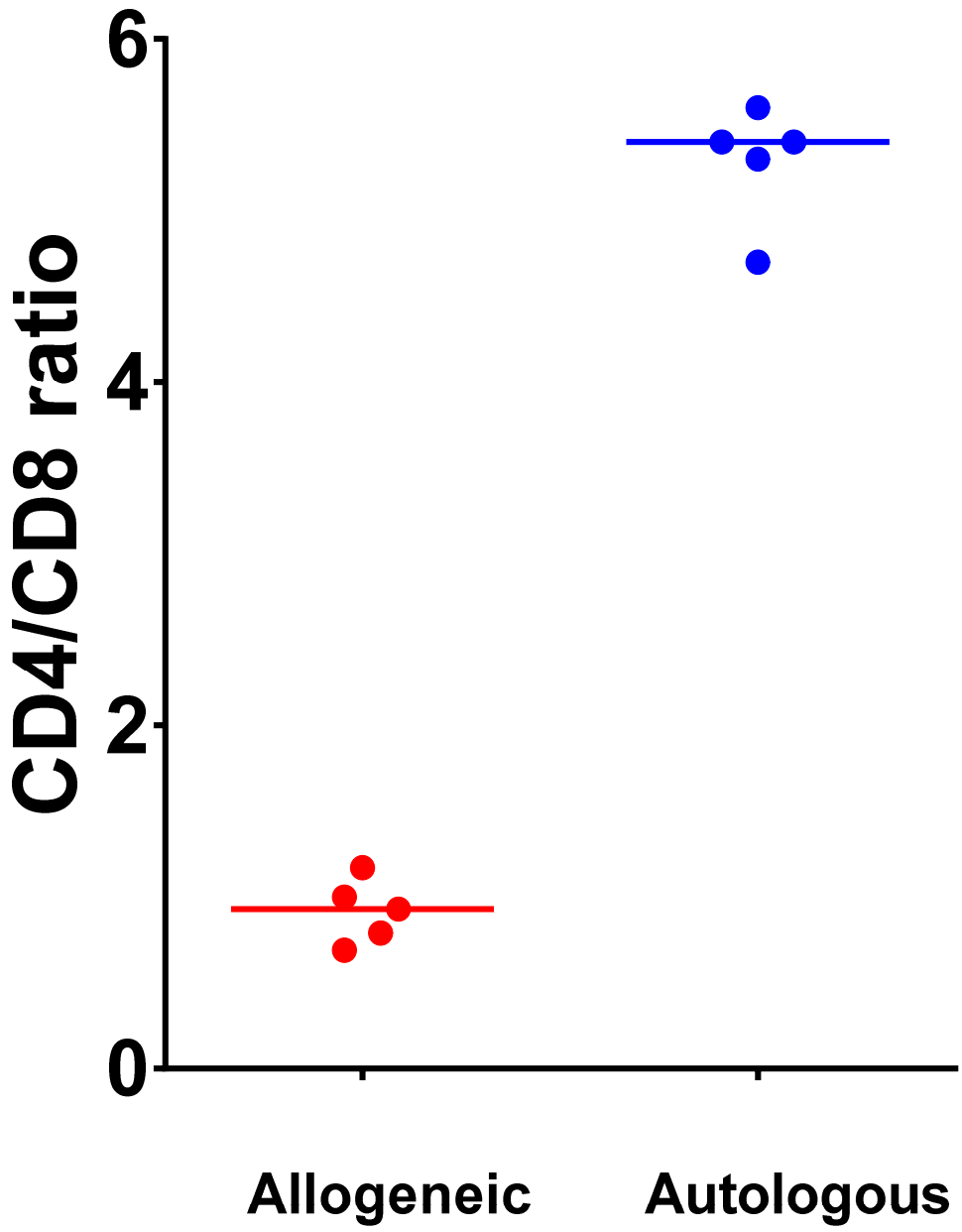

Figure 67: Reversal of CD4:CD8 ratio was observed in allogeneic cord blood T cells and not in the autologous cord blood T cells. This further indicated alloreactivity mediated by allogeneic cord blood T cells (unpaired t-test; $p<0.0001$).

Further in the additional functional experiments described in the next chapter, we continued to observe rapid regression of tumour in the cord blood T-cell group confirming enhanced alloreactivity mediated by cord blood T cells [Figure 68].

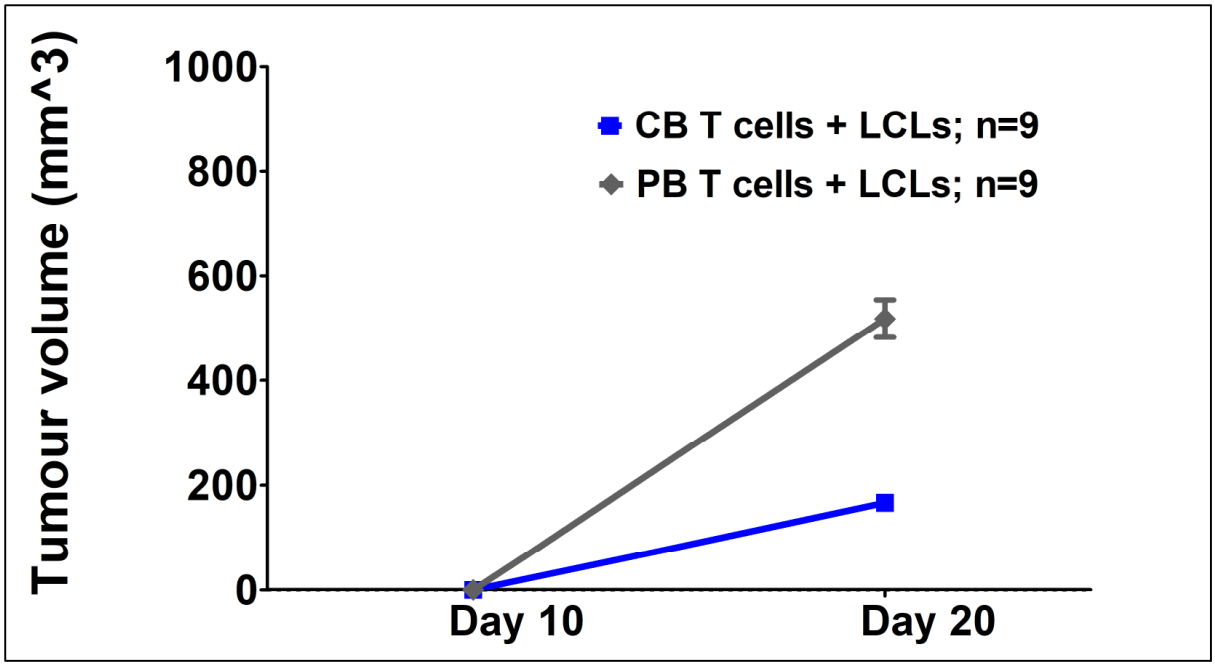

Figure 68: Cumulative tumour volumes (standard error of mean) from additional functional experiments. The tumour volumes were significantly lower in the mice injected with cord blood T cells compared with those who received equivalent numbers of peripheral blood T cells thus confirming increased alloreactive effect mediated by cord blood T cells (unpaired t-test; $p<0.0001$).

CONCLUSIONS

We have thus established a tumour model to study the allo-reactive effects of T cells. In this model, we show that cord blood T cells mediate enhanced anti-tumour effects without mediating xenogeneic GvHD. Xenogeneic GvHD was absent in the cord blood group 60 days after the injection of T cells. The absence of xenogeneic GvHD occurred despite the presence of circulating cord blood T cells at the end of experiment. The cord blood T cells did not infiltrate GvHD target organs such as liver and skin.

In contrast, 5×10^6 peripheral blood T cells failed to mediate an anti-tumour effect against 5×10^6 B-cell lymphoma cells. However, 5×10^6 peripheral blood T cells mediated an anti-tumour effect only against a lower burden of tumour i.e. 2.5×10^6 B-cell lymphoma cells. This attenuated anti-tumour effect correlated with the onset of xenogeneic GvHD which occurred 3 weeks after the injection of 5×10^6 T cells.

The enhanced anti-tumour effect in this EBV-driven tumour model was not directed against the EBV antigens but was an anti-leukaemic (allo-reactive) effect.

Our observations were intriguing because we observed enhanced anti-tumour effects mediated by cord blood T cells without xenogeneic GvHD. Although this an artificial tumour model this nicely mimics the clinical transplant situation with generally less GvHD than adult stem cell sources yet maintained or enhanced GvL effects, particularly in AML (Milano *et al.,* 2016). This suggests that cord blood T cells which are predominantly naïve undergo memory-effector induction exclusively within the B-cell lymphoma and not in the target GvHD organs of NOD/SCID/IL2rg^{null} mice. In contrast, peripheral blood T cells mediate attenuated anti-tumour effect correlating with xenogeneic GvHD. Thus, peripheral blood T cells can target both the tumour and target GvHD organs. Therefore, to further investigate the immunological basis of the differential anti-tumour and xenogeneic GvHD mediated by cord blood T cells and peripheral blood T cells we performed experiments to study recruitment of tumour-infiltrating lymphocytes and memory-effector differentiation in the tumour and in circulating lymphocytes.

Chapter seven

Tumour-infiltrating cord blood T cells mediate enhanced Tc1-Th1 immune responses compared to tumour-infiltrating peripheral blood T cells

7.0 Aims

1) To compare the kinetics of tumoural recruitment of cord blood and peripheral blood T cells.

2) To examine the role of T-cell regulation in differential anti-tumour effects mediated by cord blood and peripheral blood T cells.

3) To study the memory-effector differentiation in the circulating and tumour-infiltrating cord blood and peripheral blood T cells.

4) To compare the Tc1 induction and Th1/Th2 balance in the tumour-infiltrating cord blood and peripheral blood T cells.

7.1 Introduction

Cord blood T cells mediate enhanced anti-tumour effects compared to peripheral blood T cells. Cord blood T cells are intrinsically Tc2-Th2 biased in their natural foetal and early neonatal environment. However, in the context of allogeneic T-cell replete CBT the functionality of cord blood T cells is not being tested. Therefore, the mechanism of robust anti-leukaemia effect after T-cell replete approach is not known.

Cord blood T cells rapidly undergo memory-effector differentiation and mediate anti-viral responses after T-cell replete CBT (Chiesa *et al.,* 2012). Similarly, T-cell replete CBT significantly reduces the risk of leukaemia relapse without increasing the risk of chronic GvHD. These findings therefore raise questions about the robust anti-leukaemic effect mediated by cord blood T cells infused with the cord blood graft. How do then these intrinsically tolerant cord blood T cells mediate anti-leukaemic responses? Are there differences in the recruitment of cord blood T cells to the tumour? After recruitment to the tumour are there differences in the T-cell regulation of cord blood and peripheral blood tumour-infiltrating T cells? Do cord blood and peripheral blood tumour-infiltrating T cells distinctly orchestrate Th1 and Type 1 cytotoxic T cell responses?

In the subsequent experiments, I set out to identify the immunological basis of enhanced tumour rejection by studying the tumour-infiltrating lymphocytes.

7.2 Enhanced recruitment of cord blood T cells to the tumour may mediate a potent GvL effect

To study the immunological basis of the differential anti-tumour effect following the injection of cord blood and peripheral blood T cells, we first studied the differences in the recruitment of tumour-infiltrating lymphocytes. In a separate tumour modeling experiment, mice were injected with 5×10^6 B-cell lymphoma cells on day –2 followed by 5×10^6 cord blood ($n = 5$) or peripheral blood T cells ($n = 5$) on day 0. All mice were then sacrificed on day +15 following T cell injections, and tumour sections were studied.

Immunohistochemistry staining of tumour sections with CD3 antibody showed higher numbers of tumour-infiltrating lymphocytes in the cord blood group compared with the peripheral blood group [Figure 69].

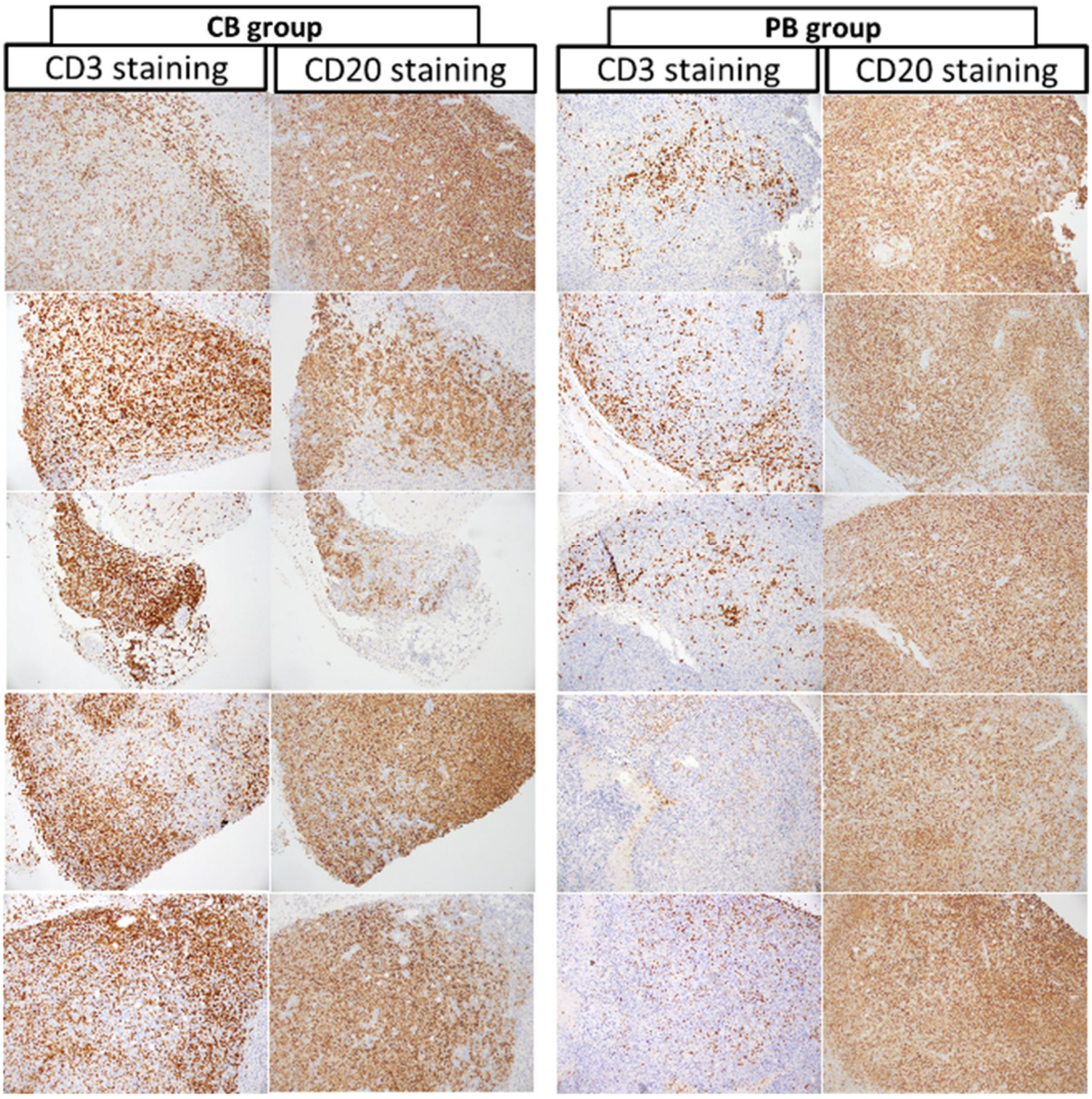

Figure 69: Contiguous tumour sections (10×) of cord blood and peripheral blood group stained with CD3 and CD20 immuno-histochemical stain. Higher numbers of tumour-infiltrating $CD3^+$ T cells was seen in the cord blood group compared with to the peripheral blood group.

Using Image J, tumour-infiltrating lymphocytes in 10 random 40× sections of each tumour were quantified as TILs/mm^2. The 10 RGB images of 40× magnification for each tumour slide were converted to black and white mask output using a calibrated threshold for each stack of images. The black output areas corresponding to the CD3 immuno-histochemical staining defined in the mask were outlined and measured in square microns.

Representative RGB mask and outline images of peripheral blood and cord blood group are shown in this figure 70. The number of infiltrating T cells in each 40× image of 94901 square microns were calculated as = Total out-lined area/Area of T-cell.

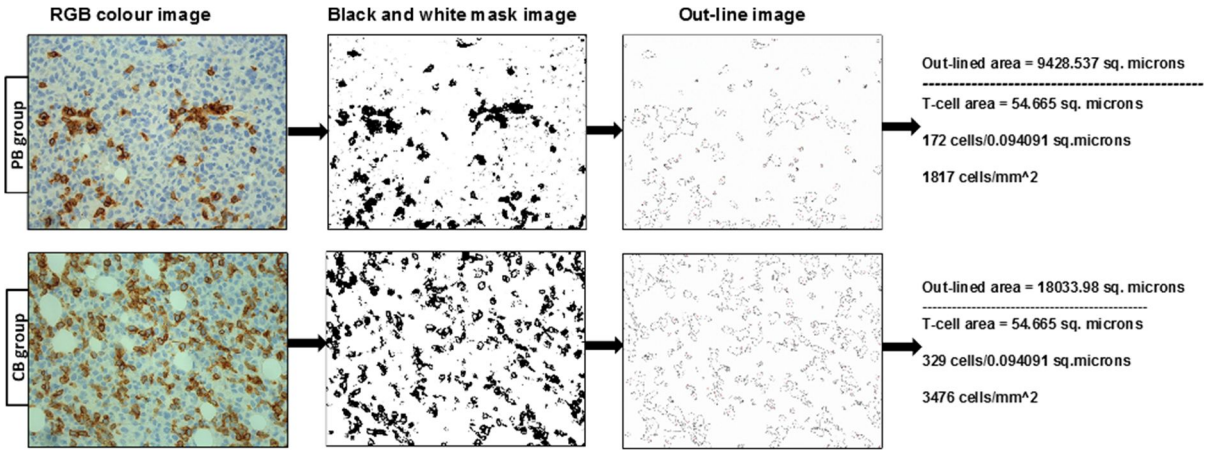

Figure 70: Ten RGB images of 40x magnification for each tumour slide were converted to black and white mask output using a calibrated threshold for each stack of images. The black output areas corresponding to the CD3 immuno-histochemical staining defined in the mask were outlined and measured in square microns. Representative RGB, mask and outline images of peripheral blood and cord blood group are shown in this figure. The number of infiltrating T cells in each 40x image of 94901 square microns were calculated as = Total out-lined area/Area of T-cell. The number of infiltrating T cells per mm^2 was derived for each image to determine the average density of T cells per mm^2 of tumour.

The number of infiltrating T cells per mm^2 was derived for each image to determine the average density of T cells per mm^2 of tumour. A significantly higher number of tumour-infiltrating were observed in the cord blood group compared to the peripheral blood group (4702 +/− 426 *vs* 1275 +/− 330; $P < 0.01$) [Figure 71]. This suggests that cord blood T cells are preferentially recruited to the tumour compared to peripheral blood T cells.

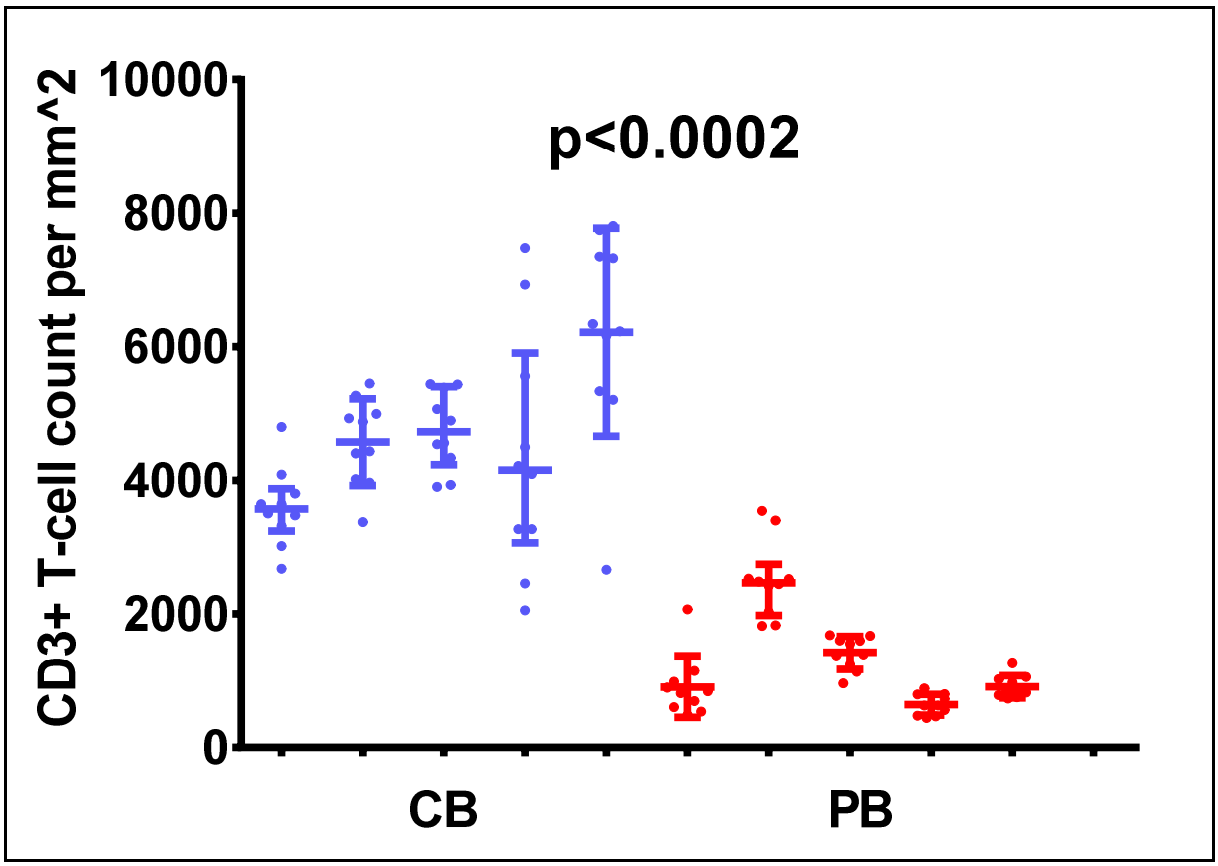

Figure 71: Density of tumour-infiltrating T cells per mm^2 (shown as scatter dot plot with median and inter-quartile range) was significantly higher in the cord blood group than in the peripheral blood group (unpaired t-test; *p<0.0002*).

Interestingly, flow-cytometric analysis of isolated tumour-infiltrating lymphocytes showed that a majority of tumour-infiltrating lymphocytes in the cord blood group were $CD8^+$ T cells, with a median CD4:CD8 ratio of 0.49 (range, 0.47–0.58). In contrast, $CD4^+$ T cells were predominant in the peripheral blood group, with a median CD4:CD8 ratio of 1.72 (range, 1.60–1.88; $P < 0.01$). This inversion of CD4:CD8 ratio in the cord blood tumour-infiltrating lymphocytes was observed despite a higher initial CD4:CD8 ratio in the injected cord blood T cells compared with the injected peripheral blood T cells (4.9 *vs* 2.9) [Figure 72].

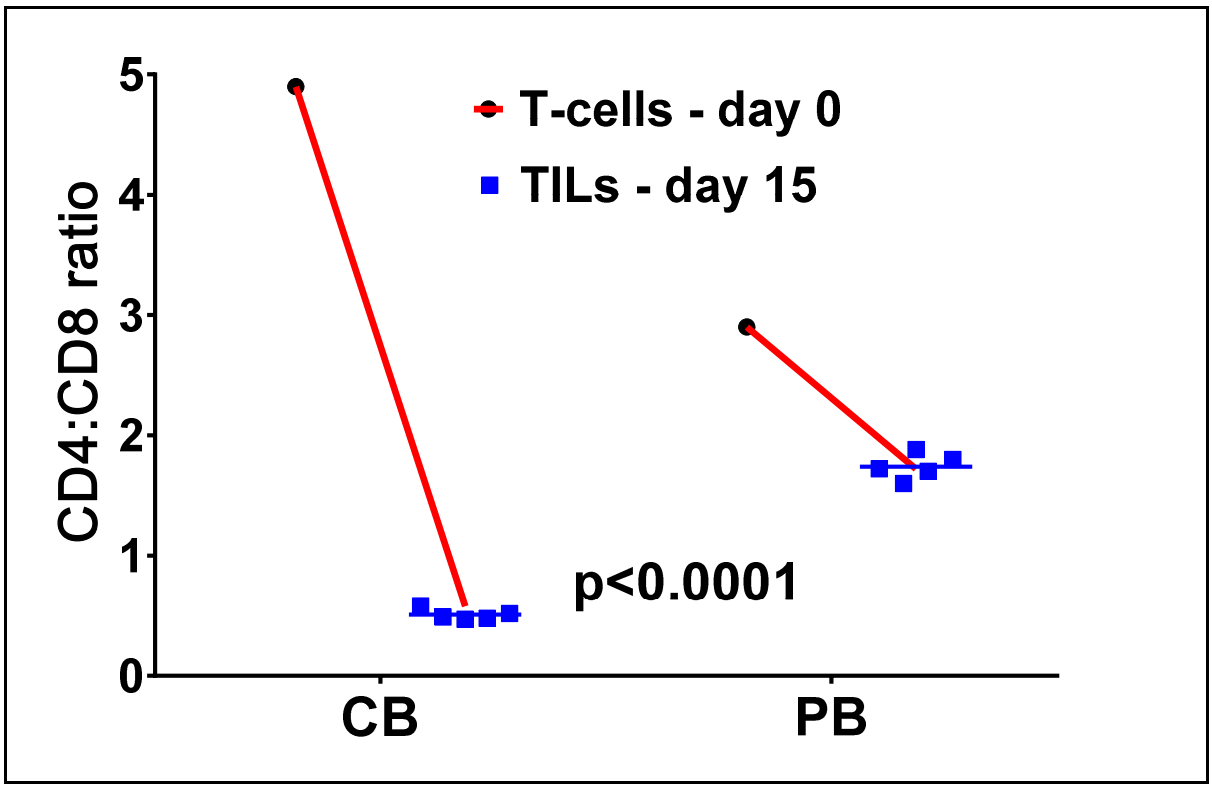

Figure 72: A significantly lower CD4:CD8 ratio was observed in cord blood TILs compared with peripheral blood TILs suggesting higher numbers of $CD8^+$ T cells infiltrated the tumour in the cord blood group.

This suggests that preferential tumoural recruitment of cord blood T cells with a $CD8^+$ T-cell bias may primarily mediate anti-tumour effects in this human-murine chimeric model.

7.3 Enhanced recruitment of cord blood TILs to the tumour occurs with $CD8^+$ T cell bias and significantly higher CD8:CD4 and CD8:$CD4^+$ T-regulatory cells ratio

To further gain insight into the kinetics of infiltration of cord blood and peripheral blood T cells in this B-cell tumour and the role of T-cell regulation in this, we compared the infiltration of $CD4^+$, $CD8^+$, and $CD4^+$ $CD25^+$ $FoxP3^+$ T-regulatory cells on day +10 and day +20 after T cell injections. In a separate experiment, we injected B-cell lymphoma (5×10^6 cells) subcutaneously on day –2, followed by 5×10^6 cord blood or peripheral blood T cells on day +0 in 8 mice each. Ten and 20 days after T-cell injections, four mice from each group were sacrificed, and isolated tumour-infiltrating lymphocytes were studied for CD4:CD8 and CD8:$CD4^+$ T-regulatory cells ratio [Figure 73]. As previously observed, the CD4:CD8 ratio in the cord blood tumour-infiltrating lymphocytes was significantly reversed compared to peripheral blood tumour-infiltrating lymphocytes. This was despite a higher initial CD4:CD8 ratio in the injected cord blood T cells compared to the injected peripheral blood T cells (3.4 *vs* 2.7). At day +10 and day +20 after T-cell injection, the median CD4:CD8 ratio in the cord blood tumour-infiltrating lymphocytes was 0.58 (range, 0.51–0.69) and 0.03 (range, 0.03–0.06), respectively, compared with a median ratio of 1.54 (range, 1.3–1.9) and 0.26 (range, 0.14–0.33) in the peripheral blood tumour-infiltrating lymphocytes ($P < 0.001$ and $P < 0.001$, respectively) [Figure 74].

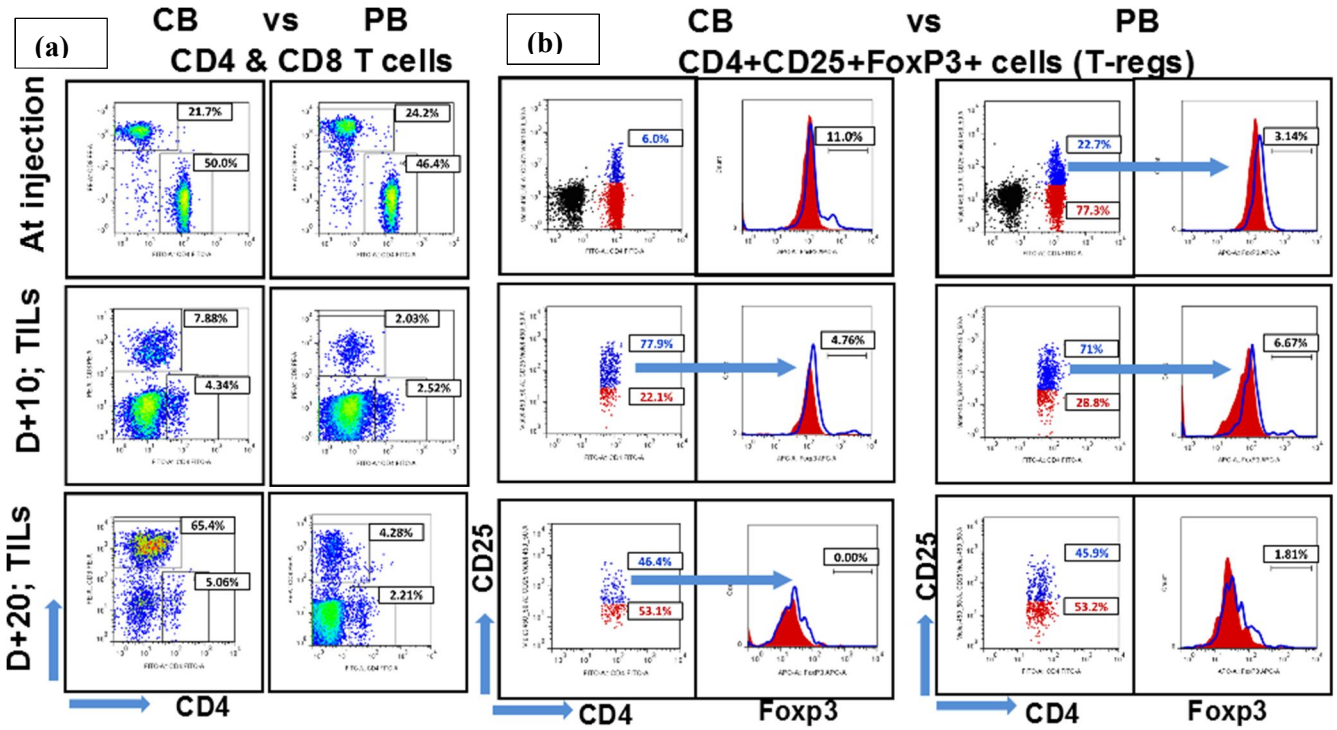

Figure 73: (a) Representative plots of $CD4^+$ and $CD8^+$ T cells and (b) $CD4^+CD25^+Foxp3^+$T cells at injection and in tumour-infiltrating lymphocytes (TILs) on day +10 and day +20.

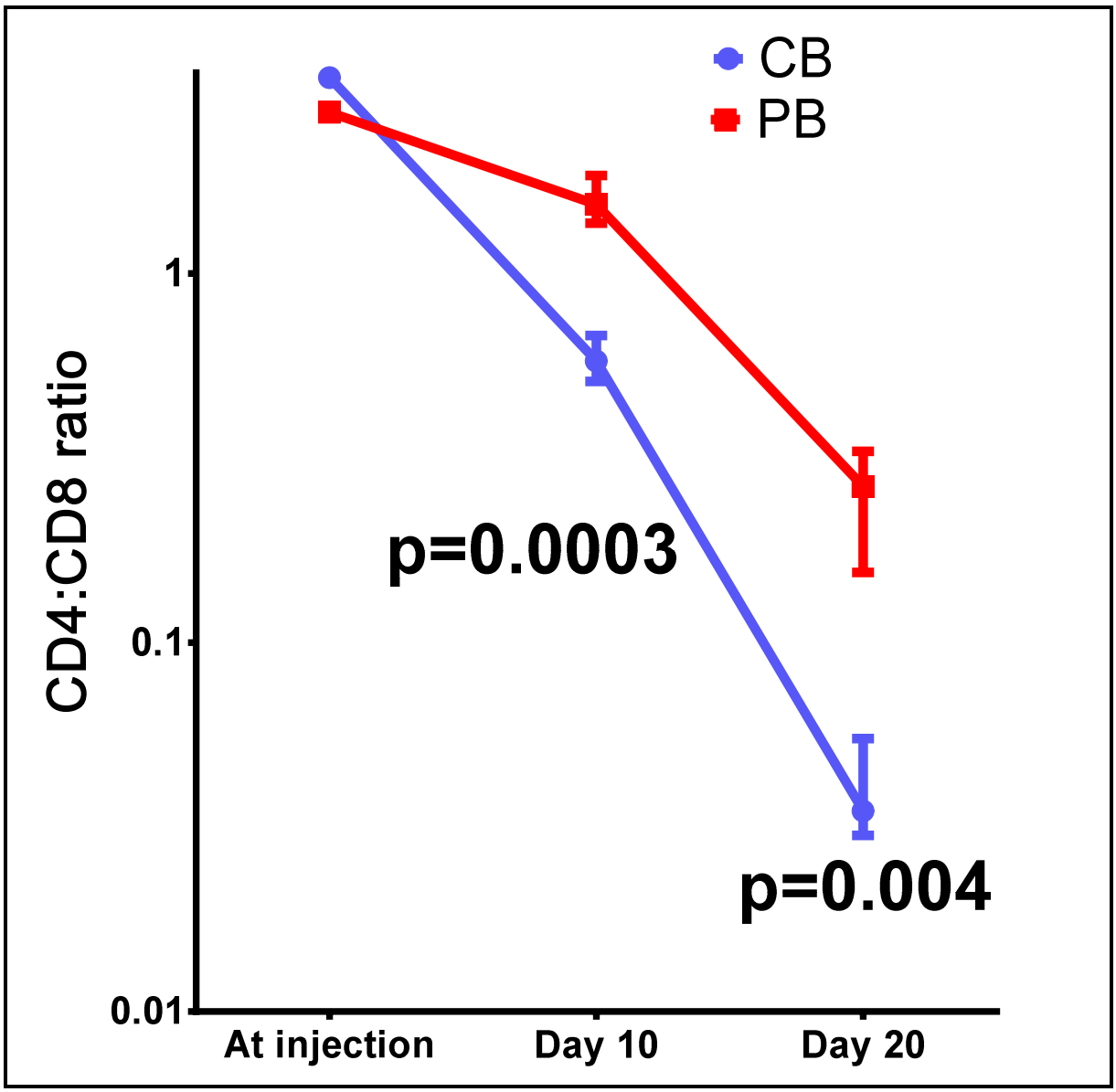

Figure 74: Line graph showing significantly lower CD4:CD8 ratio in cord blood group compared to peripheral blood group on day +10 (unpaired t-test; *p=0.0003*) and day +20 (unpaired t-test; *p=0.004*) plotted on log-scale as median and inter-quartile-range.

The above finding also correlated with a significantly higher CD8:$CD4^+$ $CD25^+$ $FoxP3^+$ ratio in the cord blood tumour-infiltrating lymphocytes compared to peripheral blood tumour-infiltrating lymphocytes both at day +10 and day +20 after T-cell injection [Figure 73 and 75]. At day +10 and day +20 after T-cell injection, the median CD8:$CD4^+$ $CD25^+$ $FoxP3^+$ ratio in the cord blood tumour-infiltrating lymphocytes was 29 (range, 25–52) and 2043 (range, 950–3288) respectively, compared with a median ratio of 11.9 (range, 7.8–15.5) and 132 (range, 72–166) in the peripheral blood tumour-infiltrating lymphocytes ($P < 0.01$ and $P < 0.01$, respectively) [Figure 75].

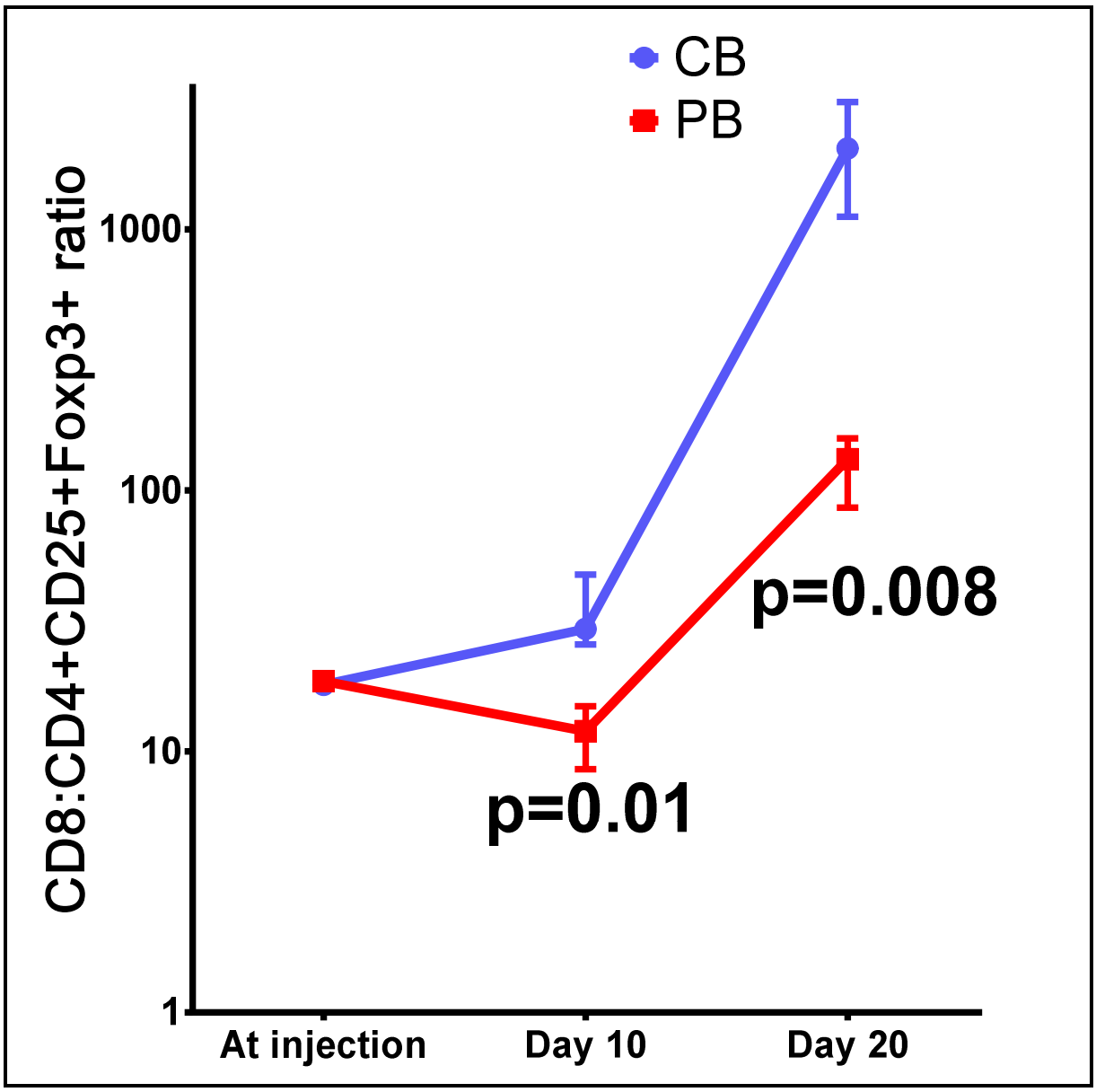

Figure 75: Line graph showing significantly higher CD8:CD4$^+$ T-regulatory ratio in cord blood group compared toperipheral blood group on day +10 (unpaired t-test; *p=0.01*) and day +20 (unpaired t-test; *p=0.008*) plotted on log-scale as median and inter-quartile-range.

This differential kinetics of T-cell infiltration indicate that, whilst cord blood CD8$^+$ T cells may be the primary mediators of the enhanced GvL effect in the cord blood group, a relatively increased tumoural recruitment of T-regulatory cells may attenuate the GvL effect in the peripheral blood group.

7.4 CCR7 enriched cord blood CD8$^+$ T cells have enhanced tumour-homing ability

Since the vast majority of cord blood CD8$^+$ T cells are CCR7^{high} [Figure 76] and CCR7 is a homing receptor for naïve T cells (De Waele *et al.,* 1988; Zhao *et al.,* 2002; Förster *et al.,*

1999), we sought to identify if $CCR7^+$ $CD8^+$ T cells predominantly infiltrate the tumour. We observed that CCR7 expression was similar in cord blood and peripheral blood $CD8^+$ TILs (median fluorescence intensity; MFI = 6854 +/– 1542 *vs* 6737 +/– 1626; p = NS). CCR7 MFI expression was significantly higher in TILs compared with circulating peripheral blood $CD8^+$ T cells (1378 +/– 10; $P < 0.01$), whilst circulating cord blood $CD8^+$ T cells remained $CCR7^{high}$ (MFI = 21128 +/– 534) [Figure 77 (a) and (b)]. This indicates that $CCR7^{high}$ $CD8^+$ T cells were primarily recruited to the tumour and higher expression of CCR7 may endow cord blood $CD8^+$ T cells with the enhanced tumour-homing ability.

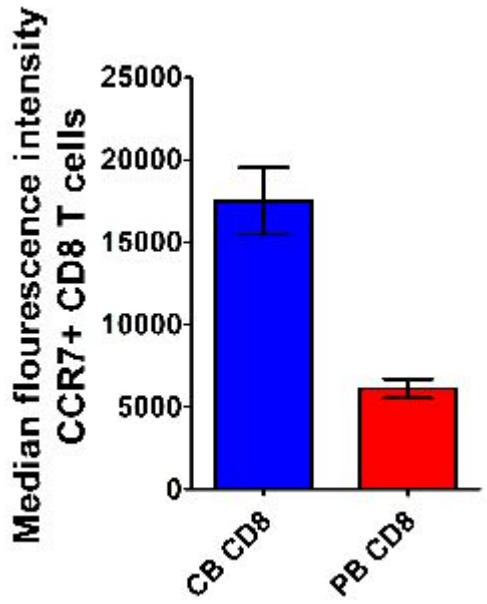

Figure 76: Normal donor cord blood CD8+ T cells have significantly higher expression of CCR7 compared with normal donor peripheral blood CD8+ T cells (expressed as mean and standard error of mean; n = 3 in each group; unpaired t-test; *P < 0.005*).

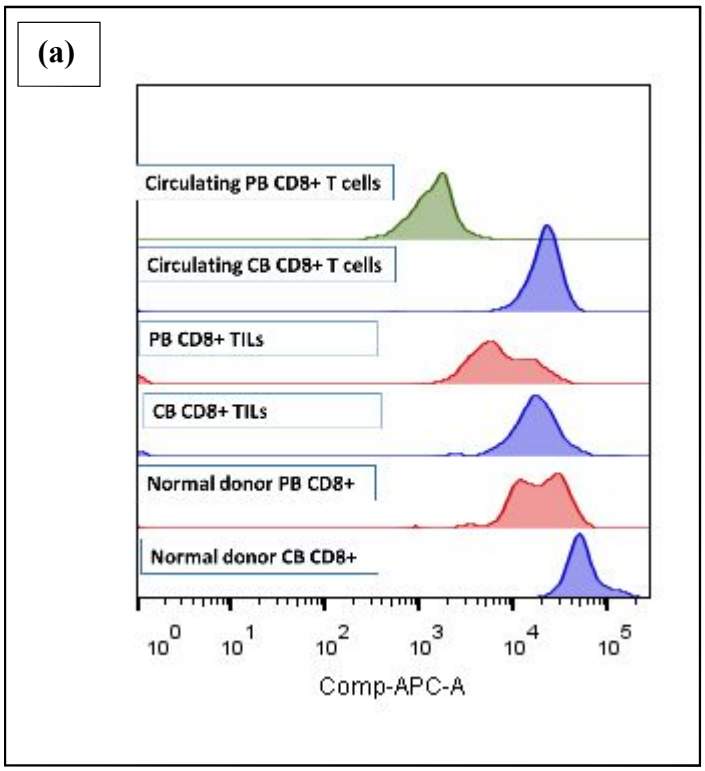

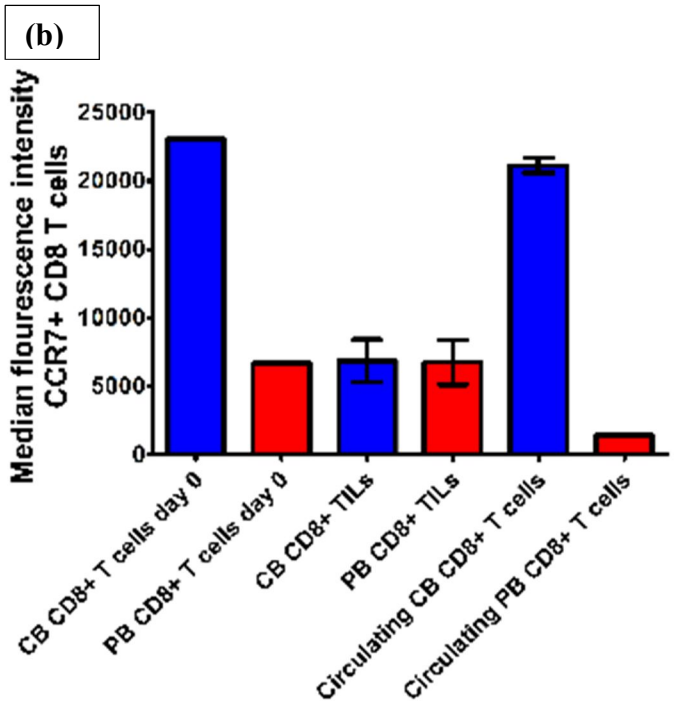

Figure 77: (a) Offset histogram plot and (b) is cumulative bar plot (mean and standard error of mean) showing fluorescence intensity of $CD8^{+}$ T cells from normal donors, tumour-infiltrating lymphocytes (TILs) and in circulation.

This figure indicates that $CCR7^{high}$ CD8+ T cells are primarily recruited to the tumour in the both the groups (p = NS), and in the peripheral blood group $CCR7^{low}$ CD8+ T cells remain in circulation (unpaired t-test; $P < 0.01$) indicating a role of CCR7 mediated chemotaxis in this tumour

7.5 Tumour-infiltrating naïve cord blood T cells rapidly differentiate into memory and effector cells

In order for naïve cord blood T cells infiltrating the tumour to provide anti-tumour effects, they must undergo memory-effector differentiation. We performed similar tumour modelling experiments and to study whether cord blood T cells undergo memory-effector differentiation at early time-points, mice in the cord blood group ($n = 4$) and peripheral blood group ($n = 4$) were sacrificed 15 days after T-cell injections.

We observed that tumour-infiltrating lymphocytes in the cord blood group rapidly underwent memory-effector differentiation, whereas circulating cord blood lymphocytes remained naïve [Figure 78 and 79]. A similar percentage of $CD8^+$ tumour-infiltrating lymphocytes were observed to have a central memory (CM) and effector memory (EM) phenotype in both groups (CM = 77.8 +/− 1.4 *vs* 78.0 +/− 1.8; EM = 1.48 +/− 0.3 *vs* 2.1 +/− 0.5; P = NS). Interestingly, compared with peripheral blood tumour-infiltrating lymphocytes, a significantly higher percentage of circulating lymphocytes in the peripheral blood group was found to have an effector memory phenotype (2.1 +/− 0.5 *vs* 8.5 +/− 0.6; $P < 0.0001$) [Figure 78 and 79].

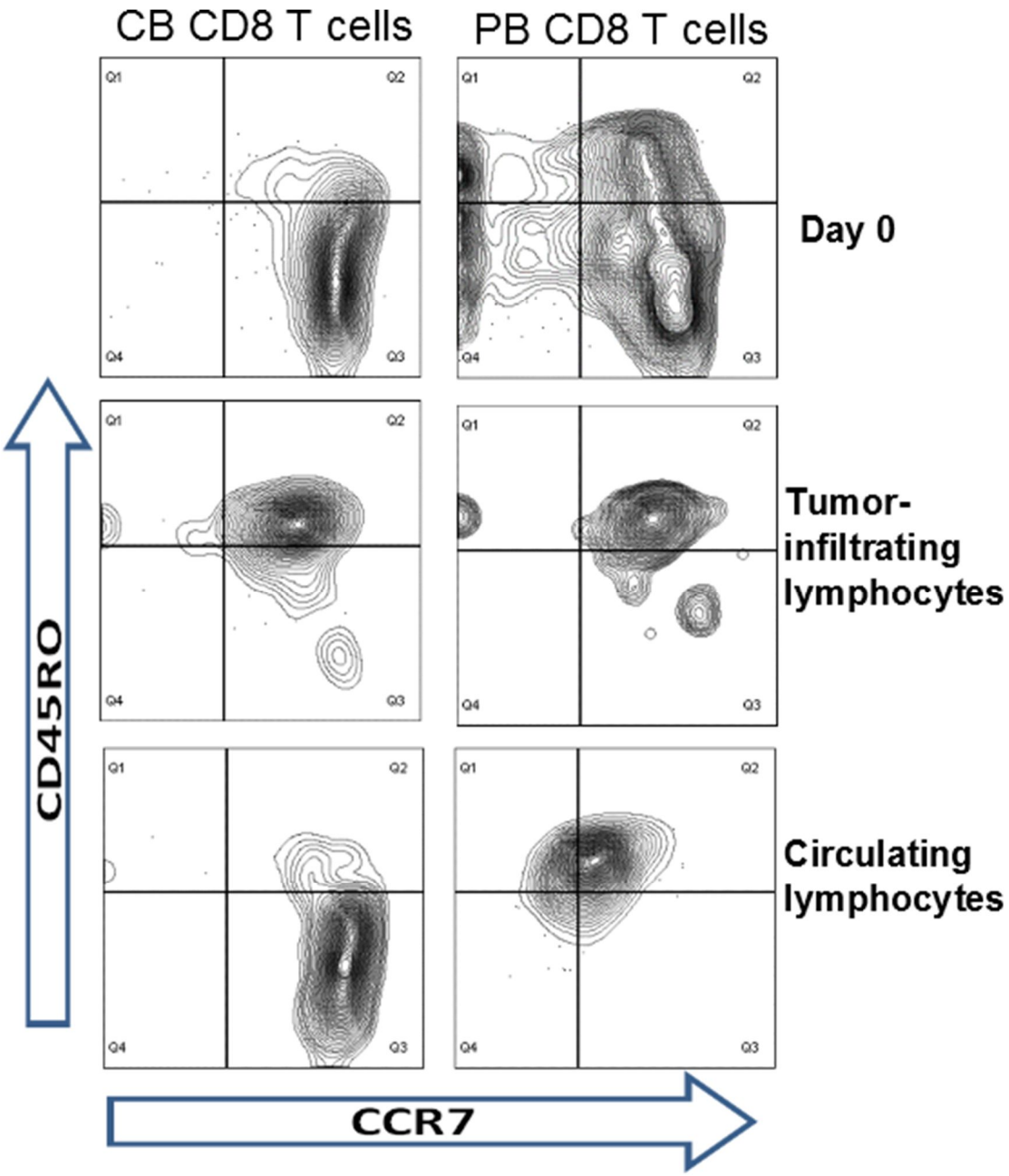

Figure 78: Representative flow-cytometry plots of $CD8^+$ T cells infused on day 0, $CD8^+$ tumour-infiltrating lymphocytes and $CD8^+$ circulating lymphocytes. Rapid switching of naïve cord blood $CD8^+$ T cells to memory/effector T cells was observed in the tumour microenvironment whilst most circulating cord blood lymphocytes remained naïve.

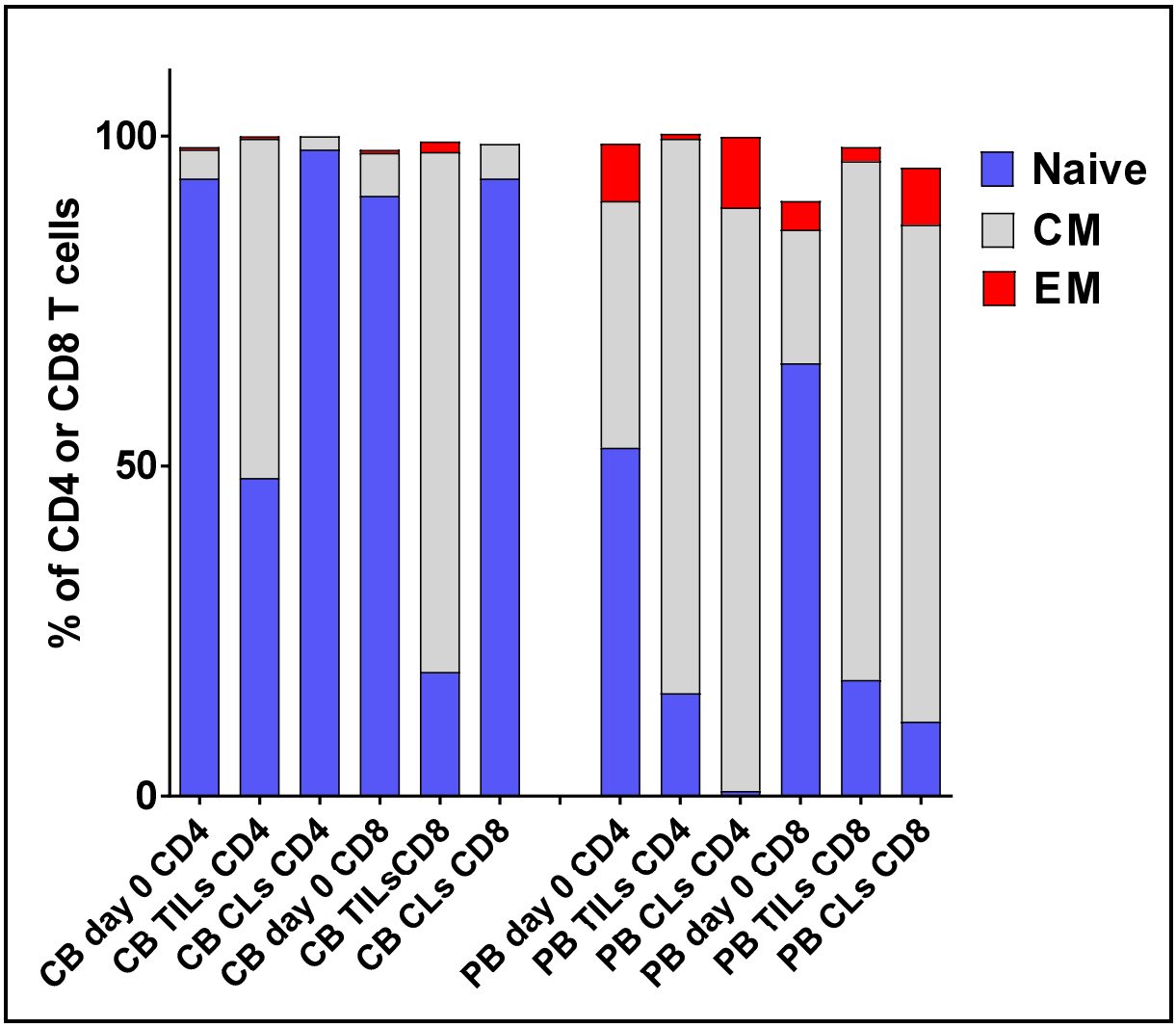

Figure 79: Comparison of median percentages of naive, central memory and effector memory subsets in tumour-infiltrating (TILs) and circulating lymphocytes (CLs) on day +15 after T-cell injection. Naive cord blood T cells rapidly switched to memory/effector phenotype in the tumour, however circulating cord blood lymphocytes remained naive. Similar percentage of $CD8^+$ TILs had central memory and effector memory phenotype in both groups (p = NS). Interestingly in the peripheral blood group, significantly higher percentage of CLs had an effector memory phenotype compared to TILs (unpaired t-test; $P < 0.0001$).

Thus, naïve cord blood T cells were rapidly and selectively observed to undergo memory-effector differentiation in this human B-cell tumour, but not in the periphery of the NOD/SCID/IL2rg^{null} model.

7.6 Naïve cord blood T cells rapidly gain IFN-γ and TNF-α effector function

Finally, to study the differences in the effector functions gained by tumour-infiltrating lymphocytes in the two groups, we performed similar tumour modeling experiments. In this experiment, we allowed the tumours to grow over the previous threshold limit of 10 mm after having obtained the permission from home office on a renewed license allowing the tumour growth of 15 mm. This was necessary because we chose to study the effector function of tumour-infiltraing lymphocytes at the onset of tumour regression. Mice in the cord blood group (n = 5) never exceeded the previous threshold of 10 mm and started to regress on day +20, whilst mice in peripheral blood group (n = 5) exceeded 10 mm size and then started to have tumour regression on day +26. Mice in both the groups were therefore sacrificed on day +26 after the injection of T cells, and tumour-infiltrating lymphocytes were studied for cytokine responses after a 6-hour *in vitro* re-challenge with lymphoma cells from the same donor. Isolated tumour-infiltrating lymphocytes were also studied for perforin expression.

$CD8^+$ tumour-infiltrating lymphocytes in both the groups demonstrated IFN-γ responses; however, despite cord blood T cells being naïve, there was no difference in the percentage of $CD8^+$ tumour-infiltrating lymphocytes expressing IFN-γ responses in the two groups (3.5 +/− 0.14 *vs* 3.4 +/− 0.15; P = NS) [Figure 80].

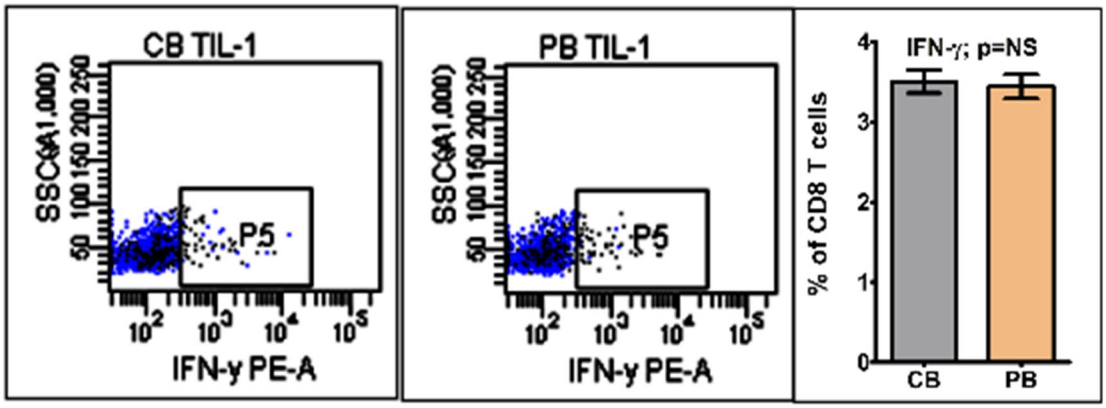

Figure 80: Representative flow-cytometry plots and cumulative bar-plots (mean and standard error of mean) of percentages of cord blood and peripheral blood $CD8^+$ TILs secreting IFN-γ. No statistically significant differences were observed in the percentage of IFN-γ secreting $CD8^+$ TILs in the two groups.

In contrast, a significantly higher percentage of cord blood $CD8^+$ tumour-infiltrating lymphocytes acquired TNF-α responses (1.2 +/− 0.07 *vs* 0.48 +/− 0.06; $P < 0.0001$) [Figure 81].

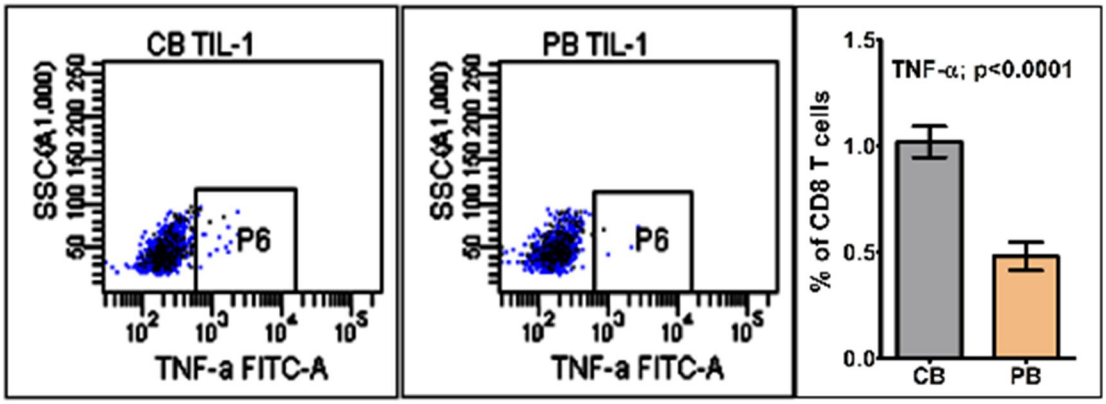

Figure 81: Representative flow-cytometry plots and cumulative bar-plots (mean and standard error of mean) of percentages of cord blood and peripheral blood $CD8^+$ TILs secreting TNF-α. A significantly higher percentages of $CD8^+$TILs in the cord blood group secreted TNF-α (unpaired t-test; *p<0.0001*).

Interestingly, a significantly higher percentage of cord blood $CD8^+$ tumour-infiltrating lymphocytes acquired dual IFN-γ^+ TNF-α^+ functions compared with peripheral blood $CD8^+$ tumour-infiltrating lymphocytes (1.0 +/− 0.08 *vs* 0.5 +/− 0.06; $P < 0.001$) [Figure 82].

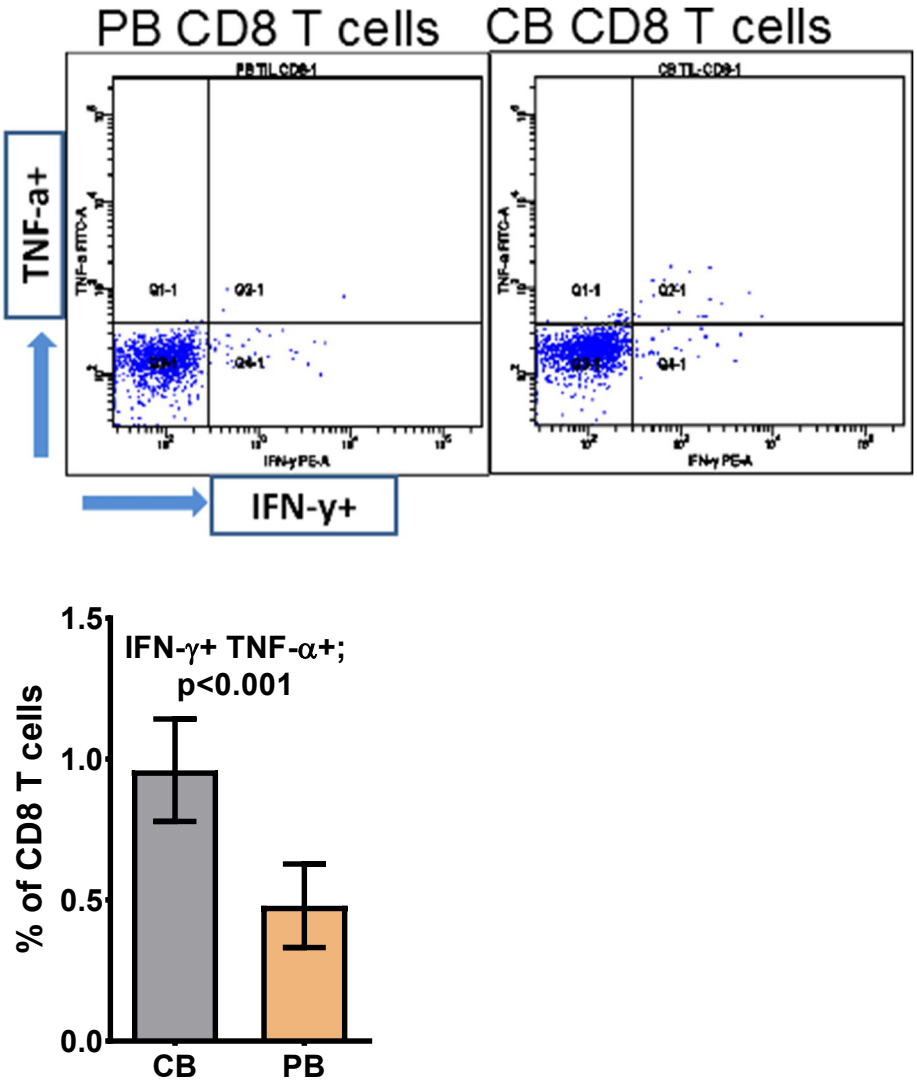

Figure 82: Representative flow-cytometry plots and cumulative bar-plots (mean and standard error of mean) of percentages of cord blood and peripheral blood $CD8^+$ TILs secreting IFN-γ^+TNF-α^+ cells are shown. Higher percentage of cord blood $CD8^+$ T cells were polyfunctional secreting dual cytokines compared to peripheral blood $CD8^+$ T cells (unpaired t-test; *p<0.001*).

The perforin expression was measured as median fluorescence intensity (MFI) and the percentage of $CD8^+$ T cells was also significantly higher in cord blood $CD8^+$ tumour-infiltrating lymphocytes compared with peripheral blood $CD8^+$ tumour-infiltrating lymphocytes (MFI = 443 +/− 7 *vs* 365 +/− 6; percentage of $CD8^+$ T cells = 75 +/− 1.3 *vs* 58 +/− 2.2; $P < 0.01$) [Figure 83].

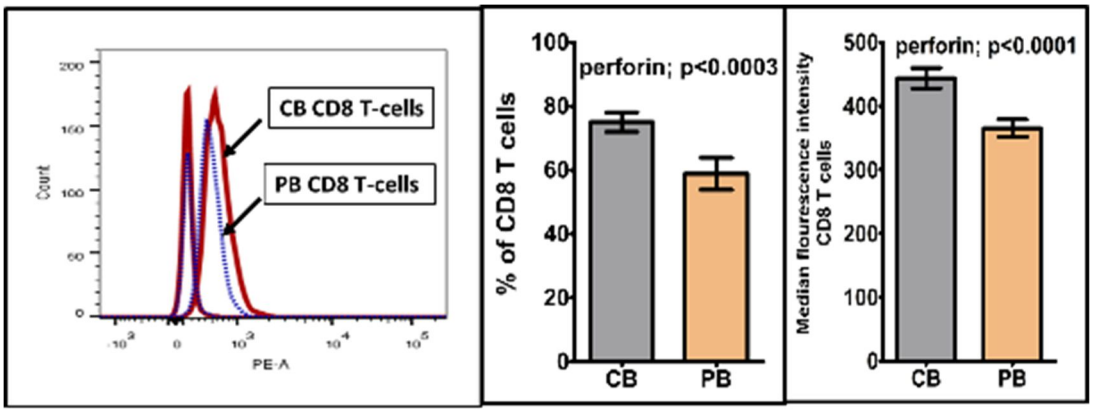

Figure 83: Representative flow-cytometry plots and cumulative bar-plots (mean and standard error of mean) of percentages of cord blood and peripheral blood $CD8^+$ TILs with perforin expression shown as percentage of $perforin^+$ cells and MFI.

We also studied effector functions gained by $CD4^+$ tumour-infiltrating lymphocytes to gain insight into the role of intra-tumoral Th1/Th2 balance on differential anti-tumour effects. $CD4^+$ tumour-infiltrating lymphocytes were identified as IFN-γ or TNF-α secreting Th1 cells and IL-4 secreting Th2 cells. Intra-tumoural Th1/Th2 balance was quantified by IFN-γ/IL-4 and TNF-α/IL-4 ratios. A significantly higher percentage of $CD4^+$ tumour-infiltrating lymphocytes were identified as Th2 tumour-infiltrating lymphocytes in the peripheral blood group compared with the cord blood group (16 +/− 0.9 *vs* 6.2 +/− 0.4; $P < 0.001$) [Figure 84]. Th1/Th2 balance measured by IFN-γ/IL-4 and TNF-α/IL-4 ratios were significantly biased towards Th1 in the cord blood group compared with the peripheral blood group (0.98 +/− 0.09 *vs* 0.3 +/− 0.02 and 0.88 +/− 0.02 *vs* 0.39 +/− 0.03; $P < 0.05$ and $P < 0.0001$, respectively) [Figure 85].

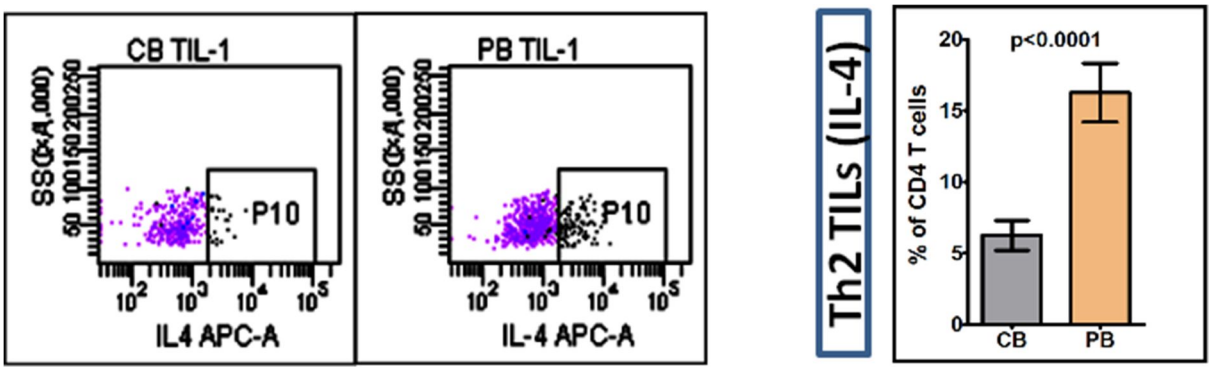

Figure 84: Representative flow-cytometry plots and cumulative bar plots (mean and standard error of mean) of IL-4 secreting $CD4^+$ T cells are shown. A significantly higher percentage of $CD4^+$ peripheral blood TILs were IL-4 secreting (plotted as mean and standard error of mean) and hence Th2 biased compared to $CD4^+$ cord blood TILs (unpaired t-test; *p<0.0001*).

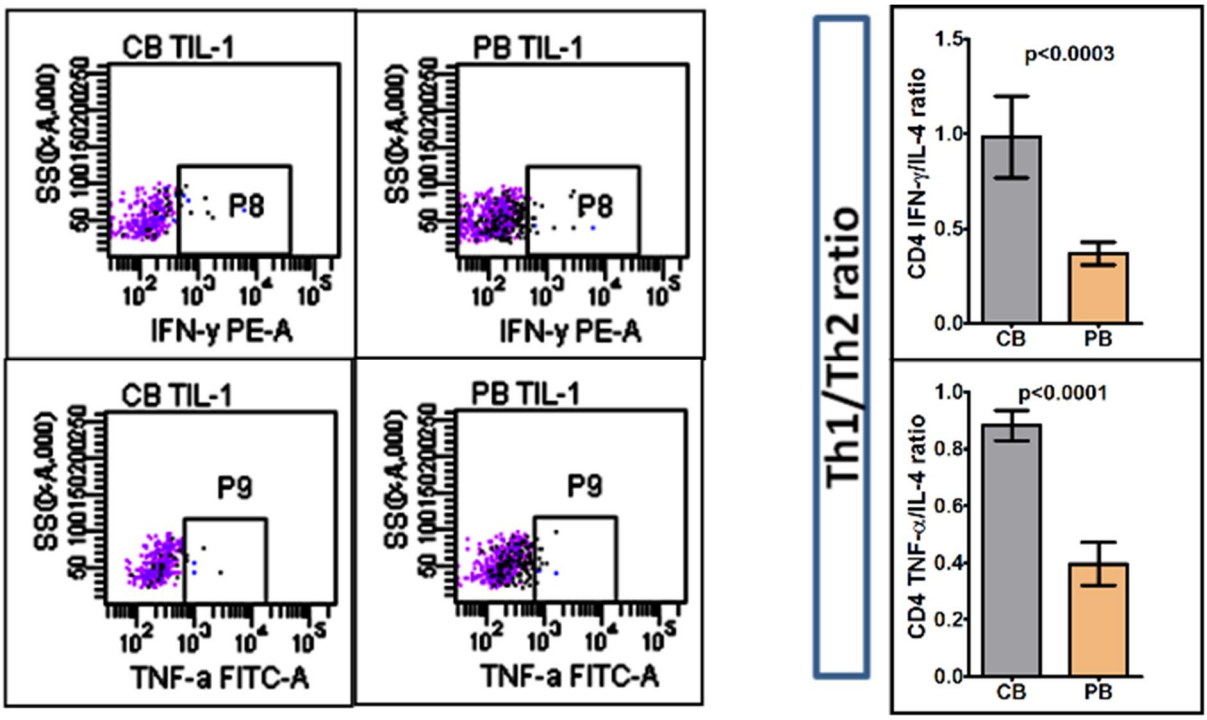

Figure 85: Representative flow-cytometry plots of IFN-γ and TNF-α secreting cord blood and peripheral blood $CD4^+$ TILs and bar plots of Th1/Th2 ratio (plotted as mean and standard error of mean) is shown. Higher Th1/Th2 ratio was observed in the cord blood TILs compared to peripheral blood TILs. (Th1/Th2 ratio was calculated as the ratio of IFN-γ/IL-4 and TNF-α/IL-4).

This suggests that naïve cord blood T cells can swiftly gain cytotoxic effector functions in the tumour microenvironment; in particular, cord blood T cells were observed to gain higher TNF-α and perforin activity compared with the peripheral blood T cells.

7.7 CONCLUSIONS

We have shown that cord blood T cells rapidly infiltrate the tumour compared to peripheral blood T cells. This tumoural infiltration of T cells in the cord blood group was particularly biased towards $CD8^+$ T cells both at early and late time points. In contrast, significant delay of $CD8^+$ T-cell tumoural infiltration was observed in the peripheral blood group. This differential infiltration of cord blood and peripheral blood $CD8^+$ T cells was observed in three separate experiments. Together with the differential infiltration of $CD8^+$ T cells in the two groups and preponderance of $CD4^+$ T-regulatory cells in the peripheral blood group may explain the differences in anti-tumour effects mediated by cord blood T cells and peripheral blood T cells.

Although cord blood T cells are predominantly naïve, we not only observed rapid tumoural infiltration of these naïve cord blood T cells, but these naïve cord blood tumour-infiltrating T cells rapidly differentiated in to memory-effector T cells. The percentage of tumour-infiltrating T cells that underwent memory-effector differentiation was similar in both the groups. The rapid tumoural infiltration of cord blood T cells together with swift memory-effector differentiation of tumour-infiltrating cord blood T cells may further explain the robust anti-tumour effects mediated by cord blood T cells.

The swift memory-effector differentiation of tumour-infiltrating cord blood $CD8^+$ T cells led to a robust cytotoxic response. The percentage of tumour-infiltrating cord blood and peripheral blood $CD8^+$ T cells demonstrated similar IFN-γ responses. However, compared with tumour-infiltrating peripheral blood $CD8^+$ T cells a significantly higher percentage of tumour-infiltrating cord blood $CD8^+$ T cells demonstrated TNF-α responses. Our most interesting finding was significantly higher percentages of cord blood $CD8^+$ T cells mediating dual IFN-γ and TNF-α responses compared with peripheral blood $CD8^+$ T cells. Similarly, higher percentages of tumour-infiltrating cord blood $CD8^+$ T cells expressed perforin compared with peripheral blood $CD8^+$ T cells.

Similar to the robust Tc1 induction of tumour-infiltrating cord blood $CD8^+$ T cells, $CD4^+$ T-cell induction also supported the cytotoxicity with a Th1/Th2 balance skewed towards Th1 induction. We observed that cord blood $CD4^+$ tumour-infiltrating T cells were biased towards cytotoxic IFN-γ and TNF-α responses whereas peripheral blood $CD4^+$ tumour-infiltrating T cells were biased towards immunosuppressive IL-4 responses.

In contrast to the cord blood tumour-infiltrating lymphocytes, circulating cord blood T cells did not undergo memory-effector differentiation whereas circulating peripheral blood T cells underwent differentiation with an effector phenotype. This finding corroborates with the absence of xenogeneic GvHD in the cord blood group and presence of severe GvHD in the peripheral blood group.

To summarise, in this model cord blood T cells selectively mediate a cytotoxic response in the tumour environment where as peripheral blood T cells mediate cytotoxicity against the tumour and target GvHD organs. The findings that cord blood T cells mediated an enhanced anti-tumour effect without exhibiting xenogeneic GvHD parallel the clinical situation in humans where CBT may exert a powerful GvL effect yet with reduced rates of GvHD.

Chapter eight

Discussion

Discussion

T-cell reconstitution after HCT occurs via thymus-dependent, and thymus-independent pathways (Mackall *et al.,* 1997; Williams *et al.,* 2007). Thymus dependent T-cell reconstitution, i.e., thymopoiesis occurs late, typically three to six months following transplantation, and results in the generation of new naïve T cells (Fallen *et al.,* 2003). In contrast, thymus-independent T-cell reconstitution occurs early, through the expansion of T cells carried with the graft. This may be driven by exposure to antigens and / or expansion of donor lymphocytes into a lymphopenic environment. This latter type of T-cell reconstitution is termed 'lymphopenia-induced proliferation' (Mackall *et al.,* 1996; Mackall *et al.,* 1997; Ge *et al.,* 2002). The relative contribution of each pathway in replenishing the peripheral T-cell pool after HCT depends on the conditioning regimens. In particular, *in vivo* T-cell depleting regimens have a significant effect on early thymus-independent proliferation.

In the context of unrelated CBT, ATG is used for *in vivo* T-cell depletion. It is now well established that *in vivo* T-cell depleting regimens lead to a significant delay in immune-reconstitution after CBT (Komanduri *et al.,* 2007; Lindemans *et al.,* 2014; Renard *et al.,* 2011). Research has indicated that CBT not only results in prolonged T-cell lymphopenia but also with impaired thymopoiesis, and skewing of late memory T cells (Komanduri *et al.,* 2007). This greatly increases the risk of viral mediated infections and mortality.

Omission of *in vivo* T-cell depletion from the conditioning regimens facilitates the restoration of adaptive immunity through thymus-independent T-cell immune-reconstitution. This form of conditioning regimen is employed for conditioning HLA-matched sibling transplants in the context of chemotherapy-resistant leukaemia. Recently, such an approach has also been used for the conditioning of unrelated cord blood grafts because of the low risk of GvHD (Chiesa *et al.,* 2012; Sauter *et al.,* 2011).

When we omitted ATG from the cord blood grafts, we observed an unexpected thymus-independent $CD4^+$ T-cell biased reconstitution (Chiesa *et al.,* 2012). In addition, we observed normal T-cell spectratype as early as 30 days post T-cell-replete CBT, which is in contrast to the previous reports of a skewed T-cell repertoire after T-cell-deplete CBT (Komanduri *et al.,* 2007). T-cell reconstitution after T-cell-replete CBT was superior to T-cell reconstitution after T-cell-replete BMT [Figure 13]. Furthermore, the T-cell reconstitution after CBT was always $CD4^+$ T-cell biased, compared to the well-recognised $CD8^+$ T-cell biased

reconstitution observed during lymphocyte recovery, after BMT (Mackall *et al.,* 1995; Hakim *et al.,* 1997; Trzonkowski *et al.,* 2008; Unsinger *et al.,* 2009; Cieri *et al.,* 2015). This observation suggests a uniquely distinct ability of cord blood $CD4^+$ T cells to expand rapidly in the post-transplant lymphopenic environment producing a diverse T-cell repertoire.

Thymic-independent T-cell expansion, following allogeneic stem cell transplantation is mediated by three processes, (1) lymphopenia-induced proliferation, (2) anti-viral expansion and (3) allo-reactive expansion.

1) Lymphopenia-induced proliferation: Non-host reactive donor T cells proliferate in response to self-MHC Class I and II molecules and / or cytokines, such as IL-7 or IL-15, and contribute to a beneficial peripheral T-cell reconstitution (Mackall *et al.,* 1996; Mackall *et al.,* 1997; Ge *et al.,* 2002).
2) Antiviral expansion: Proliferation of virus-specific T cells in response to viral reactivation.
3) Allo-reactive expansion: Host-reactive donor T cells proliferate in response to allo-antigens, causing GvHD. Allo-reactive expansion depends on the recognition of MHC:antigen complex by the T-cell receptor, engagement of co-stimulatory molecules, and clonal expansion of T cells. The most well characterized co-stimulatory molecule is the CD28/B7 family (Acuto *et al.,* 2003). However, several members of the tumour necrosis factor receptor (TNFR) superfamily - OX40, CD40, 4-1BB, CD27, CD30, and HVEM (herpes-virus entry mediator) – are being recognized as having a role in providing co-stimulation that is distinct to that of CD28/B7 (Croft *et al.,* 2003). The allo-reactive expansion is largely inhibited by immunosuppression, following HCT, and thus lymphopenia-induced proliferation is likely to be the primary mechanism in replenishing the lymphopenic environment. Thus, it is plausible that the process of lymphopenia-induced proliferation could mediate enhanced immune-reconstitution observed after T-cell replete CBT.

Rapid $CD4^+$ T-cell biased immune-reconstitution following cord blood transplantation, may be driven by upregulated homeostatic mechanisms

To study the differences in T-cell homeostasis, following cord blood and bone marrow grafts, we compared early T-cell immune-reconstitution in children (age range 0.1 to 12 years) receiving cord blood (*n = 30*) and bone marrow transplantation (*n = 40*). We observed enhanced and early T-cell reconstitution following CBT. The early T-cell reconstitution after CBT was interestingly asymmetrically $CD4^+$ T-cell biased, especially at early time-points. In contrast, early T-cell reconstitution after BMT was $CD8^+$ T-cell biased, and relatively slow (Fallen *et al.,* 2003; Fujimaki *et al.,* 2001). The enhanced T-cell immune-reconstitution after CBT occurred despite one log fewer T cells infused in the cord blood grafts, compared to the bone marrow grafts [Figure 12].

The robust $CD4^+$ T-cell expansion of cord blood T cells could be because cord blood T cells may expand with a bias towards one particular Th subset. To identify if one particular Th subset was expanding after CBT, I performed phenotyping of reconstituting $CD4^+$ T cells at one, three and six months, following CBT and BMT. A significantly increased percentage of T-regulatory cells, particularly one month after CBT compared to BMT was observed. However, by six months, the increased percentage of T-regulatory cells had gradually reduced to levels similar to those of post-BMT. The T-regulatory bias, early after CBT, was observed despite there being a similar proportion of T-regulatory cells in normal donor cord blood and adult peripheral blood (Kim *et al.,* 2012; Takahata *et al.,* 2004). The early increase in circulating regulatory T cells after CBT is an interesting finding, and perhaps reflects the rapid expansion of T-regulatory cells, or induction of T-regulatory phenotype, following cord blood graft. Despite the increased numbers of T-regulatory cells after CBT, the majority of $CD4^+$ T cells are non-regulatory cells, and hence this does not explain the enhanced $CD4^+$ T-cell biased expansion after CBT. We also found that a substantial number of T cells underwent differentiation to memory T cells, as early as 30 days post-CBT (Chiesa *et al.,* 2012). It is well known that during lymphopenia-induced proliferation, naïve T cells acquire a memory-like phenotype, and hence, the rapid conversion of naive cord blood T cells to a memory phenotype suggests the role of homeostatic mechanisms in the rapid post-CBT T-cell expansion (Surh *et al.,* 2008; Takada *et al.,* 2009; Hamilton *et al.,* 2006).

Complex homeostatic mechanisms regulate the peripheral T-cell pool. Whilst naive T cells are maintained by IL-7 and signalling from MHC-TCR contact, the memory T-cell

population is heterogeneous, and comprised of cells derived from responses to both foreign and self-antigens. Typical memory cells are kept alive, and induced to divide intermittently, by IL-7 and IL-15 (Boyman *et al.,* 2009). Therefore, to determine whether the post-CBT T-cell reconstitution is due to similar mechanism, decline in IL-7 levels post-CBT and post-BMT were compared. Higher day+30 IL-7 levels were observed in cord blood recipients compared to bone marrow recipients. More interestingly, the high day+30 IL-7 levels in the CBT recipients declined rapidly by day+90. The higher day+30 IL-7 levels in cord blood recipients compared with bone marrow recipients, could reflect the profound lymphopenic environment, due to low numbers of T cells carried with the cord blood graft, as previously described. It also suggests that the cord blood T cells are likely to be exposed to high levels of IL-7 *in vivo* for a longer period of time. The rapid decline in IL-7 after CBT by day+90 suggests that the T-cell expansion after CBT could be mediated by IL-7, a cytokine known to a role in T-cell homeostasis.

I therefore tested whether cord blood $CD4^+$ T cells are overly sensitive to homeostatic signals by comparing the proliferation of cord blood T cells and peripheral blood T cells to IL-7, IL-15 and IL-2 using a CFSE dilution assay. Cord blood $CD4^+$ T cells proliferated rapidly compared to peripheral blood $CD4^+$ T cells in the presence of supra-physiologic IL-7 concentration and showed some response to IL-15 but no response to IL-2. This hyper-responsiveness of cord blood $CD4^+$ T cells to IL-7 has also been reported by Schonland *et al.,* (Schonland; *et al.,* 2003). Thus, cord blood T cells appear to be more sensitive to homeostatic signals, compared to peripheral blood T cells, albeit at a supra-physiological dose.

In order to understand how this hyper-responsiveness to IL-7 was mediated, we studied the differences in the IL-7 pathway using flow-cytometry. IL-7 receptor-alpha expression, an upstream molecule of the IL-7 pathway, was highly expressed in cord blood $CD4^+$ T cells compared with peripheral blood $CD4^+$ T cells. Despite the higher expression of IL-7 receptor in the cord blood $CD4^+$ T cells, differential phosphorylation of the most relevant downstream molecule of IL-7 pathway (STAT5) was not observed. Thus, whilst cord blood $CD4^+$ T cells express higher levels of IL7R-alpha than peripheral blood $CD4^+$ T cells, the differences in proliferation seen between cord blood and peripheral blood $CD4^+$ T cells are not explained by STAT5 phosphorylation. Similar findings to these have been reported previously by Swainson *et al* (Swainson *et al.,* 2007). In addition, the group also studied the proliferation of cord blood $CD4^+$ T cells using 1 ng/ml of IL-7, and found that despite optimal STAT5 phosphorylation, after five days, only 10% of cord blood $CD4^+$ T cells entered cell cycle after

5 days. These finding suggests that mechanisms and/or biological processes other than the IL-7:STAT5-dependent signalling cascade may contribute to the rapid proliferation of cord blood $CD4^+$ T cells. Therefore, I studied the differences in TCR signalling between cord blood and peripheral blood $CD4^+$ T cells.

Allogeneic EBV-driven B-cell lymphoblastoid cells were used to provide strong MHC signals because they express MHC Class I and Class II molecules. After stimulation with irradiated allogeneic lymphoblastoid cells, 80% of cord blood $CD4^+$ T cells entered cell cycle and proliferated rapidly, compared with only 20% of peripheral blood $CD4^+$ T cells. This indicates that cord blood $CD4^+$ T cells are hyper-responsive to MHC signals compared to peripheral blood $CD4^+$ T cells.

The predominant $CD4^+$ T-cell population in cord blood is naïve, and the hyper-responsiveness of cord blood $CD4^+$ T cells may be a function of their naivety. To determine whether naivety mediates enhanced responsiveness to MHC signals, $CD45RA^+$ enriched fractions of CBMC and PBMC were stimulated with allogeneic EBV-driven B-cell lymphoblastoid cells. The proliferative responses of $CD4^+$ T cells in the $CD45RA^+$ enriched fractions were similar to those in unselected CBMC and PBMC fractions. Although, the CD45RA-enriched T cells may have some effector cells, similar proliferation observed in CD45RA-enriched T cells after stimulation with allogeneic LCLs suggested the hyper-responsiveness of cord blood $CD4^+$ T cells was not due to naivety but due to lower TCR signalling threshold of cord blood $CD4^+$ T cells.

Summary

The experiments described in chapter three indicate that although robust $CD4^+$ T-cell biased immune-reconstitution occurs after CBT, the majority of $CD4^+$ T cells are not regulatory. During T-cell reconstitution, naïve cord blood T cells rapidly differentiate in to memory T cells, accompanied by a rapid decline in IL-7 levels. Therefore, the differences in sensitivity of cord blood and peripheral blood $CD4^+$ T cells to IL-7 were tested. Although, cord blood $CD4^+$ T cells had higher expression of IL7R-alpha, and were significantly more sensitive than peripheral blood $CD4^+$ T cells to a supraphysiological dose of IL-7, STAT5 phosphorylation of cord blood and peripheral blood $CD4^+$ T cells at varying concentrations of IL-7 was similar. As this observation does not explain how the IL-7:STAT5 signalling cascade mediates enhanced post-CBT T-cell reconstitution, the role of TCR signalling in enhanced post-CBT T-cell reconstitution was tested. Cord blood $CD4^+$ T cells were hyper-responsive to

allogeneic MHC signals compared with peripheral blood $CD4^+$ T cells, suggesting the lower threshold for TCR signalling in cord blood $CD4^+$ T cells could explain the robust $CD4^+$ T-cell reconstitution. These observations also suggest that the T cells derived from the immune system carried with the foetal-derived cord blood graft may be distinctly regulated.

Foetal and adult lymphocytes in birds, humans, and other, mammals have been described as having distinct ontogeneic origins (Morrison *et al.,* 1995; Zanjani *et al.,* 1993; Harrison *et al.,* 1997; Ikuta *et al.,* 1990; Montecino-Rodriguez *et al.,* 2006; Havran *et al.,* 1998; Mold *et al.,* 2010). Foetal lymphocytes carried with the cord blood graft may have an enhanced ability to fill the immunological void through processes involved in lymphopenia-induced proliferation, such as TCR and cytokine signalling, and hence display distinct reconstitution kinetics following CBT. I, therefore, set out to establish whether the early adaptive immune system derived after T-cell-replete CBT recapitulates foetal ontogeny in a manner that is distinct to that of adult ontogeny following T-cell-replete BMT, and if so, whether upregulation of distinct cell signalling and biological processes during the recapitulation of foetal ontogeny explains the enhanced lymphopenia-induced proliferation following CBT.

T-cell replete cord blood transplantation recapitulates foetal ontogeny with a distinct molecular signature that supports $CD4^+$ T-cell reconstitution

There is growing evidence that supports the distinct ontogenic origins of foetal and adult lymphoid systems (Mold *et al.,* 2010; Copley *et al.,* 2013; Yuan *et al.,* 2012). Therefore, to study the effect of foetal ontogeny on T-cell replete CBT, gene expression profiling was performed on naïve $CD4^+$ T cells from (1) normal donor cord blood, (2) normal donor peripheral blood, and (3) transplant recipients two months after receiving a T-cell-replete cord blood or (4) bone marrow graft. The gene expression profiles were compared with naïve $CD4^+$ T cells from foetal lymph nodes. These studies provided compelling evidence for transcription profiles of naïve $CD4^+$ T cells from cord blood, and during early reconstitution following CBT, being distinct to those from peripheral blood. The cord blood T-cell profiles were similar to the naïve $CD4^+$ T cells from foetal lymph nodes. In contrast, the reconstituting naïve $CD4^+$ T cells following T-cell replete BMT, had a transcription profile similar to the peripheral blood $CD4^+$ T cells.

Foetal ontogeny is biased towards T-regulatory function (Silverstein *et al.,* 1964a; Silverstein *et al.,* 1964b; Michaelsson *et al.,* 2006; Takahata *et al.,* 2004). I therefore compared the relationship between naïve $CD4^+$ T cells and T-regulatory cells from foetal lymph nodes and adults. In a 2D-PCA analysis, naïve $CD4^+$ T cells and T-regulatory cells segregated, depending on their developmental stage and T-cell phenotype. Thus, the distinct profile of naïve $CD4^+$ T cells early post-CBT is due to the recapitulation of foetal ontogeny, and not due to adoption of a T-regulatory phenotype. It is well established that foetal lymphopoiesis originates from $Lin28b^+$ HSCs, and postnatally, Lin28b is down-regulated, resulting in let-7 miRNA biogenesis and an adult lymphoid program. Thus, the difference in robustness of T-cell immune-reconstitution observed after T-cell replete CBT compared with T-cell replete BMT, may be due to the distinct foetal-like transcription profile of cord blood T cells originating from $Lin28b^+$ HSCs, whereas peripheral blood T cells have a let-7 miRNA mediated adult-like transcription profile.

To establish whether the differences in transcription profiles explain the differences in regulation of T-cell homeostasis, the differentially expressed genes in the naïve $CD4^+$ T cells from the cord blood and peripheral blood were identified. In three separate experiments, the gene expression profiles of naïve $CD4^+$ T cells from cord blood and peripheral blood were

compared. Sixty genes overlapped in the three experiments. These 60 genes are therefore likely to represent the signature of cord blood $CD4^+$ T cells.

Cord blood T cells are in a highly proliferative state driven by the relatively lymphopenic environment of the foetus (Schonland *et al.,* 2003; van der Windt *et al.,* 2012; Min *et al.,* 2003). Therefore, it was speculated that cord blood T cells may be enriched with genes induced during lymphopenia-induced proliferation. To identify these genes, the expression profiles of steady-state naïve $CD4^+$ T cells from peripheral blood were compared with those from reconstituting naïve $CD4^+$ T cells following T-cell replete BMT. Nineteen of the 60 overlapping genes representing the 'signature' of naïve cord blood $CD4^+$ T cells were also differentially expressed in reconstituting naïve peripheral blood $CD4^+$ T cells following T-cell replete BMT. These 19 differentially expressed genes remained differentially expressed in the reconstituting naïve $CD4^+$ T cells following T-cell replete CBT. The up- or down-regulation of all 19 genes was higher in the post-CBT reconstituting naïve $CD4^+$ T cells than in the post-BMT cells. Thus, the differential regulation of these 19 genes in the post-transplant lymphopenic environment indicates their role in lymphopenia-induced proliferation, and the remaining 41 genes are likely to represent the rest of the foetal signature. Interestingly, of these 19 genes, *fos* and *jun* (AP-1 complex) were amongst the most up-regulated genes. Together, *fos* and *jun*, form an AP-1 complex, and are two important transcription factors that are activated, upon ligation of TCR, and represent a convergence point of several TCR-initiated signalling pathways (Brownlie *et al.,* 2013). Importantly, AP-1 complex was found to be upregulated during all the lymphopenic states. AP-1 complex was found to be more significantly upregulated in the reconstituting T cells after cord blood graft than in the reconstituting peripheral blood T cells following bone marrow graft. This finding suggests that tonic TCR signalling may be the primary driver of lymphopenia-induced proliferation, and upregulated TCR signalling may endow cord blood T cells with the property to re-populate rapidly in the lymphopenic environment.

TCR:MHC interactions and IL-7 are the two major homeostatic signals for proliferation and/or survival of T cells (Surh *et al.,* 2000; Jameson *et al.,* 2005; Deshpande *et al.,* 2013; Hennion-Tscheltzoff *et al.,* 2013), and these two signals co-operate to maintain the peripheral T-cell pool. However, the exact contribution of the TCR and IL-7 signalling pathways during lymphopenia-induced proliferation is not known. The distinct transcription profile of cord blood T cells driven by their foetal origins and significant up-regulation of AP-1 transcription

factor in the normal donor and reconstituting cord blood T cells, suggests that the TCR signalling and its related pathways may mediate enhanced immune-reconstitution after CBT.

Therefore, I performed GSEA analysis to determine which pathways are significantly upregulated in naïve $CD4^+$ T cells from normal donor cord blood T cells and reconstituting T cells after CBT and BMT, in comparison to the steady-state naïve $CD4^+$ T cells from peripheral blood. The TCR signalling pathway was upregulated in naïve $CD4^+$ T cells from all the lymphopenic conditions, such as normal donor cord blood and reconstituting T cells after CBT and BMT. It is well-established fact that TCR signalling leads to the induction of MAPkinase signalling pathways (Smith-Garvin *et al.,* 2009), and interestingly, during lymphopenic states, in addition to TCR signalling, MAPkinase signalling was also significantly upregulated. This finding indicates an essential role of endogenous TCR activation in driving lymphopenia-induced proliferation. If TCR activation to self or non-self-ligands drives lymphopenia-induced proliferation, what role does IL-7 play in T-cell homeostasis? It has been suggested that although $CD4^+$ T cells proliferate in response to IL-7, TCR stimulation increases the IL-7 responsiveness (Hennion-Tscheltzoff *et al.,* 2013). Recently it has been indicated that interruption of IL-7 signalling, with homeostatic TCR signal, is essential for the survival of naïve $CD8^+$ T cells, and persistent IL-7 signalling leads to IFN-γ mediated cell death (Kimura *et al.,* 2013). In addition, researchers have shown that the stronger the TCR signal, the more IL-7 was interrupted, and the more cells survived. Our data on the upregulation of the TCR signal during lymphopenia-induced proliferation, corroborates these findings, and suggests that during lymphopenic states, IL-7 signalling may be frequently interrupted by homeostatic TCR signal, and hence may lead to increased survival and proliferation of T cells. Thus, upregulated TCR-MAPkinase signalling in cord blood T cells is likely to be the potential mechanism of enhanced $CD4^+$ T-cell reconstitution after T-cell replete CBT.

The work done so far indicates the distinctness of TCR:MHC interactions during the development of foetal ontogeny. Therefore, to investigate the role of TCR signalling in post-CBT T-cell expansion, I attempted to generate a APC:T-cell culture system. Cord blood and peripheral blood T cells were cultured in 96 well round bottom plates with increasing concentrations of non-T cell fractions (self-APCs) to provide MHC signals. In this culture system, there was no significant effect of increasing concentration of self-APCs on peripheral blood $CD4^+$ T-cell divisions. In contrast, cord blood $CD4^+$ T cells underwent significantly

more cell divisions with increasing concentration of APCs, indicating that cord blood $CD4^+$ T cells are tuned to undergo rapid proliferation in response to self-MHC signals.

Finally, to confirm the role of upregulated TCR-AP-1 signalling pathway in the lymphopenia-induced proliferation of cord blood $CD4^+$ T cells, increasing concentrations of AP-1 inhibitor were used in the APC:T-cell culture system. Cord blood $CD4^+$ T-cell proliferation was inhibited by AP-1 inhibitor in the self APC:T-cell co-culture system, and this inhibitory effect was proportional to the increasing concentration of AP-1 inhibitor. These findings confirm the lower TCR signalling threshold of cord blood T cells to MHC ligands, and the proliferation of cord blood T cells via the TCR signalling pathway. Thus, indicating the role of TCR signalling in $CD4^+$ T-cell biased immune-reconstitution after T-cell replete CBT.

Model for CD4+ T-cell expansion after cord blood transplantation

Based on the findings of my thesis and previously described observations by other co-workers, I put forward the model of CD4+ T-cell biased expansion after cord blood transplantation.

Upregulated TCR-MAPkinase signalling in the cord blood CD4+ T cells, similar STAT5 phosphorylation of cord blood and peripheral blood CD4+ T cells to varying concentrations of IL-7 and rapid decline in IL-7 levels during expansion of cord blood T cells were the key findings of my work. Previously, essential role of both tonic TCR signalling and IL-7 signalling in proliferation and survival of naïve T cells (Surh *et al.,* 2000; Jameson *et al.,* 2005; Deshpande *et al.,* 2013; Hennion-Tscheltzoff *et al.,* 2013), and T-cell death due to persistent IL-7 signalling in the absence of MHC (Kimura *et al.,* 2013) has been described. In addition, increasing the TCR stimulation also increased the IL-7 responsiveness. Thus, it is possible to conceptualise the co-operation between tonic TCR and IL-7 signalling as key mechanisms for driving CD4+ T-cell expansion [Figure 86].

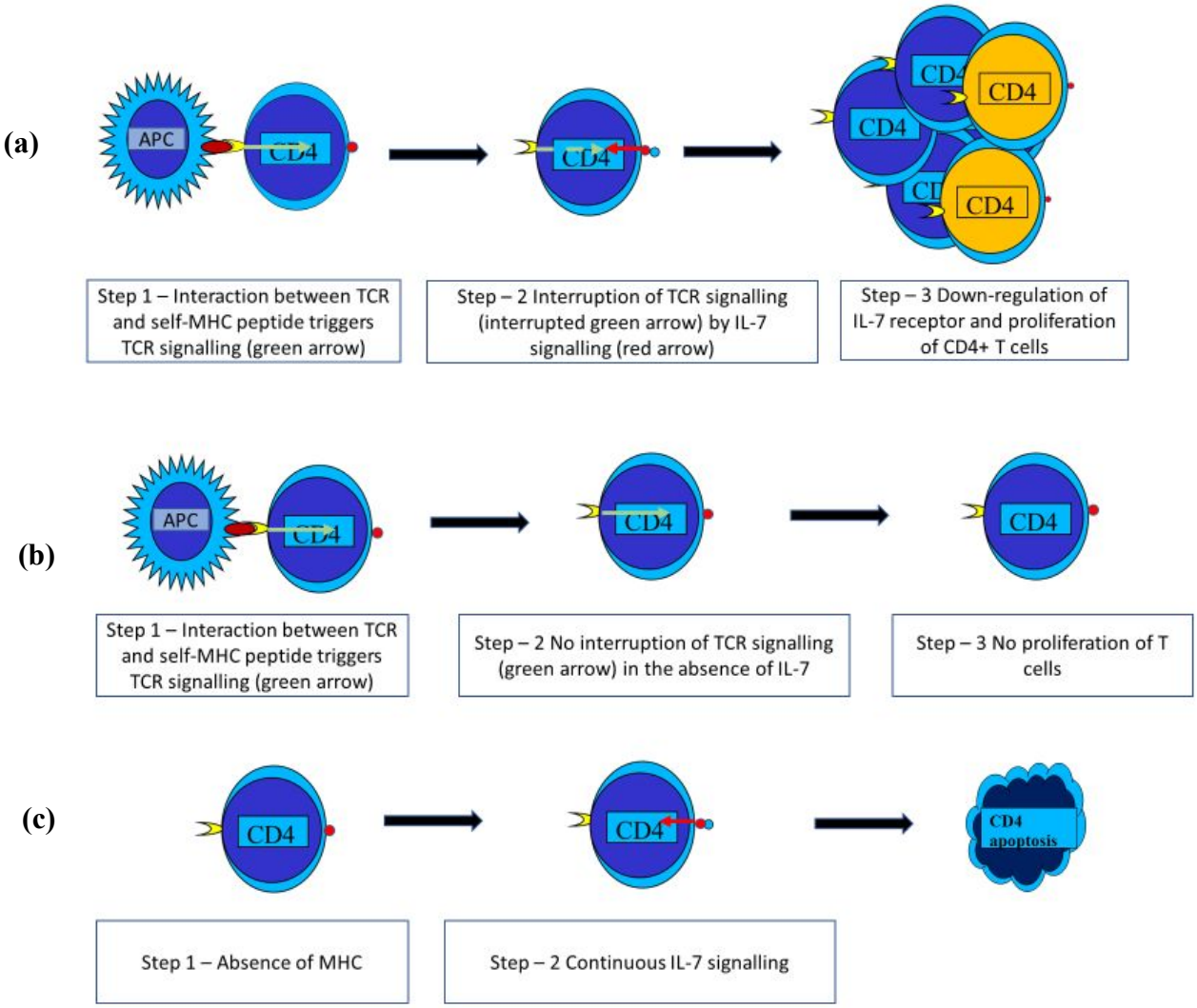

Figure 86: Mechanism of CD4+ T cell expansion after cord blood transplantation is shown. (a) shows interaction between self-MHC Class II peptide triggers TCR signalling (step 1 - shown as green arrow). The TCR signalling is interrupted by IL-7 signalling (step 2 - red arrow). This leads to downregulation of IL-7 receptor and proliferation of CD4+ T cells (step 3). (b) shows that when there is no interruption of TCR signalling by IL-7 signalling, proliferation of CD4+ T cell does not occur. (c) shows that in the absence of TCR signalling and continuous IL-7 signalling, CD4+ T-cell apoptosis occurs.

Based on the above model, one could speculate that the upregulated TCR-MAPkinase signalling in cord blood CD4+ T-cell may drive the CD4+ T-cell biased expansion after cord blood transplantation. Interestingly, it has been described recently that cord blood CD8+ T cells have downregulated TCR-MAPkinase signalling compared to their adult counterparts, and hence this TCR signalling based model of T-cell expansion would also explain delayed recovery of CD8+ T cells after cord blood transplantation (Galindo-Albarrán *et al*., 2016). Thus, the described model best fits with the theory of CD4+ and CD8+ T cells derived from

lin28b^{high} foetal HSC's may be distinctly regulated to those derived from lin28b^{low} adult HSC's. There are however other possible unexplored mechanisms for CD4+ T-cell biased expansion after cord blood transplantation. The key unexplored mechanisms that could have a role in rapid CD4+ T-cell biased expansion after cord blood transplantation are -

1) The effect of one log lower T cells transferred with the cord blood graft compared to an adult graft source and hence increased availability of sources required for CD4+ T-cell expansion,
2) The effect of naive immune system transferred with the cord blood graft vs partially differentiated immune systems transferred with an adult graft source,
   and last but not the least
3) The influence of gut microbiome of the host on cord blood T cells from the sterile foetal environment.

Summary

The molecular signature of rapidly proliferating cord blood CD4$^+$ T cells via the thymus-independent pathway is similar to foetal CD4$^+$ T cells, and hence supports the recapitulation of foetal ontogeny after T-cell replete CBT. The molecular signature of naïve cord blood CD4$^+$ T cells was found to be enriched in genes involved in TCR-MAPkinase signalling. The functional experiments further indicate that cord blood CD4$^+$ T cells proliferate rapidly in response to both self and allogeneic MHC signals. The functional experiments also show that the proliferation of cord blood CD4$^+$ T cells in response to self-MHC signals, is not only TCR-dependent but also dependent on the AP-1 complex, an important transcription factor of the TCR-MAPkinase signalling pathway. Therefore, gene expression and functional experiments confirm that cord blood CD4$^+$ T cells have a lower TCR threshold than peripheral blood CD4$^+$ T cells. The lower threshold of the TCR to MHC ligands increase their propensity to undergo lymphopenia-induced proliferation (Kassiotis *et al.,* 2003; Kieper *et al.,* 2004), and may mediate the rapid CD4$^+$ T-cell biased reconstitution after T-cell replete CBT. The increased sensitivity of cord blood T cells to MHC ligands may provide qualitatively distinct effects after T-cell replete CBT (Fulton *et al.,* 2015), therefore in the next chapters, I investigated the role of rapidly reconstituting cord blood T cells in mediating the GvL effect.

Cord blood T cells mediate enhanced Tc1-Th1 anti-leukemic effects compared with peripheral blood T cells

T-cell replete CBT is increasingly used to treat chemo-resistant leukaemia (Wagner JE Jr *et al.,* 2014; Barker *et al.,* 2015; Brunstein *et al.,* 2011; Zheng *et al.,* 2015), and as discussed before, such a T-cell replete approach leads to enhanced reconstitution after CBT (Chiesa *et al.,* 2012; Lindemans *et al.,* 2014). We also observed that these rapidly reconstituting naïve cord blood T cells differentiate into viral specific T-lymphocytes within two months of CBT, and this was associated with the rapid clearance of viral infections from the blood (both Cytomegalovirus and Adenovirus). It has been suggested that patients undergoing CBT for acute leukaemia, who reconstituted their immunity more quickly as evidenced by immune response to herpes viruses had a significantly reduced incidence of leukaemia relapse (Parkman *et al.,* 2006). Thus, despite the intrinsic bias of cord blood T cells towards anti-inflammatory Th2/Tc2 immune responses (Marchant *et al.,* 2005; White *et al.,* 2002), naive cord blood T cells can proliferate rapidly and differentiate into antigen-specific T cells following T-cell replete CBT. Whether this early and unique pattern of cord blood T-cell reconstitution mediated by strong TCR signals, could also provide an enhanced GvL effect was investigated. To determine this, the ability of cord blood *versus* peripheral blood T cells to mediate an anti-tumour effect in an EBV-driven B-cell lymphoma model of NOD/SCID/IL2rg^{null} mice was compared.

Cord blood T cells were observed to mediate a robust GvL effect compared to peripheral blood T cells in an EBV-driven B-cell lymphoma model. In comparison with cord blood T cells, peripheral blood T cells mediated an attenuated GvL effect. Although cord blood T cells mediated an enhanced GvL effect, no evidence of xenogeneic GvHD was observed. This led to the significantly improved survival of mice receiving cord blood T cells.

Xenogeneic GvHD is a well-established feature of peripheral blood T cells. Intrigued by the absence of xenogeneic GvHD in the cord blood T cells, I compared the xenogeneic potential of cord blood T cells with peripheral blood T cells. Xenogeneic GvHD was exclusively observed in the mice receiving peripheral blood T cells. This was confirmed by liver and gut histology. There was no evidence of GvHD in the cord blood group. This confirmed that cord blood T cells mediate an enhanced anti-tumour effect compared to peripheral blood T cells without exhibiting xenoreactivity. I, therefore, speculated that the xeno-reactive peripheral

blood T cells must also mediate a GvL effect, albeit an attenuated one compared with cord blood T cells.

To test the GvL effect mediated by peripheral blood T cells, the ability of 5 million peripheral blood T cells to reject a lower burden of B-cell lymphoma (2.5 million LCLs) was tested. In this model, peripheral blood T cells mediated a GvL effect against a lower burden of B-cell lymphoma, and this GvL effect correlated with the onset of xenogeneic GvHD. Thus, in comparison with cord blood T cells, peripheral blood T cells mediated an attenuated anti-tumour effect.

The B-cell lymphoma used in this model is an EBV-driven tumour that expresses viral antigens. It was, therefore, important to determine whether the effective tumour control and regression observed in the cord blood group was due to an anti-viral, or an anti-leukaemic (allo-reactive) effect. Autologous cord blood T cells lacked the ability to reject the tumour. This confirmed that the observed tumour regression in the cord blood group was an allo-reactive T-cell response, rather than an HLA-restricted anti-EBV effect.

To gain immunological insights into the enhanced allo-reactive T-cell response mediated by cord blood T cells, further tumour modelling experiments were performed to study the tumour-infiltrating lymphocytes (TILs).

Firstly, to determine the differences in recruitment of T cells to the tumour in the cord blood and peripheral blood groups, histological examination of the tumours was performed. Fifteen days after T-cell injection, mice were sacrificed, and the tumours were stained with $CD3^+$ and $CD20^+$ immuno-histochemical stains. T-cell infiltration was quantified using Image J software. A significantly enhanced infiltration of cord blood T cells was observed compared to peripheral blood T cells suggesting that cord blood and peripheral blood T cells may be distinct. Indeed, majority of cord blood T cells are antigen-inexperienced naïve T cells compared to adult peripheral blood T cells. At least, 30%–60% of adult peripheral blood T cells have a memory-effector phenotype. Furthermore, as discussed before, there is growing evidence supporting the distinct ontogenic origins of foetal and adult lymphoid immune systems. Our observations also indicate that the early adaptive immune system derived from T-cell replete CBT recapitulates a distinct molecular program of foetal ontogeny, which also includes lymphopenia-induced genes. These phenotypic and ontogenic differences between cord blood and peripheral blood T cells may not only endow cord blood T cells with the

ability to rapidly undergo lymphopenia-induced proliferation but may also confer cord blood T cells with the ability to mediate the enhanced allo-reactivity.

To further study the differences in recruitment of T cells to the tumour, flow-cytometric analysis of the isolated TILs was carried out. Majority of cord blood TILs were $CD8^+$ T cells, but in contrast, a preponderance of $CD4^+$ T cells were observed in the peripheral blood TILs. Recruitment of lymphocytes to the tumour tissue is primarily mediated by an interaction between MHC molecules expressed by the tumour cells, and the reactivity of immune cells to these molecules. It is noteworthy that despite the strong expression of MHC Class I and II molecules in this B-cell lymphoma model, and the robust proliferation of cord blood $CD4^+$ and $CD8^+$ T cells following stimulation with allogeneic lymphoma cells *in vitro*, most of cord blood TILs were $CD8^+$ T cells. This difference in the tumoural recruitment of T cells between the two groups with significantly enhanced infiltration of cord blood $CD8^+$ TILs was observed in three separate experiments. Several clinical studies on human cancer have shown that an increase in TILs is associated with a better prognosis (Leffers *et al.,* 2009; Galon *et al.,* 2006; Sato *et al.,* 2005; Zhang *et al.,* 2003). Similarly, in our tumour model, the enhanced tumoural infiltration of cord blood T cells (in particular cord blood $CD8^+$ T cells) compared with peripheral blood T cells may mediate potent anti-leukaemic effects and improve survival in the cord blood group.

The role of $CD8^+$ TILs in tumour immunology has been demonstrated in numerous murine models and in cancer patients, including those with leukaemia. In one murine model of MHC-mismatched allogeneic bone marrow transplantation for acute T-cell leukaemia, infusion of mixed donor $CD4^+$ and $CD8^+$ T cells, or donor $CD8^+$ T cells alone, mediated a potent GvL effect, whereas GvL was not observed with donor $CD4^+$ T cells alone (Johnson *et al.,* 1999). In another murine model of chronic myeloid leukaemia, GvL was also shown to be mediated by $CD8^+$ T cells (Lu *et al.,* 2012). In clinical studies, however, infusions of $CD4^+$ donor lymphocytes to treat CML relapse after HCT have induced durable remissions, although more elaborate studies have demonstrated that $CD4^+$ lymphocyte infusions led to the expansion of $CD8^+$ donor T cells and induced cytotoxic activity (Zorn *et al.,* 2002). Another recent study has also demonstrated that the response to infusions of $CD4^+$ donor lymphocytes is predicted by the percentage of pre-DLI bone marrow $CD8^+$ T cell infiltrates (Bachireddy *et al.,* 2014). It is, therefore, apparent that $CD8^+$ T cells are critical anti-leukemic effectors at the tumour site. Hence, in this human lymphoma:T-cell model, our observation of

the preferential infiltration of cord blood $CD8^+$ TILs compared with peripheral blood $CD8^+$ TILs indicates that cord blood $CD8^+$ T cells mediate enhanced anti-tumour responses.

To mediate anti-tumour effects, naïve cord blood TILs must undergo memory-effector differentiation. Therefore, the phenotype of TILs and circulating lymphocytes was studied using flow-cytometry. Majority of cord blood T cells are naïve. Despite this, the percentages of memory and effector $CD4^+$ and $CD8^+$ T cells in the cord blood TILs were similar to the peripheral blood TILs. Thus, naïve cord blood TILs were observed to undergo rapid memory-effector differentiation. Interestingly, whilst circulating lymphocytes from the peripheral blood group underwent differentiation with an effector phenotype, circulating lymphocytes in the cord blood group remained naïve. This phenotypic analysis of TILs and circulating lymphocytes, supports the observation of enhanced anti-tumour effects, with the absence of xenogeneic GvHD in the cord blood group.

To gain further insight into the enhanced anti-tumour effects mediated by cord blood T cells, the kinetics of T-cell infiltration and the regulation of T cells in the tumour microenvironment was studied. Monitoring of CD4:CD8 and CD8:$CD4^+$ T-regulatory cell ratios, both at early and late time-points was performed. A significant bias towards $CD8^+$ T cells was observed in the cord blood TILs compared to the peripheral blood TILs. In contrast, preponderance of peripheral blood TILs comprised $CD4^+$ T-regulatory cells compared to the cord blood TILs. This indicates that the rapid infiltration of cord blood $CD8^+$ T cells may mediate anti-tumour effects in the cord blood group, and a preponderance of $CD4^+$ T-regulatory cells in the peripheral blood TILs may attenuate the anti-tumour effect. Furthermore, the role of $FoxP3^+$ regulatory T-cell mediated immunosuppression is well-established as a crucial tumour immune-evading mechanism (Dunn *et al.,* 2004; Zou *et al.,* 2005; Shevach *et al.,* 2002; Sakaguchi *et al.,* 2005). In a meta-analysis of TILs in tumour sections, although $CD3^+$ and $CD8^+$ TILs were associated with good prognosis and improved survival, the $CD8^+$:$FoxP3^+$ ratio produced a more impressive hazard ratio compared with $CD3^+$ or $CD8^+$ TILs alone (Godden *et al.,* 2011).

Naïve cord blood $CD8^+$ TILs rapidly underwent memory-effector differentiation. Therefore, to study which effector activity is gained by cord blood $CD8^+$ TILs and peripheral blood $CD8^+$ TILs, cytokine staining for IFN-γ and TNF-α was performed, after stimulating isolated TILs with (B-cell) lymphoma cells *in vitro*. There were no differences in the percentage of

$CD8^+$ T cells gaining IFN-γ activity. Although, a significantly higher percentage of cord blood $CD8^+$ TILs did gain TNF-α activity compared to the peripheral blood $CD8^+$ TILs.

To further substantiate these qualitative differences between cord blood and peripheral blood TILs, perforin expression was studied. Cord blood $CD8^+$ TILs had higher expression of perforin, compared with peripheral blood $CD8^+$ TILs. Thus, higher TNF-α activity and perforin expression is likely to be the possible mechanism of enhanced anti-tumour effect mediated by cord blood $CD8^+$ T cells in this tumour model.

Next, I questioned whether the differences in the Th1/Th2 ratio of cord blood and peripheral blood $CD4^+$ TILs could explain the enhanced anti-tumour effects in the cord blood group. Th1 cells were identified as IFN-γ^+ and TNF-α^+ secreting cells, whereas Th2 cells were identified as IL-4 secreting cells. In the peripheral blood group, a significantly higher percentage of Th2 TILs was observed than in the cord blood group. On analysis of the Th1/Th2 ratio by calculating the IFN-γ^+:IL-4^+ and TNF-α^+:IL-4^+ ratios in TILs, it was observed that the Th1/Th2 ratio was significantly higher in the cord blood group compared to the peripheral blood group. Whereas $CD8^+$ TILs are apparent mediators of the GvL effect, $CD4^+$ TILs, in particular the Th1/Th2 balance also dictates tumour-specific immune responses (Tsung *et al.,* 1997; Aruga *et al.,* 1997; Fowler *et al.,* 1996). The role of the Th1/Th2 balance has also been tested in leukaemia models (Hu *et al.,* 1998). In general, immune-deviation towards Th1 effector cells mediates an anti-tumour response, whereas immune-deviation towards Th2 prevents tumour rejection. In this study, peripheral blood TILs were found to have a significantly higher Th2 responses (measured as IL-4 secreting $CD4^+$ T cells) compared to cord blood TILs, and the Th1/Th2 intra-tumoural balance (measured as IFN-γ/IL-4 and TNF-α/IL-4 ratios) in the cord blood TILs was relatively skewed toward Th1 responses compared to the peripheral blood TILs.

It is not surprising that a similar percentage of cord blood and peripheral blood $CD8^+$ TILs secrete IFN-γ because naïve cord blood and peripheral blood $CD8^+$ T cells have a comparable IFN-γ promoter methylation pattern (White *et al.,* 2002). However, the relative skewing of the Th1/Th2 balance towards Th1 in the cord blood TILs is noteworthy. This occurred even though naïve cord blood $CD4^+$ T cells are reported to be physiologically biased towards Th2, produce lower levels of IFN-γ than adult naïve T cells *in vitro* and are hypermethylated at CpG and non-CpG sites within the IFN-γ promoter (White *et al.,* 2002). Thus, under adequate priming conditions such as B-cell lymphoblastoid tumour, cord blood $CD4^+$ T cells can

rapidly mature into Th1 effectors. In contrast, a significantly lower CD8:$CD4^+$ T-regulatory ratio, a preponderance of Th2 cells and $CD4^+$ T-regulatory cells may attenuate the anti-tumour response in the peripheral blood group. Thus, a relative Th2 bias, and increased number of tumour-infiltrating T-regulatory cells in the peripheral blood group, may impair the GvL effect mediated by peripheral blood T cells in our tumour model.

Despite the naïve phenotype of cord blood T cells, we observed a similar percentage of central memory and effector memory $CD8^+$ T cells in the cord blood and peripheral blood TILs. Interestingly, circulating cord blood T cells remained naive, unlike the circulating peripheral blood T cells, which were found to have an increased percentage of effector memory T cells, compared with peripheral blood TILs. This confirms that naïve cord blood T cells mediate anti-tumour responses by rapidly undergoing memory-effector differentiation within the tumour microenvironment. However, circulating cord blood T cells continue to retain naïvety; an observation that complements the absence of xeno-reactivity in the cord blood group.

Peripheral blood T cells mediate xeno-reactivity via murine MHC Class I and II with a predominantly effector-memory phenotype (King *et al.,* 2009; Ali *et al.,* 2012; Covassin *et al.,* 2011). However, naïve T cells not only require MHC, but also require priming by co-stimulatory and differentiation signals for memory-effector differentiation (Janeway, 2005). These complex interactions for memory-effector differentiation are mediated by human APCs. In humans, following T-cell replete CBT, cord blood T cells undergo rapid memory-effector differentiation (Chiesa *et al.,* 2012). However, a lack of human APCs in our model, and the inability of naïve human T cells to interact with resting murine APCs (Lucas, *et al.,* 1995), or the defective murine APC in this model with NOD background (Shultz, *et al.,* 1995), may inhibit memory-effector differentiation. Thus, in the absence of adequate priming, circulating naïve cord blood T cells may become anergic (Janeway, 2005), and therefore, fail to cause xeno-reactivity.

In summary, cord blood T cells mediate more potent anti-tumour effects than adult T cells through the enhanced recruitment of naïve cord blood T cells (particularly cord blood $CD8^+$ T cells), prompt induction of memory-effector differentiation and gain of cytotoxic-effector functions in the tumour microenvironment. Delayed infiltration of peripheral blood T cells in the tumour and skewing of the intra-tumoural balance toward $CD4^+$ T cells, in particular suppressive T-regulatory and Th2 TILs, may impair the GvL effect mediated by peripheral

blood T cells in this model. Broadly, this work indicates that foetal-derived (ready-to-learn) cord blood T cells mediate enhanced allo-reactivity compared with adult-derived (partially-educated) peripheral blood T cells. The preferential tumour-homing of cord blood T cells compared to the peripheral blood T cells, is particularly interesting. Not only do these naïve cord blood T cells infiltrate the tumour, they also differentiate into memory-effectors and become activated. Although, manipulated tumours have been shown to attract and activate naïve $CD8^+$ T cells in the tumour microenvironment (Yu *et al.,* 2004; Schrama *et al.,* 2001; Kim *et al.,* 2004), the role of chemokine receptors in the rapid migration of T cells to the un-manipulated tumour remains to be elucidated.

The mechanisms of 1) recruitment of cord blood T cells to the tumour, 2) preferential proliferation of cord blood T cells in the tumour microenvironment, and 3) enhanced anti-tumour effects in this model remain to be elucidated and will require further work. Cord blood $CD8^+$ T cells are predominantly $CCR7^{high}$, compared with a mixture of $CCR7^{high}$ and $CCR7^{low}$ $CD8^+$ T cells in the peripheral blood. The $CD8^+$ T cells homing the tumour, in both the cord blood and peripheral blood group, were $CCR7^{high}$, whereas $CCR7^{low}$ $CD8^+$ T cells from the peripheral blood group remained in circulation. It is, therefore, possible that the high expression of CCR7 in cord blood $CD8^+$ T cells may facilitate enhanced tumour homing.

In summary, cord blood T cells mediate more potent anti-tumour effects than adult T cells in this B-cell lymphoma model. The findings that cord blood T cells mediated an enhanced GvL effect without exhibiting xeno-reactivity, parallel the clinical situation in humans, where CBT may exert a powerful GvL effect, but with reduced rates of GvHD. Our work supports the omission or minimization of serotherapy from the preparative regimens of CBT recipients for high-risk haematological malignancies to enhance T-cell mediated GvL. Whilst we recognize the limitations in extrapolating from this model system to the clinical setting, and that following cord blood grafts, other immune cells, such as natural killer cells, may also mediate a GvL effect (Gardiner *et al.,* 1998; Xing *et al.,* 2010). These findings nonetheless provide a mechanistic insight into how cord blood T cells may mediate the potent GvL effects observed after T-cell-replete CBT.

Model of GvL after cord blood transplantation

My work suggests that cord blood T cells mediate enhanced anti-leukaemic responses in this lymphoblastoid tumour model. Majority of the tumour-infiltrating cord blood T cells were CD8+ T cells and tumour-infiltrating cord blood T cells underwent rapid T-cell

differentiation with Tc1-Th1 bias. Therefore, an important question is the role of cord blood CD4+ T cells play in mediating the enhanced GvL effect. Effective antigen presentation is required for GvL effect. Lymphoblastoid cells have antigen presenting ability similar to mature dendritic cells **(**Issekutz *et al*., 1982**)**. Therefore, a standard model of GvL similar to that of chronic myeloid leukaemia is a possibility [Figure 87]. This means that the allogeneic interaction between the TCR on naïve cord blood CD4+ T cells and MHC Class II on tumour cells may activate the lymphoblastoid cells to efficiently present Class I antigens. The presentation of Class I antigens may activate the naïve cord blood CD8+ T cells leading to memory-effector differentiation, and hence cytotoxicity. Although, tumour infiltrating cord blood CD4+ T cells were low in numbers, they were all Th1-biased. The extent of contribution of CD4+ T cells in mediating GvL was not tested in this model.

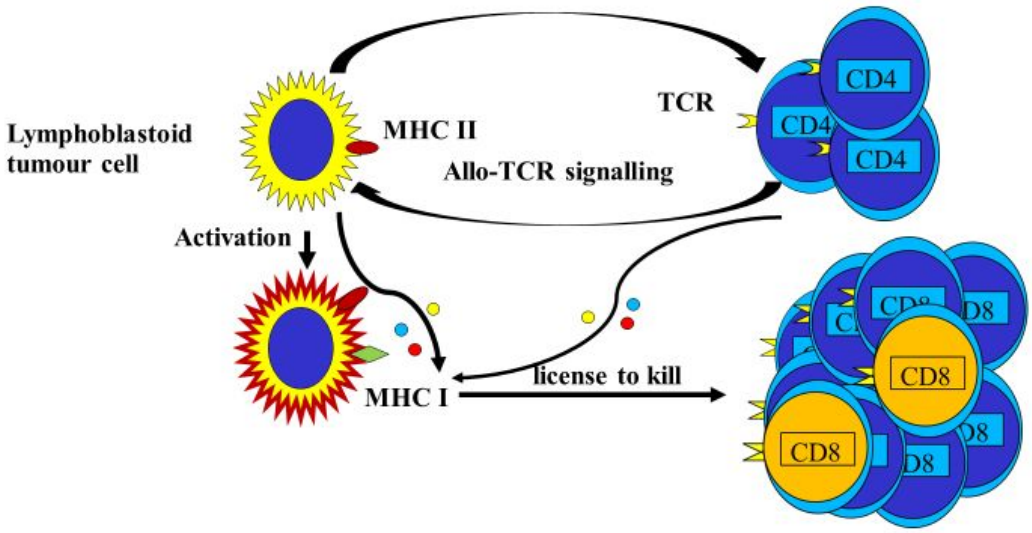

Figure 87: Mechanism of GvL in this tumour model is shown. Allogeneic cord blood CD4+ T cells interact with MHC Class II molecules on lymphoblastoid cells. This interaction activates lymphoblastoid cells leading to efficient presentation of MHC Class I molecules, and hence leading to activation of CD8+ T cells leading to differentiation and anti-tumour response. (red, blue and yellow circle represent cytokines, blue T cells are naïve and orange T cells are memory/effectors)

Therefore, another model where direct interaction between MHC Class I and naïve cord blood CD8+ T cells is also a possibility. To test the contribution of CD4+ and CD8+ T cells in mediating GvL effect, one would have to perform experiments with population of CD4+ T cells and CD8+ T cells injected in separate groups of mice with appropriate control mice, and

thus answer an important question whether CD8+ T cells can mediate GvL in the absence of CD4+ T cells.

Summary

Unrelated CBT without *in vivo* T-cell depletion is increasingly used to treat high-risk haematological malignancies. Following T-cell-replete CBT, naïve cord blood T cells undergo rapid peripheral expansion with memory-effector differentiation. Emerging data suggest that unrelated CBT, particularly in the context of HLA-mismatch and a T-cell-replete graft may reduce leukaemic relapse. To study the role of cord blood T cells in mediating graft-versus-tumour responses, and elucidate the underlying immune mechanisms for this, the ability of HLA-mismatched cord blood and adult peripheral blood T cells to eliminate Epstein-Barr virus (EBV)-driven human B-cell lymphoma was compared in a xenogeneic NOD/SCID/IL2rg^{null} mouse model. Cord blood T cells mediated enhanced tumour rejection compared to equal numbers of peripheral blood T cells, leading to improved survival in the cord blood group ($p<0.0003$). This anti-tumour effect was mediated by allo-reactive rather than EBV-specific T cells, as shown by comparing lymphoma autologous cord blood T cells with allogeneic ones. Analysis of tumour-infiltrating lymphocytes demonstrated that cord blood T cells mediated this enhanced anti-tumour effect by the rapid infiltration of the tumour with CCR7^{+} CD8^{+} T cells, and the prompt induction of cytotoxic CD8^{+} and CD4^{+} Th1 T cells in the tumour microenvironment. In contrast, in the peripheral blood group, this anti-lymphoma effect is impaired because of the delayed tumoural infiltration of peripheral blood T cells, and a relative bias toward suppressive Th2 and T-regulatory cells. Our data suggest that, despite being naturally programmed toward tolerance, reconstituting cord blood T cells may provide superior Tc1-Th1 anti-tumour effects against high-risk haematological malignancies.

Clinical applications

Upregulated TCR signals in cord blood $CD4^+$ T cells may mediate enhanced immune reconstitution and potent allo-reactivity, and hence a robust anti-leukaemic effect, as demonstrated by our work. We have shown that cord blood transplantation without serotherapy mediates a robust anti-leukaemic effect against acute myeloid leukaemia (Admiraal *et al.,* 2016). This study consolidates the idea of enhanced GvL and antiviral responses after cord blood transplant compared to an adult graft. I, therefore, envisage a retrospective European society of blood and marrow transplantation (EBMT) study to assess the role of cord blood transplantation in high-risk myeloid malignancies. It will be interesting to study the effect of *in vivo* depletion on the risk of relapse in high-risk myeloid malignancies.

Vaccination for acute myeloid leukaemia

Cord blood transplantation provides a platform for naïve and foetal T-cell therapy. Despite robust GvL effects, mediated by cord blood T cells, a substantial proportion of patients (30 to 40%) relapse after cord blood transplantation. Therefore, a cord blood transplant platform could be explored to enhance GvL using vaccination strategies. One possibility is to develop cord dendritic cell-AML tumour hybridoma vaccine, as described below.

The supernatant of cord blood washings and cord blood bags after infusion of the product contains 10 to 15 million cells. These cells could be isolated, and adherent cells cultured with granulocyte-macrophage colony stimulating factor GMCSF), IL-4, and TNF-α. The dendritic cells and AML preparations would be analyzed using immune-cytochemical staining and co-cultured with polyethylene glycol to generate DC/AML fusions, as previously described (Rosenblatt *et al.,* 2011). The irradiated dendritic cell-AML hybridoma vaccine could be injected one month after a cord blood transplant to enhance the GvL response. The vaccine induced immunologic response would be serially studied in the pre- and post-vaccination samples.

Check point blockade

Relapse of leukaemia after HCT may occur because of immune escape, and immune-checkpoint inhibitory pathways may play a role in this. Immune-checkpoint receptors, such as CTLA-4 and PD-1 have been shown to play a crucial role in tumour evasion of the donor

immune system (Davids *et al.,* 2016). The role of a checkpoint blockade in relapse following cord blood transplant has not been explored.

Off the shelf cord blood CAR T cells

CAR T-cell technology has exploded in recent years. The technology has been a great success in $CD19^+$ B-cell acute lymphoblastic leukaemia. However, autologous CAR T cells are not possible in all patients, and such patients could benefit from 'off the shelf' allogeneic CAR T cells. Off the shelf allogeneic CAR T cells, derived from peripheral lymphocytes have been manufactured using multiplex editing technology such as transcription activator–like effector nuclease (TALEN), as previously described (Poirot *et al.,* 2015; Qasim*., et al* 2017). It is likely that cord blood CAR T cells may mediate potent effects compared to peripheral blood CAR T cells, because of their proliferative potential. Off the shelf cord blood CAR T cells targeting antigens overexpressed in high risk malignancies is another potential area of development in the near future.

Relevance to Health and Disease in the Neonate

The ability of cord blood T cells, particularly CD4+ T cells, to proliferate rapidly in the post-transplant setting, converting from naïve to functional memory/effector cells with anti-viral and anti-leukaemic properties may have relevance to health and disease in the neonatal period. Clearly the ability to deal effectively with viruses in this period is vital to the newborn. However, new-borns are susceptible to viral infections. Is there a period of immune compromise during the switch over from foetal to adult lymphoid program? Could these unique properties be deleterious to the child if such cells persist in the post-natal environment i.e. lead to increased autoimmunity or diseases such as necrotising enterocolitis. The findings of these unique properties of feotal derived cord blood $CD4^+$ lymphocytes warrant further study away from the transplant setting in the neonatal period.

References

Acuto O, Michel F. CD28-mediated co-stimulation: a quantitative support for TCR signalling. Nat Rev Immunol. 2003 Dec;3 (12):939-51.

Admiraal R, Chiesa R, Lindemans CA, Nierkens S, Bierings MB, Versluijs AB, Hiwarkar P, Furtado Silva JM, Veys P, Boelens JJ. Leukemia-free survival in myeloid leukemia, but not in lymphoid leukemia, is predicted by early CD4+ reconstitution following unrelated cord blood transplantation in children: a multicenter retrospective cohort analysis. Bone Marrow Transplant. 2016 Oct;51(10):1376-1378.

Agliano A, Martin-Padura I, Mancuso P, Marighetti P, Rabascio C, Pruneri G, Shultz LD, Bertolini F. Human acute leukemia cells injected in NOD/LtSz-scid/IL-2Rgamma null mice generate a faster and more efficient disease compared to other NOD/scid-related strains. Int.J.Cancer. 2008;123:2222–2227.

Aldenhoven M, Jones SA, Bonney D, Borrill RE, Coussons M, Mercer J, Bierings MB, Versluys B, van Hasselt PM, Wijburg FA, van der Ploeg AT, Wynn RF, Boelens JJ. Hematopoietic cell transplantation for mucopolysaccharidosis patients is safe and effective: results after implementation of international guidelines. Biol Blood Marrow Transplant. 2015 Jun;21(6):1106-9.

Ali N, Flutter B, Sanchez Rodriguez R, Sharif-Paghaleh E, Barber LD, Lombardi G, Nestle FO. Xenogeneic graft-versus-host-disease in NOD-scid IL-2Rγnull mice display a T-effector memory phenotype. PLoS One. 2012;7(8):e44219.

Appelbaum FR. Haematopoietic cell transplantation as immunotherapy. Nature. 2001;411:385-389.

Apperley J, Carreras E, Gluckman E, Masszi T. The EBMT Handbook. In: Eliane Gluckman eds. Choice of the donor according to HLA typing and stem cell source. Sources and procurement of stem cells EBMT handbook; 2012: 90-107.

Apperley JF, Mauro FR, Goldman JM, et al. Bone marrow transplantation for chronic myeloid leukaemia in first chronic phase: importance of a graft-versus-leukaemia effect. Br J Haematol.1988;69:239-245.

Aringer, M. T lymphocyte activation--an inside overview. Acta Med Austriaca,2002; 29, 7-13.

Aruga A, Aruga E, Tanigawa K, Bishop DK, Sondak VK, Chang AE. Type 1 versus type 2 cytokine release by Vbeta T cell subpopulations determines in vivo antitumor reactivity: IL-10 mediates a suppressive role. J Immunol. 1997 Jul 15;159(2):664-73.

Bach FH, Albertini RJ, Joo P, Anderson JL & Bortin MM. Bone-marrow transplantation in a patient with the Wiskott-Aldrich syndrome. Lancet, ii, 1968;1364–1366.

Bachireddy P, Hainz U, Rooney M, Pozdnyakova O, Aldridge J, Zhang W, Liao X, Hodi FS, O'Connell K, Haining WN, Goldstein NR, Canning CM, Soiffer RJ, Ritz J, Hacohen N, Alyea EP 3rd, Kim HT, Wu CJ. Reversal of in situ T-cell exhaustion during effective human antileukemia responses to donor lymphocyte infusion. Blood. 2014 Feb 27;123(9):1412-21.

Bacigalupo A, Lamparelli T, Bruzzi P, et al. Antithymocyte globulin for graft-vs-host disease prophylaxis in transplants from unrelated donors: 2 randomized studies from Gruppo Italiano Trapianti Midollo Osseo (GITMO). Blood 2001;98(10):2942-2947.

Balagopalan L, Coussens NP, Sherman E, Samelson LE, Sommers CL. The LAT story: a tale of cooperativity, coordination, and choreography. Cold Spring Harb Perspect Biol. 2010 Aug;2(8):a005512.

Ballen KK, Gluckman E, Broxmeyer HE. Umbilical cord blood transplantation: the first 25 years and beyond. Blood. 2013 Jul 25;122(4):491-8.

Baran J, Kowalczyk D, Ozóg M, Zembala M. Three-color flow cytometry detection of intracellular cytokines in peripheral blood mononuclear cells: comparative analysis of phorbol myristate acetate-ionomycin and phytohemagglutinin stimulation. Clin Diagn Lab Immunol. 2001 Mar;8(2):303-13.

Barker JN, Fei M, Karanes C, et al; RCI BMT 05-DCB Protocol Team. Results of a prospective multicentre myeloablative double-unit cord blood transplantation trial in adult patients with acute leukaemia and myelodysplasia. Br J Haematol 2015;168(3):405-412.

Barker JN, Weisdorf DJ, DeFor TE, Blazar BR, McGlave PB, Miller JS, et al. Transplantation of 2 partially HLA-matched umbilical cord blood units to enhance engraftment in adults with hematologic malignancy. Blood. 2005;105(3):1343–7.

Barnes DWH & LoutitJF. What is the recovery factor in spleen? Nucleonics 1954;12, 68–71.

Barnes DWH, Corp MJ, Loutit JF & Neal FE. Treatment of murine leukaemia with X-rays and homologous bone marrow. BMJ 1956;2, 626–627.

Barrett AJ. Mechanisms of the graft-versus-leukemia reaction. Stem Cells. 1997;15:248-258.

Bender J, Mitchell T, Kappler J & Marrack P. CD4+ T-cell division in irradiated mice requires peptides distinct from those responsible for thymic selection. J. Exp. Med. 1999; 190, 367–374.

Berger F, Paulmurugan R, Bhaumik S & Gambhir SS. Uptake kinetics and biodistribution of 14C-D-luciferin--a radiolabeled substrate for the firefly luciferase catalyzed bioluminescence

reaction: impact on bioluminescence based reporter gene imaging. Eur J Nucl Med Mol Imaging, 2008;35, 2275-2285.

Berger M, Lanino E, Cesaro S, Zecca M, Vassallo E, Faraci M, De Bortoli M, Barat V, Prete A, Fagioli F. Feasibility and Outcome of Haploidentical Hematopoietic Stem Cell Transplantation with Post-Transplant High-Dose Cyclophosphamide for Children and Adolescents with Hematologic Malignancies: An AIEOP-GITMO Retrospective Multicenter Study. Biol Blood Marrow Transplant. 2016 Feb 6.

Bertaina A, Merli P, Rutella S, Pagliara D, Bernardo ME, Masetti R, Pende D, Falco M, Handgretinger R, Moretta F, Lucarelli B, Brescia LP, Li Pira G, Testi M, Cancrini C, Kabbara N, Carsetti R, Finocchi A, Moretta A, Moretta L, Locatelli F. HLA-haploidentical stem cell transplantation after removal of αβ+ T and B cells in children with nonmalignant disorders. Blood. 2014 Jul 31;124(5):822-6.

Boelens JJ. The power of cord blood cells. Blood. 2016 Jun 30;127(26):3302-3.

Bolstad BM, Collin F, Brettschneider J, Simpson K, Cope L, Irizarry RA, and Speed TP. (2005) Quality Assessment of Affymetrix GeneChip Data in Bioinformatics and Computational Biology Solutions Using R and Bioconductor. Gentleman R, Carey V, Huber W, Irizarry R, and Dudoit S. (Eds.), Springer, New York.

Boyman O, Létourneau S, Krieg C, Sprent J. Homeostatic proliferation and survival of naïve and memory T cells. Eur J Immunol. 2009 Aug;39(8):2088-94.

Brocker T. Survival of mature CD4 T lymphocytes is dependent on major histocompatibility complex class II-expressing dendritic cells. J Exp Med. 1997 Oct 20;186(8):1223-32.

Brownlie RJ, Zamoyska R. T cell receptor signalling networks: branched, diversified and bounded. Nat Rev Immunol. 2013 Apr;13(4):257-69.

Broxmeyer HE, Douglas GW, Hangoc G, Cooper S, Bard J, English D, Arny M, Thomas L & Boyse EA. Human umbilical cord blood as a potential source of transplantable hematopoietic stem/progenitor cells. Proceedings of the National Academy of Sciences of the United States of America, 1989;86, 3828–3832.

Brunstein CG, Fuchs EJ, Carter SL, et al; Blood and Marrow Transplant Clinical Trials Network. Alternative donor transplantation after reduced intensity conditioning: results of parallel phase 2 trials using partially HLA-mismatched related bone marrow or unrelated double umbilical cord blood grafts. Blood. 2011;118(2):282-288.

Buckner CD, Epstein RB, Rudolph RH, Clift RA, Storb R & Thomas ED. Allogeneic marrow engraftment following whole body irradiation in a patient with leukemia. Blood, 1970;35, 741–750.

Butz EA & Bevan MJ. Massive expansion of antigen-specific CD8+ T cells during an acute virus infection. Immunity 1998:8, 167–175.

Campana D, Janossy G, Coustan-Smith E, Amlot PL, Tian WT, Ip S, Wong L. The expression of T cell receptor-associated proteins during T cell ontogeny in man. J Immunol. 1989 Jan 1;142(1):57-66.

Cardoso AA, Schultze JL, Boussiotis VA, et al. Pre-B acute lymphoblastic leukemia cells may induce T-cell anergy to alloantigen. Blood 1996;88:41-48.

Champlin RE, Passweg JR, Zhang MJ, et al. T-cell depletion of bone marrow transplants for leukemia from donors other than HLA-identical siblings: advantage of T-cell antibodies with narrow specificities. Blood. 2000;95:3996–4003.

Chandran S, Williams S. & Denmeade S. Extended-release PEG-luciferin allows for long-term imaging of firefly luciferase activity in vivo. Luminescence, 2009;24, 35-38.

Chiesa R, Gilmour K, Qasim W, Adams S, Worth AJ, Zhan H, Montiel-Equihua CA, Derniame S, Cale C, Rao K, Hiwarkar P, Hough R, Saudemont A, Fahrenkrog CS, Goulden N, Amrolia PJ, Veys P. Omission of in vivo T-cell depletion promotes rapid expansion of naïve CD4+ cord blood lymphocytes and restores adaptive immunity within 2 months after unrelated cord blood transplant. Br J Haematol. 2012 Mar;156(5):656-66.

Cho BK, Rao VP, Ge Q, Eisen HN, Chen J. Homeostasis-stimulated proliferation drives naive T cells to differentiate directly into memory T cells. J Exp Med. 2000 Aug 21;192(4):549-56.

Cieri N, Oliveira G, Greco R, Forcato M, Taccioli C, Cianciotti B, Valtolina V, Noviello M, Vago L, Bondanza A, Lunghi F, Marktel S, Bellio L, Bordignon C, Bicciato S, Peccatori J, Ciceri F, Bonini C. Generation of human memory stem T cells after haploidentical T-replete hematopoietic stem cell transplantation. Blood. 2015 Apr 30;125(18):2865-74.

Clift RA, Buckner CD, Thomas ED, Doney K, Fefer A, Neiman PE, Singer J, Sanders J, Stewart P, Sullivan KM, Deeg J & Storb R. Treatment of chronic granulocytic leukaemia in chronic phase by allogeneic marrow transplantation. Lancet, ii, 1982;621–623.

Collier FM, Tang ML, Martino D, Saffery R, Carlin J, Jachno K, Ranganathan S, Burgner D, Allen KJ, Vuillermin P, Ponsonby AL. The ontogeny of naïve and regulatory CD4(+) T-cell subsets during the first postnatal year: a cohort study. Clin Transl Immunology. 2015 Mar 27;4(3):e34.

Collins RH, Shpilberg O, Drobyski WR, et al. Donor leukocyte infusions in 140 patients with relapsed malignancy after allogeneic bone marrow transplantation. J Clin Oncol 1997;15:433-444.

Comoli P, Labirio M, Basso S, et al. Infusion of autologous Epstein-Barr virus (EBV)-specific cytotoxic T cells for prevention of EBV-related lymphoproliferative disorder in solid organ transplant recipients with evidence of active virus replication. Blood 2002; 99: 2592–2598.

Contag PR, Olomu IN, Stevenson DK & Contag CH. Bioluminescent indicators in living mammals. Nat Med, 1998;4, 245-247.

Copley MR, Babovic S, Benz C, Knapp DJ, Beer PA, Kent DG, Wohrer S, Treloar DQ, Day C, Rowe K, Mader H, Kuchenbauer F, Humphries RK, Eaves CJ. The Lin28b-let-7-Hmga2 axis determines the higher self-renewal potential of fetal haematopoietic stem cells. Nat Cell Biol. 2013 Aug;15(8):916-25.

Covassin L, Laning J, Abdi R, Langevin DL, Phillips NE, Shultz LD, Brehm MA. Human peripheral blood CD4 T cell-engrafted non-obese diabetic-scid IL2rγ(null) H2-Ab1 (tm1Gru) Tg (human leucocyte antigen D-related 4) mice: a mouse model of human allogeneic graft-versus-host disease. Clin Exp Immunol. 2011 Nov;166(2):269-80.

Croft M. Co-stimulatory members of the TNFR family: keys to effective T-cell immunity? Nat Rev Immunol. 2003 Aug;3 (8):609-20. Review.

Dardalhon V, Jaleco S, Kinet S, Herpers B, Steinberg M, Ferrand C, Froger D, Leveau C, Tiberghien P, Charneau P, Noraz N, Taylor N. IL-7 differentially regulates cell cycle progression and HIV-1-based vector infection in neonatal and adult CD4+ T cells. Proc Natl Acad Sci U S A. 2001 Jul 31;98(16):9277-82.

Das J, Ho M, Zikherman J, Govern C, Yang M, Weiss A, Chakraborty AK, Roose JP. Digital signaling and hysteresis characterize ras activation in lymphoid cells. Cell. 2009 Jan 23;136(2):337-51.

Dausset J. Iso-leuco-anticorps. Acta Haematologica, 1958;20, 156–166.

Davids MS, Kim HT, Bachireddy P, Costello C, Liguori R, Savell A, Lukez AP, Avigan D, Chen YB, McSweeney P, LeBoeuf NR, Rooney MS, Bowden M, Zhou CW, Granter SR, Hornick JL, Rodig SJ, Hirakawa M, Severgnini M, Hodi FS, Wu CJ, Ho VT, Cutler C, Koreth J, Alyea EP, Antin JH, Armand P, Streicher H, Ball ED, Ritz J, Bashey A, Soiffer RJ; Leukemia and Lymphoma Society Blood Cancer Research Partnership. Ipilimumab for Patients with Relapse after Allogeneic Transplantation. N Engl J Med. 2016 Jul 14;375(2):143-53.

De Waele M, Foulon W, Renmans W, et al. Hematologic values and lymphocyte subsets in fetal blood. Am J Clin Pathol. 1988;89: 742-746.

deKoning J, van Bekkum DW, Dicke KA, Dooren LJ, Radl J & van Rood JJ. Transplantation of bone-marrow cells and fetal thymus in an infant with lymphopenic immunological deficiency. Lancet, i, 1969;1223–1227.

Dermime S, Mavroudis D, Jiang YZ, et al. Immune escape from a graft-versus-leukemia effect may play a role in the relapse of myeloid leukemias following allogeneic bone marrow transplantation. Bone Marrow Transplant 1997;19:989-999.

Deshpande P, Cavanagh MM, Le Saux S, Singh K, Weyand CM, Goronzy JJ. IL-7- and IL-15-mediated TCR sensitization enables T cell responses to self-antigens. J Immunol. 2013 Feb 15;190(4):1416-23.

Di Terlizzi S, Zino E, Mazzi B, et al. Therapeutic and diagnostic applications of minor histocompatibility antigen HA-1 and HA-2 disparities in allogeneic hematopoietic stem cell transplantation: a survey of different populations. Biol Blood Marrow Transplant. 2006;12:95-101.

Do JS, Min B. Differential requirements of MHC and of DCs for endogenous proliferation of different T-cell subsets in vivo. Proc Natl Acad Sci U S A (2009) 106(48):20394–8.

Dunn, G. P., Old, L. J. & Schreiber, R. D. The immunobiology of cancer immunosurveillance and immunoediting. Immunity. 2004 21, 137–148.

Eapen M, Rubinstein P, Zhang MJ, Stevens C, Kurtzberg J, Scaradavou A, Loberiza FR, Champlin RE, Klein JP, Horowitz MM, Wagner JE. Outcomes of transplantation of unrelated donor umbilical cord blood and bone marrow in children with acute leukaemia: a comparison study. Lancet. 2007 Jun 9;369(9577):1947-54.

Elmaagacli AH, Beelen DW, Trenn G, Schmidt O, Nahler M, Schaefer UW. Induction of a graft-versus-leukemia reaction by cyclosporin A withdrawal as immunotherapy for leukemia relapsing after allogeneic bone marrow transplantation. Bone Marrow Transplant. 1999;23(8):771.

Epstein RB, Storb R, Clift RA & Thomas ED. Transplantation of stored allogeneic bone marrow in dogs selected by histocompatibility typing. Transplantation, 1969;8, 496–501.

Ernst B, Lee DS, Chang JM, Sprent J & Surh CD. The peptide ligands mediating positive selection in the thymus control T-cell survival and homeostatic proliferation in the periphery. Immunity 11, 173–181 (1999).

Fallen PR, McGreavey L, Madrigal JA, Potter M, Ethell M, Prentice HG, Guimarães A, Travers PJ. Factors affecting reconstitution of the T cell compartment in allogeneic haematopoietic cell transplant recipients. Bone Marrow Transplant. 2003 Nov;32(10):1001-14.

Feeney ME, Draenert R, Roosevelt KA, et al. Reconstitution of virus-specific CD4 proliferative responses in pediatric HIV-1 infection. J Immunol. 2003;171:6968–75.

Fefer A, Buckner CD, Clift RA, Fass L, Lerner KG, Mickelson EM, Neiman P, Rudolph R, Storb R & Thomas ED. Marrow grafting in identical twins with hematologic malignancies. Transplantation Proceedings, 1973;5, 927–931.

Ferreira C, Barthlott T, Garcia S, Zamoyska R & Stockinger B. Differential survival of naive CD4 and CD8 T cells. J. Immunol. 2000; 165, 3689–3694.

Fichtelius KE. The gut epithelium: a first level lymphoid organ? Exp Cell Res 1967;49:87.

Ford CE, Hamerton JL, Barnes DWH & LoutitJF. Cytological identification of radiation-chimaeras. Nature 1956;177, 452–454.

Förster R, Schubel A, Breitfeld D, et al. CCR7 coordinates the primary immune response by establishing functional microenvironments in secondary lymphoid organs. Cell. 1999 Oct 1;99(1):23-33.

Foster AE, Dotti G, Lu A, Khalil M, Brenner MK, Heslop HE, Rooney CM & Bollard CM. Antitumor activity of EBV-specific T lymphocytes transduced with a dominant negative TGF-beta receptor. J Immunother, 2008;31,500-505.

Fowler DH, Breglio J, Nagel G, Hirose C, Gress RE. Allospecific CD4+, Th1/Th2 and CD8+, Tc1/Tc2 populations in murine GVL: type I cells generate GVL and type II cells abrogate GVL. Biol Blood Marrow Transplant, 2 (1996), pp. 118–125.

Fujimaki K, Maruta A, Yoshida M, Kodama F, Matsuzaki M, Fujisawa S, Kanamori H, Ishigatsubo Y. Immune reconstitution assessed during five years after allogeneic bone marrow transplantation. Bone Marrow Transplant. 2001 Jun;27(12):1275-81.

Fulton RB, Hamilton SE, Xing Y, Best JA, Goldrath AW, Hogquist KA, Jameson SC. The TCR's sensitivity to self peptide-MHC dictates the ability of naive CD8(+) T cells to respond to foreign antigens. Nat Immunol. 2015 Jan;16(1):107-17.

Gale RP, Horowitz MM, Ash RC, Champlin RE, Goldman JM, Rimm AA, Ringdén O, Stone JA, Bortin MM. Identical-twin bone marrow transplants for leukemia. Ann Intern Med. 1994;120(8):646.

Galon J, Costes A, Sanchez-Cabo F, Kirilovsky A, Mlecnik B, Lagorce-Pages C, Tosolini M, Camus M, Berger A, Wind P, Zinzindohoue F, Bruneval P, Cugnenc PH, Trajanoski Z, Fridman WH, Pages F. Type, density, and location of immune cells within human colorectal tumors predict clinical outcome. Science. 2006;313:1960–1964.

Gans H, Yasukawa L, Rinki M, et al. Immune responses to measles and mumps vaccination of infants at 6, 9, and 12 months. J Infect Dis. 2001;184:817–26.

Gardiner CM, Meara AO, Reen DJ. Differential cytotoxicity of cord blood and bone marrow-derived natural killer cells. Blood 1998;91(1):207-213.

Gasparoni A, Ciardelli L, Avanzini A, Castellazzi AM, Carini R, Rondini G, Chirico G. Age-related changes in intracellular TH1/TH2 cytokine production, immunoproliferative T lymphocyte response and natural killer cell activity in newborns, children and adults. Biol Neonate. 2003;84(4):297-303.

Gatti RA, Meuwissen HJ, Allen HD, Hong R & Good RA. Immunological reconstitution of sex-linked lymphopenic immunological deficiency. Lancet, ii, 1968;1366–1369.

Ge Q, Hu H, Eisen HN, Chen J. Different contributions of thymopoiesis and homeostasis-driven proliferation to the reconstitution of naive and memory T cell compartments. Proc Natl Acad Sci U S A. 2002 Mar 5;99(5):2989-94.

Gianni AM, Siena S, Bregni M, Tarella C, Stern AC, Pileri A & Bonadonna G. Granulocyte-macrophage colony stimulating factor to harvest circulating haemopoietic stem cells for autotransplantation. Lancet, ii, 1989;580–585.

Gibbons DL, Haque SF, Silberzahn T, Hamilton K, Langford C, Ellis P, Carr R, Hayday AC. Neonates harbour highly active gammadelta T cells with selective impairments in preterm infants. Eur. J. Immunol. 2009; 39, 1794–1806.

Gibbons D, Fleming P, Virasami A, Michel ML, Sebire NJ, Costeloe K, Carr R, Klein N, Hayday A. Interleukin-8 (CXCL8) production is a signatory T cell effector function of human newborn infants. Nat. Med. 2014; 20, 1206–1210.

Gluckman E, Broxmeyer HE, Auerbach AD, Friedman HS, Douglas GW, Devergie A, Esperou H, Thierry D, Socie´ G, Lehn P, Cooper S, English D, Kurtzberg J, Bard J & Boyse EA. Hematopoietic reconstitution in a patient with Fanconi's anemia by means of umbilical-cord blood from an HLA-identical sibling. New England Journal of Medicine, 1989;321, 1174–1178.

Gluckman E. Choice of the donor according to HLA typing and stem cell source. EBMT Handbook 6th Edition 2012; Chapter 6:93.

Goldman JM, Gale RP, Horowitz MM, et al. Bone marrow transplantation for chronic myelogenous leukemia in chronic phase: increased risk for relapse associated with T-cell depletion. Ann Intern Med. 1988;108:806-814.

Goldrath AW, Bevan MJ. Selecting and maintaining a diverse T-cell repertoire. Nature. 1999;402:255–262.

Gooden MJ, de Bock GH, Leffers N, Daemen T, Nijman HW. The prognostic influence of tumour-infiltrating lymphocytes in cancer: a systematic review with meta-analysis. Br J Cancer. 2011 Jun 28;105(1):93-103.

Goulmy E, Schipper R, Pool J, Blokland E, Falkenburg JH, Vossen J, Gratwohl A, Vogelsang GB, van Houwelingen HC, van Rood JJ. Mismatches of minor histocompatibility antigens between HLA-identical donors and recipients and the development of graft-versus-host disease after bone marrow transplantation. N Engl J Med. 1996 Feb 1;334(5):281-5.

Grewal SS, Barker JN, Davies SM, Wagner JE. Unrelated donor hematopoietic cell transplantation: marrow or umbilical cord blood? Blood. 2003 Jun 1;101(11):4233-44.

Guimond M, Veenstra RG, Grindler DJ, Zhang H, Cui Y, Murphy RD, Kim SY, Na R, Hennighausen L, Kurtulus S, Erman B, Matzinger P, Merchant MS, Mackall CL. Interleukin 7 signaling in dendritic cells regulates the homeostatic proliferation and niche size of CD4+ T cells. Nat Immunol. 2009 Feb;10 (2):149-57.

Ganusov VV. Discriminating between different pathways of memory CD8+ T cell differentiation. J Immunol. 2007 Oct 15;179(8):5006-13.

Gutman JA, Turtle CJ, Manley TJ, Heimfeld S, Bernstein ID, Riddell SR, Delaney C. Single-unit dominance after double-unit umbilical cord blood transplantation coincides with a specific CD8+ T-cell response against the nonengrafted unit. Blood. 2010 Jan 28;115(4):757-65.

Hakim FT, Cepeda R, Kaimei S, et al. Constraints on CD4 recovery postchemotherapy in adults: Thymic insufficiency and apoptotic decline of expanded peripheral CD4 cells. Blood 1997; 90: 3789–3798.

Hamilton SE, Wolkers MC, Schoenberger SP, Jameson SC. The generation of protective memory-like CD8+ T cells during homeostatic proliferation requires CD4+ T cells. Nat Immunol. 2006;7:475–481.

Harrison DE, Zhong RK, Jordan CT, Lemischka IR, Astle CM. Relative to adult marrow, fetal liver repopulates nearly five times more effectively long-term than short-term. Exp Hematol. 1997;25:293.

Haynes BF, Singer KH, Denning SM, Martin ME. Analysis of expression of CD2, CD3 and T cell antigen receptor molecules during early human fetal thymic development. J Immunol 1988;141:3776-3784.

Haynes BF, Denning SM, Singer KH, Kurtzberg J. Ontogeny of T cell precursors: a model for the initial stages of human T cell development. Immunol Today 1989;10:87.

Havran WL, Allison JP. Developmentally ordered appearance of thymocytes expressing different T-cell antigen receptors. Nature. 1988;335:443.

Hebel K, Weinert S, Kuropka B, Knolle J, Kosak B, Jorch G, Arens C, Krause E, Braun-Dullaeus RC, Brunner-Weinzierl MC. $CD4^+$ T cells from human neonates and infants are poised spontaneously to run a nonclassical IL-4 program. J. Immunol. 2014 192, 5160–5170.

Henderson RA, Watkins SC, Flynn JL. Activation of human dendritic cells following infection with Mycobacterium tuberculosis. J Immunol. 1997;159:635–43.

Hennion-Tscheltzoff O, Leboeuf D, Gauthier SD, Dupuis M, Assouline B, Grégoire A, Thiant S, Guimond M. TCR triggering modulates the responsiveness and homeostatic proliferation of CD4+ thymic emigrants to IL-7 therapy. Blood. 2013 Jun 6;121(23):4684-93.

Hermann E, Truyens C, Alonso-Vega C, et al. Human fetuses are able to mount an adultlike CD8 T-cell response. Blood. 2002;100:2153–8.

Hobbs JR, Hugh-Jones K, Barrett AJ, Byrom N, Chambers D, Henry K, James DC, Lucas CF, Rogers TR, Benson PF, Tansley LR, Patrick AD, Mossman J, Young EP. Reversal of clinical features of Hurler's disease and biochemical improvement after treatment by bone-marrow transplantation. Lancet. 1981 Oct 3;2(8249):709-12.

Horowitz MM, Gale RP, Sondel PM, et al. Graft-versus-leukemia reactions after bone marrow transplantation. Blood 1990;75:555-562.

Hu HM, Urba WJ, Fox BA. Gene-modified tumor vaccine with therapeutic potential shifts tumor-specific T cell response from a type 2 to a type 1 cytokine profile. J Immunol 1998;161:3033–3041.

Hunder NN, Wallen H, Cao J, Hendricks DW, Reilly JZ, Rodmyre R, Jungbluth A, Gnjatic S, Thompson JA, Yee C. Treatment of metastatic melanoma with autologous CD4+ T cells against NY-ESO-1. N Engl J Med. 2008 Jun 19;358(25):2698-703.

Ikuta K, et al. A developmental switch in thymic lymphocyte maturation occurs at the level of the hematopoietic stem cells. Cell. 1990;62:863.

Jacobson LO, Marks EK, Robson MJ, Gaston EO & Zirkle RE. Effect of spleen protection on mortality following X-irradiation. J. Lab. Clin. Med. 1949;34, 1538–1543.

Jameson SC. T cell homeostasis: keeping useful T cells alive and live T cells useful. Semin Immunol. 2005 Jun;17(3):231-7. Review.

Janeway CA. Immunobiology 6th edition. In: T Cell-Mediated Immunity. New York and London: Garland Science; 2005: 319-366.

Johnson BD, Becker EE, Truitt RL. Graft-vs.-host and graft-vs.-leukemia reactions after delayed infusions of donor T-subsets. Biol Blood Marrow Transplant. 1999;5(3):123-32.

Johnson FL, Look AT, Gockerman J, Ruggiero MR, Dalla-Pozza L & Billings FT. Bone-marrow transplantation in a patient with sickle-cell anemia. New England Journal of Medicine, 1984;311, 780–783.

Johnson WE, Li C, Rabinovic A (2007) Adjusting batch effects in microarray expression data using empirical Bayes methods. Biostatistics 8: 118-127.

Juttner CA, To LB, Haylock DN, Dyson PG, Bradstock KF, Dale BM, Enno A, Sage RE, Szer J & Toogood IRG. Approaches to blood stem cell mobilisation: initial Australian clinical results. Bone Marrow Transplantation, 1990;5, 22–24.

Kagi D, Vignaux F,Ledermenn B, et al. Fas and perforin pathways as major mechanisms of T cell-mediated cytotoxicity.Science 1994; 265:528–530.

Kaminski BA, Kadereit S, Miller RE, Leahy P, Stein KR, Topa DA, Radivoyevitch T, Veigl ML, Laughlin MJ. Reduced expression of NFAT-associated genes in UCB versus adult CD4+ T lymphocytes during primary stimulation. Blood. 2003 Dec 15;102(13):4608-17.

Kanda J, Kaynar L, Kanda Y, Prasad VK, Parikh SH, Lan L, Shen T, Rizzieri DA, Long GD, Sullivan KM, Gasparetto C, Chute JP, Morris A, Winkel S, McPherson J, Kurtzberg J, Chao NJ, Horwitz ME. Pre-engraftment syndrome after myeloablative dual umbilical cord blood transplantation: risk factors and response to treatment. Bone Marrow Transplant. 2013 Jul;48(7):926-31.

Kassiotis, G., Zamoyska, R., and Stockinger, B. Involvement of avidity for major histocompatibility complex in homeostasis of naive and memory T cells. J. Exp. Med. 2003; 197, 1007–1016.

Kaye J. Niche marketing: regulation of the homeostasis of naive CD4+ T cells. Nat Immunol. 2009 Feb;10 (2):136-8.

Kedl RM, Rees WA, Hildeman DA, Schaefer B, Mitchell T, Kappler J, Marrack P. T cells compete for access to antigen-bearing antigen-presenting cells. J Exp Med. 2000 Oct 16;192 (8):1105-13.

Kedl RM, Schaefer BC, Kappler JW & Marrack P. T cells down-modulate peptide-MHC complexes on APCs in vivo. Nature Immunol. 3, 27–32 (2002).

Keever CA, Small TN, Flomenberg N, Heller G, Pekle K, Black P, Pecora A, Gillio A, Kernan NA, O'Reilly RJ. Immune reconstitution following bone marrow transplantation: comparison of recipients of T-cell depleted marrow with recipients of conventional marrow grafts. Blood. 1989 Apr;73(5):1340-50.

Kessinger A, Armitage JO, Landmark JD, Smith DM, Weisenburger DD. Autologous peripheral hematopoietic stem cell transplantation restores hematopoietic function following marrow ablative therapy. Blood. 1988 Mar;71(3):723-7.

Kieper WC, Burghardt JT, Surh CD. A role for TCR affinity in regulating naive T cell homeostasis. J Immunol. 2004 Jan 1;172(1):40-4.

Kieper, W.C., Burghardt, J.T., and Surh, C.D. A role for TCR affinity in regulating naive T cell homeostasis. J. Immunol. 2004; 172, 40–44.

Kieper WC, Troy A, Burghardt JT, Ramsey C, Lee JY, Jiang HQ, et al. Recent immune status determines the source of antigens that drive homeostatic T cell expansion. J Immunol 2005 174(6):3158–63.

Kim H, Moon HW, Hur M, Park CM, Yun YM, Hwang HS, Kwon HS, Sohn IS. Distribution of CD4+ CD25 high FoxP3+ regulatory T-cells in umbilical cord blood. J Matern Fetal Neonatal Med. 2012 Oct;25(10):2058-61.

Kim HJ, Kammertoens T, Janke M, Schmetzer O, Qin Z, Berek C, Blankenstein T. Establishment of early lymphoid organ infrastructure in transplanted tumors mediated by local production of lymphotoxin alpha and in the combined absence of functional B and T cells. J Immunol. 2004 Apr 1; 172(7):4037-47.

Kim YJ, Broxmeyer HE. Immune regulatory cells in umbilical cord blood and their potential roles in transplantation tolerance. Crit Rev Oncol Hematol. 2011 Aug;79(2):112-26. Review.

Kimura MY, Pobezinsky LA, Guinter TI, Thomas J, Adams A, Park JH, Tai X, Singer A. IL-7 signaling must be intermittent, not continuous, during $CD8^+$ T cell homeostasis to promote cell survival instead of cell death. Nat Immunol. 2013 Feb;14(2):143-51.

King MA, Covassin L, Brehm MA, Racki W, Pearson T, Leif J, Laning J, Fodor W, Foreman O, Burzenski L, Chase TH, Gott B, Rossini AA, Bortell R, Shultz LD, Greiner DL. Human peripheral blood leucocyte non-obese diabetic-severe combined immunodeficiency interleukin-2 receptor gamma chain gene mouse model of xenogeneic graft-versus-host-like disease and the role of host major histocompatibility complex. Clin Exp Immunol. 2009 Jul;157(1):104-18.

Komanduri KV, St John LS, de Lima M, McMannis J, Rosinski S, McNiece I, Bryan SG, Kaur I, Martin S, Wieder ED, Worth L, Cooper LJ, Petropoulos D, Molldrem JJ, Champlin RE, Shpall EJ. Delayed immune reconstitution after cord blood transplantation is characterized by impaired thymopoiesis and late memory T-cell skewing. Blood. 2007 Dec 15;110(13):4543-51.

Krampera M, Tavecchia L, Benedetti F, Nadali G, Pizzolo G. Intracellular cytokine profile of cord blood T-, and NK- cells and monocytes. Haematologica. 2000 Jul;85(7):675-9.

Kurnick NB, Montano A, Gerdes JC, et al: Preliminary observations on the treatment of postirradiation hematopoietic depression in man by the infusion of stored autogenous marrow. Ann Intern Med 1958;49:973-986.

Langrish CL, Buddle JC, Thrasher AJ, Goldblatt D. Neonatal dendritic cells are intrinsically biased against Th-1 immune responses. Clin Exp Immunol. 2002 Apr;128(1):118-23.

Latthe M, Terry L, Macdonald TT. High frequency of CD8aa homodimer bearing T cells in human fetal intestine. Eur J Immunol 1994;24:1703-1705.

Law JP, Hirschkorn DF, Owen RE, et al. The importance of Foxp3 antibody and fixation/permeabilization buffer combinations in identifying CD4+CD25+Foxp3+ regulatory T cells. Cytometry A. 2009 Dec;75(12):1040-50.

Lee YT, de Vasconcellos JF, Yuan J, Byrnes C, Noh SJ, Meier ER, Kim KS, Rabel A, Kaushal M, Muljo SA, Miller JL. LIN28B-mediated expression of fetal hemoglobin and production of fetal-like erythrocytes from adult human erythroblasts ex vivo. Blood. 2013 Aug 8;122(6):1034-41.

Leeansyah E, Loh L, Nixon DF, Sandberg JK. 2014. Acquisition of innate-like microbial reactivity in mucosal tissues during human fetal MAIT-cell development. Nat. Commun. 5, 3143.

Leffers N, Gooden MJ, De Jong RA, Hoogeboom BN, ten Hoor KA, Hollema H, Boezen HM, van der Zee AG, Daemen T, Nijman HW. Prognostic significance of tumor-infiltrating T-lymphocytes in primary and metastatic lesions of advanced stage ovarian cancer. Cancer Immunol Immunother. 2009;58:449–459.

Levine JE, Braun T, Penza SL, Beatty P, Cornetta K, Martino R, Drobyski WR, Barrett AJ, Porter DL, Giralt S, Leis J, Holmes HE, Johnson M, Horowitz M, Collins RH Jr. Prospective trial of chemotherapy and donor leukocyte infusions for relapse of advanced myeloid malignancies after allogeneic stem-cell transplantation. J Clin Oncol. 2002;20(2):405.

Lindemans CA, Chiesa R, Amrolia PJ, Rao K, Nikolajeva O, de Wildt A, Gerhardt CE, Gilmour KC, B Bierings M, Veys P, Boelens JJ. Impact of thymoglobulin prior to pediatric unrelated umbilical cord blood transplantation on immune reconstitution and clinical outcome. Blood. 2014 Jan 2;123(1):126-32.

Lisciandro JG, Prescott SL, Nadal-Sims MG, Devitt CJ, Richmond PC, Pomat W et al. Neonatal antigen-presenting cells are functionally more quiescent in children born under traditional compared with modern environmental conditions. J Allergy Clin Immunol. 2012 Nov;130(5):1167-1174.

Lochte HL Jr, Levy AS, Guenther DM, Thomas ED, Ferrebee JW. Prevention of delayed foreign marrow reaction in lethally irradiated mice by early administration of methotrexate. Nature. Dec 1962;15;196:1110-1.

Lorenz E, Uphoff D, Reid TR & Shelton E. Modification of irradiation injury in mice and guinea pigs by bone marrow injections. J. Natl Cancer Inst. 1951;12, 197–201.

Loughlin PM, Cooke TG, George WD, et al. Quantifying tumour-infiltrating lymphocyte subsets: a practical immuno-histochemical method. J Immunol Methods. 2007 Apr 10;321(1-2):32-40.

Lu YF, Gavrilescu LC, Betancur M, Lazarides K, Klingemann H, Van Etten RA. Distinct graft-versus-leukemic stem cell effects of early or delayed donor leukocyte infusions in a mouse chronic myeloid leukemia model. Blood. 2012 Jan 5;119(1):273-84.

Lucarelli G, Polchi P, Izzi T, Manna M, Agostinelli F, Delfini C, Porcellini A, Galimberti M, Moretti L, Manna, A, Sparaventi G, Baronciani D, Proietti A & Buckner CD. Allogeneic marrow transplantation for thalassemia. Experimental Hematology, 1984;12, 676–681.

Lucas PJ, Bare CV, Gress RE. The human anti-murine xenogeneic cytotoxic response. II. Activated murine antigen-presenting cells directly stimulate human T helper cells. J Immunol. 1995 Apr 15;154(8):3761-70.

Mackall CL, Fleisher TA, Brown MR, et al. Age, thymopoiesis, and CD4+ T-lymphocyte regeneration after intensive chemotherapy. N Engl J Med 1995; 332: 143–149.

Mackall CL, Granger L, Sheard MA, Cepeda R, Gress RE. T-cell regeneration after bone marrow transplantation: differential CD45 isoform expression on thymic-derived versus thymic-independent progeny. Blood. 1993 Oct 15; 82(8):2585-94.

Mackall C, Hakim F, Gress R. T - cell regeneration: all repertoires are not created equal. Immunol Today. 1997;18(5):245–51.

Mackall CL, Bare CV, Granger LA, Sharrow SO, Titus JA, Gress RE. Thymic-independent T cell regeneration occurs via antigen-driven expansion of peripheral T cells resulting in a repertoire that is limited in diversity and prone to skewing. J Immunol.1996;156(12):4609–16.

Majhail NS, Brunstein CG, Wagner JE. Double umbilical cord blood transplantation. Curr Opin Immunol. 2006 Oct. 18(5):571-5.

Marchant A, Goldman M. T cell-mediated immune responses in human newborns: ready to learn? Clin Exp Immunol. 2005;141(1):10-18[Review].

Markiewicz MA, Brown I, Gajewski TF. Death of peripheral CD8+ T cells in the absence of MHC class I is Fas-dependent and not blocked by Bcl-xL. Eur J Immunol. 2003 Oct;33(10):2917-26.

Marmont A, Horowitz MM, Gale RP, et al. T-cell depletion of HLA-identical transplants in leukemia. Blood. 1991;78:2120-2130.

Martin CE, Kim DM, Sprent J, Surh CD. Is IL-7 from dendritic cells essential for the homeostasis of CD4+ T cells? Nat Immunol. 2010 Jul;11 (7):547-8; author reply 548.

Maury S, Salomon B, Klatzmann D, Cohen JL. Division rate and phenotypic differences discriminate alloreactive and nonalloreactive T cells transferred in lethally irradiated mice. Blood. 2001 Nov 15;98(10):3156-8.

McVay LD, Jaswal SS, Kennedy C, Hayday A, Carding SR. The generation of human cd T cell repertoires during fetal development. J Immunol 1998;160:5851-5860.

Mehta J, Powles R, Singhal S, Iveson T, Treleaven J, Catovsky D. Clinical and hematologic response of chronic lymphocytic and prolymphocytic leukemia persisting after allogeneic bone marrow transplantation with the onset of acute graft-versus-host disease: possible role of graft-versus-leukemia. Bone Marrow Transplant. 1996;17(3):371.

Michaëlsson J, Mold JE, McCune JM, Nixon DF. Regulation of T cell responses in the developing human fetus. J Immunol. 2006 May 15; 176(10):5741-8.

Mikkola HK, Orkin SH. The journey of developing hematopoietic stem cells. Development. 2006 Oct;133(19):3733-44. Review.

Milano F, Gooley T, Wood B, Woolfrey A, Flowers ME, Doney K, Witherspoon R, Mielcarek M, Deeg JH, Sorror M, Dahlberg A, Sandmaier BM, Salit R, Petersdorf E, Appelbaum FR, Delaney C. Cord-Blood Transplantation in Patients with Minimal Residual Disease. N Engl J Med. 2016 Sep 8;375(10):944-53.

Min B, McHugh R, Sempowski GD, Mackall C, Foucras G, Paul WE. Neonates support lymphopenia-induced proliferation. Immunity. 2003 Jan;18(1):131-40.

Min B, Yamane H, Hu-Li J, Paul WE. Spontaneous and homeostatic proliferation of CD4 T cells are regulated by different mechanisms. J Immunol 2005; 174(10):6039–44.

Min B. Spontaneous T Cell Proliferation: A Physiologic Process to Create and Maintain Homeostatic Balance and Diversity of the Immune System. Front Immunol. 2018 Mar 19;9:547.

Mold JE, Venkatasubrahmanyam S, Burt TD, et al. Fetal and adult hematopoietic stem cells give rise to distinct T cell lineages in humans. Science. 2010 Dec 17;330(6011):1695-9.

Molldrem JJ, Lee PP, Wang C, Champlin RE, Davis MM. A PR1-human leukocyte antigen-A2 tetramer can be used to isolate low-frequency cytotoxic T lymphocytes from healthy donors that selectively lyse chronic myelogenous leukemia. Cancer Res.1999;59:2675-2681.

Montecino-Rodriguez E, Leathers H, Dorshkind K. Identification of a B-1 B cell-specific progenitor. Nat Immunol. 2006;7:293.

Morrison SJ, Hemmati HD, Wandycz AM, Weissman IL. The purification and characterization of fetal liver hematopoietic stem cells. Proc Natl Acad Sci. 1995;92:10302.

Neubert R, Delgado I, Abraham K, Schuster C, Helge H. Evaluation of the age-dependent development of lymphocyte surface receptors in children. Life Sci. 1998;62(12):1099-110.

Nguyen VT, Morange M & Bensaude O. Firefly luciferase luminescence assays using scintillation counters for quantitation in transfected mammalian cells. Anal Biochem, 1988;171, 404-408.

Niehues T, Rocha V, Filipovich AH, Chan KW, Porcher R, Michel G, Ortega JJ, Wernet P, Göbel U, Gluckman E, Locatelli F. Factors affecting lymphocyte subset reconstitution after either related or unrelated cord blood transplantation in children -- a Eurocord analysis. Br J Haematol. 2001 Jul;114(1):42-8.

Nijmeijer BA, Willemze R, Falkenburg JH. An animal model for human cellular immunotherapy: specific eradication of human acute lymphoblastic leukemia by cytotoxic T lymphocytes in NOD/scid mice. Blood 2002;100:654-660.

Nitsche A, Zhang M, Clauss T, Siegert W, Brune K, Pahl A. Cytokine profiles of cord and adult blood leukocytes: differences in expression are due to differences in expression and activation of transcription factors. BMC Immunol. 2007 Aug 31;8:18.

Nowell PC, Cole LJ, Habermeyer JG & Roan PL. Growth and continued function of rat marrow cells in X-radiated mice. Cancer Res. 1956;16, 258–261.

Okada R, Kondo T, Matsuki F, Takata H, Takiguchi M. Phenotypic classification of human CD4+ T cell subsets and their differentiation. Int Immunol. 2008 Sep;20(9):1189-99.

Opiela SJ, Koru-Sengul T, Adkins B. Murine neonatal recent thymic emigrants are phenotypically and functionally distinct from adult recent thymic emigrants. Blood. 2009 May 28;113(22):5635-43.

Ota MO, Vekemans J, Schlegel-Haueter SE, et al. Hepatitis B immunisation induces higher antibody and memory Th2 responses in new-borns than in adults. Vaccine. 2004;22:511–9.

Pages H, Carlson M, Falcon S and Li N (2017). AnnotationDbi: Annotation Database Interface. R package version 1.16.19.

Park M, Lee SH, Lee YH, Yoo KH, Sung KW, Koo HH, Kang HJ, Park KD, Shin HY, Ahn HS, Chung NG, Cho B, Kim HK, Koh KN, Im HJ, Seo JJ, Han DK, Baek HJ, Kook H, Hwang TJ, Lee EK, Hah JO, Lim YJ, Jung HJ, Park JE, Jang MJ, Chong SY, Oh D; Korean

Cord Blood Transplantation Working Party. Pre-engraftment syndrome after unrelated cord blood transplantation: a predictor of engraftment and acute graft-versus-host disease. Biol Blood Marrow Transplant. 2013 Apr;19(4):640-6.

Parkman R, Cohen G, Carter SL, Weinberg KI, Masinsin B, Guinan E, et al. Successful immune reconstitution decreases leukemic relapse and improves survival in recipients of unrelated cord blood transplantation. Biol Blood Marrow Transplant. 2006;12:919–927.

Passweg JR, Tiberghien P, Cahn JY, et al. Graft-versus-leukemia effects in T lineage and B lineage acute lymphoblastic leukemia. Bone Marrow Transplant 1998;21:153-158.

Patel KJ, Rice RD, Hawke R, Abboud M, Heller G, Scaradavou A, Young JW, Barker JN. Pre-engraftment syndrome after double-unit cord blood transplantation: a distinct syndrome not associated with acute graft-versus-host disease. Biol Blood Marrow Transplant. 2010 Mar;16(3):435-40.

Poirot L, Philip B, Schiffer-Mannioui C, Le Clerre D, Chion-Sotinel I, Derniame S, Potrel P, Bas C, Lemaire L, Galetto R, Lebuhotel C, Eyquem J, Cheung GW, Duclert A, Gouble A, Arnould S, Peggs K, Pule M, Scharenberg AM, Smith J. Multiplex Genome-Edited T-cell Manufacturing Platform for "Off-the-Shelf" Adoptive T-cell Immunotherapies. Cancer Res. 2015 Sep 15;75(18):3853-64.

Politikos I, Kim HT, Nikiforow S, Li L, Brown J, Antin JH, Cutler C, Ballen K, Ritz J, Boussiotis VA. IL-7 and SCF Levels Inversely Correlate with T Cell Reconstitution and Clinical Outcomes after Cord Blood Transplantation in Adults. PLoS One. 2015 Jul 15;10(7):e0132564.

Ponce DM, Hilden P, Devlin SM, et al. High disease-free survival with enhanced protection against relapse after double-unit cord blood transplantation when compared with T cell-depleted unrelated donor transplantation in patients with acute leukemia and chronic myelogenous leukemia. Biol Blood Marrow Transplant 2015;21(11):1985-1993.

Prasad VK, Kurtzberg J. Emerging trends in transplantation of inherited metabolic diseases. Bone Marrow Transplant. 2008 Jan;41(2):99-108.

Puel A, Ziegler SF, Buckley RH, Leonard WJ. Defective IL7R expression in T(-)B(+)NK(+) severe combined immunodeficiency. Nat Genet. 1998 Dec;20(4):394-7.

Qasim W, Zhan H, Samarasinghe S, Adams S, Amrolia P, Stafford S, Butler K, Rivat C, Wright G, Somana K, Ghorashian S, Pinner D, Ahsan G, Gilmour K, Lucchini G, Inglott S, Mifsud W, Chiesa R, Peggs KS, Chan L, Farzeneh F, Thrasher AJ, Vora A, Pule M, Veys P. Molecular remission of infant B-ALL after infusion of universal TALEN gene edited CAR Tcells. Sci Transl Med. 2017 Jan 25;9(374).

Quezada SA, Simpson TR, Peggs KS, Merghoub T, Vider J, Fan X, Blasberg R, Yagita H, Muranski P, Antony PA, Restifo NP, Allison JP. Tumor-reactive CD4(+) T cells develop

cytotoxic activity and eradicate large established melanoma after transfer into lymphopenic hosts. J Exp Med. 2010 Mar 15;207(3):637-50.

Rénard C, Barlogis V, Mialou V, Galambrun C, Bernoux D, Goutagny MP, Glasman L, Loundou AD, Poitevin-Later F, Dignat-George F, Dubois V, Picard C, Chabannon C, Bertrand Y, Michel G. Lymphocyte subset reconstitution after unrelated cord blood or bone marrow transplantation in children. Br J Haematol. 2011 Feb;152(3):322-30.

Rénard C, Barlogis V, Mialou V, Galambrun C, Bernoux D, Goutagny MP, Glasman L, Loundou AD, Poitevin-Later F, Dignat-George F, Dubois V, Picard C, Chabannon C, Bertrand Y, Michel G. Lymphocyte subset reconstitution after unrelated cord blood or bone marrow transplantation in children. Br J Haematol. 2011 Feb;152(3):322-30.

Rezvani K, Grube M, Brenchley JM, et al. Functional leukemia-associated antigen specific memory CD8+ T cells exist in healthy individuals and in patients with chronic myelogenous leukemia before and after stem cell transplantation. Blood. 2003;102:2892-2900.

Rocha V, Cornish J, Sievers EL, Filipovich A, Locatelli F, Peters C, Remberger M, Michel G, Arcese W, Dallorso S, Tiedemann K, Busca A, Chan KW, Kato S, Ortega J, Vowels M, Zander A, Souillet G, Oakill A, Woolfrey A, Pay AL, Green A, Garnier F, Ionescu I, Wernet P, Sirchia G, Rubinstein P, Chevret S, Gluckman E. Comparison of outcomes of unrelated bone marrow and umbilical cord blood transplants in children with acute leukemia. Blood. 2001 May 15;97(10):2962-71.

Rocha V, Wagner JE Jr, Sobocinski KA, Klein JP, Zhang MJ, Horowitz MM, Gluckman E. Graft-versus-host disease in children who have received a cord-blood or bone marrow transplant from an HLA-identical sibling. Eurocord and International Bone Marrow Transplant Registry Working Committee on Alternative Donor and Stem Cell Sources. N Engl J Med. 2000 Jun 22;342(25):1846-54.

Rooney CM, Smith CA, Ng CY, et al. Infusion of cytotoxic T cells for the prevention and treatment of Epstein-Barr virus-induced lymphoma in allogeneic transplant recipients. Blood. 1998;92:1549-1555.

Rosenblatt J, Vasir B, Uhl L, Blotta S, Macnamara C, Somaiya P, Wu Z, Joyce R, Levine JD, Dombagoda D, Yuan YE, Francoeur K, Fitzgerald D, Richardson P, Weller E, Anderson K, Kufe D, Munshi N, Avigan D. Vaccination with dendritic cell/tumor fusion cells results in cellular and humoral antitumor immune responses in patients with multiple myeloma. Blood. 2011 Jan 13;117(2):393-402.

Rubinstein P, Carrier C, Scaradavou A, Kurtzberg J, Adamson J, Migliaccio AR, Berkowitz RL, Cabbad M, Dobrila NL, Taylor PE, Rosenfield RE, Stevens CE. Outcomes among 562 recipients of placental-blood transplants from unrelated donors. N Engl J Med. 1998 Nov 26;339(22):1565-77.

Saini M, Pearson C, Seddon B. Regulation of T cell-dendritic cell interactions by IL-7 governs T-cell activation and homeostasis. Blood. 2009 Jun 4;113 (23):5793-800.

Sakaguchi, S. Naturally arising Foxp3-expressing CD25+CD4+ regulatory T cells in immunological tolerance to self and non-self. Nature Immunol. 2005 6, 345–352.

Sato E, Olson SH, Ahn J, Bundy B, Nishikawa H, Qian F, Jungbluth AA, Frosina D, Gnjatic S, Ambrosone C, Kepner J, Odunsi T, Ritter G, Lele S, Chen YT, Ohtani H, Old LJ, Odunsi K. Intraepithelial CD8+ tumor-infiltrating lymphocytes and a high CD8+/regulatory T cell ratio are associated with favorable prognosis in ovarian cancer. Proc Natl Acad Sci USA. 2005;102:18538–18543.

Sauter C, Abboud M, Jia X, Heller G, Gonzales AM, Lubin M, Hawke R, Perales MA, van den Brink MR, Giralt S, Papanicolaou G, Scaradavou A, Small TN, Barker JN. Serious infection risk and immune recovery after double-unit cord blood transplantation without antithymocyte globulin. Biol Blood Marrow Transplant. 2011 Oct;17(10):1460-71.

Savoldo B, Rooney CM, Di Stasi A, Abken H, Hombach A, Foster AE, Zhang L, Heslop HE, Brenner MK, Dotti G. Epstein Barr virus specific cytotoxic T lymphocytes expressing the anti-CD30zeta artificial chimeric T-cell receptor for immunotherapy of Hodgkin disease. Blood 2007;110(7):2620-2630.

Schetelig J, Kiani A, Schmitz M, Ehninger G, Bornhauser M. T cell-mediated graft-versus-leukemia reactions after allogeneic stem cell transplantation. Cancer Immunol Immunother. 2005;54:1043-1058.

Schönland SO, Zimmer JK, Lopez-Benitez CM, Widmann T, Ramin KD, Goronzy JJ, Weyand CM. Homeostatic control of T-cell generation in neonates. Blood. 2003 Aug 15;102(4):1428-34.

Schrama D, thor Straten P, Fischer WH, McLellan AD, Bröcker EB, Reisfeld RA, Becker JC. Targeting of lymphotoxin-alpha to the tumor elicits an efficient immune response associated with induction of peripheral lymphoid-like tissue. Immunity. 2001 Feb; 14(2):111-21.

Seddon B, Zamoyska R. Regulation of peripheral T-cell homeostasis by receptor signalling. Current opinion in immunology. 2003;15:321–324.

Seddon B, Zamoyska R. TCR and IL-7 receptor signals can operate independently or synergize to promote lymphopenia-induced expansion of naive T cells. J Immunol. 2002 Oct 1;169(7):3752-9.

Sekine T, Marin D, Cao K, Li L, Mehta P, Shaim H, Sobieski C, Jones R, Oran B, Hosing C, Rondon G, Alsuliman A, Paust S, Andersson B, Popat U, Kebriaei P, Muftuoglu M, Basar R, Kondo K, Nieto Y, Shah N, Olson A, Alousi A, Liu E, Sarvaria A, Parmar S, Armstrong-James D, Imahashi N, Molldrem J, Champlin R, Shpall EJ, Rezvani K. Specific combinations

of donor and recipient KIR-HLA genotypes predict for large differences in outcome after cord blood transplantation. Blood. 2016 Jul 14;128(2):297-312.

Shevach, E. M. CD4+ CD25+ suppressor T cells: more questions than answers. Nature Rev. Immunol. 2002 2, 389–400.

Shimoni A, Gajewski JA, Donato M, Martin T, O'Brien S, Talpaz M, Cohen A, Korbling M, Champlin R, Giralt S. Long-Term follow-up of recipients of CD8-depleted donor lymphocyte infusions for the treatment of chronic myelogenous leukemia relapsing after allogeneic progenitor cell transplantation. Biol Blood Marrow Transplant. 2001;7(10):568-75.

Shultz LD, Ishikawa F, Greiner DL. Humanized mice in translational biomedical research. Nat.Rev Immunol. 2007;7:118–130.

Shultz LD, Schweitzer PA, Christianson SW, Gott B, Schweitzer IB, Tennent B, McKenna S, Mobraaten L, Rajan TV, Greiner DL, et al. Multiple defects in innate and adaptive immunologic function in NOD/LtSz-scid mice. J Immunol. 1995 Jan 1;154(1):180-91.

Silverstein AM, Prendergast RA, Kraner KL. Fetal response to antigenic stimulus. IV. Rejection of skin homografts by the fetal lamb. J Exp Med. 1964a;119:955-964.

Silverstein AM. Ontogeny of the immune response. Science. 1964b;144(3625):1423-1428.

Silva-Santos B, Schamel WW, Fisch P, Eberl M. gammadelta T-cell conference 2012: close encounters for the fifth time. Eur. J. Immunol. 2012; 42, 3101–3105.

Simpson-Abelson MR, Sonnenberg GF, Takita H, Yokota SJ, Conway TF, Jr., Kelleher RJ, Jr., Shultz LD, Barcos M, Bankert RB. Long-term engraftment and expansion of tumor-derived memory T cells following the implantation of non-disrupted pieces of human lung tumor into NOD-scid IL2Rgamma(null) mice. J.Immunol. 2008;180:7009–7018.

Smith-Garvin JE, Koretzky GA, Jordan MS. T cell activation. Annu Rev Immunol. 2009;27:591-619.

Socié G, Schmoor C, Bethge WA, et al. Chronic graft-versus-host disease: long-term results from a randomized trial on GVHD prophylaxis with or without anti–T cell globulin ATG-Fresenius. Blood 2011;117(23):6375-6382.

Spencer J, Macdonald TT, Finn T, Isaacson PG. The development of gut associated lymphoid tissue in the terminal ileum of fetal human intestine. Clin Exp Immunol 1986;64:536.

Sprent J, Surh CD. Normal T cell homeostasis: the conversion of naive cells into memory-phenotype cells.Nat Immunol. 2011;12:478–484.

Storb R, Epstein RB, Graham TC & Thomas ED. Methotrexate regimens for control of graft-versus-host disease in dogs with allogeneic marrow grafts. Transplantation, 1970;9, 240–246.

Storb R, Epstein RB, Ragde H, Bryant J, Thomas ED. Marrow engraftment by allogeneic leukocytes in lethally irradiated dogs. Blood. 1967 Dec;30(6):805-11.

Storb R, Prentice RL & Thomas ED. Treatment of aplastic anemia by marrow transplantation from HLA identical siblings. Prognostic factors associated with graft versus host disease and survival. J. Clin. Invest. 1977;59, 625–632.

Storb R, Thomas ED, Buckner CD, Clift RA, Johnson FL, Fefer A, Glucksberg H, Giblett ER, Lerner KG & Neiman P. Allogeneic marrow grafting for treatment of aplastic anemia. Blood, 1974;43, 157–180.

Subramanian A, Tamayo P, Mootha VK, Mukherjee S, Ebert BL, Gillette MA et al. Gene set enrichment analysis: a knowledge-based approach for interpreting genome-wide expression profiles. Proc Natl Acad Sci U S A. 2005 Oct 25;102 (43):15545-50.

Surh CD, Sprent J. Homeostasis of naive and memory T cells. Immunity. 2008;29:848–862.

Surh CD, Sprent J. Homeostatic T cell proliferation: how far can T cells be activated to self-ligands? J Exp Med. 2000 Aug 21;192(4):F9-F14. Review.

Susskind B, Shornick MD,Iannotti MR, et al. Cytolytic effector mechanisms of human CD4+ cytotoxic T lymphocytes. Human Immunol 1996; 45:64.

Swainson L, Kinet S, Mongellaz C, Sourisseau M, Henriques T, Taylor N. IL-7-induced proliferation of recent thymic emigrants requires activation of the PI3K pathway. Blood. 2007 Feb 1;109(3):1034-42.

Tan JT, Ernst B, Kieper WC, LeRoy E, Sprent J, Surh CD. Interleukin (IL)-15 and IL-7 jointly regulate homeostatic proliferation of memory phenotype CD8+ cells but are not required for memory phenotype CD4+ cells. J Exp Med 2002; 195(12):1523–32.

Takada K, Jameson SC. Naive T cell homeostasis: from awareness of space to a sense of place. Nat Rev Immunol. 2009;9:823–832.

Takahata Y, Nomura A, Takada H, Ohga S, Furuno K, Hikino S, Nakayama H, Sakaguchi S, Hara T. CD25+CD4+ T cells in human cord blood: an immunoregulatory subset with naivephenotype and specific expression of forkhead box p3 (Foxp3) gene. Exp Hematol. 2004 Jul;32(7):622- 9.

Tan JT, Dudl E, LeRoy E, Murray R, Sprent J, Weinberg KI, Surh CD. IL-7 is critical for homeostatic proliferation and survival of naive T cells. Proc Natl Acad Sci U S A. 2001 Jul 17;98(15):8732-7.

Thomas ED, Buckner CD, Sanders JE, Papayannopoulou T, Borgna-Pignatti C, De Stefano P, Sullivan KM, Clift RA & Storb R. Marrow transplantation for thalassaemia. Lancet, ii, 1982;227–229.

Thomas ED, Buckner CD, Storb R, Neiman PE, Fefer A, Clift RA, Slichter SJ, Funk DD, Bryant JI & Lerner KG. Aplastic anaemia treated by marrow transplantation. Lancet, i, 1972;284–289.

Thomas ED, Lochte HL Jr, Cannon JH, Sahler OD & Ferrebee JW. Supralethal whole body irradiation and isologous marrow transplantation in man. J. Clin. Invest. 1959;38, 1709–1716.

Thomas ED, Lochte HL Jr, Lu WC & Ferrebee JW. Intravenous infusion of bone marrow in patients receiving radiation and chemotherapy. N. Engl. J. Med. 1957;257, 491–496.

Thomas ED, Storb R, Clift RA, Fefer A, Johnson FL, Neiman PE, Lerner KG, Glucksberg H & Buckner CD. Bone marrow transplantation. New England Journal of Medicine, 1975;292, 832–843, 895–902.

To LB & Juttner CA. Peripheral blood stem cell autografting: a new therapeutic option for AML? British Journal of Haematology, 1987;66, 285–288.

Tonon SS, Goriely E, Aksoy O, et al. Bordetella pertussis toxin induces the release of inflammatory cytokines and dendritic cell activation in whole blood: impaired responses in human newborns. Eur J Immunol. 2002;32:3118–25.

Trzonkowski P, Zilvetti M, Chapman S, et al. Homeostatic repopulation by CD28-CD8+ T cells in alemtuzumab-depleted kidney transplant recipients treated with reduced immunosuppression. Am J Transplant 2008; 8: 338–347.

Tsung K, Meko JB, Peplinski GR, Tsung YL, Norton JA. IL-12 induces T helper 1-directed antitumor response. J Immunol. 1997 Apr 1;158(7):3359-65.

Tu W, Chen S, Sharp M, Dekker C, et al. Persistent and selective deficiency of CD4+ T cell immunity to cytomegalovirus in immunocompetent young children. J Immunol. 2004;172:3260–7.

Unsinger J, Kazama H, McDonough JS, Hotchkiss RS, Ferguson TA. Differential lymphopenia-induced homeostatic proliferation for CD4+ and CD8+ T cells following septic injury. J Leukoc Biol 2009; 85: 382–390.

Uphoff DE. Alteration of homograft reaction by A-methopterin in lethally irradiated mice treated with homologous marrow. Proc Soc Exp Biol Med. 1958;99(3):651-3.

van der Windt DJ, Dons EM, Montoya CL, Ezzelarab M, Long C, Wolf RF, Ijzermans JN, Lakkis FG, Cooper DK. T-lymphocyte homeostasis and function in infant baboons: implications for transplantation. Transpl Int. 2012 Feb;25(2):218-28.

van Rood JJ, Eernisse JG & van Leeuwen A. Leukocyte antibodies in sera from pregnant women. Nature, 1958;181, 1735–1736.

van Rood JJ, Oudshoorn M. Eleven million donors in Bone Marrow Donors Worldwide! Time for reassessment? Bone Marrow Transplant. 2008 Jan;41(1):1-9.

Vekemans J, Ota MO, Wang EC, et al. T cell responses to vaccines in infants: defective IFNgamma production after oral polio vaccination. Clin Exp Immunol. 2002;127:495–8.

Veys P, Wynn RF, Ahn KW, Samarasinghe S, He W, Bonney D, Craddock J, Cornish J, Davies SM, Dvorak CC, Duerst RE, Gross TG, Kapoor N, Kitko C, Krance RA, Leung W, Lewis VA, Steward C, Wagner JE, Carpenter PA, Eapen M. Impact of immune modulation with in vivo T-cell depletion and myleoablative total body irradiation conditioning on outcomes after unrelated donor transplantation for childhood acute lymphoblastic leukemia. Blood. 2012 Jun 21;119(25):6155-61.

von Hoegen P, Sarin S, Hrowka JF. Deficiency in T cell responses of human fetal lymph node cells: a lack of accessory cells. Immunol Cell Biol 1995;73:353-361.

Wagner JE Jr, Eapen M, Carter S, et al; Blood and Marrow Transplant Clinical Trials Network. One-unit versus two-unit cord-blood transplantation for hematologic cancers. N Engl J Med. 2014;371(18):1685-1694.

Wange RL. LAT, the linker for activation of T cells: a bridge between T cell-specific and general signaling pathways. Sci STKE. 2000 Dec 19;2000(63):re1.

Weiden PL, Flournoy N, Thomas ED, Prentice R, Fefer A, Buckner CD, Storb R.Antileukemic effect of graft-versus-host disease in human recipients of allogeneic-marrow grafts. N Engl J Med. 1979;300(19):1068.

Weiden PL, Sullivan KM, Flournoy N, Storb R, Thomas ED. Antileukemic effect of chronic graft-versus-host disease: contribution to improved survival after allogeneic marrow transplantation. N Engl J Med. 1981;304(25):1529.

White GP, Watt PM, Holt BJ, Holt PG. Differential patterns of methylation of the IFN-gamma promoter at CpG and non-CpG sites underlie differences in IFN-gamma gene expression between human neonatal and adult CD45RO- T cells. J Immunol. 2002;168(6):2820-2827.

Wiegering V, Eyrich M, Wunder C, Günther H, Schlegel PG, Winkler B. Age-related changes in intracellular cytokine expression in healthy children. Eur Cytokine Netw. 2009 Jun;20(2):75-80.

Willemze R, Rodrigues CA, Labopin M, Sanz G, Michel G, Socié G, Rio B, Sirvent A, Renaud M, Madero L, Mohty M, Ferra C, Garnier F, Loiseau P, Garcia J, Lecchi L, Kögler G, Beguin Y, Navarrete C, Devos T, Ionescu I, Boudjedir K, Herr AL, Gluckman E, Rocha V; Eurocord-Netcord and Acute Leukaemia Working Party of the EBMT. KIR-ligand incompatibility in the graft-versus-host direction improves outcomes after umbilical cord blood transplantation for acute leukemia. Leukemia. 2009 Mar;23(3):492-500.

Williams KM, Hakim FT, Gress RE. T cell immune reconstitution following lymphodepletion. Semin Immunol. 2007 Oct;19(5):318-30. Epub 2007 Nov 19.

Xie Y, Akpinarli A, Maris C, Hipkiss EL, Lane M, Kwon EK, Muranski P, Restifo NP, Antony PA. Naive tumor-specific CD4(+) T cells differentiated in vivo eradicate established melanoma. J Exp Med. 2010 Mar 15;207(3):651-67.

Xing D, Ramsay AG, Gribben JG, et al. Cord blood natural killer cells exhibit impaired lytic immunological synapse formation that is reversed with IL-2 exvivo expansion. J Immunother 2010;33(7):684-696.

Yan CH, Liu DH, Liu KY, Xu LP, Liu YR, Chen H, Han W, Wang Y, Qin YZ, Huang XJ. Risk stratification-directed donor lymphocyte infusion could reduce relapse of standard-risk acute leukemia patients after allogeneic hematopoietic stem cell transplantation. Blood. 2012 Apr;119(14):3256-62.

Yu P, Lee Y, Liu W, Chin RK, Wang J, Wang Y, Schietinger A, Philip M, Schreiber H, Fu YX. Priming of naive T cells inside tumors leads to eradication of established tumors. Nat Immunol. 2004 Feb; 5(2):141-9.

Yuan J, Nguyen CK, Liu X, Kanellopoulou C, Muljo SA. Lin28b reprograms adult bone marrow hematopoietic progenitors to mediate fetal-like lymphopoiesis. Science. 2012 Mar 9;335(6073):1195-200.

Zanjani ED, Ascensao JL, Tavassoli M. Liver-derived fetal hematopoietic stem cells selectively and preferentially home to the fetal bone marrow. Blood. 1993;81:399.

Zhang L, Conejo-Garcia JR, Katsaros D, Gimotty PA, Massobrio M, Regnani G, Makrigiannakis A, Gray H, Schlienger K, Liebman MN, Rubin SC, Coukos G. Intratumoral T cells, recurrence, and survival in epithelial ovarian cancer. N Engl J Med. 2003; 348:203–213.

Zhao Y, Dai ZP, Lv P, Gao XM. Phenotypic and functional analysis of human T lymphocytes in early second- and third-trimester fetuses. Clin Exp Immunol. 2002;129: 302-308.

Zheng C, Luan Z, Fang J, et al. Comparison of conditioning regimens with or without antithymocyte globulin for unrelated cord blood transplantation in children with high-risk or advanced hematological malignancies. Biol Blood Marrow Transplant. 2015 Jan 15.

Zorn E, Wang KS, Hochberg EP, Canning C, Alyea EP, Soiffer RJ, Ritz J. Infusion of CD4+ donor lymphocytes induces the expansion of CD8+ donor T cells with cytolytic activity directed against recipient hematopoietic cells. Clin Cancer Res. 2002 Jul;8(7):2052-60.

Zou, W. Immunosuppressive networks in the tumour environment and their therapeutic relevance. Nature Rev. Cancer 2005; 5, 263–274.

Appendix 1

Hiwarkar P, Qasim W, Ricciardelli I, Gilmour K, Quezada S, Saudemont A, Amrolia P, Veys P. Cord blood T cells mediate enhanced antitumor effects compared with adult peripheral blood T cells. Blood. 2015 Dec 24;126(26):2882-91.

Appendix 2

Prashant Hiwarkar, Mike Hubank, Waseem Qasim, Robert Chiesa, Kimberly C. Gilmour, Aurore Saudemont, Persis J. Amrolia and Paul Veys. Cord blood transplantation recapitulates fetal ontogeny with a distinct molecular signature that supports $CD4^+$ T-cell reconstitution. Blood Advances 2017 1:2206-2216.